DEVELOPMENT OF THE NEW UE38 UNDULATOR FOR THE ATHOS BEAMLINE IN SwissFEL

H. Joehri[†], M. Calvi, M. Hindermann, L. Huber, A. Keller, M. Locher, Th. Schmidt, X. Wang,
A. Zandonella, Paul Scherrer Institute, 5232 Villigen, Switzerland

Abstract

For Athos, the second beamline of SwissFEL, we profit from the experience of the U15 undulator development. The U15 undulator is in use at the Aramis-beamline in SwissFEL. But for Athos, there are new requirements, because it will be a polarized undulator with a period of 38mm. We developed a new arrangement of the drives in a X-arrangement. The magnet keepers are optimized for bigger forces also in the beam direction. A vacuum pipe with only 0.2mm of wall thickness is realized.

Currently, the undulator is in fabrication at MDC Max Daetwyler AG. All the main parts are manufactured and the assembly is close to be finished. For measurement and alignment, separate tools had to be designed.

For the vacuum pipe we have a prototype, which is close to the requirements. Some points of the fabrication process have to be optimized to realize a better straightness.

OVERVIEW

The general arrangement is an Apple II undulator, but the movements of the magnets are not in vertical direction. The opening of the gaps, is like an X (Figure 1).
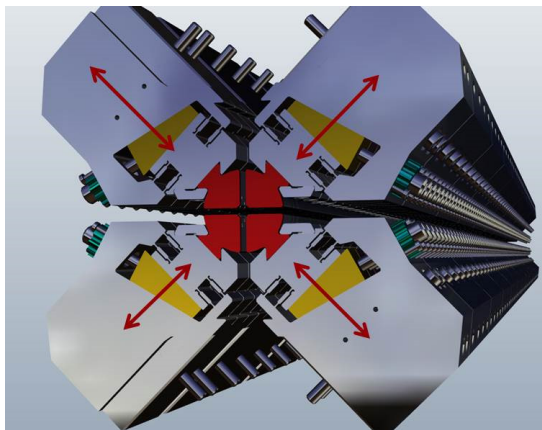

Figure 1: X – Arrangement.

Each magnet can be adjusted with a screw. The screw with two different threads moves a wedge. This wedge moves the magnet in the direction of the gap movement. This enables to use a robot system to adjust each magnet individually within a tolerance of 1.5 µm

___
† haimo.joehri@psi.ch

Main Specification

Length	: 2 m
Number of periods	: 52
Length of period	: 38 mm
Gap range	: 3 – 21 mm
Shiftrange	: +/- 21 mm
Magnetic force in X	: 1.6 tons
Magnetic force in Y	: 1.6 tons
Magnetic force in Z	: 2.0 tons

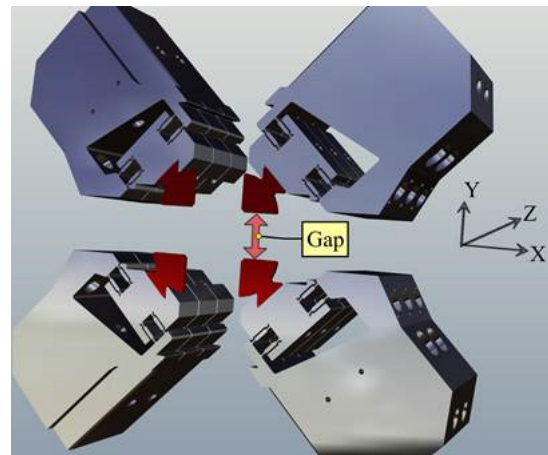See figure 2 for the definition of gap and the direction of the forces

Figure 2: Definition of gap and the coordinates.

DRIVES AND ENCODERS

One goal of the development was to find an arrangement in a way, that the drives are independent of each other (see figure 3).

The gap is changed by a wedge drive. The wedge is driven by a servomotor and a spindle with a satellite roller screw. The slope of the spindle is 0.5 mm.

The shift drive is solved directly with a spindle and a servo-motor. Also here, a spindle with satellite roller screws is used. The slope is 1.0 mm.

To allow the baseplate with the keepers to move in both directions (gap and shift), a separate plate is positioned between the frame and the baseplate (violet plate in figure 3). This plate is connected to the frame with 7 linear guides to give the stiffness of the system.

All movements are controlled by linear encoders
Motors: Beckhoff AM8023-OE21
Encoders: Heidenhain LC 415-ML70

Accelerators

Insertion Devices

APPLE II INSERTION DEVICES MADE AT MAX IV

A. Thiel, M. Ebbeni, H. Tarawneh, MAX IV Laboratory, Lund, Sweden

Abstract

At present five Apple II insertion devices were made and installed at MAX IV [1], three of them in the 1.5GeV-ring, and two in the 3GeV-ring. The assembly of the last one of a total number of six Apple II undulators made at MAX IV is currently going on. The undulators have period lengths of 48mm (two devices), 53mm, 58mm, 84mm and 95.2mm. The operational gap range of the 3GeV devices is between 11mm and 150mm, the range of the 1.5GeV devices is 14mm to 150mm. Structural analysis was applied to assure a minimum deflection of the main frame and the magnet array girders. The main frame is made of nodular cast iron, while the girders are made of aluminium alloy. In order to optimize the magnetic tuning the position of the magnet keepers can be adjusted by wedges. The undulators were fiducialized before the installation in the ring tunnel and were aligned in the straight section using their magnetic centre as reference. All MAX IV made undulators have three feet with vertical adjustment and separate horizontal adjusters. This paper describes the design, assembly, shimming and installation of the MAX IV Apple II devices in more detail.

OVERVIEW OF INSTALLED APPLE II

Three Apple II undulators (EPU: elliptically polarising undulator) are in place at the 1.5GeV-ring and two EPU's in the 3 GeV-ring. A sixth EPU is currently in assembly for the 3 GeV-ring. Table 1 shows the overview of the EPU's with some characteristic properties.

Table 1: Summary of Styles

	Beam-line	Period length	Inst. length	Magn. gap	K_{eff}
3 GeV	Hippie	53mm	4m	11mm	3.30
	Veritas	48mm	4m	11mm	3.30
	Softimax	48mm	4m	11mm	3.30
1.5 GeV	Bloch	84mm	2.6m	14mm	8.65
	FinEst	95.2mm	2.6m	14mm	10.40
	MAX peem	58mm	2.6m	14mm	4.95

These six undulators were manufactured at the MAX IV magnet laboratory between 2015 and 2018. The initial design bases on an EPU designed in collaboration with Bessy (HZB) [2].

MECHANICAL DESIGN FEATURES

Undulator Cast Frame

The backbone of MAX IV EPU's is the cast iron frame made of nodular cast iron EN-GJS-400-18-RT according to DIN EN1563. The material combines high strength and good machining properties with low deformation at present forces. The cast pattern of the frame was designed by the foundry based on the calculated magnet forces and estimated magnet array weight. Figure 1 shows the force pattern and Table 2 the allowable deformation.
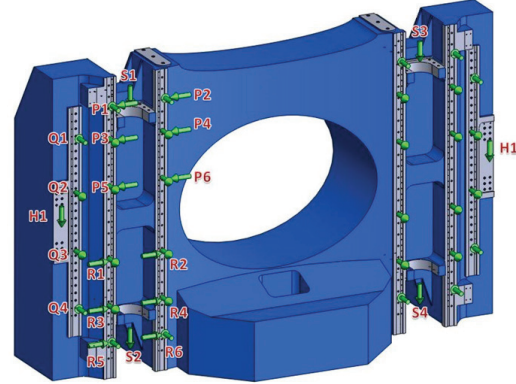

Figure 1: Force pattern on the EPU-model frame.

Table 2: Maximum Allowable Deformation

	Horizontal [mm]	Vertical [mm]
P-R		< 0.050
P1-P6 / R1-R6	< 0.015	
Q1-Q2 / Q3-Q4	< 0.010	
Q1-Q4	< 0.020	

The foundry's engineering team optimized the cast model respectively [3], also in regard of the manufacturing procedure. MAX IV used two standardized wooden cast patterns to cover the two different straight section lengths of the two storage rings. The cast frames have a weight of approximate 6.2t. Figure 2 shows the EPU53 cast frame during machining.
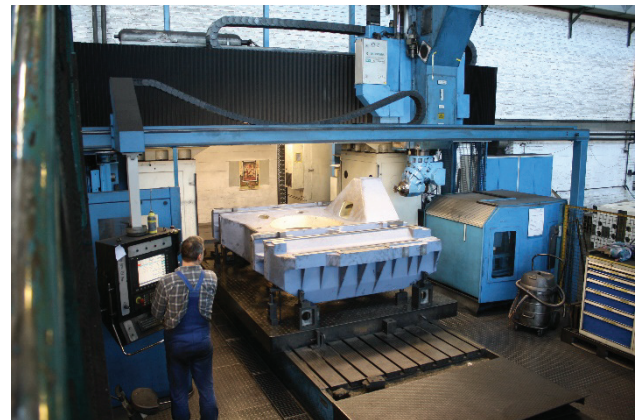

Figure 2: EPU53 cast frame during machining.

Undulator Feet Arrangement

The EPU's manufactured by MAX IV have three feet, which carry the entire weight. Three additional side adjusters take care of the horizontal alignment. The

RF FINGERS FOR THE NEW ESRF-EBS STORAGE RING

Th. Brochard[†], L. Goirand, P. Brumund, J. Pasquaud, S. White
European Synchrotron Radiation Facility, 38043 Grenoble, France

Abstract

In the new ESRF-EBS (Extremely Brilliant Source) storage ring vacuum chambers assembly, with a reduced aperture and the new omega shape, RF fingers are a key component to ensure good vacuum conditions and reach the best possible machine performance. As a result, dedicated efforts were put into producing a more compact more robust more reliable and easier to assemble RF finger design for the new machine. The work was done in parallel on the beam coupling impedance reduction, which have a direct impact on the electron beam lifetime, and on the mechanical aspect with FEA validation and geometry optimization. Many test have been made, in a mechanical laboratory, including high resolution 3D computed tomography images in order to measure the electrical contact, and also in the existing ESRF storage ring with the electron beam, to validate the final design before launching the series production.

INTRODUCTION

In order to absorb chamber-to-chamber misalignments, thermal expansion, for instance during bake-out, bellows are used to inter-connect a large number of chambers along the ring circumference. These bellows however are seen as resonant cavities by the beam hence breaking the geometrical continuity of the beam pipe and leading to degraded vacuum and stability performance. The continuity is restored by electrically shielding the bellows from the beam using so-called RF fingers which consist of conductors matching the vacuum chamber profile and connecting the beam pipes on either side of the bellow. The RF fingers are meant to absorb mechanical movements while providing the best possible mechanical and geometrical continuity: designing such a device is therefore far from trivial since many aspects have to be carefully optimized.

The new omega-shaped chamber profile is not compatible with the present RF finger design if geometrical continuity is to be enforced. A dedicated in-house design based on new concepts and principles was therefore devised for the ESRF-EBS ring. Figure 1 shows the final design. It is the result of several iterations and optimizations of beam coupling impedance and mechanical properties.
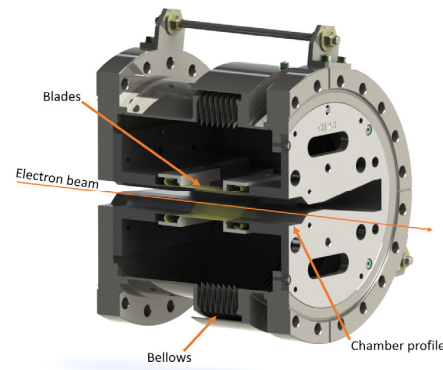

Figure 1: RF Finger placed in a bellows.

BEAM COUPLING IMPEDANCE REDUCTION

The first step was to ensure that the cavity formed by the bellow was properly shielded from the beam. This was achieved by 10 blades (5 top and 5 bottom) as seen in Fig. 2. Once the bellow is invisible to the beam, the beam coupling impedance is strictly given by geometrical discontinuities of the inner volume: in this case the steps and tapers angle at the entrance and exit of the RF fingers can be seen in Fig. 2. The step height was fixed to 0.3mm for mechanical criteria and the only parameter left for optimization was the taper angle, a good compromise was found with a reduction of the taper angle from 5º to 2º leading to a reduction of the beam coupling impedance by a factor 4. This result was found satisfactory as the resulting full contribution of the RF fingers to the total impedance of the machine became significantly smaller than the contribution of beam pipes themselves.
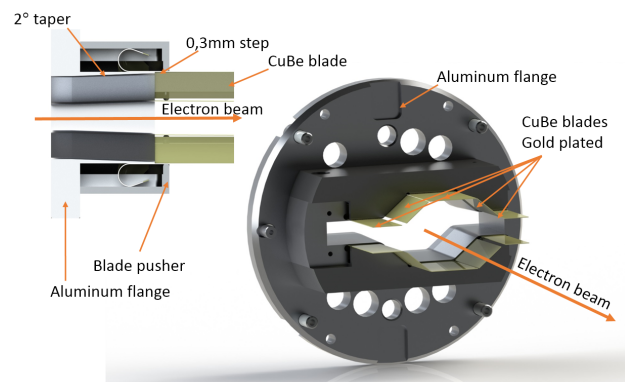

Figure 2: RF Finger cut view.

---

† brochard@esrf.fr

DEFORMABLE RF FINGERS WITH AXIAL EXTENSION

S. Sharma[†], F. DePaola, F. Lincoln, J. Tuozzolo, NSLS-II, BNL, 11973 Upton, NY, USA

Abstract

RF fingers in a bellows assembly provide electrical continuity for the image current between adjacent vacuum chambers. They are required to absorb all misalignments between the two chambers while minimizing abrupt changes in the beam aperture. In addition, during bake-outs of the chambers the fingers are required to accommodate their large thermal expansions. The latter is achieved either by having a sliding-contact finger design or a deformable finger design. In this paper we describe a version of the deformable finger design which permits large compression, significant misalignments and axial extension. A novel method of fingers' fabrication, FE analysis and test results are presented.

INTRODUCTION

Bellows assemblies are used as flexible interconnections between adjacent vacuum chambers. The flexibility of the stainless steel bellows compensates for transverse misalignments and axial gap of ~ 2 mm for the NSLS-II chambers. During bake-outs of the vacuum chambers the bellows compress by ~ 10 mm to absorb the combined thermal expansion of the chambers. RF fingers made from copper alloys are used inside the bellows to provide electrical continuity and the continuity of the beam aperture. These fingers must also compensate for the chambers' misalignment, axial gap and thermal expansion.
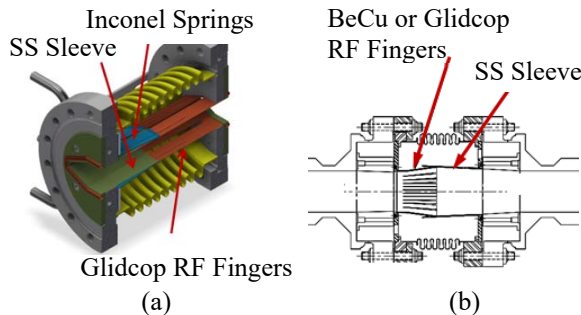

Figure 1: Conventional designs of RF fingers sliding on SS sleeve, (a) outside sliding type, (b) inside sliding type.

The conventional design of RF fingers relies on the fingers sliding on the outside surface or on the inside surface of a sleeve usually made from stainless steel. RF fingers for NSLS-II [1] and APS [2], shown in Fig. 1(a) and 1(b), are examples of the two designs. In the case of the outer-sliding RF finger design the fingers are compressed by cantilevered Inconel springs to ensure good contact pressure. A lack of good contact pressure can lead to thermal deformation and even melting of the fingers in storage rings with high beam current or high current per bunch.

† sharma@bnl.gov

A deformable finger design with fixed contacts has been proposed recently [3, 4] for the interconnection module of the LHC vacuum chambers. The RF fingers are pre-deformed in a corrugated shaped (Fig. 2(a)). The design is optimized to prevent buckling and over-extension. In the as-installed position, Fig. 2 (a), the fingers are compressed. During operation the fingers are almost fully extended (Fig. 2(b)) leaving some slack to compensate for axial gap.

Figure 2: LHC deformable finger design, (a) as installed, (b) in operation.

In this paper we present a fixed-contact RF finger design that utilizes large nonlinear deformation including buckling to compensate for thermal expansion of the chambers. The RF fingers in this single-piece design can be offset by up to 2 mm to compensate for transverse misalignments between the vacuum chambers. They can also be extended by up to 2 mm to compensate for axial gaps. The RF fingers are designed to remain straight during operation.

PROPOSED DESIGN

Figure 3 depicts the proposed design of the RF fingers with typical overall dimensions. RF fingers are made as a single-piece spool (Fig. 3(a)) from a stock of CuCrZr or Glidcop (AL-15) alloys. These alloys are chosen in place of a more commonly used alloy, BeCu, because of their higher electrical and thermal conductivities (Table 1). Glidcop RF fingers are in use at PEP-II [5], APS and NSLS-II, and CuCrZr RF fingers have been proposed for the ITER project [6].
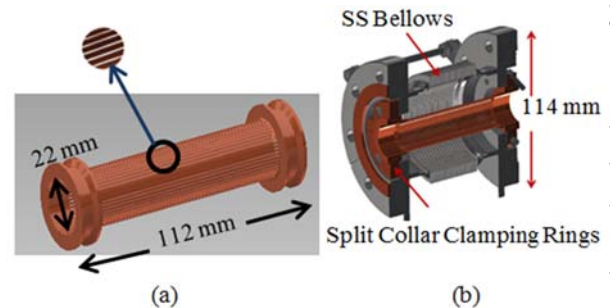

Figure 3 : Proposed RF finger design, (a) single-pièce RF finger spool, (b) assembly inside SS bellows using split collar clamping rings.

INSTALLATION AND ALIGNMENT OF SESAME STORAGE RING

T. Abu-Hanieh, SESAME, P. O. Box 7, Allan 19252, Jordan

Abstract

SESAME (Synchrotron-light for Experimental Science and Applications in the Middle East) is the first international 3rd generation synchrotron light source in the Middle East region. This paper presents the method used for installing the Storage ring girders, magnets, vacuum chambers, straight sections, and how the alignment was done. The Installation have been done in a short time with few staff. It was hard and difficult but went great.

A substantial progress has been made in the design, construction and installation of the SESAME Mechanical Systems. All Storage Ring accelerator systems are ready and commissioned.

INTRODUCTION

SESAME was officially opened in Allan (Jordan) on 16 May 2017. It is the Middle East's first major international research centre [1]. It is a cooperative venture by scientists and governments of the region set up on the model of CERN although it has very different scientific aims. Figure 1 shows SESAME building at Allan, Jordan, almost 35km northwest of Amman, and Fig. 2 shows SESAME machine components.

Figure 1: The SESAME building.

Figure 2: The SESAME machine.

STORAGE RING STRUCTURE

The storage ring is composed from 16 cells connected with straight sections, as shown in Fig. 3.

Figure 3: SESAME Storage Ring.
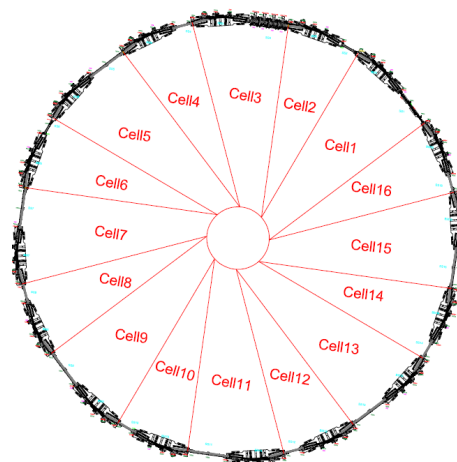
Girder length = 5.2m, Flatness error < ± 50 µm, Magnet position error < ± 50 µm. Girder-to-girder position error < ± 100 µm, Girder deflection under load < 50 µm.

Figure 4 shows the magnets of the main ring after installation; with a list of all parts of the main ring. Table 1 shows the parameters of SESAME storage ring.

Figure 4: Magnets of main ring.

Table 1: Storage Ring Parameters

Parameter	Unit	Value
Energy	GeV	2.5
Circumference	m	133.2
Electron beam current	mA	100 - 400

COLLIMATOR FOR ESRF-EBS

J. Borrel[*], Y. Dabin, F. Ewald, P. Van Vaerenbergh, ESRF, Grenoble, France

Abstract

The function of the Collimator is to localize the majority of the electron losses in the ESRF-EBS storage ring (SR). In addition, the Collimator of the ESRF-EBS should absorb about 1200 W of synchrotron radiation. For ESRF-EBS, the electron losses due to intra bunch scattering (Touschek scattering) will be higher than in the current ESRF SR. To limit the level of radiation outside the storage ring, and the activation level of the vacuum chambers, it is more efficient to localize the electron losses and block the radiations at one place rather than reinforce all of the SR tunnel shielding. Once the collimator is put on line with the electron beam at nominal intensity, it will no longer be possible to intervene on it (due to the activation of the materials). As a consequence, a high level of reliability is required.

The design takes into account all the diverse requirements from a safety, accelerator physics, thermal and mechanical point of view.

INTRODUCTION

The ESRF-EBS storage ring is very different with the previous one. Electron losses from intra bunch beam scattering is higher. This is the raison to introduce a Collimator to localize the majority of electron losses in two places, surrounded by a heavy concrete block.
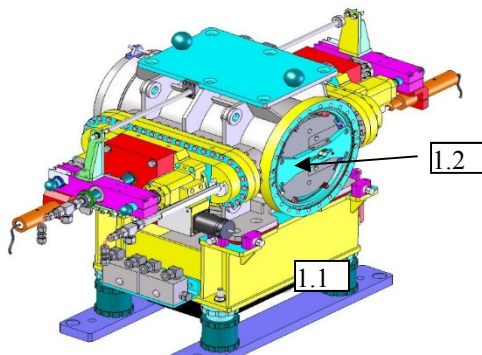

Figure 1: Collimator General assembly.

DESCRIPTION

As shown in Figures 1 to 3, the ESRF-EBS Collimator is composed of: the vacuum chamber and its support (1.1), the inner fixed shielding (1.2), fixed blades (2.1) and movable blades (2.2), its motorization (3.1) and the guiding system (3.2). In addition, concrete fixed shielding (Fig. 10) is placed around the collimator to absorb radiations outside

_____
* Email address: borrel@esrf.fr

the collimator vacuum chamber. This paper will only describe the Collimator itself (Fig. 1). The ESRF-EBS Collimator is designed to have a 300 mm active length with a 15 mm fixed aperture in the vertical and 12 mm (+/-2 mm) adjustable aperture in the horizontal plane. The maximal horizontal opening is 32 mm.

At the entrance and at the exit of the Collimator there are "RF fingers" (Fig. 4.1). Their specific shape makes the transition between the omega internal shapes of the ESRF-EBS high profile chamber and the square shape of the Collimator inner section (Fig. 2).
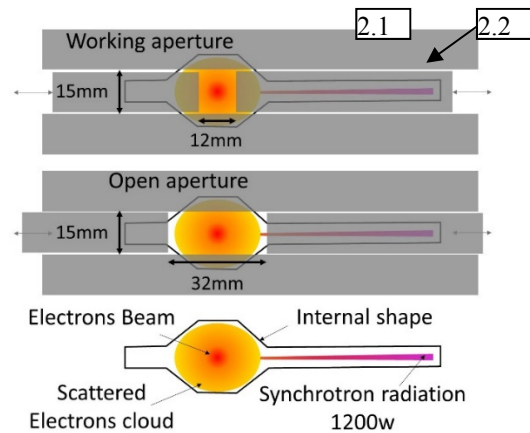

Figure 2: section of the collimator blades in two positions: the working position and fully open.
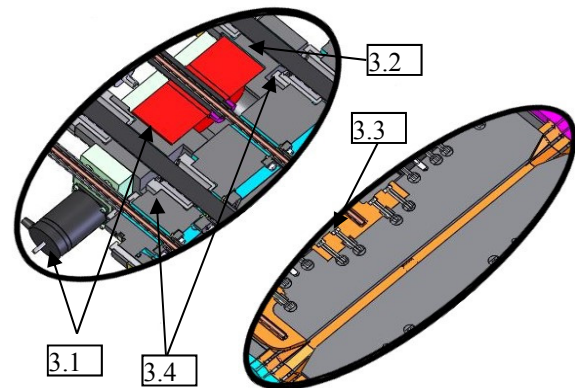
Figure 3: Details of internal view in horizontal cut.

Inside the collimator there is an absorber (Fig. 4.2) to stop the synchrotron radiation from the upstream dipoles. This absorber is made in "Glidcop Al 15©" with cooling in a concentric shape.

In order to adapt the shape of the horizontal blades as smoothly as possible, there is a 30mm taper at each end of the horizontal blades.

In addition to the blades (fixed and movable), there is a fixed shielding (Fig. 8) in the vacuum chamber to block the radiation from the scattering of the electrons absorbed by the Inermet IT180 blades.

U15 DESIGN AND CONSTRUCTION PROGRESS

F. Briquez, C. Arrachart, N. Baron, N. Béchu, P. Berteaud, F. Blache, C. Bourgoin, M.-E. Couprie,
J. Da Silva Castro, C. De Oliveira, J.-M. Dubuisson, J.-P. Duval, C. Herbeaux, F. Lepage,
A. Lestrade, F. Marteau, A. Mary, F. Michel, S. Morand, M.-H. Nguyen, A. Rouquié, M. Sebdaoui,
G. Sharma, K. Tavakoli, M. Tilmont, M. Valléau, M. Vandenberghe, J. Vétéran,
Synchrotron SOLEIL, Gif-sur-Yvette, France.

Abstract

A 15 mm period PrFeB Cryogenic Permanent Magnet Undulator (CPMU) is under construction at SOLEIL, relying on the experience gained from the two PrFeB CPMU already installed at SOLEIL [1, 2]. The improved design includes a magnetic length of 3 m and a minimum gap of 3 mm, leading to a polyvalent device of interest for both synchrotron radiation sources and free electron lasers. A dedicated magnetic measurement bench is also under development to perform measurements at cryogenic temperature, based on the SAFALI system. The designs of both undulator and measurement bench will be explained, the construction progress will be detailed and first results will be given.

INTRODUCTION

The SOLEIL synchrotron light source has been in operation since 2006. 27 insertion devices are installed, including 4 electromagnetic undulators [3, 4], 12 APPLE-II ones [5], 8 in-vacuum ones [6], 2 wigglers [7, 8] and one EMPHU-type device [9]. Two of the in-vacuum devices are cryogenic U18 undulators and a third device of the same type was built and installed at the COXINEL experiment [10, 11], which is part of the LUNEX5 project [12]. A fourth CPMU is under construction in the frame of a collaboration agreement with the MAX-IV laboratory. This U15 undulator is called a cryo-ready one since it can be used at both cryogenic and room temperatures, thanks to the high coercivity material used for the permanent magnets. This particularity leads to a polyvalent device of interest for both synchrotron light sources and Free Electron Lasers. A view of the whole device design is shown in Figure 1.
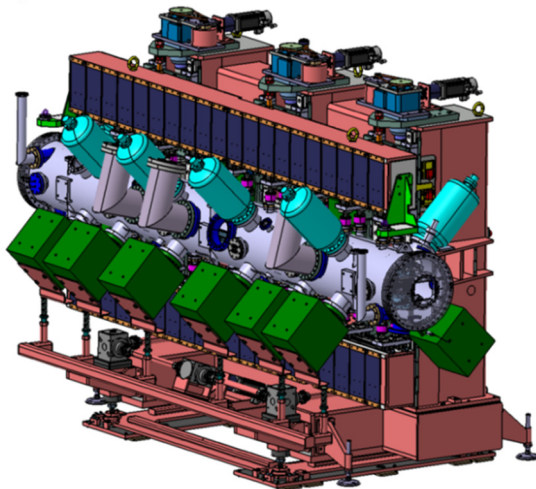

Figure 1: Design of the fully equipped U15 undulator.

MAIN PARAMETERS

The U15 design can be seen as an improvement of the SOLEIL U18 CPMU one since it is longer, has a reduced period, and can reach a smaller gap. The main parameters of both CPMU are compared in Table 1. With these characteristics, U15 has twice periods as compared to U18, leading to a higher radiated flux. By decreasing the period and increasing the peak field, one enlarges the wavelength range of the light emitted by the device.

Table 1: U15 Main Parameters Compared To U18 Ones

Parameter	U15	U18
Length (m)	3	2
Period (mm)	15	18
Min. gap (mm)	3	5.5
Max. field @77 K (T)	1.35	1.15
Nb. Periods	200	100

MAGNETIC DESIGN

The magnetic structure is a hybrid one with poles made of Vanadium Permendur and permanent magnets made of $Pr_2Fe_{14}B$ (CR53 grade). As this material does not experiment Spin Reorientation Transition phenomenon [2], it is thus possible to cool down the magnets directly at liquid nitrogen temperature with no remanent field reduction, leading to a quite simple thermal scheme [13]. The magnetic system characteristics are given in Table 2.

Table 2: U15 Permanent Magnet Properties

Parameter	Value
Remanent field @293 K (T)	1.32
Remanent field @77 K (T)	1.55
H_{cB} @293 K (kA/m)	1016
H_{cJ} @293 K (kA/m)	1906
Pole dimensions (mm)	33x26x1
Magnet dimensions (mm)	50x30x5.5

UNDULATOR MECHANICAL DESIGN

The general design is based on the usual SOLEIL CPMU concept: the jaws are made of extruded aluminium parts which are drilled all along, enabling the liquid nitrogen to flow directly in the material and obtain an efficient magnet cooling. The main element designs are very similar between the two undulators, once taken into account the higher length of the device and the stronger magnetic force between the jaws, which is expected to reach 10 t. In order to support this strength, the carriage includes 3 motorized axes rather than 2. Moreover, the design also offers the possibility to generate a 1.5 mm taper, which can be very useful, especially for FEL operation.

PROGRESS ON THE FINAL DESIGN OF THE APS-UPGRADE STORAGE RING VACUUM SYSTEM

J. Carter, B. Billett, B. Brajuskovic, M. Lale, A. McElderry, J. Noonan, M. O'Neill, K. Wakefield,
D. Walters, G. Wiemerslage, J. Zientek, Argonne National Laboratory, Lemont, IL, USA

Abstract

The final design phase is underway for the APS-Upgrade project's storage ring vacuum system. Many aspects of the design are being worked on to address challenging interfaces and to optimize vacuum system performance. Examples of recent work include updates to ray tracing and vacuum analysis, new developments in vacuum chamber and photon absorber design, and further refinement of vacuum pumping plans to achieve the best possible pressure distributions. Recent R&D work and results from a vacuum system sector mockup have also informed designs and installation plans. An overview of progress in these areas and remaining challenges is presented.

APS-U VACUUM SYSTEM REQUIREMENTS

The APS-Upgrade will retrofit the existing 1.1 km circumference APS storage ring with a new 6 GeV, 200 mA storage ring optimized for brightness above 4 keV. The scope of the APS-U storage ring vacuum system design group includes the vacuum system and component design of 40 sector arcs as shown in Figure 1 and 5x specialty 'Zone F' straight sections. The goal is to install and commission the new ring with only one year of down time for the users and to condition vacuum to 2 nTorr average pressures at 200 mA beam current by 1000 A*hrs conditioning time.
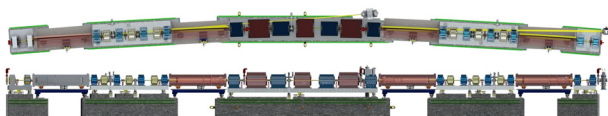

Figure 1: One 22 meter length sector of APS-U storage ring (excludes straight section).

The new storage ring design pushes magnet poles close to the electron beam and calls for narrow vacuum chambers, typically with a 22 mm inner diameter and 1 mm wall thickness. This is a substantial reduction from the previous APS design with an 84 mm wide x 42 mm tall elliptical aperture, see Figure 2 for comparison. A standard, 22 meter length arc of the vacuum system (not including straight sections) will include 27x custom vacuum chambers, 14x BPMs, 2x gate valves, 6x photon absorbers, 3x gauges, and photon extraction chambers. Of the 27x vacuum chambers, 19x will be round and NEG coated, 2x are keyhole, 2x vacuum crosses, and 4x are extruded aluminum 'L-bend' chambers. In total, 11.2 meters of the 22.1 meter length will be NEG coated.
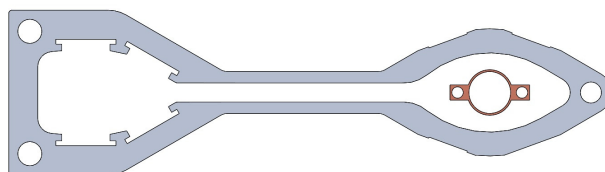

Figure 2: Cross section comparison of current APS-style vacuum chamber to new APS-U-style chamber.

INTERFACES

The APS-U vacuum systems are designed around careful interfaces with the needs of APS-U physics, magnets, and more. Vacuum components, flange seals, and absorbers must minimize impedance losses through the use of subtle transitions and reliable rf seals. The magnet's quantities, spacing, and narrow pole gaps drive thin walled vacuum chamber designs with narrow spaces to seal flanges and rout cooling water. Figure 3 demonstrates narrow installation and maintenance access between magnets to a compact BPM housing assembly. The vacuum system is also designed around numerous internal interfaces. Photon absorbers, both mounted and compact 'inline' style, are used to shadow and protect uncooled components such as BPM's, flange joints, and gate valves.

Figure 3: Narrow access between magnets to a compact BPM assembly demonstrated on a mockup.

VACUUM SYSTEM ANALYSIS

Ray tracing and vacuum analyses are performed using both 2D and 3D tools to understand and improve the limits of the vacuum system and to ensure design requirements are met. An analysis of vacuum pressures using programs like VACCALC for 2D models and MolFlow+ for 3D models helps predict the pressure profile through a hybrid pumping system. A standard arc pressure profile at 1000 A*hrs conditioning is shown in Figure 4. Pressures are typically low where distributed pumping is incorporated and

DESIGN OF A RADIATION TOLERANT, INDEXING PROFILE MONITOR FOR THE LCLS ELECTRON BEAM*

A. Cedillos†, R. Clive Field, SLAC National Accelerator Laboratory, 94025 Menlo Park, CA, USA

Abstract

The Linac Coherent Light Source (LCLS) electron beam can damage YAG:Ce scintillation screens. After one year of use, the existing profile monitor has diminished fluorescence of the screen. The decrease in performance has resulted in distorted beam images which can compromise the acquired data. Scheduling a YAG screen replacement is difficult, resulting in weeks of diminished performance. We have developed a unique profile monitor that incorporates multiple YAG screens (Ø40 mm, 50 um thick) and methods to reduce device downtime. This device uses unique geometry to direct coherent optical transition radiation (COTR) away from the optical path, which preserves the high resolution beam image. We are presenting the operational requirements, device design and installed device operational results.

INTRODUCTION

The profile monitor upstream of the electron beam dump is used to image the beam after passing through a transverse accelerating radio frequency (RF) cavity situated 30 meters upstream [1]. The LCLS electron beam, with an intensity range of 1.5-2.0 pC per pulse at 120 Hz, damages the YAG:Ce after one month of usage. Retracting the YAG screen when not in use increases the lifespan of the screen to 10-12 months but damage still occurs. Even if damage is not visible, beam tests have shown that fluorescence in a localized area is diminished which greatly compromises the useable data from the beam image. Using a green-or-ange filter and a blue light, instead of the usual UV light, this damage can be seen as a dark discoloration on the YAG screen. The shape of the damage matches the beam profile which is elongated vertically due to the upstream bend magnets (Figure 1).

One solution is to replace the YAG screen after one year of usage but this is costly and inconvenient. Replacing the YAG screen requires shutting the beam off for 8 hours which is problematic. This paper describes the key components of the updated profile monitor that improve the service interval period, serviceability and operation.
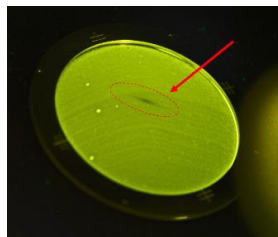

Figure 1: Photo of YAG with indicated damage.

DESIGN REQUIREMENTS

The first requirement of the upgraded profile monitor was multiple YAG screens to increase the service interval period. The second requirement was to allow immediate operation after installation to reduce user downtime. This second requirement dictates that the new device use the proven geometry which successfully directs the OTR away from the optics path. To further decrease the potential for damage, the third requirement was that the device not fail into the beam during a power failure. The fourth requirement was to have easily removable YAG scintillators and a fifth requirement was to assess damage in situ.

Motion

Having the device near the electron beam dump prohibits the use of motors with onboard electronics or optical encoders which are susceptible to radiation. We chose a guided, double-acting pneumatic actuator because it achieves the required maximum stroke of 134.6 mm with a compact design (Figure 2). The actuator is sized to overcome the combined vacuum, spring and gravity force of 250 N while providing adjustable velocities to minimize shock to the YAG screens. Since compact pneumatic actuators don't exist with four positions, a manually adjusted hard stop is used to set the YAG screen location (Figure 2). This feature makes it quick and easy to change to the next YAG screen and simplifies the control scheme to two positions.
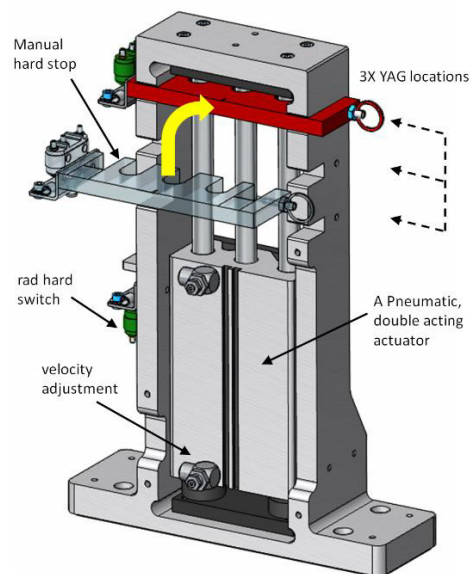

Figure 2: Actuator assembly using a 2-position pneumatic actuator to achieve 4 total positions.

ALUMINIUM AND BIMETALLIC VACUUM CHAMBERS FOR THE NEW ESRF STORAGE RING (EBS)

F. Cianciosi, P. Brumund, L. Goirand,
ESRF (European Synchrotron Radiation Facility), 38000 Grenoble, France

Abstract

The ESRF is proceeding with the design and procurement of its new, low emittance EBS storage ring (Extremely Brilliant Source project). This completely new storage ring requires a new vacuum system including UHV chambers with complex shape and strict geometrical and dimensional tolerances. Due to these complexities, it was decided to build some of the chambers in an aluminium alloy machined from bulk material; the only technology permitting to respect these challenging requirements. This project now consists of 128 chambers, 2.5m long, built in alloy 2219 with custom-built Conflat flanges made by explosion bonding. The production phase is nearly finished and the chambers that have been produced fully satisfy expectations. A second generation of experimental aluminium chambers was also designed as a substitute for some of the steel chambers in an attempt to resolve part of the geometrical difficulties. These chambers are highly complex as they contain steel-aluminium junctions in the body in order to accommodate bellows and beam position monitor buttons. The delivery of the first prototype of this type of chamber is planned for June 2018.

CHOICE OF THE TECHNOLOGY

The new storage ring requires a very complex vacuum chamber system [1]. The magnets lattice and its dimensions leave very little space for the chambers, resulting in a rather complex shape. Furthermore, the beam has a very curved path, due to the presence of 4 dipole arrays (each comprising 5 permanent magnet modules with 5 different bending radii), and 3 dipole-quadrupoles. For the chambers inside the dipoles, the only technology that can be used to produce such a difficult shape is machining from bulk material. For the other chambers, it is possible to use a construction of formed and welded sheet metal.

CHOICE OF MATERIALS

The material of the chambers shall have a very low magnetic permeability, sufficient strength at bake-out temperature (150°C), to be electrically conductive and, of course,

UHV compatible (down to pressure levels of $10^{-10} mBar$). The only affordable choice for the dipole chambers that are made of bulk material was an aluminium alloy, while for the other chambers the best option was stainless steel AISI316LN ESR, which is more resistant in thin sheets and easily weldable [2]. The decision to make some of the chambers from steel meant that the EBS cell could be designed in such a way that all the bellows and the BPMs could be located on the chambers. These components are very difficult to integrate in aluminium chambers (see Fig. 1). A careful analysis of the available weldable aluminium alloys for the dipole chambers revealed that the best material used at high temperatures during bake-out is the 2219T851 (ultimate tensile strength at 150C for 1000h: $\sigma_{UTS} = 220MPa$ [3]).

MECHANICAL DESIGN

Flanges

Two types of flanges were investigated, both based on the CF standard. The first is the aluminium type produced by *Kurt J. Lesker*. It has the advantage of being made of the same alloy as the chambers (2219 T851). However, these flanges are only compatible with pure aluminium gaskets and are sensitive to damage. The second flange type was a bimetallic flange, which is compatible with copper gaskets and is more robust, although they do present a danger of galvanic corrosion and leaks in the joint between the two materials. After a profound analysis of tender offers for the production of these flanges, the ESRF accepted the tender from *CECOM*, Italy, whose proposal consisted of custom-made bimetallic flanges machined from bimetallic sheets carefully controlled in order to avoid the risk of leaks due to bad bonding. *CECOM* assumed full responsibility for the quality of the flanges even after their installation on the chamber, thus avoiding liability issues in the event of problems between the supplier of the bimetallic material and the manufacturer of the chambers.
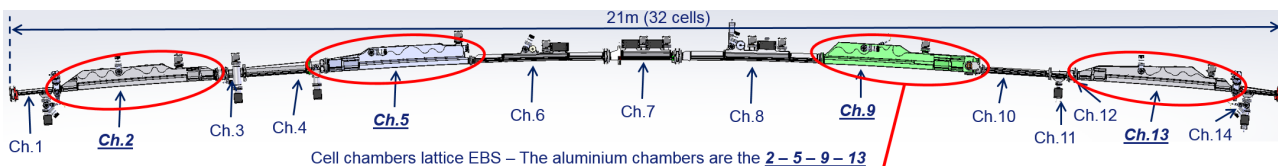

Figure 1: Vacuum chambers on one cell of EBS.

FRICTION STIR WELDING AND COPPER-CHROMIUM ZIRCONIUM: A NEW CONCEPT FOR THE DESIGN OF SIRIUS' HIGH-POWER ABSORBERS

G.V. Claudiano†, L.M. Volpe, P.T. Fonseca, E.B. Fonseca[1], M.H.S. Silva,
Brazilian Synchrotron Light Laboratory (LNLS), Brazilian Center for Research in Energy and Materials (CNPEM), 13083-970, Campinas, Sao Paulo, Brazil
[1] also at School of Mechanical Engineering, University of Campinas, 13083-860 Campinas, Sao Paulo, Brazil

Abstract

Sirius, the new Brazilian fourth-generation synchrotron light source, is currently under construction. Due to the high brilliance and low emittance of its source, the photon beam on each undulator beamline can have power densities as high as 55 W/mrad². To protect the components downstream, the Front-End power absorbers need to manage this power in a limited space, but also having precision in alignment and being reliable all over their lifetime. To achieve this behaviour, the selected alloy was the copper-chromium-zirconium (CuCrZr, commercially known as C18150) because of improved thermal and mechanical properties. In order to seal the vacuum chamber (path on which the cooling water flows), friction stir welding was the selected joining method. During the welding process, the material passes through a grain refinement process which results in a high-resistance joint. The manufacturing process could also result on a reduction of costs and lead times. Finally, it will be presented the final versions of the component with its support and the characterizations done to validate the welded joint under vacuum and water pressure requirements.

INTRODUCTION

Sirius is the new 3-GeV low-emittance high-brightness fourth-generation Brazilian synchrotron light source. As a research facility, it is going to provide resources for high-level scientific studies after its beamlines are finished. Also, as can be seen by the monochromators [1] and mirrors projects [2], new concepts and technologies are already being developed.

Regarding the undulator-beamlines FE (Front-end) power absorbers (*i.e.* fixed mask, photon shutter and high-power slits), their designs were already finished, tested and validated. Those are the components which manage the high power emitted by the storage ring, protecting the components downstream by blocking portions of the white beam. On [3], it can be found specifically the function of each power absorber along with their apertures and design criteria. Their design was based on brazing of Glidcop [4] and stainless-steel parts as described on [5].

Despite of their proven utility, their manufacture chain was highly demanding in some points, such as: human sources, time and machining services (in order to refine mechanical adjustments between parts). Those facts were the main motivation for the proposal of the system optimization done in the current study. A copper-chromium-zirconium alloy (CuCrZr, commercially known as C18150) was the chosen alloy for this application because of the following reasons: it is cheaper and available on national market, its mechanical and thermal properties are alike the Glidcop [6], and it is vacuum compatible [7] It should also be emphasized that other synchrotron facilities have already replaced Glidcop by CuCrZr alloy on their FE power absorbers [8-9].

On other hand, due to their high thermal conductivity, copper and copper alloys are difficult to weld using conventional techniques (*i.e.* techniques that involve fusion). Usually, a high heat input is necessary to melt the material and it is particularly compromising when working with precipitated-hardened alloys, such as CuCrZr [10], once strengthening nano-precipitates can be largely eliminated due to the welding thermal cycle. During welding, the previous thermal cycle usually effaces the heat treatment, and along with recrystallization, results in lower yield and ultimate strength than the aged base metal [10, 11]. Moreover, copper is susceptible to embrittlement due to oxygen dissolution into the melt pool. Furthermore, reference [12] points out that a long exposure of the CuCrZr alloy to high temperatures could cause over aging and recrystallization. Thus, it is necessary not only to limit the temperatures durring manufacturing of the component, but also during its operation in the beamline. It was defined as a constraint because of a proposal to do the flange manufacturing on the CuCrZr workpiece itself as a manner to reduce the number of welding spots (a reduced material strength could cause a greater deformation on the flange's knife, leading to a vacuum leakage.

Differently from conventional processes, friction stir welding (FSW) is a solid-state joining technique capable of overcoming the problems related to welding of copper [13]. FSW consists of a rotating non-consumable tool, which is inserted in the material and translates along the weld path to create a joint. The tool generates heat from friction and deformation. Since maximum temperatures lay

---

† gabriel.claudiano@lnls.br

INTERFACES WITH OPERATIONAL SYSTEMS
APS UPGRADE REMOVAL AND INSTALLATION*

R. Connatser, Argonne National Laboratory, Argonne, IL, USA

Abstract

A critical time for the Advanced Photon Source Up-grade (APS-U) Project is the twelve month dark period in which the current accelerator, front ends, and insertion devices will be removed and the new MBA will be installed. In addition to the technical interfaces, there are a number of operational support systems and utilities that will be affected. For the dark period to be a success, all of these interfaces need to be described and their interaction with the removal and installation processes defined. This poster describes some of these systems and their interfaces.

ASSEMBLY, REMOVAL, AND INSTALLATION

The APS-U project will have an extended pre-installation phase where the 200 magnet modules will be assembled and tested prior to being placed in storage. The dark period will be kicked off with an extensive Lock Out Tag Out procedure prior to the removal of the current accelerator. The current plan calls for installation of all tray, cabling, fibers, and any other modifications to the tunnel to be complete prior to installation of the new magnet modules. Once installed, all necessary connections will be made up and testing without beam can commence.

Access Control Interlock System

The Access Control Interlock System (ACIS) of the APS consists of control systems, shutters, physical personnel gates and barriers, and associated control and sensor cabling. A block diagram is indicated in Figure 1. Entering the tunnel via various penetrations, the cabling in the tunnel runs in dedicated conduit or in shared cable trays. In order to facilitate the removal and installation work, a majority of the physical barriers and gates that are part of the ACIS will be removed at the beginning of the dark period. The sensors and interlocks that are conjoined with this equipment will need to accounted for in that period. The current plan is that the physical barriers will be reinstalled at the same locations after the installation of the new MBA.mplates are provided for recommended software and authors are advised to use them. Please consult the individual conference help pages if questions arise.
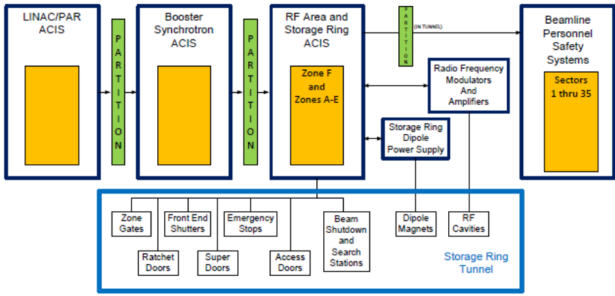
Figure 1: ACIS block diagram.

Cooling Water and Bakeout System

Cooling water for the APS storage ring is routed via two different headers and piped in parallel to the accelerator components. During the removal phase the connectors to the components will be severed after the headers are drained. The APS-U configuration has yet to be fully engineered. The current storage ring at the APS has dedicated, hot water based, bakeout systems. For the 40 storage rings sectors of the APS, there are 20 independent bakeout systems and cooling systems, located in the even sectors. The baking skid is typically located in the maintenance corridor on the inboard of the SR tunnel while the cooling skids are on the mezzanine, as shown in Figure 2. These systems are planned to be reused for the new MBA, so how they are disconnected during the removal phase, and how much work there will be during the installation to bring these systems will need to sorted out during the removal and installation planning.
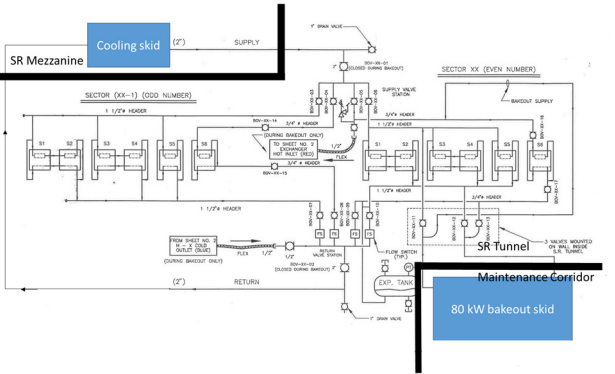

Figure 2: Water systems block diagram.

Vacuum System

The APS-U storage ring vacuum system for each sector will consist of a pair of racks with controllers located on

RETRACTABLE ABSORBER (MASK) AND WHITE BEAM IMAGER DIAGNOSTIC FOR CANTED STRAIGHT SECTION

J. Da Silva Castro, M. Labat, F. Lepage, N. Hubert, N. Jobert, A. Mary, K. Tavakoli, N. Béchu,
C. Herbeaux, Synchrotron SOLEIL, 91190 Gif-sur-Yvette, France

Abstract

At the SOLEIL synchrotron, as in other accelerators, two canted sources can coexist on the same straight section for space and economic reasons. For its two long beamlines (ANATOMIX source upstream and NANOSCOPIUM source downstream) SOLEIL has made the choice to equip one of his long straight section with two canted insertion devices capable to operate simultaneously. That implies to take into account the degradation risk management of equipment, due to radiation. As the beam power deposition from the upstream undulator can seriously degrade the downstream one, or even other equipment. To handle these risks, Soleil first designed and installed in 2016 a retractable vertical absorber between both insertions to protect the downstream source from the upstream one. In 2017, Soleil then designed and installed a white beam imager, redundant an existing photon beam monitor (XBPM), to verify the correct positioning / alignment of equipment and beams relative to each other. For the vertical absorber as for the white beam imager SOLEIL had to meet some interesting technological and manufacturing aspects that we propose to present in a poster.

INTRODUCTION

In one of the long straight sections of SOLEIL, SDL13, two canted insertion devices have been installed for X-rays delivery to the ANATOMIX (upstream) and NANO-SCOPIUM (downstream) beamlines. For the insertion devices to be operated and used simulatneously by those two independent beamlines, they were canted in the horizontal plane. But the canting angle remains small, so that the upstream ID radiation passes through the downstream ID. To prevent any damage of the downstream ID magnets from the upstream ID radiation, it was first decided to install an absorber in between the two IDs, to shadow the downstream ID magnets. But the efficiency of this mask relies on an accurate relative alignment of the upstream ID, the mask itself and the downstream ID. Those diagnostics to do the survey are mandatory. An XBPM in the beamlines front-end is in operation since 2016. But to ensure a redundancy in the measurements, it was decided in 2017 to add nearby a white imager. This paper summarizes the design of both the absorber and the white imager.

THE ABSORBER

The absorber first aim was to shadow the downstream ID magnets from the upstream ID radiation. Installed in between the two IDs, this gave a vertical aperture of 2.8 mm. Detailed studies were then carried out to define its geometry in order not to jeopardize the performance of the storage ring in terms of collective effect induced instabilities, beam losses, injection efficiency and beam time. The absorber is a piece of copper with an asymmetric 90 degree U-shape (see Figure 1). It encloses the photon beam produced upstream while the electron beam is located at -11 mm from the U-border of the absorber (see inset in Figure 1 b).

(a) Schematic

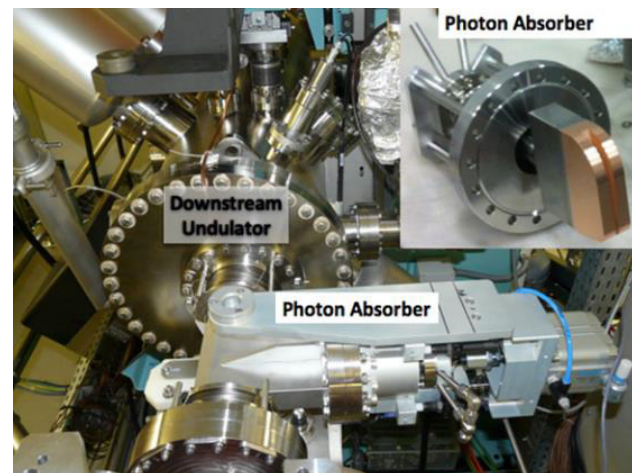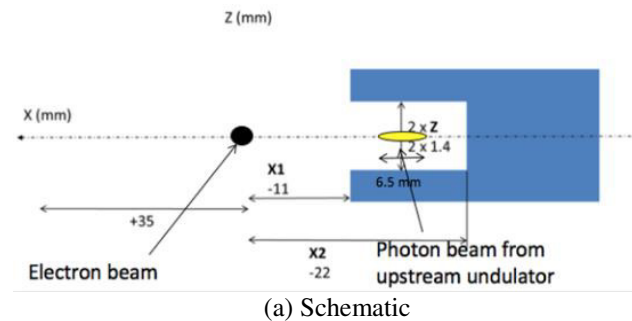(b) Pictures before (inset) and after installation
Figure 1: Schematic and pictures of the absorber.

The absorber is maintained inserted in between the IDs using a spring based system. For security reason, the stage is by default inserted. It can be retracted when needed, thanks to a remote controlled jack (see Figure 4).

MULTIPOLE INJECTION KICKER (MIK), A COOPERATIVE PROJECT SOLEIL AND MAX IV

J. Da Silva Castro, P. Alexandre, R. Ben El Fekih, S. Thoraud, Synchrotron SOLEIL, 91190 Gif-sur-Yvette, France

Abstract

The cooperative MIK project SOLEIL / MAX IV started in 2012 and is part of the Franco-Swedish scientific collaboration agreement, signed in 2009 and followed by framework agreements signed in 2011. The MIK is a particular electromagnet using theoretical principles of the 1950s and recently used by the new generation of synchrotrons to significantly improve the Top-Up injection of electrons into the storage rings. Indeed, this type of magnet can drastically reduce disturbances on stored beams and also offers substantial space savings. The MIK is a real opportunity for synchrotrons wishing to upgrade their facilities. One of the first MIK developed by BESSY II in 2010 gave significant results. These results motivated SOLEIL and MAX IV to develop together their own MIK. Many technical challenges have been overcome in the area of mechanical design and manufacture as well as in magnetic and high voltage design of the MIK. Currently the first series is in operation at MAX IV and displays already outstanding performances. Optimization work is in progress.

COMPLEMENTARY DESCRIPTION

Figure 1 shows the principles of the MIK. Figure 2 shows more technical details. The MIK is composed of a chamber in two part of synthetic monocrystalline Sapphire. Parts are assembled by diffusion bonding (Kyocera Japan). Chamber can also be made in alumina with two parts assembled by glass gluing or brazing depending on the subcontractor (Friatec or Coorstek). The chamber has to be machined with a very high precision to ensure a good magnet. 8 grooves positioning the 8 conductors (copper) are machined in the hundredth of a millimeter. The conductors formed and there insulating bars (alumina) are glued in the grooves, with specific tools designed and used by Soleil team. The connection between the chamber and the flanges is ensured by a brazed Sapphire/copper interface, then a brazed copper/ stainless steel interface and finally a stainless steel / flange weld.

A titanium coating of a few microns inside the sapphire vacuum chamber (made at ESRF) allows the flow of the image current without disturbing the magnetic field.

Shape of transversal magnetic field (By(x)) to minimise effects on Circulating electron beam on the center (S). Only electron beam to be injected (I) sees a significant magnetic field.

(I) Injected electrons beam

(S) Circulating electrons beam on storage ring

- Special Octupole with 8 copper conductor, diameter 2 mm, in series
- 13 200V
- Half-sine current pulse 7700 peak Amps
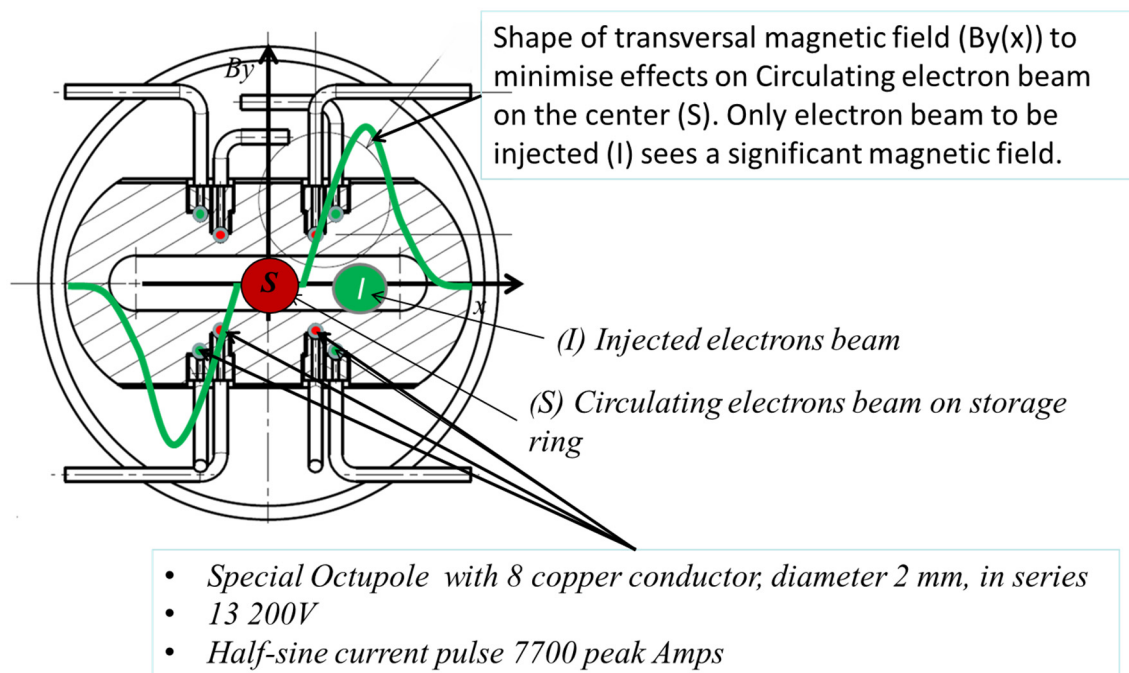
Figure 1: Cross-sectional view and principals of the MIK.

MECHANICAL DESIGN CHALLENGES BUILDING A PROTOTYPE 8-POLE CORRECTOR MAGNET

F. DePaola, R. Faussete, S. Sharma, C. Spataro
Brookhaven National Laboratory (BNL), Upton, New York, USA
A. Jain, M. Jaski, Argonne National Laboratory (ANL), Lemont, Illinois, USA

Abstract

An innovative design was developed for an 8-pole corrector magnet for the APS upgrade program. This is a combined function magnet consisting of horizontal and vertical correctors as well as a skew quadrupole. This paper describes technical challenges presented by both the magnetic design and the interface constraints for the magnet. A prototype magnet was built, and extensive testing on the magnet confirmed that all magnetic and mechanical requirements were achieved. The final design of the magnet has incorporated improvements that were identified during the manufacturing and testing of the prototype magnet.

INTRODUCTION

Multi-purpose 12-pole corrector magnets have been used in the past at several laboratories [1] but these tend to be quite large and there is not much space between the poles for mounting the coils. An 8-pole structure was developed which is more compact than a 12-pole design, yet offers a way to zero out the sextupole and decapole terms in the dipole mode and the skew octupole term in the skew quadrupole mode [2]. The magnet was designed to meet the requirements shown in Table 1.

Table 1: Design Parameters

Parameter	Value	Units
DC steering (at 6 GeV)	≥ 300	microradian
Dipole H-V field integral	≥ 0.006	T-m
Skew Quad filed integral	≥ 0.25	T
Maximum Current	15	A
Maximum required power	minimized	W
Steering at 1 kHz	> 1% or 3	microradian
Cooling method	Air cooled	
Maximum insertion length	160	mm
Maximum insertion length with feet	90-U/S, 106-D/S	mm
Minimum Aperture	26	mm
Minimum Pole tip-to-pole tip gap	10	mm
Minimum coil-to-coil gap	16	mm
Magnet center height	279.5 ± 0.25	mm
Maximum Half-width from the vertical mid-plane	270	mm

Extensive testing was performed on the prototype 8-pole corrector magnet, photo shown in (Figure 1). This testing confirmed that the magnet is capable of providing the horizontal and vertical steering and skew quadrupole strength with good field quality and meets the specifications within the given space constraints.
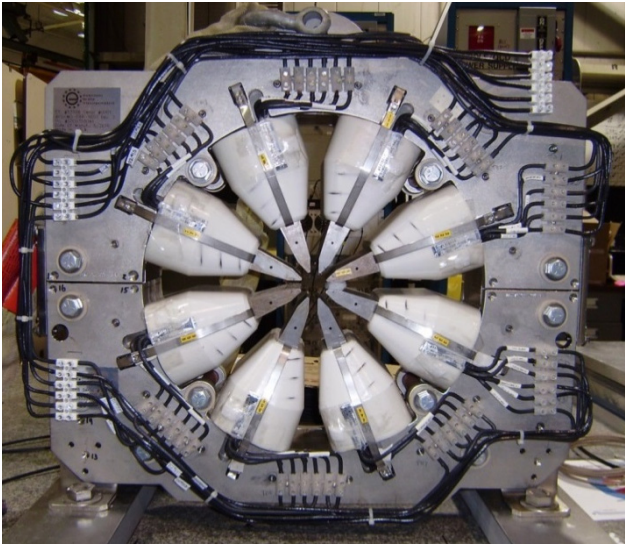
Figure 1: Prototype 8-Pole Corrector Magnet.

The magnet aperture was chosen to achieve a minimum pole-tip to pole-tip gap of 10 mm. Pole length and thickness are optimized to fit all the coils with a minimum coil-to-coil gap of 16 mm which is required at the horizontal mid-plane for the vacuum chamber extraction ports. The backleg thickness is optimized for low peak field, mechanical strength, and overall size.

COIL ASSEMBLIES

The coil pack for the 8-pole corrector magnet features three different coils on each pole, which are combined in series in a specific sequence to produce normal and skew dipole steering as well as a skew quadrupole corrector (see Figure 2).

Red
D1 Coil (1 layer)
29 turns

Blue
Skew Quad Coil
(2 layers)
28+25 = 53
total turns

Green
D2 Coil (4 layers)
22+19+16+13 = 70
total turns

All coils use 8 AWG square copper wire

Figure 2: Coil Configuration.

STATUS OF THE CONCEPTUAL DESIGN OF ALS-U*

C. Steier[†], A. Allézy, A. Anders, K. Baptiste, E. Buice, K. Chow, R. Duarte, G. Cutler, R. Donahue,
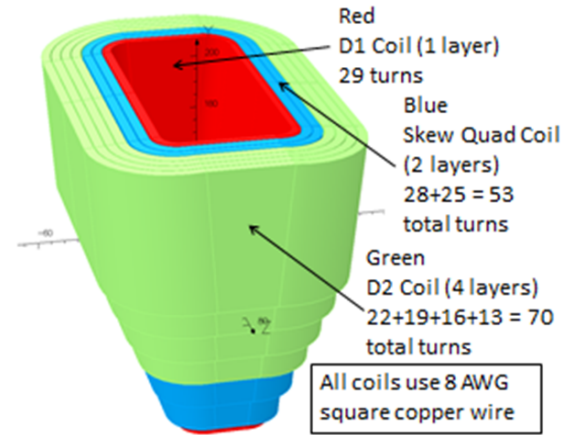D. Filippetto, J. Harkins, T. Hellert, M. Johnson, J.-Y. Jung, S. Leemann, D. Leitner, M. Leitner,
T. Luo, H. Nishimura, T. Oliver, O. Omolayo, J. Osborn, C. Pappas, S. Persichelli, M. Placidi,
G. Portmann, S. Reyes, D. Robin, F. Sannibale, S. De Santis, C. Sun, C. Swenson, M. Venturini,
S. Virostek, W. Waldron, E. Wallén, LBNL, Berkeley, CA 94720, USA

Abstract

The ALS-U conceptual design promises to deliver diffraction limited performance in the soft x-ray range by lowering the horizontal emittance to about 70 pm rad resulting in two orders of brightness increase for soft x-rays compared to the current ALS. The design utilizes a nine bend achromat lattice, with reverse bending magnets and on-axis swap-out injection utilizing an accumulator ring. This paper shows some aspects of the completed conceptual design of the accelerator, as well as some results of the R&D program that has been ongoing for the last years.

INTRODUCTION

To achieve diffraction-limited performance for soft x-rays, ALS-U uses a nine bend achromat lattice with on-axis swap out injection. The improvement in coherent flux will be achieved by a big reduction of the emittance as well as smaller horizontal beta functions and insertion devices with smaller gaps (vertically and horizontally). This requires to replace the existing triple bend achromat lattice with a multi bend Achromat (MBA) lattice [1, 2]. The design produces round beams of 70 pm rad emittance, about 30 times smaller than the horizontal emittance of the existing ALS. ALS-U received approval of Mission Need (CD-0) from DOE/BES in September 2016 and the conceptual design was finished in spring 2018 and has been reviewed by a series of nine external technical reviews. Table 1 summarizes the main accelerator parameters and Figure 1 shows the nine bend achromat including the magnet supports based on plinths and rafts.
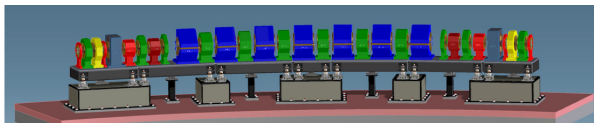

Figure 1: CAD model of ALS-U showing one of the twelve sectors of the nine bend achromat lattice as well as the support system based on plinths and rafts.

Because ALS-U is a low energy machine (with strong intrabeam scattering), it requires design solutions different from those of hard x-ray projects. Therefore an R&D program was started in early FY14 with the goal of reducing the

Table 1: Parameter List Comparing ALS with ALS-U

Parameter	Current ALS	ALS-U
Electron energy	1.9 GeV	2.0 GeV
Beam current	500 mA	500 mA
Hor. emittance	2000 pm rad	70 pm rad
Vert. emittance	30 pm rad	70 pm rad
rms beam size (IDs)	251 / 9 µm	≤14 / ≤14 µm
rms beam size (bends)	40 / 7 µm	≤7 / ≤10 µm
Energy spread	0.97×10^{-3}	1.04×10^{-3}
Bunch length	60–70 ps	120–140 ps
(FWHM)	(harm. cavity)	(harm. cavity)
Circumference	196.8 m	~196.5 m
Bend magnets per arc	3	9

technical risks. The main areas studied were swap-out injection, harmonic cavities with large lengthening factors [3, 4], vacuum design/NEG coating, and high gradient magnets. Substantial progress has been made in all areas and an improvement in brightness by two orders of magnitude at 1 keV is achievable (see Figure 2).
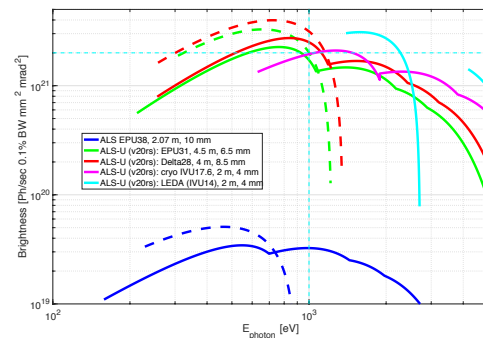
Figure 2: Soft x-ray brightness of planned new insertion devices on ALS-U compared to th existing ALS showing 2 orders of magnitude improvement at 1 keV.

LATTICE

During the conceptual design phase, a defined process was used to improve the lattice and, once a significant improvement was achieved, to update the baseline lattice, after evaluating the impact on the design of the individual technical systems. The work first focused on making the lattice more robust to errors, and to improve the lifetime. Later on, 5 T Superbends were included to maintain the ALS hard

FRICTION STIR WELDING ATTEMPTS FOR UHV APPLICATIONS: STAINLESS STEEL/ALUMINUM

A. Ermakov[†], C. Martens, U. Naujoks, DESY, Hamburg, Germany

Abstract

At DESY in Hamburg an investigation was started to join aluminium chambers with stainless steel flanges by friction stir welding. First results will be presented.

It will be shown that there is only a small effect of hardening in the contact zone at the stainless-steel side, a small amount of particles are given and the diffusion zone is about 3 microns, but with a very irregular effect on the structured junction.

Because of that, the influence of the surface and the welding parameters on the process will be investigated in the future.

OBJECTS FOR WELDING

The choice between different materials in UHV applications becomes more and more important. An investigation was started to combine aluminium chambers with standard UHV-flanges from stainless steel. Friction stir welding attempt was implied on standard UHV-flange type of NW100 (316LN) with Al insert (AN EW 6082 T6) as blind flanges for UHV usage. An industrial enterprise welded a series of flanges with different welding parameters (part of flange presented on Fig. 1). The samples #1, 2 taken from two welded flanges were investigated by means of hardness (Vickers, HV1), X-Ray fluorescence (Al is not visible due to technical limitations) and SEM/EDX element analysis measurements.
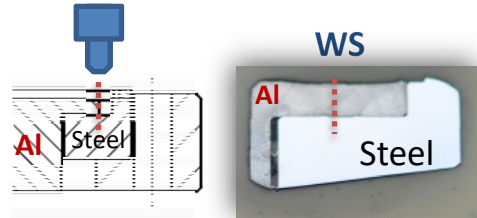

Figure 1: Part of flange with Al-insert. Position of welding seam.

HARDNESS

On Fig. 2 shown the results of hardness measurements in welding seam HAZ/TMAZ areas of sample #1. The hardness values in Aluminium part along the joint interface in WS area has in average 61.5HV1.

In both HAZ/TMAZ in measured region the Al alloy material is ca. 10% harder as in welding seam. The initial hardness of Al alloy is about 90HV so the softening of Al alloy close to welding seam area is obviously due to the temperature rise by welding. The distribution of hardness values in stainless steel shows the hardening of material in welding seam area close to joint interface. Due to relative lower thermal conductivity of stainless steel the hardness values are normalized in distance of about 1mm away to the hardness of stainless steel of ca. 160HV1. Similar variation of hardness of welding partners observed in articles [1-3]. It is reasonable to assume that hardening of material can be caused by at least 3 factors: one of them is deformation or pressure from the welding tool coming from Al side, temperature influence or the building of associated phases.
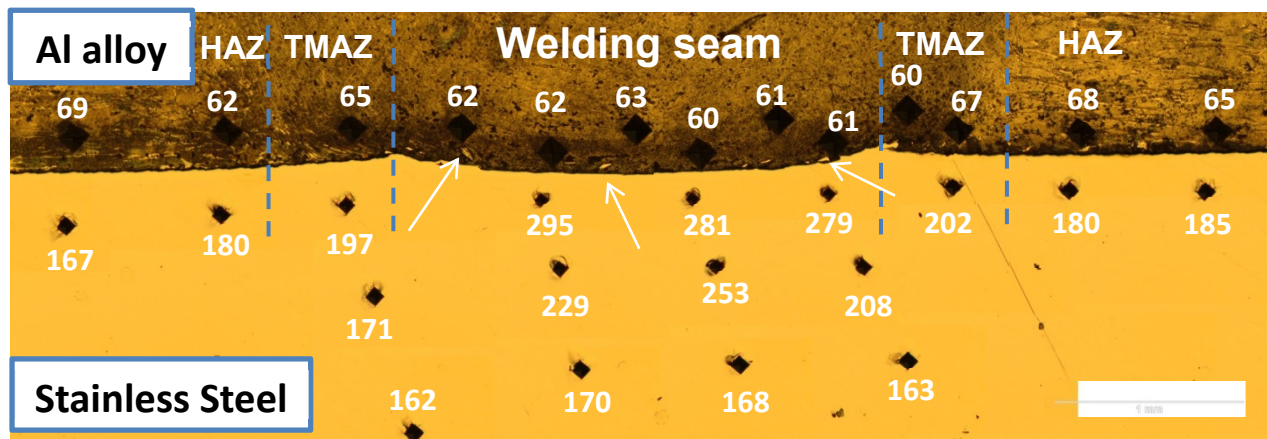

Figure 2: Distribution of HV hardness values measured along welding seam area and TMAZ/HAZ areas. Arrows show the small particles of stainless steel fraction mixed by welding with Al alloy.

---

† alexey.ermakov@desy.de

HAMMERHEAD SUPPORT DESIGN AND APPLICATION AT SSRF*

F. Gao, R.B.Deng ,S.W.Xiang, Z.Q.Jiang, L.X.Yin
Shanghai Institute of Applied Physics,CAS, 201204 Shanghai, China
S.Sharma, NSLS-II, Brookhaven National Laboratory, NY, USA

Abstract

Electron beam stability is very important for Shanghai Synchrotron Radiation Facility (SSRF). One of the major players on beam stability is the vibration stability of magnet support systems. This paper describes several kinds of hammerhead magnet support prototypes with different structures, materials and ground fixation. Modal and response analyses of these prototypes are contrasted by finite-element analysis (FEA) and tests. The design can be applied to guide and improve the mechanical structures and the stability of magnet support systems at SSRF and other light source facilities.

INTRODUCTION

The Shanghai Synchrotron Radiation Facility (SSRF) is a third-generation light source, which requires high electron beam stability [1-2]. The electron beam stability is one of the most import elements that influence the properties of light sources. SSRF locates near the Huangpu River which flows to the east sea from west to east of Shanghai, which makes the soil soft. What makes things worse is the heavy traffic day and night and the nearby magnetic levitation. So the fact is that the ground vibrations at SSRF are larger than at other light sources due to altogether these factors [3].

The important demands of electron beam stability result in the high mechanical stability requirement for the light sources key parts such as quadruple magnets. Since the mechanical support system for the magnets provides supporting, location and position adjustment, the high mechanical stability of the support is indirectly expected. The first eigenfrequency is an important index for the stability and performance of girders, based on the condition of SSRF, which motivates us to take measures to improve the stability of mechanical support system for magnets.

Marble bases produced from Shandong Province of China have been used as the main component of the support for quadruple in Shanghai Soft X-ray FEL (SXFEL) infrastructure [4]. S. Sharma proposed a girder-free support system. The system took account of several main aspects such as mechanical stability and thermal stability [5]. Based on these references, we developed several kinds of girder prototype for magnets at SSRF.

This paper describes an attempt to understand and increase the first eigenfrequency of different kinds of hammerhead support with different structures, materials and

ground fixation to improve the stability. Modal hammering experiments and the Finite-element (FE) analysis of prototypes were carried out at SSRF. The results are discussed in this paper.

STRUCTURE OF PROTOTYPES DESIGN

Figure 1 shows the mechanical structure of hammerhead support design for magnets. Figure 2 shows the size of one support. Two hammerhead supports are connected with two C-channel beams. The beams bolted to hammerhead supports are 2.9m in length and 0.4m in height, welded by steel plates. Magnets are assembled accurately on the top of supports with required good alignment techniques. Eight wheels fixed on both sides of the hammerhead supports can make the heavy support system move easier in the tunnel in the future. One prototype is about 2m long, with two quadrupoles and two sextupoles. Different materials and fixation methods between supports and floor are used for the design of prototypes.
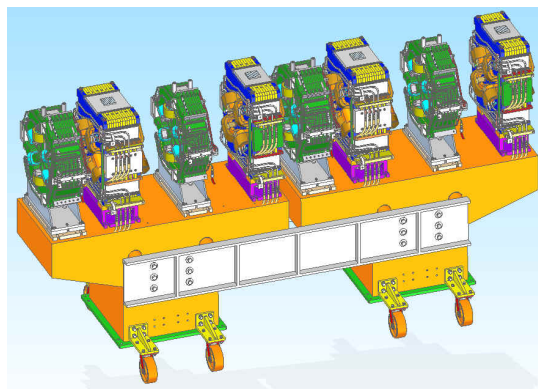

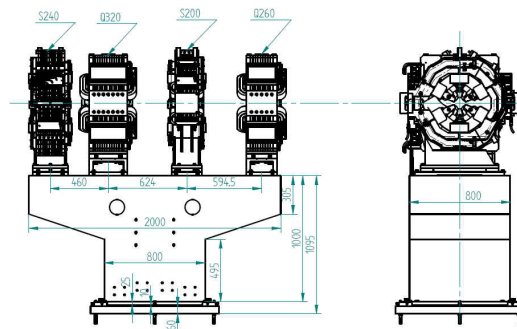Figure 1: Structure of the hammerhead support system.

Figure 2: Size of the hammerhead support.

DESIGN CONSIDERATIONS ASSOCIATED WITH THE REPLACEMENT OF A SEXTUPOLE MAGNET BY A SHORT WIGGLER IN A CELL OF THE DIAMOND STORAGE RING LATTICE

N. P. Hammond, I. P .S. Martin, Diamond Light Source, Oxfordshire, UK

Abstract

All of the original straight sections in the Diamond storage ring are now occupied, and novel ways of converting bending magnet beamline locations into insertion device beamlines are being considered. Recently one cell of the 24 cells was reconfigured in to a Double-Double Bend Achromat (DDBA) to provide a new location for an Undulator and enable a formerly designated bending magnet beamline to become an Insertion Device Beamline [1]. Extending this concept for the new Dual Imaging and Diffraction (DIAD) Beamline proved to have a strong impact on lifetime and injection efficiency, so instead a proposal was made to remove a Sextupole magnet in the corresponding storage ring cell and substitute it with a short fixed gap Wiggler. The accelerator physics, mechanical and electrical design aspects associated with the change are described.

INTRODUCTION

One of the proposals emerging from the initial studies into a suitable cell configuration for an upgraded Diamond Storage Ring was a modified 4-bend achromat [1], referred to as DDBA. This had the additional benefit of providing a new achromat mid-straight for locating an Insertion Device (ID), which could replace the original bending magnet as a beamline source. Although initially developed as an upgrade for the whole storage ring it was decided to trial it in one cell to provide a new ID source for the VMX beamline. A number of factors described below prevent this solution from being deployed in a second location to provide an ID for the DIAD Beamline.

A SECOND DDBA CELL?

Although the ability of the Storage Ring to function under all operating conditions has been proved for a single DDBA cell [2], detailed studies (unpublished) have indicated that adding cells, reconfigured to a DDBA, reduces the dynamic and momentum apertures; and hence injection efficiency and lifetime to an unacceptable extent, refer to Figs. 1 and 2.

Additionally, modifying a cell to a DDBA configuration requires a complete new suit of reduced aperture magnets and vacuum vessels. Combined with re-cabling, the capital expenditure required is considerable, in the region of £2.6M excluding the cost of the new Insertion Device.

Limiting the shutdown for DDBA installation time to a maximum of eight weeks required an extensive programme of cabling up to two years in advance of the girder exchange. A set of temporary cables replicating the existing ones was installed. The existing cell was then reconnected to the temporary cables, once this was completed the existing cables could be removed and replaced by the new DDBA cables. This way when the new girder assemblies were installed they could readily be connected to the pre-terminated cables [1]
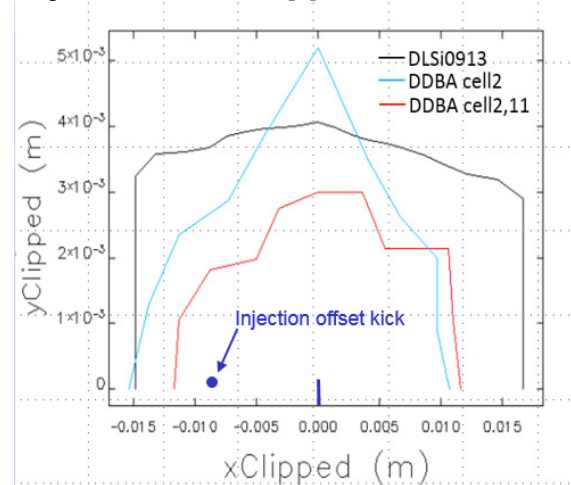
Figure 1: Reducing Dynamic Aperture for successive DDBA cell reconfigurations
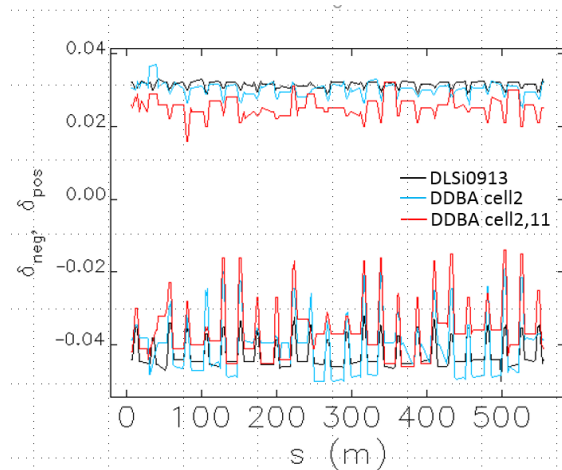
Figure 2: Reducing Momentum Aperture for successive DDBA cell reconfigurations.

The reduced machine performance combined with the associated costs of procurement, preparation, and installation have made an alternative configuration an attractive proposition.

An alternative reconfiguration was proposed whereby the first sextupole magnet upstream of the second dipole in the standard DBA configuration was replaced by a short 10 pole fixed gap Wiggler.

VACUUM PERFORMANCE TEST OF CuCrZr PHOTON ABSORBERS

Q. Li[†], P. He, D. Z. Guo, B. Q. Liu, Y. S. Ma, T. Z. Qi, X. J. Wang,
Institute of High Energy Physics Chinese Academy of Sciences, Beijing, China
P. Manini, SAES Getters S.p.A., Lainate, Italy

Abstract

To test the pumping performance of NEG coated CuCrZr absorber, we performed a comparative experiment on the two absorbers, one with NGE coating and the other one without coating. First, we run the Monte Carlo simulation by using MolFlow+ code to estimate the pressure inside test chamber at different thermal outgassing rate. And then two absorbers are mounted inside the chamber for the pressure vs. time profiles testing. The experimental set-up and pressure profiles will be presented here.

INTRODUCTION

We have developed two absorbers made of CuCrZr materials. The CuCrZr alloy is the right material for handing high heat load of synchrotron radiation. It has high yield and tensile strength, it has much lower cost than GlidCop, also it can be easily welded with stainless-steel (no brazing process) and also UHV compatibility. The two absorbers were similar in structure and the vacuum sealing flange was integrated with the absorber without any brazed or welded junctions. The 1st absorbers are similar to the ALBA absorber structure [1] and parts of the surface have NGE coating as shown in Fig. 1. The other one refers to the ESRF EBS [2] absorber structure but has no NEG coating on its surface, see Fig. 2. These two absorbers were made up by SAES RIAL and 1st one NEG coated by SAES Getters.

This experiment is to measure the pump-down curves of two absorbers and to see whether the NEG coating on the absorber has pumping effect. In the following sections, we will show the experimental set-up and present the measurement results.
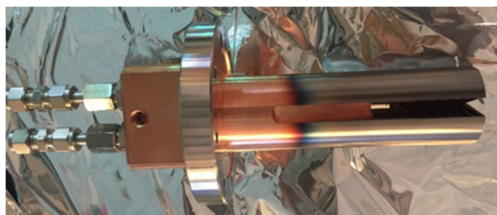
Figure 1: 1st absorber with NEG coating.

Figure 2: 2nd absorber without NEG coating.

---

† liqi@ihep.ac.cn

MONTE CARLO SIMULATION

In order to choose the structure of a reasonable experimental system, we performed a simulation calculation using the Monte Carlo simulation code MolFlow+ which was developed at CERN [3].

We designed two types of experimental systems. One was to connect the vacuum chamber directly with a 150 L ion pump. The other was to add a 10mm diameter orifice conductance to the ion pump port. The simulation model is shown in Fig. 3. The simulated pressure results at different thermal outgassing rates are shown in Table 1.
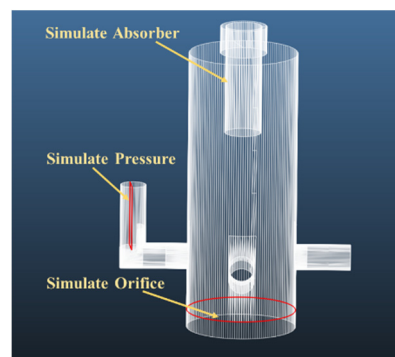
Figure 3: Simulation model.

Based on the simulation results, we set up the experimental chamber with small orifice conductance, so as to the pressure difference between the two absorbers can be more clearly displayed.

EXPERIMENTAL PROCEDURE

NEG coating can be activated after 24 hours baking at temperatures above 180°C. Before NEG coating activation, we need to bake the vacuum chamber to desorb the adhering gas on the inner surface. We developed our own activation curve with reference to the programs of SAES [4] and SOLEIL [5] and combined with the actual conditions of our baking, see Fig. 4.

Bake out operation procedure:

- Assemble the vacuum system including one of two absorbers and flanges.
- Put on the heating equipment (thermocouples and heating tapes) in three parts (absorber and vacuum chamber up and down).
- Start pump-down by primary pump and TMP.
- Switch on Helium Mass Spectrometer Leak Detector to perform leak detection.
- Keeping TMP pumping.

A MECHANICAL UNDULATOR FRAME TO MINIMIZE INTRINSIC PHASE ERRORS

Jui-Che Huang[†], Chih-Sheng Yang, Ching-Kang Yang, Cheng-Hsing Chang, Ching-Shiang Hwang,
National Synchrotron Radiation Research Center, Hsinchu, Taiwan
H. Kitamura, RIKEN / SPring-8, 1-1-1 Kouto, Mikazuki-cho, Sayo-gun, Hyogo, Japan
S. Mizumoto, T. Kohda, NEOMAX ENGINEERING Co., Ltd , Suita-shi, Osaka, Japan

Abstract

A PrFeB-based cryogenic permanent magnet undulator (CPMU) is under construction at the Taiwan Photon Source (TPS) to generate brilliant X-rays. When magnets are cooled to 77 K, a CPMU with a period length of 15 mm can generate an effective magnetic field of 1.32 T in a gap of 4 mm. A main feature of the TPS CPMU is its low-intrinsic-phase errors by the installation of force-compensation modules on the out-of-vacuum girders in a four-support-points configuration. Moreover, adjusting the spring settings one can obtain very low undulator phase errors. In this paper, a mechanical frame design for the TPS-CPMU with force-compensating spring modules will be discussed. Observations of deformation effects of the out-of-vacuum girders on the CPMU will be presented.

INTRODUCTION

Together with a high strength parameter, low phase errors are required characteristics an undulator to allow the generation of higher harmonics without significant degradation of SR brilliance and are therefore an important consideration to evaluate the undulator magnetic field quality. The X-ray brilliance degradation (I/I_0) due to RMS phase errors scales like $I/I_0 = \exp[-(n\sigma_{PE})^2]$ [1], where n is the undulator harmonic order and σ_{PE} the RMS phase error. The phase error derives from magnetic field errors, which can result from (1) differences of individual magnet blocks, such as remnant field and height of the magnet, (2) gap errors from manufacturing tolerances, such as the flatness of the in-vacuum girder, the length of link rods and assembly accuracy of the mechanical frame, (3) gap errors caused by mechanical deformations and (4) thermal effects in magnet arrays. During the construction of a TPS-CPMU, individual differences of magnet blocks can be greatly eliminated by magnet sorting. Gap errors from manufacturing tolerances can be corrected by adjusting gaps locally. These two error sources are of a static nature and careful corrections can be made to minimize phase errors. The gap errors caused by mechanical deformations are gap-dependent, since the magnetic forces increase exponentially with decreasing undulator gap. A counter force system, especially at small gaps, becomes necessary to retain low intrinsic RMS phase errors. Thermal effect in the magnet arrays can be corrected by temperature control systems, which however will not be discussed in this note.

---

† email address : huang.juiche@nsrrc.org.tw

MECHANICAL FRAME WITH FORCE-COMPENSATING SPRING MODULS

The magnetic force in the CU15 reaches up to 32 kN at a gap of 4 mm and 77 K, so a conventional two-support configuration is no longer rigid enough to keep the net RMS phase errors small. Yet, an optimized four-support configuration can reduce the intrinsic rms phase errors to less than 0.5 degrees [2]. Moreover, strong magnetic forces not only cause gap errors but also the deformation of the mechanical frame and heavy load to the gap drive system. Based on these considerations, the design goal of a counter force system in a four-support configuration of the mechanical frame is not only to compensate the magnetic force but also to obtain a mostly stress-free mechanical frame. Therefore, a force-compensation spring module in a compact and moment-free design is introduced and installed on four support-points of the mechanical frame (Fig. 1). The spring module is an invention of Hitachi Metals Co. Ltd. and international patents are pending. Attractive characteristics of the force-compensating spring modules are, (1) that the system is set-up in-air, so the adjustment of springs is easy, (2) machined -springs results in good reproducibility, (3) the low weight and compact design allows easy removal of the spring module during maintenance and assembly of vacuum components and (4) effective compensation of strong magnet forces without undesirable side effects. The spring module is installed between upper and lower out-of-vacuum girder and can compensate the attractive magnetic forces by repulsive spring forces. The rotational moments of the upper and the lower girders act in opposite directions as shown in Fig. 1b. The linear guides have sufficient stiffness to allow the changes of the magnetic gap while absorbing the rotational moments since, there is no mechanical connection between spring module and the pillars of the mechanical frame. The deformed spring module can keep the mechanical frame mostly stress-free with only a small deformation.

Figure 2 illustrates the deformation of the mechanical frame with and without spring modules by a finite element analysis. With the spring module, the transverse pillar tilt becomes small and the deformation of the out-of-vacuum girder due to magnetic forces can be reduced from 2.1 um to 0.12 um for a force of 32 kN (Fig. 3). Including the in-vacuum-girder deformation, the intrinsic phase errors are estimated to be less than 1 degrees. The spring module will deform and compensate the magnetic force, so the stress and deformation of the out-of-vacuum girders and pillars are reduced.

DESIGN OF VERTICAL AND HORIZONTAL LINEAR FLEXURE STAGE FOR BEAM SIZE MONITOR SYSTEM

W.Y. Lai, S.Y. Perng, H.S. Wang, C.J. Lin, D. G. Huang,
H.C. Ho, K.H. Hsu, T.C. Tseng, C. K. Kuan
National Synchrotron Radiation Research Center, No 101, Hsin-Ann Road, Hsinchu 30076, Taiwan

Abstract

Taiwan photon source is a third-generation accelerator with low emittance and high brightness. The electric beam size is one of important parameters to indicate the stability and to measure the emittance and coupling of light source. The aperture size of beam slitter is a crucial part to calculate the value of beam size in the X-ray pine-hole system. In order to obtain the more precise result of beam size, the flexure mechanism on beam slitter is applied for the adjustment of the aperture. This paper shows that the design concept and the measurement of the beam size are obtained by the new adjustment system.

INTRODUCTION

The Taiwan Light Source (TPS) is a 3-GeV synchrotron radiation light facility. The construction started on February 2010 and after five years of construction and hardware developments, commissioning of the beam began on December 2014, and the 8 insertion devices were installed from April 2015 to now for user of beam line. Now the beam current of TPS storage ring can be up to 400mA for beam line used. TPS is a third-generation accelerator with the characters of low emittance and low coupling. Those beam parameters are routinely measured by the synchrotron radiation light produced from a dipole magnet, and the emittance can be measured indirectly by obtaining the transverse beam size. There is a dedicated beamline for photon diagnostics at the TPS storage ring utilized visible light and X-ray of the synchrotron radiation [1].

The structure of X-ray pine hole was oxidized seriously by the ozone resulted from reaction of ultraviolet in air after serval years. It made the measurement of beam size to be instable and unreliable, because of that there was some fluff on the aperture of X-ray pine hole generated by the oxidation of structure. The measurement of beam size is relating to the aperture of beam slitter sensitively and the energy peak of spectrum slightly [2]. Considering of that, the X-ray slitter at upstream is designed to be ability of scanning for obtaining the optimum aperture at different spectrum situation.

MECHANISM DESIGN

The previous measurement of the beam size at TPS was about 63μm and 40μm in the X and Y direction respectively. The result is large than the result of calculation [3]. In order to get the more precise beam size of TPS, the existing equipment need to be upgraded. To find the best

aperture at the dedicated beam is the direction of promotion. Considering the purpose, an adjustable aperture mechanism with the ability of high resolution in a limited space was designed. The advantages of compliant structure are well known in no backlash motion and absence of lubrification and wear. Considering that the requirement of a stroke is also few and the requirement of space is limited, an adjustment system with vertical and horizontal linear flexure stage was designed at dedicated beam line as shown in Figure 1.

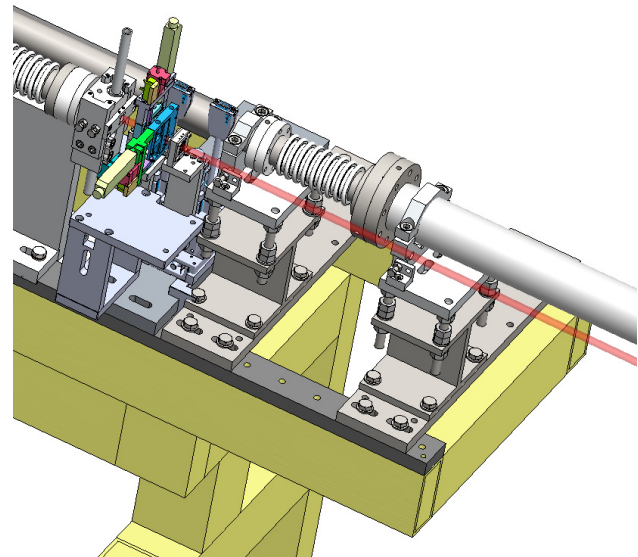Figure 1: Layout of the adjustment system.

Introduction of Components

Figure 2 shows all the components of adjustment mechanism. The original structure of X-ray pine hole was set on commercial X, Y stages. The new adjustment system was set on the other X, Y stages. We can choose one those slitters by using those stages. Another function of stages is tuned for scanning the position of X-ray.

STUDY ON COOLING TECHNOLOGY OF THE SUPERCONDUCTING UNDULATOR AT SSRF *

Yiyong Liu[†], Li Wang, Jian Wang, Sen Sun, Shuhua Wang
Shanghai Institute of Applied Physics, CAS, Shanghai, China

Abstract

A superconducting undulator (SCU) prototype with the period of 16 mm and the magnetic gap of 9.5 mm has been designed and fabricated at the Shanghai Synchrotron Radiation Facility (SSRF) since late 2013. A set of cooling system is designed to cool down cold masses, this paper presents the details of their design, calculation and test: 4 small cryogenic refrigerators are used as cold sources, and the superconducting coil and beam pipe are independently cooled down; The 4.2 K superconducting coil is mainly cooled by the liquid helium tube of thermal siphon loop; The 10~20 K ultra-high vacuum beam tube is cooled by Cu strips conduction. The main sources and mechanism of thermal loads for the SCU were analyzed. And experimental test of cooling technology for SCU prototype had been performed, the feasibility of cooling scheme and the rationality of the cooling structure for the SCU prototype were verified. The cryogenic test and operation of the SCU doesn't require the input of liquid helium from the outside, and is not limited by the liquid helium source. This is the characteristic of SSRF's SCU cooling technology.

INTRODUCTION

The superconducting undulator (SCU) with the advantage of producing high peak magnetic field at smaller period length can bring higher photon brilliance, as a result, technologies of SCU attract more and more attention for the synchrotron facilities in the world [1].

The Shanghai Institute of Applied Physics (SINAP) has started the research and development of SCU technology such as the winding skill of the coils since 2009. SINAP decided to develop one SCU prototype in order to study all the key technologies including coil winding, cooling technology, magnetic field measurement, cryomodule integration and alignment for the future FEL (Free Electron Laser) projects and SSRF (Shanghai Synchrotron Radiation Facility) upgrade project in China in 2013. The SCU prototype mainly consists of superconducting coil, beam chamber and cryostat. The coils include one set of main coils, two sets of end coils, their support frames and quench protection diodes. The SCU prototype is expected to be installed at the SSRF for online test in the winter of 2018.

The SCU superconducting coils are made from commercial copper matrix niobium titanium conductors. Both the pole and the mandrel are made of the soft iron.

The parameters of the SCU prototype are summarized in Table 1.

Table 1: Parameters of Superconducting Undulator Prototype

SC conductors	NbTi/Cu=0.93(+/-0.05):1
Material of pole and mandrel	Soft iron (DT4C)
Period length (mm)	16
Period number	50
Magnetic gap (mm)	9.5
Minimal beam gap (mm)	7.5
Central peak field (T)	≥0.67
Phase error (degree)	≤4
Operating current (A)	Main coil: 400A；2 End coils: 34 A
Magnetic storage energy (kJ)	7
Coil length (mm)	800+32=832
Length of Cryostat along the beam line (m)	1.8

COOLING SCHEME

High efficient and stable cryogenic cooling system is a necessary condition to ensure the operation of the SCU. In order to realize and maintain the cryogenic environment for superconducting coils, the cooling technology needs to be studied in consideration of the complicated structure of the coil arrays, UHV beam chamber, current leads, and thermal loads and so on.

The coils length of the SCU prototype is only 0.9 m, using low temperature superconducting material NbTi / Cu wound, the running temperature margin for the coils is only about 0.8 K, the operating current of the main coils is 400 A. The magnetic clearance and beam clear area of the prototype is 9.5 mm and 7.5 mm respectively, and the thickness of beam chamber is 0.5 mm, that means 0.5 mm space between the coils and the beam chamber. Considering that the measured dynamic heat load of the SSRF beam is about 30 W, in order to avoid the direct influence of beam dynamic thermal load on the stable operation of the coils, the overall cooling scheme of the SCU is as follow:

1. Using 4 cryogenic refrigerators as cold sources, which is more easier for operation and maintenance, and the equipment cost and operating cost is lower compared with large helium refrigerator system.

2. The coils and the beam chamber are independently cooled: The two upper refrigerators cooled the coils, the two down refrigerators cooled the beam chamber. The 4.2 K superconducting coil is mainly cooled by the liquid

FIELD QUALITY FROM TOLERANCE ANALYSES
IN TWO-HALF SEXTUPOLE MAGNET*

J. Liu†, M. Jaski, A. Jain, A. Donnelly, C. Doose, R. Dejus
Argonne National Laboratory, 60439, Argonne, USA

Abstract

Sextupole magnets are used extensively in particle accelerators, synchrotrons, and storage rings. Good magnetic field quality is needed in these magnets, which requires machining the magnet parts to high precision and is the primary driver of the high fabrication costs. To minimize the fabrication costs, a magnetic field quality study from tolerance analyses was conducted. In this paper, finite element analysis (FEA) using OPERA was performed to identify key geometric factors that affect the magnetic field quality and identify the allowable range for these factors. Next, geometric and dimensional tolerance stack-up analyses are carried out using Teamcenter Variation Analysis to optimize the allocation of the geometric tolerances to parts and assemblies. Finally, the analysis results are compared to magnetic measurements of a R&D sextupole magnet.

INTRODUCTION

The Advanced Photon Source (APS) at Argonne National Laboratory (ANL) is upgrading the current double-bend achromat, 7-GeV, 3rd generation storage ring to a 6-GeV, 4th generation storage ring with a multi-bend-achromat lattice that provides dramatically enhanced hard x-ray brightness and coherent flux [1]. The new lattice has 40 sectors with 13 bending magnets per sector, including six reverse bends. Each sector includes 6 sextupoles of two different types. One has steel pole tips and produces nominal integrated sextupole field of up to 727 T/m, and the other contains vanadium permendur (VP) pole tips and produces nominal integrated sextuple field of up to 1315 T/m.

The allowable rms values for random multipole errors in units at 10 mm reference radius for the sextupoles (one unit is 0.01% of the main field component) are listed in Table 1. The requirement for magnet-to-magnet alignment within a module consisting of four quadrupoles and three sextupoles is 30 μm rms. The magnetic center of each magnet should be close to its mechanical center for ease of alignment using mechanical reference surfaces. Furthermore, the magnetic roll angle should be less than 0.4 mrad rms. These requirements place stringent demands on the magnet fabrication tolerances.

In order to achieve the required magnetic field quality and alignment accuracy at reasonable fabrication cost, magnetic and mechanical tolerance analyses are conducted to identify the key driving factors and their allowable limits, and to specify the proper mechanical tolerances for parts and assembly to control the driving factors within allowable limits.

Table 1: Allowable rms Values for Rrandom Fractional Multipole Errors for Sextupoles at 10 mm Radius

Harmonic	Normal (unit)	Skew (unit)
Octupole	8.9	8.9
Decapole	9.1	9.1
Dodecapole	4.5	0.9
14-pole	2.6	1.8
16-pole	0.7	0.7
18-pole	0.8	0.3

MAGNETIC TOLERANCE ANALYSES

Sextupoles for APS Upgrade are made of two solid steel yoke halves (top and bottom) with removable poles tips [2]. This study was carried out on the sextupole with VP pole tips, but the results can be applied to both magnets. For a two-piece design, since it is assembled from outside yokes inward to the pole tips, all the machining errors, including size, form, orientation, and location on mating features, contribute to the variation of the final pole tip surface locations. The machining and assembly errors that will affect the magnetic field quality include: i) pole tip surface profile errors; ii) top half offset horizontally; iii) top half offset vertically; iv) top half rotated relative to the bottom half; and v) pole tips misalignment along the mounting surfaces. Opera-2D finite element analyses are carried out to study the effect of these mechanical errors on the field quality. The geometric configuration for magnetic analyses in Opera is shown in Figure 1.
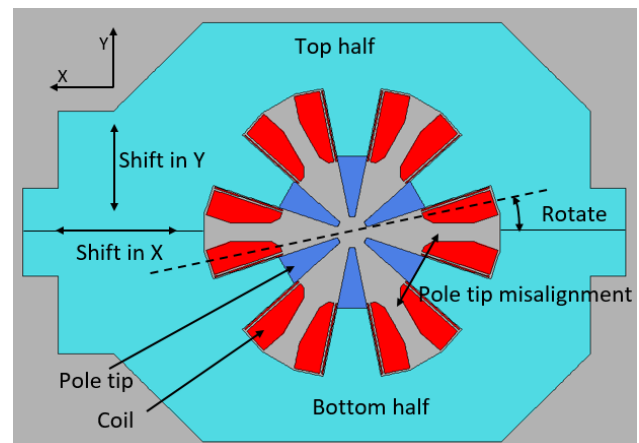

Figure 1: Configuration for magnetic analyses.

FRONT END OF DUAL IMAGING AND DIFFRACTION BEAMLINE AT DIAMOND LIGHT SOURCE

X. Liu[†], R. K. Grant, N. P. Hammond, R. K. Rawcliffe, Diamond Light Source, Oxfordshire, UK

Abstract

The Dual Imaging and Diffraction (DIAD) beamline X-ray source is a ten-pole mini wiggler. By locating the mini wiggler in place of an existing sextupole magnet, the DIAD beamline is built at a bending magnet beamline position in Diamond. To accommodate the unusual beam trajectory, a new front end was designed for the DIAD beamline. The particular designs and specifications, including an improved front end slits design, as well as the synchrotron and dipole ray tracing of the front end are presented in this paper. The development process of delivering the front end - the project challenges, approach and activities are also described along with the technical challenges.

INTRODUCTION

All of the original straight sections in the Diamond storage ring are now occupied. After an extensive study at the beginning of the DIAD beamline project, the decision was made that the DIAD beamline would be built at a bending magnet (BM) beamline position by replacing an existing sextupole magnet with a ten-pole permanent magnet wiggler [1]. DIAD X-ray beam radiates in the same direction as the first bend of the double-bend achromat. The schematics of the beam trajectory are shown in Figure 1. The field strength of the mini wiggler is 1.56T, the period length is 117mm and the total power at 500mA is 4.8kW.
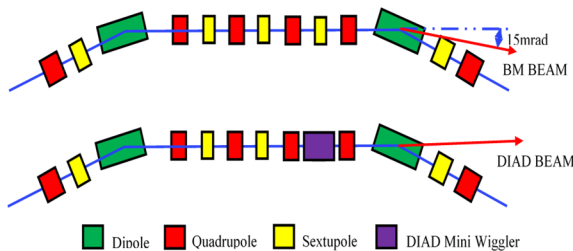

Figure 1: Top: Schematic diagram of the double-bend achromat layout. Bottom: Schematic diagram of the mini-wiggler replacing the sextupole.

This unusual beam trajectory means that the front end will be exposed to the radiation from the dipoles of the double-bend achromat. It will be necessary to shield the uncooled part of the front end from dipole radiation. Further engineering challenges include the front end having to cope with a wide wiggler beam of a fan size of 6 (horizontal) x 0.4 (vertical) mrad. The beamline also requires the front end slits to be the first optics of the beamline. It is important for the front end slits to perform according to the beamline needs.

---
xia.liu@diamond.ac.uk

The delivery of the Front End is on the critical path of the beamline project. A new approach of "Management of the Fuzzy Front End of Innovation" [2] was tried in the concept design stage to manage the technical uncertainties effectively at the early stage of the project. We have gained more understanding of how to be more efficient in the design and development of front ends, which is an innovation process, and deliver the project successfully.

ENGINEERING SOLUTIONS

The DIAD front end design is shown in Figure 2. It consists of Zero Aperture module, 1st Aperture module, Absorber module and fast shutter, Access Pipe module, Slits module, Twin Port Shutter Module and Optics Hutch module. Radiation shielding and modules using DLS generic designs [3] are not part of the discussions in this paper. The more challenging front end ray trace and front end slits will be discussed.

Front End Ray Trace and General Layout

Ray tracing using AutoCAD was employed to study the optical path of the wiggler X ray radiation and dipole radiations and to identify aperture needs. General Layout of the front end was carried out in parallel with the ray tracing to optimise the component sizes and locations of assembly modules. The ray tracing (Figure 3) has the following findings:

- A zero module is necessary to connect the front end to the storage ring (SR) as it is almost 12 meters from the end of the SR vessel to the ratchet wall, while the standard length of an undulator front end at Diamond is around 10.4 meters.
- The crotch absorber in the SR vessel needs to be wider to provide more shielding to prevent radiation from dipole 2 shining on the uncooled zero module vessel.
- A zero aperture, in addition to the wider crotch absorber, is also needed to provide shielding to the uncooled zero module vessel. The zero aperture is also designed to replace the Beam Port Absorber fitted at the end of the SR vessel to make the easy connection of the front end to the storage ring.
- For the benefit of the project timescale and cost, a decision was made at the ray tracing stage that Absorber, Access Pipe, Twin Port Shutter and Optics Hutch module will use DLS generic designs [3]. However, the 6mrad wiggler beam size is too wide for the standard 1st Absorber. The solution was to design the 1st Aperture to trim the wiggler beam to 0.86(H) x 0.34(V) mrad so that the standard 1st Absorber can be used.

MORPHOLOGIES OF OXYGEN-FREE TITANIUM AND PALLADIUM/TITANIUM THIN FILMS: NEW NON-EVAPORABLE GETTER (NEG) COATINGS

T. Miyazawa[*], SOKENDAI (The Graduate University for Advanced Studies), 305-0801 Tsukuba, Japan

A. Hashimoto[1], M. Yamanaka, National Institute for Materials Science, 305-0047 Tsukuba, Japan

T. Kikuchi, K. Mase[2], KEK, 305-0801 Tsukuba, Japan

[1]also at University of Tsukuba, 305-0047 Tsukuba, Japan

[2]also at SOKENDAI (The Graduate University for Advanced Studies), 305-0801 Tsukuba, Japan

Abstract

Non-evaporable getter (NEG) coatings are ideal for maintaining an ultrahigh vacuum (UHV) in the range 10^{-8} Pa and they are widely used for accelerators because they are oil free, magnetic-field free, vibration free, economical, space saving, and energy efficient. We recently fabricated new NEG coatings consisting of low-oxygen-content Ti or oxygen-free Pd/Ti by sublimation under a clean UHV in the range 10^{-8} to 10^{-7} Pa. Here, we report the determination of the morphologies of these films by scanning electron microscopy, transmission electron microscopy, scanning transmission electron microscopy, and energy-dispersive X-ray spectroscopy. The Ti and Pd films had almost uniform thicknesses of about 1.3 μm and 50 nm, respectively, and the Pd film completely overcoated the Ti film. Both the Pd and Ti thin films were uniformly deposited in plane on the stainless steel 304L substrate and they had polycrystalline structures. The interface between the Pd and Ti thin films was not abrupt.

INTRODUCTION

A non-evaporable getter (NEG) is a material, such as Al, Ti, V, Zr, Hf, Ta, Nb, Fe, or their alloys, that can evacuate reactive residual gases after activation under a clean ultrahigh vacuum (UHV) [1–3]. The NEG coating technique involves coating the inner walls of a vacuum chamber with thin film of a NEG material [4–6] and it is widely used in accelerators for synchrotron radiation facilities, because NEG thin films suppress outgassing from substrates and pump reactive residual gases, and because they are space saving. The most popular NEG coating consists of Ti, Zr, and V, deposited by dc magnetron sputtering; this technique was developed by Benvenuti *et al.* [4,5]. The resulting TiZrV thin film can be fully activated by baking at 180 °C for 24 hours. Recently, thin films of TiZrHfV deposited by dc magnetron sputtering have been reported to be fully activated by baking at 150–160 °C for 24 hours [6].

We recently developed a new NEG coating, and named it as oxygen-free Pd/Ti coating, principally for pumping H_2 and CO [7,8]. The oxygen-free Pd/Ti coating has the following advantages: (1) it can be activated after baking at 133 °C for 12 hours; (2) the Pd overcoat prevents oxidation of the Ti film, even after repeated venting–baking cycles; (3) the initial and running costs are low; (4) its fabrication does not require skilled technicians; (5) it can be applied to chambers having a complex structure; and (6) it can be applied to narrow tubes, where Pd and Ti filaments can be arranged.

To produce this coating, a thin film of Ti is initially deposited and subsequently overcoated with Pd under clean UHV conditions in the range 10^{-8} to 10^{-7} Pa. The activation and pumping processes for the oxygen-free Pd/Ti thin film differ from those used for conventional NEG coatings [9]. In the activation process of conventional NEG, C and O atoms chemisorbed on the NEG surface diffuse into the bulk to provide a clean and reactive surface [3]. Consequently, the activation temperature of conventional NEG films is determined mainly by the diffusion activation energies of C and O atoms. On the other hand, the oxygen-free Pd/Ti thin film is activated by the diffusion of H atoms from the Ti film through the Pd overcoating to the surface, where they desorb into the vacuum as H_2 molecules. The activation energies for surface adsorption and bulk dissolution of H are −0.53 and −0.1 eV, respectively, for Pd, and −0.92 and −0.47 eV, respectively, for Ti [10]. During this activation process, CO chemisorbed on the Pd surface is also desorbed, leaving the surface available for CO absorption [11]. Because the activation temperature of oxygen-free Pd/Ti thin film is determined by the diffusion and desorption energies of hydrogen as well by the desorption energy of CO, the activation temperature can be reduced to as low as 133 °C [7,8]. When an ionization gauge is used in a vacuum system, oxygen-free Pd/Ti is expected to pump hydrogen-containing molecules, such as H_2O or CH_4, because electrons emitted from the gauge dissociates these molecules into H atoms and radicals such as O and C.

Here, we report the morphologies of the low-oxygen-content Ti and oxygen-free Pd/Ti thin films as determined by scanning electron microscopy (SEM), transmission electron microscopy (TEM), scanning transmission electron microscopy (STEM), and energy-dispersive X-ray spectroscopy (EDS).

---

*miyazate@post.kek.jp

A QUASI-PERIODICELLIPTICALLY POLARIZED UNDULATOR AT THE NATIONAL SYNCHROTRON LIGHT SOURCE II*

M. Musardo[†], T. Tanabe, O. Chubar, Y. Hidaka, D. Harder, J. Rank, P. Cappadoro and T. Corwin,
Energy Sciences Directorate, Brookhaven National Laboratory, 11973 Upton, NY, USA
C. A. Kitegi, Synchrotron SOLEIL, Saint-Aubin, France

Abstract

A 2.8 m long quasi-periodic APPLE II type undulator has been commissioned at the National Synchrotron Light Source II (NSLS-II) for the Electron Spectro-Microscopy (ESM) beamline in the framework of the NEXT (NSLS-II Experimental Tools) project [1]. It provides high brilliance photon beams in circularly and linearly polarized radiation from VUV to soft X-Rays. The mechanical structure implemented to achieve the quasi-periodicity in the magnetic field profile is described together with the optimization techniques utilized to correct the undesirable phase-dependent errors. The final magnetic results are presented as well as the spectral performance of the device. Although this EPU (Elliptically Polarizing Undulator) was procured as a turn-key device, the vendor was only responsible for the mechanical frame and the control system. Sorting and assembly of the magnet modules and the magnetic field tuning - Virtual Shimming and Magic Finger - were performed at the NSLS-II Magnetic Measurement Lab.

MAGNETIC AND MECHANICAL STRUCTURE

The magnetic structure of EPU105 is configured as four Halbach arrays in four adjacent quadrants. The support structure is equipped with four translation units for the polarization control (linear, circular, and elliptical). The period length (λ) is 105 mm and the minimum magnetic gap of the device is 16 mm. The main magnet dimensions are 34 mm (H) x 34 mm (V) x 26.25 mm (L). The remanence of the NdFeB magnets is 1.25 T. The longitudinal air-gap between the magnets is 50 µm and the gap between the magnet arrays is 1 mm. The full length of the magnetic core is 2654.25 mm, excluding girder movement and the trim magnet holders. The device has two different types of terminations, both composed of one vertically magnetized full block, two vertically magnetized half blocks and four horizontally magnetized half blocks. The end section configuration block width and the space between blocks is optimized to minimize trajectory steering and field integrals. A NEG-coated vacuum chamber with current strip corrections used for dynamic field integral correction is employed [2]. ESM EPU105 is a quasi-period undulator (QPU). The Quasi-Periodicity (Q-P) is obtained by modulating the magnetic field amplitude along the length of the device. This is achieved by vertical displacement of B-magnets (blocks magnetized longitudinally) at six specific locations. In order to reduce the magnetic field strength at

those locations the standard magnet holders were replaced with special holders that displace the magnets vertically by 13 mm with respect to the mid-plane, as shown in Fig. 1.
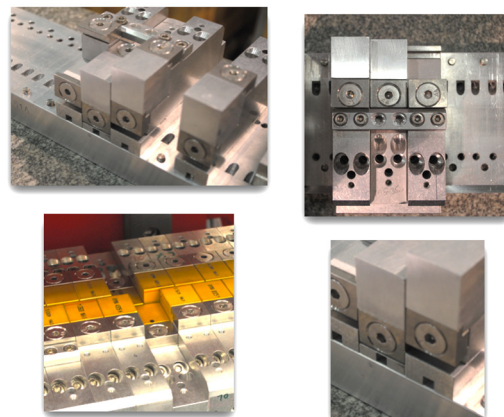

Figure 1: Magnet holders for the Q-P configuration.

During the assembly process only those magnets with longitudinal magnetization are shifted in order to minimize the deleterious effects of the Q-P adjustment on the first and second magnetic field integrals. Figure 2 shows the measured magnetic field on-axis and the 3 GeV electron trajectory in the horizontal plane at the minimum gap and phase 0.
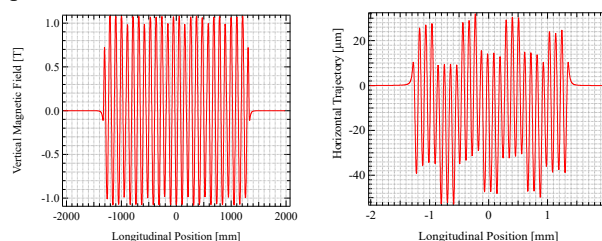
Figure 2: Measured vertical magnetic field on axis (left) and horizontal trajectory (right) in the Q-P configuration.

The quasi-periodicity in the magnetic field profile was introduced in order to modify the properties of the emitted photon beam - a reduction in intensity and shift in energy of the higher harmonics compared to the fundamental. Because of the shift in energy the higher harmonics are no longer proportional to an integer multiple of the fundamental energy, which drastically reduces the amount of unwanted higher harmonic radiation transmitted through the monochromator in the ESM beamline.

Quasi-periodic undulators were originally proposed as a method to reduce contamination from high order spectral harmonics where optical filtering is not possible or convenient [3].

STRUCTURE DESIGN OF A MULTI-WIRE TARGET*

Xiaojun Nie [†], Anxin Wang, Jilei Sun, Taoguang Xu, Ling Kang, Jiebing Yu, Huayan He, Jia-xin Chen, Donghui Zhu, Lei Liu, Changjun Ning, Guangyuan Wang, Yongji Yu, Junsong Zhang, Dongguan Branch of the Institute of High Energy Physics, Chinese Academy of Science(CAS), 523803 Dongguan, China

Abstract

Introduce a structure design of a Multi-Wire Target. The plan of wire alignment was decided by analysis. The wire tightening device with interlaced alignment was used to solve the wire alignment in narrow space. The vacuum chamber was designed by optimization. The displacement pickup was used to make the movement control of translation stages.

INTRODUCTION

The multi-wire target is a device which is used to measure the section of beam. The measuring mental wire is bombarded by the beam and gets the low-energy electron. The low-energy can output the voltage signals. The multi-wire target can use this signal to measure the density of beam section. The mental wires are aligned according to the beam measuring requirement.

The multi-wire target has a complex structure, which includes measuring part, vacuum chamber, moving part and so on. It also demands high motion accuracy to reach high measuring accuracy. According to the running requirement of China Spallation Neutron Source, one multi-wire target (RDMWS) is demanded on the ring to dump transportation to the beam section[1-2].

WIRE ALIGNMENT PLAN

Wire alignment plan is the wire distribution pattern. Two group wires, which are vertical each other, are designed to detect two directions of beam. The horizontal and vertical directions are selected the wire directions to simplify the structure of multi-wire target. According to the beam parameter, the dimension of beam section can be reached. The dimension（1σ）of

horizontal direction is 20mm,while the dimension（1σ）of another direction is 10mm. The wire alignment plan can be concluded by the above information, which is stated as the following.

(1)Wire direction: horizontal and vertical directions.

(2)Wire quantity on horizontal direction: 35 wires are distributed on this direction. The distance between the wires is 7mm. The width of covered area is about 238mm. 17 wires are include in 6σ range (σ_x=20mm).

(3)Wire quantity on vertical direction: 41 wires are distributed on this direction. The distance between the wires is 6mm. The width of the covered area is about 240mm. 10 wires are include in 6σ range (σ_y=10mm).

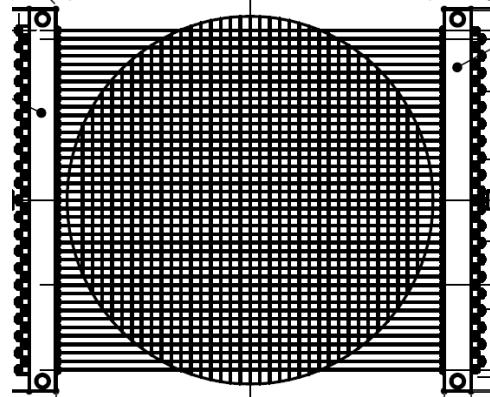The wire distribution figure can be reached by the plan, which is illustrated as Figure 1.

Figure 1: Wire distribution plan.

DESIGN OF WIRE TIGHTEN COMPONENT

Design Requirements

Wire tighten component is an important part for the multi-wire target, which is used to locate and fix the wires. It is important to optimize this part because of the dense distribution of wires in narrow space.

The component should fix and locate wires reliably. Any two components should avoid position interference each other. The material for this part should not be hard. Otherwise it is easy to harm the wires. Meanwhile any two wires should be insulated each other. The vacuum working condition should also be considered for design.

Structure of Wire Tighten Component

Wire tighten component is composed of wire tighten clamps, located blocks and tighten bolts. The oxygen-free copper was selected as the material of wire tighten clamp, while the ceramic was selected for the located block. Each wire is strained by the spring and fixed by bolts. The tungsten wire is used for measurement, which has good electrical conductivity and mechanical property. But the diameter of the wire is very small to ensure the measuring precision. So the stretching force of the spring should not be too high.

One group stepped holes were designed on the located block. The stepped holes can be used to locate the wire tighten clamps and install the springs. The distribution of wire tighten clamps are very dense. So they are aligned by interlaced alignment to get a gap between two clamps and avoid short circuit for the rotation of wire tighten clamp. In order to make interlaced alignment, two type clamps

CALCULATION OF ORBIT DISTORTIONS FOR THE APS UPGRADE DUE TO GIRDER RESONANCES*

J. Nudell[†], Z. Liu, V. Sajaev, C. Preissner, Argonne National Laboratory, Argonne, IL, USA

Abstract

Maintaining sub-micron-scale beam stability for the APS-U Multibend Achromat Lattice places strict requirements on the magnet support system. Historically, magnet vibration requirements have been based on physics simulations which make broad generalizations and assumptions regarding the magnet motion. Magnet support systems have been notoriously difficult to analyze with FEA techniques and as a consequence, these analyses have been underutilized in predicting accelerator performance. The APS has developed a procedure for accurate modeling of magnet support systems. The girder mode shapes are extracted from these analyses and exported to accelerator simulation code *elegant* to calculate the static beam amplification factor for each mode shape. These amplification factors, along with knowledge of damping coefficients and the character of the tunnel floor motion, may then be used to predict the effect of girder resonances on beam stability and validate the magnet support designs.

INTRODUCTION

Typical magnet support stability requirements for light sources are specified by physicists with a girder-to-girder motion specification and a magnet-to-magnet motion specification (for elements mounted on a common girder) as shown in Table 1 for the APS Upgrade (APS-U). As the required stability of fourth-generation light sources becomes more stringent, so too do the requirements for support systems. The goal for APS-U is to limit mechanical sources of beam motion to less than one micron in each direction, without orbit feedback.

Table 1: APS-U Vibration Tolerances [1]

Specified over 1-100 Hz	X (rms)	Y (rms)
Girder Vibration	20 nm	20 nm
Quadrupole Vibration	10 nm	10 nm

Although the tolerances in Table 1 are useful to provide engineers with simple design requirements, they are based on broad generalizations regarding the character of the magnet motion which may be inaccurate. For instance, magnet-to-magnet vibration within a girder is simulated by physicists as uncorrelated motion, when in reality, this motion is mostly correlated and due to girder deformations (which can be simulated). In addition, the specifications are based upon a particular magnet grouping arrangement, making it difficult to accurately evaluate alternate magnet grouping arrangements in terms of beam dynamics.

The APS has developed a procedure for modeling of magnet support system dynamics which has proven to be accurate in predicting modal response within 10%, as shown in reference [2]. The paper below describes a procedure for utilizing these modal analyses in order to predict the effect of measured ground motion and simulated magnet support system dynamics on beam motion. The procedure has been used to evaluate a previous magnet support grouping, as described in reference [3] and the results here are used to evaluate a new magnet support grouping.

APS-U MAGNET GROUPING

The APS-U magnets will be placed on three long and two short supports (girders) per sector. Three larger supports will rest on three concrete plinths, and two smaller supports will straddle between the three plinths. The plinths are used to effectively raise the floor and reduce the height of the girders. The middle module containing focusing and defocusing quadrupoles and dipoles is called "FODO", and the side modules, which contain the quadrupole doublet, longitudinal gradient dipole, and multipoles, are called "DLM-A" and "DLM-B".

The tolerances listed in Table 1 assume a magnet grouping arrangement where all quadrupoles between dipoles are located on a common girder. This arrangement does not allow for bellows in between modules, which makes fabrication, installation, and alignment of the accelerator components infeasible given the short period of time allotted for installation. The new magnet grouping arrangement places the quadrupoles adjacent to the dipole magnets on a common support with bellows on either end, called "QMQ". Since the tolerances in Table 1 do not reflect this grouping, the strategy described in this paper is used to evaluate the magnet support design. The new and old magnet grouping arrangements are shown in Figure 1.
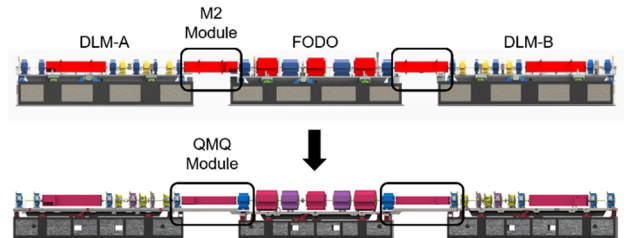

Figure 1: Previous (top) and current (bottom) APS-U magnet grouping arrangement.

GIRDER VIBRATION MODES

The girder modal analysis is performed using ANSYS Mechanical, Release 18.1 [4]. In order to accurately predict the modal response of the modules, dynamic stiffness testing is completed on the support components. Each support component is preloaded between two weights, hung from

NEXT GENERATION X-RAY BEAM POSITION MONITOR SYSTEM FOR THE ADVANCED PHOTON SOURCE MBA UPGRADE*

S. Oprondek[†], F. Westferro, S.H. Lee, B. Yang, Y. Jaski, J. Downey, J. Mulvey,
and M. Ramanathan, Advanced Photon Source, Argonne National Laboratory,
Lemont, IL 60439, USA

Abstract

The Advanced Photon Source (APS) upgrade from double-bend achromats (DBA) to multi-bend achromats (MBA) lattice has increased the need for reliable diagnostic systems. This upgrade will decrease the size of the photon beam drastically and beam current will be increased from 100 mA to 200 mA. The small beam and intense heat loads provided by the upgraded APS requires unique and innovative approaches to beam position monitoring. To meet the need for a reliable diagnostic system for the APS upgrade, the next generation X-ray Beam Position Monitoring System (XBPM) is required which includes the first XBPM (XBPM1), the Intensity Monitor (IM1) and the second XBPM (XBPM2). This paper presents progress and status of the current configuration of the XBPM system especially the development work involving the IM1 and XBPM2.

The R&D work to develop an alternative XBPM1 using the Compton scattering principle is also presented.

INTRODUCTION

Improved beam stability is critical for the Advanced Photon Source Upgrade (APS-U). The APS-U will require keeping short-term beam angle change below 0.25 µrad and long-term angle drift below 0.6 µrad. In conjunction with four Radio Frequency Beam Position Monitors (RFBPM) in the accelerator ring, the front ends of the APS-U will have three diagnostic components devoted to maintaining orbit control. Beam stability will rely on two unique components that will detect X-Ray Fluorescence (XRF): the first XBPM (XBPM1) and the Intensity Monitor (IM1). The second XBPM (XBPM2) will use photoemission current to help maintain beam stability. The XBPM1 is the initial source of feedback control during user operation. The IM1 and XBPM2 are secondary devices that provide complementary data during user operation. The IM1 provides intensity measurements while a photon shutter is closed and is used to calibrate the XBPM1. The XBPM2 is not in the orbit feedback loop and is mainly used to assess feedback performance. The layout for the devices is shown in simplified form in Figure 1.
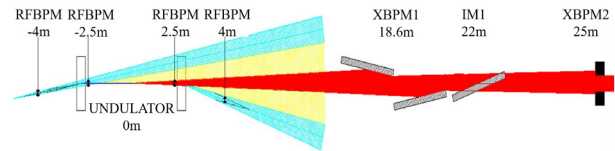
Figure 1: Layout of XBPM system.

FIRST X-RAY BEAM POSITION MONITOR (XBPM1)

The XBPM1 for the high heat load front ends (HHLFE) for the APS-U [1] uses pinhole optics and an array of silicon PIN photodiodes to monitor both vertical and horizontal displacement of the X-Ray beam as the beam is absorbed by two grazing incident insertion device (GRID) GlidCop absorbers. The XBPM1 is called the GRID-XBPM for this reason. The HHLFE is downstream of two inline undulators. The GRID absorbers are incident with the beam at 1° and will absorb 11.5 kW during normal operation. Missteering conditions require the absorbers to be able to withstand absorbing 17 kW and for this reason, GlidCop was the necessary material for this application. A cross-section of one of the GRID masks and detectors is shown in Figure 2.
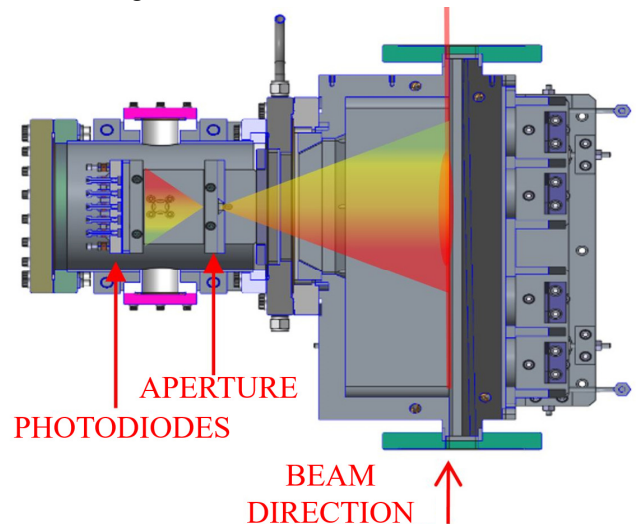
Figure 2: Cross-section of one GRID mask, with fluorescence overlay.

The unique design of the detectors is the major upgrade for this component as the GRID-XBPM style of XBPM1 has been proven effective in the current APS [2]. The detector uses an array of nine photodiodes as shown in Figure 3.

ALBA SYNCHROTRON LIGHT SOURCE LIQUEFACTION HELIUM PLANT

M.Prieto†, Y. Nikitin‡, C. Colldelram§, J. Casas#
ALBA Synchrotron Light Source, 08290 Cerdanyola del Vallès, Spain

Abstract

ALBA is a 3rd generation Synchrotron Light facility with: 8 operational Beam Lines (BLs), a 2nd BL of Phase II under construction and 3 first Phase III BLs in design phase. Some user experiments require Liquid Helium (LHe) as a coolant. The resulting LHe consumption at ALBA is about 650 l/week.

Thus far the vaporized helium, which results from the refrigeration of experiments and equipment, has been released into the atmosphere without being reused. Due to the increasing price of LHe, ALBA agreed with ICN2 (Catalan Institute of Nanoscience and Nanotechnology) to invest in a Liquefaction Helium Plant. Internal staff has carried out the project, installation and pressure equipment legalization of the plant, which is located in a new 80 m² construction. Under operation the plant allows recycling up to 24960 litres of LHe per year, which is an 80% of the helium consumed at ALBA, by making the gaseous helium undergo through 3 main stages: recovery, purification and liquefaction.

The plant, unique in Catalonia, will entail cost savings about 77% and will reduce vulnerability to supply disruptions. ICN2 will benefit from a part of the production due to their initial investment.

SIGNIFICANCE OF RECYCLING HELIUM

Due to the fact that helium is an inert gas and it has a really low boiling-point (-268.93 ºC) [1], it is used in a wide range of applications.

Once gaseous helium is released into the atmosphere there is no economical way to recovery it, because most of it escapes into the space; leading to a very low and relatively constant atmosphere helium concentration of only 5.2 ppm [2], which is too low so as to separate it from air. By contrast, the highest helium content is in a few natural gas fields around the globe.

Owing to the balance between increasing demand and helium availability, helium is a finite non-renewable resource. Thus, gaseous helium should be recovered.

OPERATION

So as to meet ALBA's liquid helium demand, the plant subjects the vaporized helium to 3 stages: **recovery**, **purification** and **liquefaction**.

_____

† mprieto@cells.es
‡ ynikitin@cells.es
§ ccolldelram@cells.es
# jcasas@cells.es
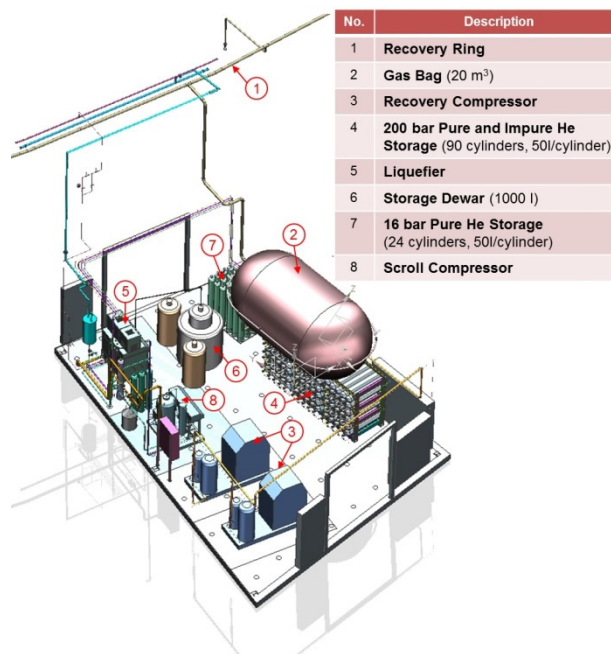
Figure 1: Liquefaction Helium Plant (LHeP) equipment identification.

Recovery

The **recuperation** initiates when the vaporized helium, which results from the thermal exchange between the liquid helium and the beamlines' components to cool, is slightly heated and inserted in the 400 m perimeter **recovery ring** that carries the gaseous impure helium to a **20 m³ gas balloon.** The helium warm-up is vital prior to being introduced into the recovery ring in order to avoid damaging the canvas, which composes the 20 m³ gas bag, because it cannot handle extreme temperatures. The helium stored in the balloon is compressed up to 200 bar by the **recovery compressor** for the purpose of saving space as well as averting the bag's collapse. The resulting 200 bar helium is stored in the **200 bar impure helium storage** (see Fig. 1 and Fig. 2).

Purification

Prior to liquefying this gas, it must be purified by the **liquefier**'s internal purifier (see Fig. 2) that is capable to clean helium gas with up to 10 % air impurity. Thus, once the 200 bar storage contains a reasonable amount of impure helium, the **purification** commences starting the **liquefier** up.

The liquefier's purifier works as long as it is cooled below pre-set temperatures, which can solely be reached by circulating cold pure helium through it. The required pure helium is sucked of the **16 bar pure helium storage**,

DEVELOPMENT OF A REVOLVER TYPE UNDULATOR

T. Ramm*, M. Tischer, Deutsches Elektronen-Synchrotron DESY, 22607 Hamburg, Germany

Abstract

A revolver-type undulator is developed for the SASE section of the FLASH Free-Electron Laser (FEL) at DESY. Currently, a 1.2 GeV linear accelerator injects electrons into two undulator lines to provide fully coherent VUV light to different experimental stations in two experimental halls. The more recently built FLASH2 branch consists of 12 planar undulators with a fixed magnet structure of 32 mm period length.

Within plans for refurbishment of the original FLASH1 undulator section and also to open up new operation schemes with an extended photon energy range, an undulator development was started that allows for a change of different magnet structures. Once installed, it will be possible to change the wavelength range or the FEL operation scheme within a short period of time. Magnet structures can then be switched at any time without any observable effect on the electron beam orbit or the photon beam position.

The single design steps are described in the following article: profile of requirements, choice of an applicable changing mechanism, development of a new magnet structure, the position of the bearing points, a new floor assembly and improvement of the cantilever arm.

INTRODUCTION

The motivation for the development of a magnet structure changing undulator is to open up the photon energy range for the users within a short period of time without manpower-intensive hardware exchange in the tunnel or impact on the beamline. This development is still ongoing; the paper reflects the present status of design.

PROFILE OF REQUIREMENTS

The magnet structure changing undulator should be based upon the currently installed planar insertion devices with a length of 2.5 m. Its new dimension should neither exceed the available space nor result in changing a lot of assemblies in the surroundings. Another requirement for the construction is to switch between as many as possible magnet structures automatically within a short period of time. Effects on the electron beam are undesirable. The currently installed magnet structure shall possibly be used further on and also be part of the new ones. The changing mechanism is to be mounted on the currently used base frame of the FLASH2 insertion device (ID) with all its installed components. The length of the new ID should still be 2.5m and the whole assembly shouldn't pass the existing limits. The shutdown-time for exchanging the undulators with another magnet structure and the necessary manpower has to be minimized.

* torsten.ramm@desy.de

SELECTION OF THE CHANGING-MECHANISM

There are at least four different concepts how an exchangeable magnet structure has been realized in the past. Generally it is required to open the gap before changing the magnet arrays.

The first type has been built at DESY already in the early days of undulators and has a rotating cylinder pivot-mounted and electrically driven at the outer ends (see Fig. 1). The advantages are that you are free at the number of installed magnet structures and only restricted by their magnitude. Also, there are no disturbing influences on the magnetic field along the magnet structure. However, the cylinders, not pivot-pointed at the "Bessel-points", causing a large bending in the middle of the ID, which varies with gap and also from one to the other magnet structure [1].

The second version is similar to the first one with the difference that the pivot-points are positioned at the calculated "Bessel-points" or at the four optimum points in case of two further links. Both, upper and lower cylinder can carry three structures at maximum because the other space is preserved for bow bearings. This is the most common way of design and has been built at several labs [2, 3].

In the third solution the magnet structures are mounted side by side on an intermediate plate which can be moved transversally on a stiff magnet girder in order to change the structure. It has the advantage that a rotating mechanism with inevitable angular and phase errors can be avoided. On the other hand, the full magnetic force of all three structures is always present. In principle, the magnetic attraction of the girders can be canceled e.g. by compensation magnets beside the actual magnets which of course holds for any of the four discussed schemes. Besides, large and exact linear guides and adjustments are required [4, 5].

The fourth solution is an ID with a rotation mechanism based on multiple strap hinges which connect the movable with the fixed part of the girder. This is an innovative, compact and rigid design. Drawbacks of this concept are the limitation to only two magnet structures and in particular a complex and expensive fabrication of the strap hinge as a bearing [3].

The four alternatives have been investigated in detail and assessed under consideration of various boundary conditions with different impact, among those: an integration of possibly three magnet structures, compatibility with the existing magnet structure, keeping the 2.5 m girder length, minimization of girder bending, small overall size, reuse of the well-proven undulator frame, further use of the existing vacuum chamber, and finally costs.

Accelerators

Insertion Devices

OVERVIEW OF SESAME WATER COOLING SYSTEM DESIGN & OPERATION*

M. Al Shehab[†], SESAME, 19252 Allan, Jordan
M. Quispe, ALBA, 08290 Barcelona, Spain

Abstract

SESAME started operation in January 2017. In order to receive heat deposited in various synchrotron devices during operation, a low-conductivity water cooling system was installed. Within this paper the design, construction and operation of the water cooling system will be discussed, Both Hydraulic and Thermal Behaviour of the system will be analysed and discussed with numerical simulation means as well as real operation pressure and temperature data for the purpose of a better understanding of the cooling system.

INTRODUCTION

SESAME cooling system basically based on two Air-cooled chillers, with a total capacity of 2314Kw. The cooling water coming from chillers feeds thermally insulated buffer tank, the buffer tank provides the cooled water to the accelerator subsystems (injector, Booster, Storage Ring & Beamlines) through two plate heat exchangers with a total capacity on 1762Kw of thermal exchange.

The air temperature inside the experimental Hall, Booster & Storage Ring tunnels are conditioned through five AHU's, two of them are used for the Experimental Hall with a total capacity of 500Kw, one for the Booster Tunnel with a capacity of 500Kw, and two for the Ring Tunnel with a total capacity of 30kw.

The general scheme of SESAME cooling system is shown in Figures 1 and 2, and the accelerator thermal loads are shown in Table 1 below. for this phase of operation at SESAME the only existing beamlines are (XAFS/XRFS) and IR Beam line including the Front ends. a future plane is foreseen to increase the cooling capacity through the installation of a third chiller of 1157kw cooling capacity and increase the Heat exchange with a third heat exchanger of 880Kw exchange capacity to cope with the future needs at SESAME which includes the Air Conditioning of the Experimental and optical Hutches as required for the current

Table 1: Thermal Loads for Subsystems

Component	Power (Kw)
SR	774.8
RF+Dipole PS	640
Booster+Injector	70
AHU'S	600

operation the hydraulic system is working in manual mode. The group of pumps is fixed to a constant RPM, through VFD system, the users select manually the percentage of RPM that they need and do a final optimization by controlling the differential pressure sensor available between the inlet and outlet rings. This operational mode is stable if the system is a circuit closed without and modification to the local consumption. For the moment the system meets the criteria but in future operation the scenario will be different: the map of pressure and water flow velocities will be not constant for different reasons
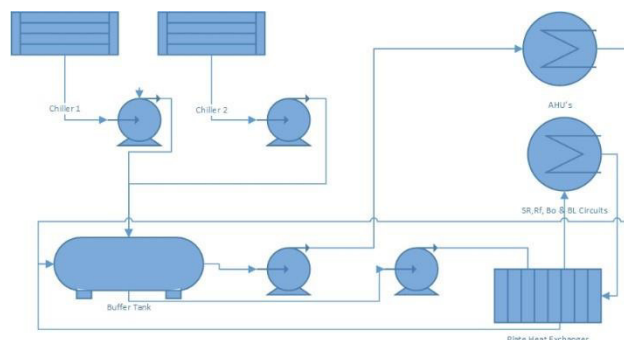
Figure 1: General scheme of the cooling system.
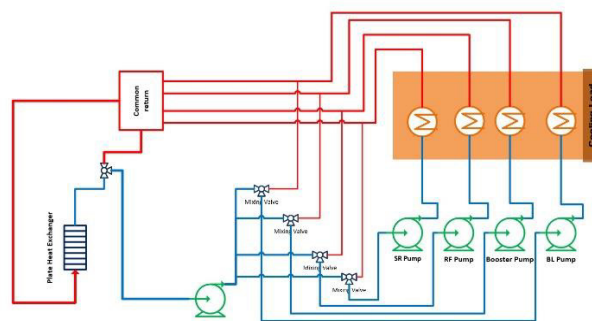
Figure 2: Scheme of the cooling circuits of the accelerator (SR,RF,Bo& Bl).

SR COOLING SYSTEM

For the Storage Ring the main supply cooling pipe line Starts with DN150 Pipe size which is divided by a Tee and reduced gradually from DN100, DN80, DN65 and Ends with DN50 Pipe size, the total Flow in the SR Circuit is 24L/s with a differential pressure of 8bars. The water flow inside the ring is 180° Circulated with Zero Velocity Point at the ends (Figure 3), at each girder the flow is branched with a supply and return cross equipped with a

VIBRATION MEASUREMENT & SIMULATION OF MAGNET & GIRDER IN SESAME*

M. Al Shehab[†], SESAME, 19252 Allan, Jordan

E. Lakovakis, L. Lancy, 1211 Geneva, Switzerland

Abstract

SESAME (Synchrotron-light for Experimental Science and Applications in the Middle East) started operation in January 2017. During the design phase several FEA studies were performed to optimize the girder and the magnet design taking into account all the constraints such as the tight spacing between magnets, the vacuum chamber installation interactions with the magnets. In this paper the experimental and Numerical modal analysis are presented as well as the result comparison between the experimental and simulation work.

INTRODUCTION

Finite Element Analysis Using ANSYS were used during the design phase in order to calculate the Eigen Frequencies and to extract the mode shapes of the Girder-Magnets Assembly [1]. After that experimental modal analysis had been conducted at CERN vibration labs. The outcome results are then used to perform Model Tuning for the Girder-Magnet assembly FEA model used in the calculations of Eigen frequency and mode shape as well as the magnets PSD response to the ground vibration.

INITIAL FEA MODEL RESULTS

Initial Modal Analysis for the girder system design before modifications during manufacturing phase was performed using ANSYS workbench15 finite element analysis software. In which over 20 modes have been extracted. the lowest natural frequency found to be 22 Hz with a longitudinal bending shape (bending the around beam axis), as shown on Table 1. The second mode Eigen frequency was 23 Hz with a longitudinal bending shape as well, the 3rd mode related to the dipole magnet with a transversal shape (rotation around beam direction) and 45.4 Hz frequency, for the 4th mode the mode take a longitudinal bending shape with an Eigen frequency of 62.8 Hz related to the long quadrupoles magnets.

Table 1: Eigen Frequencies For The Initial Design

Mode	Freq.(Hz)	Shape
1	22	Sext Longitudinal Bending
2	23	SQ Longitudinal Bending
3	45.4	Dipole Transversal Rotation
4	62.8	LQ Longitudinal Bending

PROTOTYPE EXPERIMENTAL MODAL ANALYSIS

In the following part of this paper the results of the experimental modal analysis performed by the Mechanical Measurement Lab of the EN -MME group at CERN to characterize the dynamical behaviour of the magnets and the girder impact of SESAME are described.

Test Setup

For measuring the dynamic response of the structure, five tri-axial accelerometers were used, two PCB Piezotronics 356A33 (sensitivity of 10 mV/g, frequency range from 2 Hz to 7 kHz and a mass of 5 grams) & two PCB Piezotronics 356B08 (sensitivity of 100 mV/g, frequency range from 0.5 Hz to 5 kHz and a mass of 50 grams. One PCB Piezotronics 356A15(sensitivity of 100 mV/g, frequency range from 2 Hz to 5 kHz and a mass of 10 grams).

In addition to the accelerometers, two impact hammers (PCB Piezotronics models 086D05 and 086D20) were used to excite the magnets and the girder respectively.

Measurement Positions

The measurement positions of the accelerometers were chosen in order to know the behaviour of the different parts of the structure. The measurements were carried out for four separate parts of the structure: the sextuple, the long and the short quadrupole and the girder as shown in Figure 1. The girder was not fixed to the floor during the measurements.
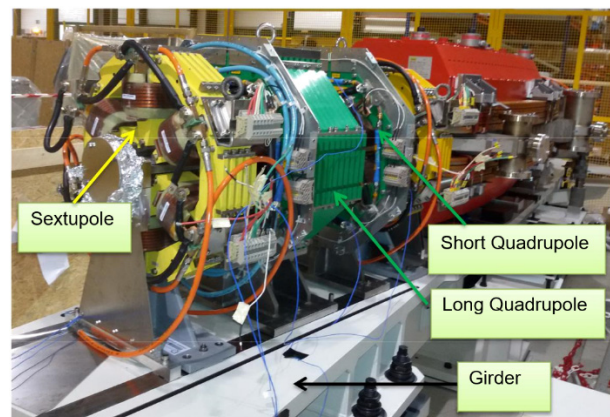

Figure1: Position of the accelerometers.

THE USE OF AM TECHNOLOGIES FOR HV AND UHV COMPONENTS AND VESSELS

A. Stallwood, G. Duller, D. Butler, Diamond Light Source, Didcot, England

Abstract

AM (Additive Manufacturing) technology (3D Printing) in plastics and metals has now been in commercial use for over 30 years. However, the application of this technology in vacuum environments has been limited, due to the material porosity and additives used in the manufacturing techniques. This paper reports on the testing and use of FDM (Fused Deposition Modelling) PEEK (Polyether ether ketone) and DMLS (Direct Metal Laser Sintering) metal components inside a UHV (Ultra-High-Vacuum) environment. Specifically covering the use of DMLS to successfully produce a complex vacuum vessel operating at 10^{-6} mbar, as used on the new VMXm beamline at Diamond Light Source. Vacuum testing the vessel has demonstrated that this manufacturing technique has the potential to produce vessels that are capable of holding 10^{-10} mbar.

FDM PEEK

FDM Technology and Material Development

FDM technology has increased in popularity over the last 10 years since the launch of the RepRap self-build hobby machines in 2005. These cheap machines with open source software has allowed hobbyists and engineers to invest in the technology at home and in small offices.

The boom lead to a number of competitors copying the technology and then an increased number of materials on offer. Initially limited to thermoplastics such as PLA (Polylactic acid), ABS (Acrylonitrile Butadiene Styrene) and Nylon, now materials include high percentages of fillers such as wood and metal to generate different material finishes and properties. In 2015 the German company INDMATEC [1] (now Apium) produced the first FDM PEEK material.

FDM PEEK

PEEK is a popular material to choose when looking for a vacuum compatible plastic; it has low moisture absorption, good stability and is very strong compared with other plastics. Its most useful property is the high temperatures it can withstand, thus enabling PEEK components to go through the vacuum bake out process.

Having the ability to produce complex parts locally and quickly would clearly be a benefit. However, the common low cost FDM machines cannot reach the temperatures required for the production of PEEK parts.

Specialised FDM machines have been produced to combat the issues with high temperature heads, heated beds and enclosed build areas.

Vacuum Testing FDM PEEK

The vacuum group at Diamond tested 19 samples supplied by Apium. The samples were specified by Apium as 100% build density and were in the form of flat tensile test samples with a surface area of 1.42 cm^2 each.

Testing the samples uncleaned, as delivered direct from the supplier, the outgassing rate reached 1.33×10^{-6} mbar l s^{-1} cm^{-2}. Ultrasonic cleaning in IPA (Isopropyl alcohol) made the outgassing increase to 1.7×10^{-6} mbar l s^{-1} cm^{-2}. After baking at 150⁰ C for 12 hours the outgassing rate improved significantly to 3.98×10^{-11} mbar l s^{-1} cm^{-2} meeting our specifications for use in UHV.

These results compared favourably to machined PEEK components and it is possible that they could be baked longer to improve outgassing rates.

Forming Components Using FDM PEEK
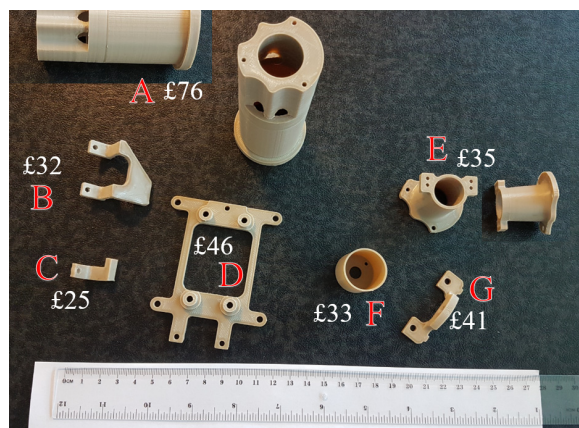
Figure 1: PEEK components produced using FDM, with costs in sterling 2017.

Seven components were ordered from Apium and a visual and dimensional inspection was carried out on five of them (A-E).

The visual inspection clearly showed some build issues:
- Poor surface finish
- Unpredictable distortion
- Unpredictable component shrinkage

Detailed inspection reports were carried out on the components using a CMM. Although many feature dimensions were within tolerance, components B, C and D (Figures 1 and 2) were distorted and warped by up to 1 mm in the extremes. Component E showed no signs of warping and most dimensions within ±0.1 mm. Component A showed no signs of warping, but the internal diameter was 1 mm undersize and the outer flange diameter 0.5 mm oversize.

Surface finishes also varied considerably; the base plate build surface came out polished while all other external

STAINLESS STEEL VACUUM CHAMBERS
FOR THE EBS STORAGE RING

P. Van Vaerenbergh[*], J.-C. Biasci, D. Einfeld, L. Goirand,
J. Léonardon, H. P. Marques, J. Pasquaud, K. Scheidt,
ESRF, 38000 Grenoble, France

Abstract

The upgrade of the ESRF (ESRF-EBS) is a highly challenging project in many respects. One major challenge is to manufacture vacuum chambers within extremely tight tolerances. Indeed, the chamber envelope is constrained by the very limited space available between the beam stay clear and the magnets pole tips, requiring profile tolerances of just 500 µm over the full length of the chamber for a width of 55 mm. An additional challenge is guaranteeing the perpendicularity (up to 0.75 mrad) between the CF flanges and the chamber body. While a design using discrete removable absorbers was chosen, one family of chambers contains a distributed absorber required to protect the insertion devices from 600 W of upstream dipole X-rays. Two companies have been selected to produce a total of 296 stainless steel chambers. Given the unusual tolerance requirements, the manufacturers have been obliged to adapt and develop their production techniques to overcome the challenges. During manufacture, vacuum leaks were discovered on some of the BPM buttons. This paper will also present the two techniques that ESRF has developed in order to prevent the integration of potentially leaking buttons.

INTRODUCTION

After the successful delivery of the first phase of the upgrade programme in the period 2009-2015, the ESRF launched in May 2015 the ESRF – Extremely Brilliant Source (ESRF – EBS) project [1, 2]. This ambitious 150 M€ programme aimed, amongst other things, to construct and commission a brand new 844 m circumference ESRF-EBS storage ring. The goal is to increase by a factor of 100 the brilliance and coherence of the beam whilst reducing by 20 % the electrical cost of operating the storage ring.

In 2015, the Mechanical Engineering Group of ESRF initiated the design and calculations for the EBS project vacuum chambers. The design difficulties of these chambers included the narrow aperture constraint within the magnets, the density of equipment (free space between magnets within a cell is 3.4 m instead of 8 m previously), the overall ring impedance budget and synchrotron radiation handling.

---

* email address: vanvaer@esrf.fr

GENERAL DESIGN OF A STANDARD CELL

Besides the exception of the injection cell, all 32 cells of the storage ring share an identical vacuum chamber shape (with minor variations in the diagnostic equipment installed on some chambers that replaces the generic CH12).

The design phase led to a set of 424 vacuum chambers of which 296 were designed in 316LN stainless steel and 128 in 2219 aluminium alloy. Aluminium vacuum chambers are equipped with bimetal Conflat flanges (custom made from the chamber supplier by explosion bonding) [3]. All BPM blocks are part of the stainless-steel vacuum chambers. Some of the stainless-steel chambers can also accommodate fast correctors operating at high frequencies that cannot be installed on aluminium chambers due to the Eddy current. Figure 1 presents the general layout of a cell as well as the associated vacuum assembly.

DESIGN OF THE CHAMBERS

Space constraints and tight tolerances were the major challenges in the chamber design and production. The chambers were made as large as possible within the magnets, using anti-chambers to improve conductance and discrete absorbers to collect the synchrotron radiation. The limited available space also restricts the locations where vacuum chamber hardware such as flanges, bellows, pumps and the diagnostic equipment can be installed. Typically, the stainless-steel chambers have an "elliptical shape" with variable dimension antechambers to provide the path for X-ray extraction. The wall thickness is 1.625 mm with reinforcement at the location of the antechambers. In order to fit inside the magnets, a strict geometrical tolerance of the profile was compulsory. Figure 2 shows that for 55 mm width, and over the full length of the chamber, we have limited the shape deviation to 500 µm. Such tolerances have been verified, during the Factory Acceptance Tests, by using customised "Go-No-Go" jigs [4] and CMM (portable of fix devices).

Electron beam welding has been widely used to limit the distortion of the 316LN sheets during the welding process.

The stainless-steel chambers family has been split in two categories, the "High Profile" and the "Low Profile" (see Fig. 2 and Table 1). The vacuum chambers pass through the inside of the lattice magnets (quadrupoles, sextupoles, octupoles) with a minimum clearance smaller than 1 mm. This limited space has to accommodate the bake-out environment, the manufacture tolerances and the alignment errors (see Fig. 3).

METAL 3D ADDITIVE MACHINING FOR IN-VACUUM BEAM INSTRUMENTATION

R. Veness, W. Andreazza, D. Gudkov, A. Miarnau Marin, S. Samuelsson,
CERN, Geneva, Switzerland

Abstract

3D additive machining by selective laser melting (SLM) has great potential for widespread use in the field of accelerator instrumentation. However, as with any new process or material, it must be adapted and qualified for use in the specific in-vacuum accelerator environment.

This paper outlines recent developments of this technology for beam instrumentation in CERN accelerators. It covers topological optimisation, design and production methods for SLM, validation and testing of samples and components to qualify the production process. It also reports on experience with operation in multiple machines.

INTRODUCTION

The CERN Beam Instrumentation Group manages more than 2000 in-vacuum instruments across the whole accelerator chain with several hundred different designs. With tens of designs in progress at any time for consolidation and new projects, there is a strong interest in taking advantage of emerging technologies and processes that offer either enhanced functionality or more cost effective production.

SLM offers both of these possibilities, allowing for the simple and rapid production of forms that are not readily machinable. In addition, it is a process that is well suited to the small series of parts generally required.

The capital cost of metal SLM equipment is falling rapidly and desktop plastic 3D printing equipment allows easy prototyping.

SLM LIMITS AND QUALIFICATION

There are a number of well-documented constraints that apply to SLM. Typical powder grain size of 30 μm limits feature sizes and wall thicknesses to a minimum of ~0.4 mm, as a minimum number of fused grains are required to ensure mechanical integrity. This also limits achievable surface roughness without post-machining to Ra 12.5 (ISO N10). Tolerances are limited by thermal deformations and component design, but typically are not better than 0.1 mm between two separated points. Although many geometries that are not possible using conventional machining can be produced by SLM, some forms, particularly flats parallel to the plane of product build-up are not possible. Thus an understanding of the production process is needed by the designer. A specific training course for CERN designers on 3D additive manufacture was therefore organised with a manufacturer.

Additional constraints are imposed by the application of the final component to an in-vacuum, accelerator environment. SLM uses a powder semi-product of which only a small fraction is integrated into the part. The rest is re-used in successive cycles, sometimes up to 20 times. This recycling was considered a risk factor for introducing impurities into the powder, particularly as it is an abrasive dust manipulated by technicians with plastic gloves. Any powder sintering process such as SLM tends to produce products with some porosity and reduced mechanical strength compared with smelted materials. This could also cause problems of virtual leaks if pores are open.

In order to address these potential issues, three cuboid samples were produced using SLM with dimensions $2 \times 2 \times 1$ cm. One sample was made with new powder the second with powder after 10 re-uses and the third with powder after 18 re-uses. They were tested on a standard 'vacuum qualification' bench at CERN, measuring outgassing rate via pressure variation across a known conductance and measuring gas spectra with a Residual Gas Analyser (RGA) [1]. No difference was seen between the three samples either for outgassing or in the RGA spectrum, within the limits of the measurement (1.55×10^{-8} mbar.l.s^{-1}.cm^{-2}, limited by the background outgassing). A further test, putting all three samples together gave a value for total outgassing of 6.23×10^{-9} mbar.l.s^{-1}.cm^{-2} H$_2$0 equivalent after 10 hours of pumping. The pump-down curve showed a 1/t slope, typical of a clean, unbaked, metallic surface. The RGA was also typical of an unbaked, metal surface with mass elements greater than 44 all 4 orders of magnitude below the 18 (H$_2$O) peak, indicating no heavy contamination (see Figure 1).
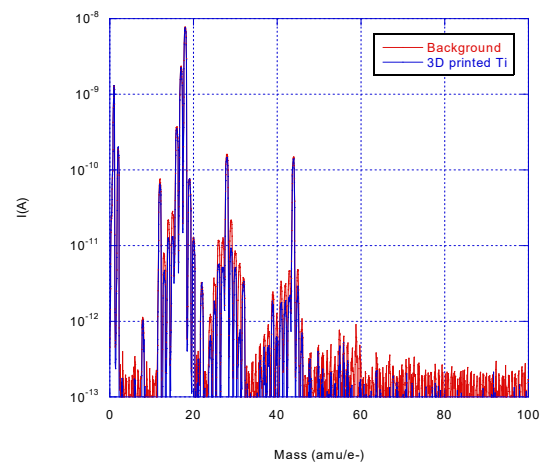

Figure 1: RGA scan of titanium blocks made by SLM from 'recycled' powder blocks.

A NEW SEALING TECHNOLOGY FOR HIGH PRECISION WIDE OPEN UHV VACUUM FLANGE AND WAVEGUIDE CONNECTIONS WITH METAL GASKETS

S. Vilcins*, M. Holz, DESY, 22607 Hamburg, Germany
D. Bandke, DESY, 15738 Zeuthen, Germany

Abstract

The European-XFEL X-Ray laser facility is located in Hamburg. Since its commissioning in September 2017, this large X-ray laser opens new research opportunities for industrial users and scientists. For many beam diagnostic devices ultra-high vacuum components with high mechanical precision and additional strict requirements on particle cleanliness were produced. A vacuum chamber for the bunch compressor (BC) with a cross section of 400 mm*40.5 mm made of stainless steel blocks 1.4429 (316 LN) has been installed. These chambers have integrated flange-connections for large VATSEAL® gaskets. The tolerances for these flanges are extremely tight to ensure save vacuum tight sealing.

This contribution will report of a new technology for such large rectangular or other large flange surfaces. Furthermore this contribution will compare the present with this new technology. This new technology can be used as well for other vacuum flange metals like aluminium or titanium. Using of this technology for applications under special conditions, like particle free applications due to the non-lubricated conditions, are conceivable.

INTRODUCTION

The European X-ray Free-Electron Laser (E-XFEL) [1] is a 3.4 km long international facility, starting from DESY in Hamburg/Lurup and ending in Schenefeld (Schleswig-Holstein) in Germany. The bunch is compressed in two of three magnetic chicanes by factors of 20 and 5, respectively. Details about the chicane properties can be found in [2].

Particle accelerators like the E-XFEL are using various beam diagnostics, e.g. Beam Position Monitors (BPM) for measuring the beam orbit and diagnostics to measure longitudinal beam properties [3]. The XFEL bunch compressor (BC) incorporated three magnetic chicanes. These BC's are equipped with large vacuum chambers to ensure a beam transport with no losses under different conditions. In each of the straight sections of BC 1 and BC 2 beam diagnostic elements are located, namely an 'Energy' BPM (BPMS) and an Optical Transition Radiation (OTR) station. The vacuum chamber for these devices had to be extended to a rectangular cross section of 400 mm * 40.5 mm to fit the large vacuum beam pipe. This big cross section causes a new sealing technology of the vacuum

chambers and their flanges. The flange connections have to be leak tight up to Ultra-High-Vacuum (UHV) properties better than $1*10^{-10}$ mbar leak rate.

GASKETS FOR NON-SYMMETRICALLY APERTURES

For wide open or non-symmetrically flange apertures flange connections with VATSEAL [4] gaskets are used, instead of normal Conflat (CF) with copper gasket rings. VATSEAL connections are made for special vacuum connections, RF structures and as well as for synchrotron beamlines. Further requirements for all-metal seal connections with VATSEAT gaskets are low permeation, low outgassing, baked-able, no hydrocarbons, low particle emission and radiation resistive. Figure 1 shows a few VATSEAL gaskets.
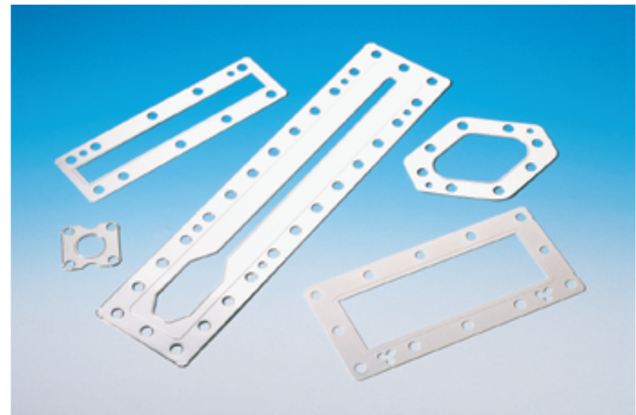
Figure 1: VATSEAL gaskets from VAT, CH [4].

A VATSEAL gasket consists of an all-metal gasket with a raised, contiguous "gasket lip" on both sides. The cross section of the raised sealing strip is highly precise and designed to follow the real vacuum outline, close to the inner diameter. Most of VATSEAL gaskets are conceptual costumer design. The major factor of reliable vacuum connections is the quality and appearance of the stainless-steel flange surfaces. The applied manufacturing process after machining vacuum chambers is a handmade process step! This technology will be described in the next chapter before the new technology will be discussed.

---

* silke.vilcins@desy.de
® Trademark of http://www.vatvalve.com/home

PRELIMINARY DESIGN OF THE MAGNETS OF HALS*

Bo Zhang[†], Zhiliang Ren, Hongliang Xu, Xiangqi Wang, Wang Yong
University of Science and Technology of China, Hefei, Anhui, China

Abstract

The Hefei Advanced Light Source (HALS) is a future soft X-ray diffraction-limited storage ring at National Synchrotron Radiation Laboratory (NSRL) of China. This project aims to improve the brilliance and coherence of the X-ray beams and to decrease the horizontal emittance. The lattice of the HALS ring relies on magnets with demanding specifications, including combined function dipole-quadrupoles (DQs) with high gradients, longitudinal gradient dipoles (DLs), high gradient quadrupoles and sextupoles. All these magnets have been designed using Radia and POSSION, as presented in this paper.

INTRODUCTION

Hefei Light Source (HLS) at National Synchrotron Radiation Laboratory is a dedicated secondary generation VUV and soft X-ray light source. The upgrade of HLS was completed in 2014 and the performance has been improved a lot. With the development of accelerator technologies and requirements from the user community, a new light source named Hefei Advanced Light Source (HALS) was brought forward about three years ago. HALS will be a soft X-ray diffraction-limited storage ring. Pre-research project of HALS was funded by Chinese Academy of Sciences and Anhui Province of China in 2017. Most key technologies, such as lattice design, vacuum, magnet, radio frequency, will be studied in the next two years.

According to the accelerator physics design, longitudinal gradient dipoles, combined dipole quadrupoles, quadrupole and sextupole magnets will be studied and prototypes of them will be constructed. Preliminary design of them will be stated in this paper.

STORAGE RING OF HALS

The lattice of the HALS has been studied using a new concept of multi-bend achromatic (MBA), locally symmetric MBA, which can promise large dynamic aperture and momentum acceptance [1,2]. Main Parameters of the HALS is shown in Table 1. It should be noted that the lattice is still evolving, and the parameters will be changed with it.

Table 1: Main Parameters of HALS

Parameter	Value	Units
Energy	2.4	GeV
Average current	300	mA
Natural emittance	18.4	pm·rad
Circumference	~680	m
Number of cells	32	-
Long straight section	5.1	m
Energy loss per turn	220	keV

MAGNETS OF HALS

In the MBA lattice of HALS, high gradient quadrupole magnets are used to compress the beam emittance, sextupole magnets are used to correct the chromaticity, longitudinal gradients dipole magnets (DLs) are used to bend the beam and weaken the negative effect of sextupole on dynamic aperture, and combined dipole-quadrupoles (DQs) are good for saving space. The magnets need to be studied are shown in Table 2.

Table 2: Magnets of HALS

	DL	DQ	Quad	Sextu
Field strength	0.2~0.5T	0.5T 25T/m	80T/m	4000T/m^2
Bore diameter		26 mm		
Reference radius		3 mm		
Homogeneity	5×10^{-4}	5×10^{-4}	5×10^{-4}	1×10^{-3}

All magnets except the DL should be optimized to improve the field quality. The shape optimization method developed in ESRF [3] was adopted. Pole profiles of the magnets are parameterized using Legendre polynomials. A cost function such as the sum of multipole field are reduced with Newton-Gauss iteration until the optimized profile is obtained.

Longitudinal Gradient Dipole

Permanent magnets (PM) have drawn much attention in recent years, although there exist some challenges such as the variation of remanent field with the temperature and radiation damage. The greatest advantage of PM is the almost zero operation cost. So, we design a PM based longitudinal gradient dipole, as shown in Fig. 1.

The DL magnet has seven modules. All modules have the same gap and pole shape but are filled with different amounts of permanent magnet volumes to achieve the longitudinal field gradient. The PM material used for the

THE DESIGN OF LCLS-II PHOTON BEAM CONTAINMENT SYSTEM

H. Wang*, Y. Feng, S. Forcat Oller, J. Krzywinski, E. Ortiz and M. Rowen
SLAC National Laboratory, Menlo Park, USA

Abstract

LCLS-II will produce very powerful and collimated FEL photon beams. Unlike conventional synchrotrons, the LCLS-II beam containment components withstand not only the high average beam power and/or power density, but also the instantaneous thermal shocks from the pulsed beam structure, which can potentially reach 9mJ/pulse. With a beam repetition rate up to 1MHz, regular metal based beam collimators and absorbers used in synchrotrons will no longer work, because of the likelihood of fatigue failure. And because of the poor thermal conductivity, the old LCLS B4C based absorber would need very shallow glancing angle and take valuable beamline space. Hence, a low-Z and high thermal conductivity CVD diamond based photon beam collimator and absorber systems have been developed in LCSLII. The initial damage tests using LCLS FEL beam provided positive results that graphite coated CVD diamond can endure per pulse dose level to 0.5eV/atom. For the beamline and personnel safety, in addition to the passive CVD diamond collimators and absorbers, newly developed photon diode beam mis-steer detection systems and conventional SLAC pressurized gas burn-through monitors have been also introduced in the photon beam containment system design.

INTRODUCTION

At a typical third generation synchrotron light source, the photon beam divergence can range from a few mrads for undulator beamlines and up to 10 mrad for some wiggler beamlines. The beam containment systems are designed to trim the beam divergence and define a beam size that can be accepted for experiments, as well as addressing the beam mis-steering conditions. It is not the same case for LCLS-II photon beams, which have divergence ranging from a couple of μrad to a few tens of μrad and highly coherent. The conventional scheme for containing a synchrotron photon beam won't be appropriate for the LCLS-II photon beams. On the one hand, the collimators or apertures for LCLS-II are not used to define the size of the beam, and in contrary, the photon collimators apertures try to stay clear from the beam to avoid generating noises for the experiments. On the other hand, the collimators are still needed to contain the beams in case of beam mis-steered away from its normal course, i.e. the golden trajectory. Moreover, due to the FEL beam pulses may carry tremendous power that can damage most materials by single shot ablations, and high repetition rates (up to 1MHz) may cause the fatigue failure for most of the metals even for lower beam fluences. Therefore, low atomic weight (low-Z) materials that can tolerate thermal shocks with high repetition rates may be suitable for the

construction of beam containment component. B4C is one of the low-Z materials used LCLS and other FEL facilities. However, because the LCLS-II beam can potentially have up to 880W of integrated power, good thermal conductivity becomes necessary for the application. In the meantime, large and thick chemical vapor deposition (CVD) diamond has become economically viable, hence, it has been chosen as the major heat absorption material [1].

In this article, firstly, a brief description of engineering design and analysis of the CVD diamond based beam containment components, i.e. collimators and stoppers, are presented. Secondly, in order to detect a breach caused by the FEL beam to the collimators and stoppers, diode and gas based sensing systems are also integrated with the design. And finally, the basic working principle of the photon beam containment system is briefly described.

LCLS-II BEAM PARAMETERS

Table 1 and Table 2 show the beam parameters that can produce the most thermal loads to the devices. In some extreme cases, the power load on the collimator upstream can be up to 1000 W/mm². For the soft-xray beamline, single pulse fluence (up to approx. 9mJ/pulse) may even induce damages that are not purely due to thermal effects, but directly breakdown of the bond between atoms.

GRAPHITE COATED CVD DIAMOND PHOTON ABSORBERS

To further improve the thermal shock resistance, a thin pyrolytic graphite is coated on all sides of the diamond used in collimators and stoppers. Figure 1 shows the transient behavior of a single pulse FEL beam hits the diamond absorber with 4μm coating. One can see that the sharp instantaneous temperature rise is located in the thin graphite coating. The temperature in diamond doesn't have this sharp rise. Figure 2 shows one of the damage tests done to the graphite coated diamond by taking LCLS beam with a fluence of approx. 0.6 ±0.15eV/atom. After 100,000 shots, one can visually observe the footprints of the beam, but no obvious morphological damage to the coating [2].

Figure 3 shows an absorber assembly with graphite coated CVD diamond and light-tight box installed.

A BRIEF DESCRIPTION OF LCLS-II PHOTON BEAM CONTAINMENT SYSTEM

Even equipped with graphite coated diamond absorbers, under extreme conditions, a few photon collimators upstream won't survive the extreme heat loads and ablations. As described previously, under normal operation conditions, the

---

* hengzi@slac.stanford.edu

Core technology developments

New Technologies

INVESTIGATION OF REGULATION PLAN FOR THE VIBRATION UTILITY EQUIPMENT OF HEPS

Fang Yan[†], Gang Xu, Zhizhuo Wang, Daheng Ji, Yi Jiao, Chunhua Li
Key Laboratory of Particle Acceleration Physics and Technology, Institute of High Energy
Physics (IHEP), Chinese Academy of Sciences, Beijing, China
Qilong Sun, Longwei Lai, Zhiqiang Jiang, Shanghai Institute of Applied Physics (SINAP),
Shanghai, China

Abstract

For the third or fourth generation synchrotron light sources, the brilliance of the x-ray beam is 2 to 3 orders higher than other generations, and in the meanwhile the beam emittance is at least one order smaller. To ensure the stability of the beam, the vibration caused beam motion is usually controlled to be within 10% of the RMS beam size. Thus the smaller beam emittance is, more restrict of the regulation plan to the vibration sources should be. Inside of the light source site, one major vibration source is the utility equipment such as water pump, compressors and so on. There are two controlling approaches for the vibration amplitude of those sources, one is damping, and another way is decay. However reasonable specification is the key of the controlling method. This work will present the detailed establish process of the regulation plan for HEPS in China.

INTRODUCTION

Currently, the low emittance storage ring has considered being the future development direction of the photo sources. However, with the decreasing of the designed emittance of the ring, the problems caused by the ambient ground motion have been increasingly highlighted. Delicate research has to be done during the design stage for the inducing beam instabilities caused by those sources. HEPS has a very challenging beam stability requirements with the transverse beam emittance specification of 0.1 nm.rad and designed natural emittance of ~0.03nm.rad while the effective vertical emittance of ~5pm.rad [1-2]. To ensure the stability of the beam on the experimental station, the vibration caused beam size increment has to be controlled being smaller than 10% of the RMS beam size. Thus, according to the current designed 34pm.rad lattice, the RMS beam position and angular motion has to be smaller than 1μm & 0.2μrad, 0.3μm & 0.1μrad, transverse and longitudinal respectively. [2] Special cares are mandatory in developing site vibration specifications, stable building design concepts, and passive and active ways to minimize effects on the stability of the photon beam and critical accelerator and beamline components caused by ambient ground motion sources.

To investigate the vibration influence to the beam, one has to identify the critical vibration sources, including the Egan frequencies and the amplitudes of the vibrations. There are two controlling approaches for the vibration amplitude of those ambient ground sources, one is damping,

---

† yanfang@ihep.ac.cn

and another way is decay. The vibration amplitude attenuate with distance as it propagates along the ground from the source to each element of the main ring with certain speed. The ambient ground motions caused by all sources transmit through the slab and girder-magnet assembling inducing orbit instability of the beam. Usually these two methods have to be combined together to realize the final specifications, and the damping level is determined, to some extent, by the decay ability of the HEPS ground. Once the critical vibration sources are identified and the decay of the vibration on HEPS ground is measured, the specification and regulation plan for the ambient ground motion of HEPS could be established.

AMBIENT GROUND MOTION SOURCES

The ambient ground motion includes ground motion of the HEPS site and other ambient motions caused by critical vibration sources around the HEPS ring including utilities (such as pump, compressor, air conditioner et. al), machine related vibrations sources (such as pulsed booster magnet, water flow et. al) and cultural noises which has day-night cycle (such as traffic and other human activities). The former one has been introduced in another paper [3], this paper will only focus on the latter one.

2 Hz Booster

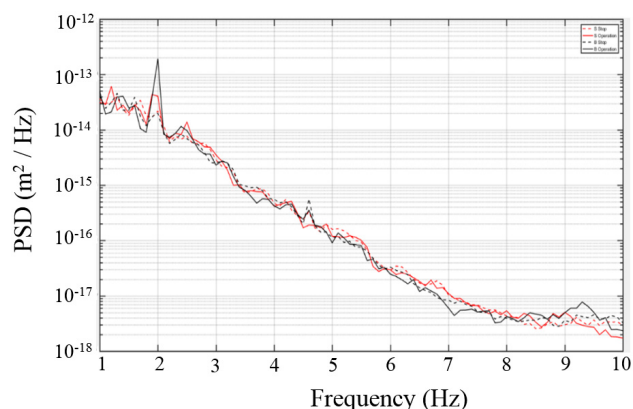Figure 1: The black line and dash line represent PSD spectrum (in x direction) measured at booster derivation part while booster on (real line) and off operation (dash line) respectively, the red line and dash line represent PSD spectrum on main ring ground while booster on (real line) and off operation (dash line) respectively.

The HEPS booster will be operated on pulsed mode with repetition rate of 2Hz. As the AC dipole of the

A NOVEL ATTEMPT TO DEVELOP A LINEAR POLARIZATION ADJUSTABLE UNDULATOR BASED ON MAGNETIC FORCE COMPENSATION TECHNOLOGY *

W. Zhang[†], Y. Zhu, Shanghai Institute of Applied Physics, CAS, Shanghai, China

Abstract

A linear polarization adjustable undulator is proposed in this paper. This undulator can reach 1.5T magnetic peak field with a period length 68mm and magnet length 4m. By adding two repulsive magnet arrays beside centre array the magnetic force between girders can be reduced from 70kN to near zero. Such an approach can result in a significant reduction of the undulator volume, simplification of the strong back design and fabrication. By means of rotating through the centre of undulator we can achieve magnetic field from vertical orientation to horizontal orientation. The linear polarization of radiation can be adjusted between zero and 90 degree.

INTRODUCTION

In majority of linear polarized PM undulators operating in synchrotrons and FELs, magnetic field strength is controlled by varying the gap between magnet arrays by moving arrays in vertical plane. Usually, arrays are mounted using rails on C-shape strong back. The C-shape enables lateral access to magnetic field region. Because of magnetic forces between arrays are very strong and required precision for the gap control is very high, the strong back structures must be extremely rigid. To provide such rigidity, these structures are usually built with massive and heavy components. As a result, gap varying undulators are very large, heavy and quite expensive.

There are three different method have been developed to cancel the attractive force [1-5]. One is the mechanical system composed of a number of springs having different lengths and coefficients attached to the both sides of the main magnets, which was applied to an in-vacuum wiggler developed at Synchrotron SOLEIL and SSRF for CLS. Spring-8 suggested that adding magnetic system composed of two rows of magnet array generating a repulsive force attached to the both sides of the main magnets. None of them led to a reduction in undulator dimensions or noticeable simplification of the undulator mechanical system. APS used a custom-designed conical spring system for the dynamic compensation of the undulator magnetic forces and achieved vertically polarized radiation in one 3.4-meter-long undulator prototype [6]. Such an approach resulted in a significant reduction of the undulator volume, simplification of the strong back design and fabrication but needed dozens spring tuning and calibration work.

Table 1: U68 Specifications

Periodic Length	68 mm
Length/Segment	4.0 m
Number of Periods	58
Maximum Field	1.5 T
Minimum Gap	7.2 mm
Nominal Gap	7.5 mm
Maximum Gap	80 mm
Magnet Material	NdFeB
Magnet Structure	PPM
Beam Deformation	Less than 10μm

In this paper we propose a relative compact undulator design based on Spring-8 suggestion that using repulsive magnet arrays method. Thanks to the magnetic force cancellation for all gap range 7.2-80 mm we design a very compact and thin aluminum alloy girder 80mm thickness as magnet array base beam. The deformation of the beam is just from gravity-induced deformation which is stable 5μm as the magnetic gap changes. The C-shape strong back can be simplified and the whole undulator can be weight loss less than 2t. The undulator mechanical system designed can be rotated around the centre axis. We can achieve magnetic field from vertical orientation to horizontal orientation. The linear polarization of radiation can be adjusted between zero and 90 degree.

CRITICAL DESIGN FEATURES

This U68 has 58 periods with period length 68 mm corresponds to six standard Halbach-type magnet arrays which consist of two centre magnet arrays provided the magnetic field 1.5T and four magnet arrays beside the centre arrays above and below to produce repulsive force. The specification of the undulator is list in Table 1.
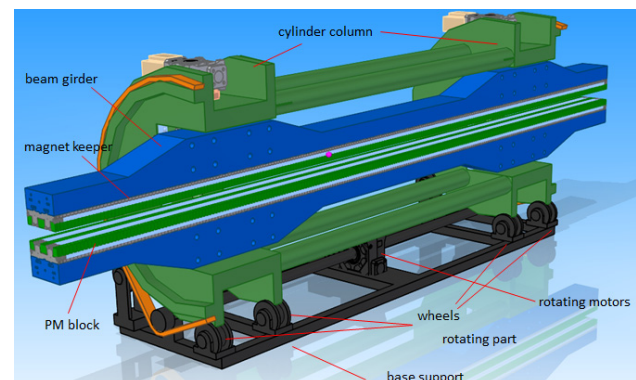

Figure 1: Overview of undulator structure: (1) –cylinder column; (2) -permanent magnet blocks soldered to aluminum keepers (3); (4) – beam girder ;(5) – base support

---

THE LNLS METROLOGY BUILDING – ENVIRONMENTAL CONTROL RESULTS*

H. G. P. de Oliveira†, M. Bazan, C. S. N. C. Bueno, L. Sanfelici, LNLS, Campinas, Brazil

Abstract

Modern synchrotron light sources require high mechanical stability throughout its facilities, frequently demanding characterization processes in the micro and nanometer scales. In this context, the Brazilian Synchrotron Light Laboratory (LNLS) built a new facility with several controlled environment rooms to minimize disturbances during optical and mechanical metrology procedures and to support advanced instrumentation development for the new Sirius' beamlines. The building design imposed very strict requirements regarding temperature, humidity and particles. This work presents the environmental control validation results and the floor vibration assessment enlightening the influence of the building machinery. Temperature variations below ± 0,1 °C were successfully achieved for all rooms, relative humidity is also better than 50 ± 5 % and the floor RMS displacement did not exceed 15 nm. The building is fully operational since early 2017 and currently hosting several tests on monochromators, mirrors, front-ends and many other systems for the Sirius beamlines.

INTRODUCTION

Sirius is a 4th generation 3 GeV synchrotron light source currently under construction [1] by the Brazilian Synchrotron Light Laboratory (LNLS), designed to provide high brilliance and coherent flux based on a 5-bend achromat lattice with 0.25 nm·rad natural emittance [2,3]. The beamlines of this new generation synchrotron have started to be designed with highly demanding requirements to preserve the extraordinary properties of the source. To achieve such requirements, it is necessary to develop high-end mechanical and optical elements and instrumentation able to guarantee precision and stability during beamline operation. However, before installation of any instrumentation in the beamlines, it is necessary to validate the equipment performance, which can only be done with precision metrology. Also, to take reliable measurements, several parameters must be considered, like the uncertainties of the measurement equipment, the test setup and the environmental disturbances, which can be related to temperature stability, air convection and turbulence, air cleanness, atmospheric pressure and humidity, and vibration [4].

This paper describes the environmental control results of the new LNLS Metrology Building, whose design concepts were detailed at the 2016 MEDSI Conference [5]. Also, the performance of the inertial bases/floor on top of which the metrology laboratories were installed is presented considering the influence of the building machinery.

PROJECT REQUIREMENTS

The LNLS Metrology Building was designed following a layer-based architecture, in which the outer layers have a proper environmental control that contributes for the stability of the inner ones. The goal of this architecture is to provide the laboratories (inner layers) a highly stable environment, minimizing the influence of the large thermal and humidity variations that may naturally occur outside the building [5]. The building contains three layers and each of them has one or more rooms controlled by independent air handling units (AHUs). The design requirements for each area inside the building are presented at Table 1:

Table 1: Environmental Requirements

Room	T [°C]	RH [%]	Particle
Building Shed	23±1.5	-	-
Assembly Room 1	22±1.0	50±10	-
Assembly Room 2	22±0.5	50±10	-
Mech. Metrology	22±0.1	50±5	-
Optical Metrology	22±0.1	50±5	ISO 7
Gowning Room and Buffers	22±0.1	50±5	ISO 8

ENVIRONMENTAL CONTROL RESULTS

The whole layer concept efficiency is based on stabilizing an outer layer to diminish the external thermal load on the inner layers walls. Aiming to that result, the first system tuned was the main shed, which has the more relaxed requirements and where more general and less precise tests take place. Figure 1 shows the comparison between the shed and external temperature variation, measured along a day. All the results displayed on this paper refer to the same day, 28/04/2018.
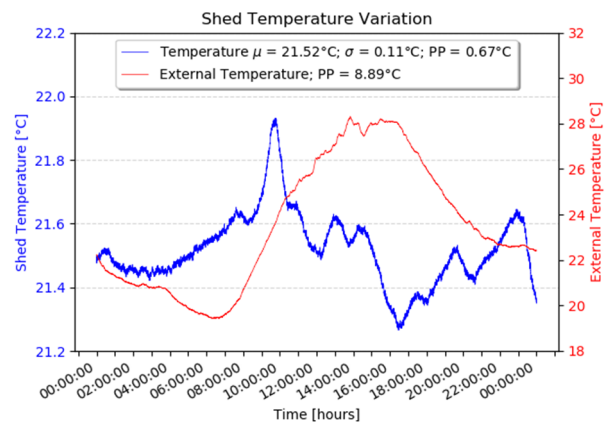

Figure 1: Temperature variation inside and outside the Metrology Building over one day.

THE STATUS OF THE NEW HIGH-DYNAMIC DCM FOR SIRIUS

R. R. Geraldes[†1], R. M. Caliari, G. B. Z. L. Moreno, M. Saveri Silva, L. Sanfelici,
H.C.N. Tolentino, H. Westfahl Jr., Brazilian Synchrotron Light Laboratory (LNLS),
Brazilian Center for Research in Energy and Materials (CNPEM), Campinas, São Paulo, Brazil
T. A. M. Ruijl, R. M. Schneider, MI Partners, Eindhoven, The Netherlands
[1]also at Technische Universiteit Eindhoven, Eindhoven, The Netherlands

Abstract

The monochromator is known to be one of the most critical optical elements of a synchrotron beamline, since it directly affects the beam quality with respect to energy and position. Naturally, the new 4th generation machines, with their small emittances, start to bring higher stability performance requirements, in spite of factors as high power loads and variations, high radiation levels, ultra-high vacuum compatibility and vibration sources. In response to that, an innovative concept of a high-dynamic vertical DCM (Double Crystal Monochromator) with angular range between 3 and 60 degrees (equivalent to 2.3 to 38 keV with Si(111)) has been developed at the Brazilian Synchrotron Light Laboratory. A highly repeatable dynamic system, with servo control bandwidth of 250 Hz, has been achieved and will be installed at Sirius macromolecular crystallography beamline – MANACA – still in 2018. The complete offline results of the in-vacuum cryocooled high-dynamic DCM, showing stability between crystals around 15 nrad RMS up to 2.5 kHz, even during the Bragg angle motion for flyscans, are presented.

INTRODUCTION

The beamlines of the new generation of synchrotrons, the so-called Diffraction Limit Storage Rings (DLSR), have started to be built with ever more demanding requirements to preserve the extraordinary properties of the sources. In double-crystal monochromators (DCMs), the main performance bottleneck has been proven to be the stability of the parallelism between the two crystals, since it affects the position of the virtual source with a scaling factor given by the distance to the source, which is typically about 30 m [1]. Indeed, for sources of a few microns, this angular stability must be kept within a few nrad to keep the variation of the virtual source within about 10% of its size.

Considering the frequency range between 0 and 2.5 kHz, figures as low as 20 nrad RMS (root mean square) have been reported for horizontal DCMs [2], whereas for vertical DCMs the best performances seemed to be stuck around 50 nrad RMS [3]. Yet, it must be noticed that still today most of the available data about DCMs unfortunately cannot be directly compared to each other. This is because, although for given disturbance levels the outcome of a measurement does strongly depend on acquisition parameters like frequency and integration time, the RMS values are hardly ever displayed as a function of frequen-

cy, but often mentioned as single numbers without further acquisition details. This means that many official numbers show averaged optimistic values, which may not be consistent with the needs and timescales of different experiments at the beamlines. Indeed, with experiments reaching the sub-millisecond range, performances in the kHz range must be proven. Moreover, it must be emphasized that even the best results rely on braked systems only, whereas about 100 nrad RMS could be expected in active control [3]. Finally, during energy flyscans, the stability levels may exceed the microradian range. Consequently, to the best of our knowledge, no vertical DCM had been close to the 10-nrad-level performance as required by DLSR beamlines.

Convinced that incremental improvements in traditional systems was insufficient to reach the new requirements, the Brazilian Synchrotron has developed over the last three years an innovative DCM, the so-called High-Dynamic DCM (HD-DCM), an active high-performance mechatronic system with a closed-loop bandwidth of 250 Hz [4]. The conceptual design, the mechatronic principles and thermal management solutions were presented in MEDSI 2016 [5–7]. More recently, the results of in-air validation of the core, together with system identification and control techniques, were presented in ICALEPCS 2017 [8,9]. In the following sections, the most recent updates, together with the offline performance of the full in-vacuum cryocooled system, are presented, showing unprecedent stability and scanning performances.

The HD-DCM is now ready to be tested online and is expected to be installed at Sirius macromolecular crystallography beamline – MANACA – in the second semester of 2018. Sirius is in an advanced construction phase, with the LINAC and the booster currently being commissioned and installed, respectively.

SYSTEM STATUS

Goniometric System

Figure 1 shows the complete system and highlights its sub-modules, including the goniometric system, the vacuum vessel and the granite bench, which were not addressed in previous publications.

As planned from the beginning, the goniometric system was realized by means of double-side bearings, to improve the load capacity and stiffness in a symmetric design. To save development time and costs, a commercial direct-drive ball-bearing rotary stage has

---

† renan.geraldes@lnls.br

SAMPLE STABILIZATION FOR TOMOGRAPHY EXPERIMENTS IN PRESENCE OF LARGE PLANT UNCERTAINTY

T. Dehaeze[1,†], M. Magnin-Mattenet, ESRF, Grenoble, France
C. Collette[1], Université Libre de Bruxelles, BEAMS department, Brussels, Belgium
[1]also at Precision Mechatronics Laboratory / A&M department, Liege, Belgium

Abstract

A new low emittance lattice storage ring is under construction at the ESRF. In this new instrument, an upgraded end station for ID31 beamline must allow to position the samples along complex trajectories with a nanometer precision. In order to reach these requirements, samples have to be mounted on high precision stages, combining a capability of large stroke, spin motion, and active rejection of disturbances. First, the end station will be presented with the associated requirements. However, the precision is limited by thermal expansion and various imperfections that are not actively compensated. Our approach is to add a Nano Active Stabilization System (NASS) which is composed of a 6DoF Stewart platform and a 6 DoF metrology system. A 3D model of the end station updated with experimental data is developed. As the mass of the samples may vary by up to two orders of magnitudes, robust control strategies are required to address such plant uncertainty. The proposed control strategy are presented and applied on the developed model by conducting time domain simulations of tomography experiment in presence of instrumentation noise and system uncertainty.

INTRODUCTION

Within the framework of the ESRF Phase II Upgrade Programme, a new state-of-the-art end station for the high-energy beamline ID31 is under development. Research in many scientific areas such as material and life sciences are increasingly looking for instruments with higher spatial resolution. The design of the new end station will enable many hard X-ray characterization techniques such as reflectivity, wide angle diffraction and diffraction tomography. The need of great versatility induces many constrains on the end station such as combining large stroke ($\approx 10\,\text{mm}$), high precision ($\approx 10\,\text{nm}$) while accepting samples with mass ranging from $1\,\text{kg}$ to $50\,\text{kg}$.

Many positioning end stations have been developed with an increasing positioning precision [1–3].

However, when nanometer precision is needed, thermal expansion and vibrations are becoming the main source of positioning error that cannot be compensated by encoders used for each stage. Therefore, a direct metrology system is usually needed [2].

The aim of this study is to develop a short stroke Stewart platform that actively stabilize the sample position and compensate for all sources of perturbations and imperfection.

---

† thomas.dehaeze@esrf.fr

This paper is organized as follows into three sections. The first section presents the ID31 positioning end station and its associated specifications. The second section is dedicated to the Nano Active Stabilization System (NASS) and the associated metrology frame. A model of the ID31 positioning station is also developed and presented. In the third section, after presenting the control strategy, simulations of tomography experiments are conducted using the developed model. These measurements are used to estimate the performance gain of using such active stabilization system.

ID31 SAMPLE-STATION

In order to position the samples along complex trajectories with a nanometer precision, a versatile positioning platform is developed. A simplified schematic representation of the system is shown Fig. 1.
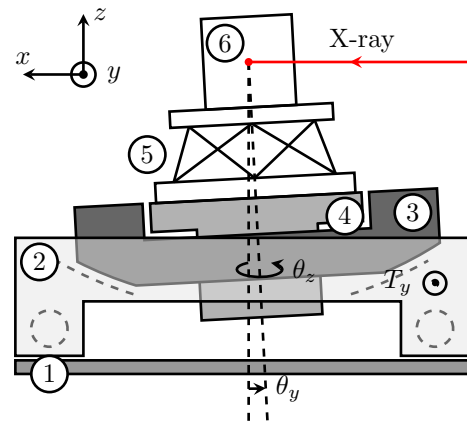
Design

Figure 1: Schematic representation of the ID31 end station. (1) granite, (2) Translation Stage, (3) Tilt Stage, (4) Spindle, (5) Long Stroke Hexapod, (6) Sample.

This platform consists of multiple stacked stages, each of which is described below.

First, a translation stage offers a travel range of $T_y = \pm 5\,\text{mm}$ in the y direction which permits to scan the sample through the X-ray. A linear encoder is used to drive a brushless linear motor in a feedback loop with a Proportional-Integral-Derivative (PID) control law.

A tilt stage then rotates the sample around the y axis by $\theta_y = \pm 3°$. The rotation axis is aligned with the focusing point of the X-ray in order to allow experiments such as X-ray reflectivity. The tilt stage is driven by a stepper motor and a PI position feedback using linear encoders.

HIGH-ACCURACY SMALL ROLL ANGLE MEASUREMENT METHOD BASED ON DUAL-GRATING DIFFRACTION HETERODYNE INTERFEROMETER*

S. Tang[†, 1, 2], M. Li[†, 1, 2], H. Liang[1], W. Sheng[1, 2], J. Yang[2], Beijing Synchrotron Radiation Facility,
Institute of High Energy Physics, Beijing 100049, P. R. China
[1]also at Laboratory of X-ray Optics and Technology, Institute of High Energy Physics,
Beijing, P. R. China
[2]also at University of Chinese Academy of Sciences, School of Physics, Beijing, P. R. China

Abstract

Small roll angle (ROLL) is a crucial parameter for the motion performances of ultra-precision guide way often applied in fine mechanics and instruments of synchrotron radiation, such as long trace profiler (LTP). However, it is difficult to be measured by conventional methods including interferometer and autocollimator owing to their low sensitivities in axial direction. There is an orthogonal dilemma between measured direction and angular displacement plane for ROLL measurement. Therefore, a novel method based on dual-grating diffraction heterodyne interferometer is presented, which uses the combining scheme of diffraction grating and heterodyne interferometer to overcome the orthogonal problem. Moreover, the design of differential structure with dual-grating and grating interferometer instead of pure interferometer is adopted to improve the practicability against the environment, e. g. air fluctuation, inconstant rotation centre. It has inherited advantages of high-resolution up to 2nrad, high sampling rate up to 50kHz, and contactless by mathematical model and analysis. So, theoretical and experimental verifications are both implemented to its validation.

INTRODUCTION

Nano-radian accuracy small roll angle (ROLL) measurement method would be very urgent for the ultra-precision optical metrology and precision instrument [1-5], especially, long trace profiler (LTP). It will be benefit the development of two-dimensional LTP used for the test of X-ray mirrors. Besides, the ROLL is also important issue in the field of the industries, such as Numerical Control (NC) machine tools, Coordinate measuring machines (CMM), advanced manufacturing technology, and precision motion engineering. No matter which field, there is indeed a common technique which is application of precision linear motion guideway pair. But, it is very difficult to achieve high-performance measurement for the ROLL, especially field testing. Because the orthogonal problem of Roll displacement plane and linear motion direction of the

guideway disables the typical methods of interferometer and autocollimator, compared with pitch or yaw measurement, as shown in Fig. 1.
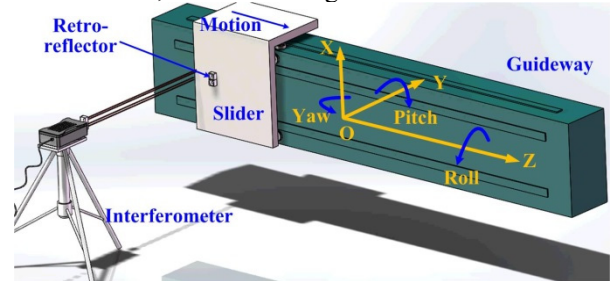

Figure 1: The diagram of angle deviations of the guideway.

So, there are exploration researches on it, such as:

1) Polarization detecting based on interferometry, including intensity [6, 7] and phase sensing [8-15].

2) Using special shape component based on interferometry, such as using wedge prism and its derivative [16, 17].

3) Geometrical transfer test using position sensitive detector (PSD) [18-20].

4) Synthetization of other optical methods [21-24], such as grating interferometer for ROLL measurement.

And there are maybe other instruments like level meter or inclinator. They are all proved the progress in laboratory. However, there is a little far way for practical application, especially, ROLL compensation of LTP and 3-axis NC machine tools or CMM. In this paper, a synthetization dual-grating heterodyne interferometric ROLL measurement method is presented, which uses grating for overcoming the orthogonal problem and heterodyne interferometer for high-accuracy, good stability, high-sampling rate.

CONFIGURATION AND MATHEMATICAL MODELING

As show in Fig. 2, the configuration of proposal method is composed of dual-frequency laser measuring head, polarizing beam splitter (PBS), right-angle prism (RAP), dual-grating, and dual-retroreflector (using RAPs), etc.

A beam emitted by the dual-frequency laser measuring head, containing two orthogonal linear polarized compounds with a stable frequency difference of ~3 MHz, which is split into two beams (called P-beam and

THE DESIGN OF EXACTLY-CONSTRAINED
X-RAY MIRROR SYSTEMS FOR SIRIUS

R. R. Geraldes, G.V. Claudiano, L.M. Volpe, M. S. Souza, A. Sikorski, V. Z. Ferreira, L. Sanfelici, H.C.N. Tolentino, H. Westfahl Jr., Brazilian Synchrotron Light Laboratory (LNLS), Brazilian Center for Research in Energy and Materials (CNPEM), 13083-970, Campinas, Sao Paulo, Brazil.

Abstract

The first set of Sirius beamlines is expected to start operating in early 2019. Regarding X-ray mirror systems, a single design concept has been possible thanks to the standardization of side-bounce fixed-shape mirrors. To preserve the extreme quality of both the mirror figures and the source, the main design targets were minimizing mechanical and thermal distortions in the mirrors while maximizing mechanical and thermal stabilities. A deterministic high-resolution exactly-constrained flexure-based mirror support provides pitch tuning within 100 nrad and resonances above 150 Hz, while dealing with clamping and thermal expansion effects. The adopted cooling strategy was indirect cryocooling via cryostats, drastically minimizing thermal gradients and distortions in the mirrors, decoupling vibration sources and simplifying cooling circuits. Finally, a 5-degree-of-freedom granite bench, based on high-resolution levellers and air-bearing solutions, support the vacuum chamber, on which the internal mechanics is stiffly mounted. The specifications, design and partial results are presented.

INTRODUCTION

The design of mirror systems is one of the most revisited topics in beamline designs, since ever-increasing power management and figure error requirements continuously drive either innovative or optimized concepts, particularly for cooling and figure shaping [1–6]. For many solutions, however, it is often unclear how complex mechanics and cooling schemes may limit performance either in terms of slope errors or mechanical stability.

To comply with height and slope budget errors as low as a few nanometers and tens of nanoradians, respectively, Sirius X-ray mirrors were standardized in fixed-figure configuration, thus preventing the use of benders. Next, looking forward to superior passive mechanical stability, the decision for side-bounce deflection standardization was made. These two conditions, together with generally low absorbed power levels, i.e. below 50 W, have created the opportunity for the development of an alternative standard design for mirror systems, as illustrated in Fig. 1.

From the experience gained with the High-Dynamic Double Crystal Monochromator (HD-DCM) [7], deterministic design concepts have been applied to seek simple yet accurate and highly-stable thermo-mechanical solutions. Details about the vacuum vessel, cryocooling scheme based on cryostats and cooling braids, fixation of the mirrors and internal mechanics are given in the following sections. More information about the granite bench and the

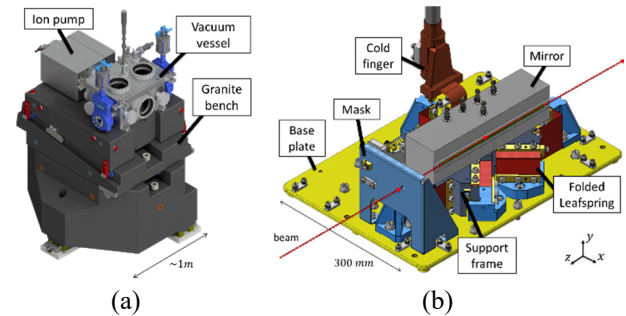designing process for the mirrors are found in [8] and [9], respectively.

Figure 1: Example of the new standard mirror systems for Sirius X-ray beamlines. (a) Vacuum vessel on granite bench; (b) mirror mounted to fine-tuning mechanism.

CONCEPTUAL DESIGN

The concept of the mirror systems was, from the very beginning, based on a few deterministic design guidelines. From the bottom to the top, the mirrors should be built on highly stable granite benchs, having only as many of degrees of freedom (DoF) as those necessary for positioning and alignment at the beamline [8]. Then, as approached in the HD-DCM, the vessel should be treated as an interface between the mirror and the bench, and by no means as a reliable and stable mounting structure in itself. Next, the mirrors should be deterministically fixed to an UHV-compatible high-resonance-frequency fine-tuning mechanism, which should be directly mounted to the vessel to benefit from the high stiffness of the bench. Finally, mechanically complex colling schemes should be avoided. Then, gathering the specifications, error budgets and alignment requirements for the mirrors of the first set of Sirius X-ray beamlines, common ground could be defined for the development of standard systems. The summarized specs are gathered in Table 1.

Table 1: X-ray Mirror Systems Summarized Specs

Description	Spec
Ry range:	> 1 mrad
Ry resolution:	< 100 nrad
Ry stability:	< 30 nrad $RMS_{2.5kHz}$
Resonances:	> 150 Hz
Thermo-mechanically induced slope errors:	< 50 nrad
Power load:	< 50 W
Cooling scheme:	indirect cryocooling via copper braid and cryostat

FE MODEL OF A NANOPOSITIONING FLEXURE STAGE FOR DIAGNOSIS OF TRAJECTORY ERRORS

S. P. Kearney, D. Shu,

Advanced Photon Source, Argonne National Laboratory, Argonne, IL., USA

Abstract

The Advanced Photon Source Upgrade project includes upgrading several beamlines, which desire nanopositioning and fly-scan capabilities. A step towards achieving this is through the use of flexure stages with minimal trajectory errors. Typically, parasitic motion is on the order of micrometer-level displacements and tens of microradian-level rotations. The cause of such errors is difficult to diagnosis due to the scale and complexity of the overall mechanism. Therefore, an FE model of a flexure pivot nanopositioning stage with centimeter-level travel range [1, 2] has been developed to aid in trajectory error diagnosis. Previous work used an FE model and relative error analysis to quantify the effects of assembly error on trajectory errors [3]. Relative error analysis was used due to the difficulty in validating a complex FE model. This study develops an experimentally validated FE model of a single joint to quantify the expected error in the full FE model. The full model is then compared experimentally to the flexure stage to assess the model accuracy and diagnosis trajectory errors.

INTRODUCTION

The Advanced Photon Source Upgrade project includes upgrading several beamlines, which desire nanopositioning and fly-scan capabilities. This will require a better understanding the cause of trajectories that are typically on the order of micrometer displacements and mircoradian rotations [1]. We have previously developed a flexure pivot nanopositioning stage with centimeter-level travel range [1, 2] that could benefit from more focused analysis of its trajectory errors. Previously, relative error analysis was used due to the difficulty in validating a complex FE model. This study hopes to improve the quality of the FE model to be used in absolute analysis. In this paper we will present a more accurate model of the single flexure pivot that was validated through experiment, and use this more accurate model in the complete flexure stage model. The flexure stage FE model will then be compared to experimental results.

The flexure stage has four main components in its construction. A commercially available flexure pivot from C-Flex Bearing Co., Inc. and Riverhawk Co, Fig. 1, is used at each mechanical joint. These pivots are then assembled in a deformation compensated orientation four-bar mechanism, see Fig. 2. Two of these four-bar mechanisms can be joined (Fig. 3), known commonly as a double parallelogram mechanism [4], to provide rectilinear motion with the parasitic motion of the four-bar cancelled. However, there is now two degrees of freedom with the double parallelogram so we employ a 2:1 stabilizing mechanism (Fig. 4 item 2) to control the floating middle-bar, which is similar to the mechanism in [5]. A complete flexure stage, Fig. 4,

can then be assembled using these fundamental units, a vertical stage using these units can be seen in [3]. The stage in Fig. 4 will be used in this analysis.
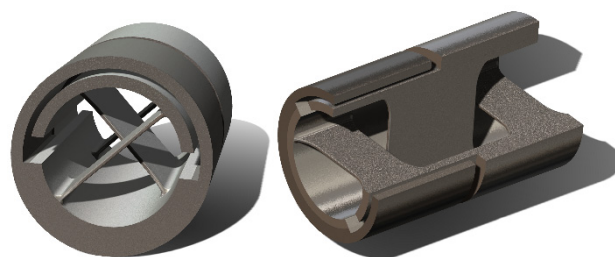

Figure 1: Flexure pivot used as a main element in the flexure stage design.

Figure 2: Four-bar deformation compensated flexure mechanism.

Figure 3: Double four-bar deformation compensated flexure mechanism.

APPLICATION OF ADDITIVE MANUFACTURING IN THE DEVELOPMENT OF A SAMPLE HOLDER FOR A FIXED TARGET VECTOR SCANNING DIFFRACTOMTER AT SwissFEL

Xinyu Wang[†], Jan Hora, Patrick Hirschi[1], Haimo Jöhri, Claude Pradervand, Bill Pedrini,
Paul Scherrer Institut, 5232 Villigen, Switzerland
[1]also at HELVETING Engineering AG, Neuenhof, Switzerland

Abstract

Whilst the benefit of additive manufacturing (AM) in rapid prototyping becomes more and more established, the direct application to 3D printing is still demanding. Exploitation of AM opens the door for complex and optimized parts which are otherwise impossible to fabricate. Therefore, consistent efforts are currently directed to gain specific knowledge on the numerical simulation and the design process.

For a vector scanning diffractometer foreseen for fixed target protein crystallography at the Swiss X-ray free electron laser (SwissFEL) [1], we developed, manufactured and tested a 3D-printed sample holder with carbon fibre reinforced polyamide material. The diffractometer serves to collect diffraction patterns at up to 100 Hz rate on many small protein crystals (< 5 µm) by scanning the sample in the X-ray beam following the custom trajectories. The large accelerations in the motion plane transverse to the beam require the holder, which is tightly fixed on the diffractometer stages, to be particularly light and stiff.

Our work on the design and the dynamic tests for the 3D-printed holder is presented here. For sake of comparison, the numerical analysis and tests were extended on a CNC-machined aluminium holder realized to fulfil the same function.

INTRODUCTION

The collection of X-ray diffraction images with the fixed target protein crystallography instrument SwissMX [2], currently under realization at SwissFEL, relies on scanning the sample in the X-ray beam using an advanced diffractometer with translation axes in x- and y-directions (Fig. 1). In the specified error budget of 1.2 µm in total between the impact position of a femtosecond SwissFEL X-ray pulse and protein crystal position, the contribution from the deformation of sample holder is restricted to be less than 200 nm. The benchmark motion of the stages is sinusoidal with 50 Hz frequency and a maximum acceleration of 2.5 m/s^2, corresponding to a motion amplitude of 25 µm. The weight of the sample holder is crucial due to the large accelerations acting on the moving parts. The

total mass allowed by the performances of the stages must be below 100g. Given the weight of the sample unit of 30 g (including sample chip, sample pin and pin-holder magnet), the sample holder maximal weight is 70g. The natural frequencies of the sample holder have been requested to be above 400 Hz.
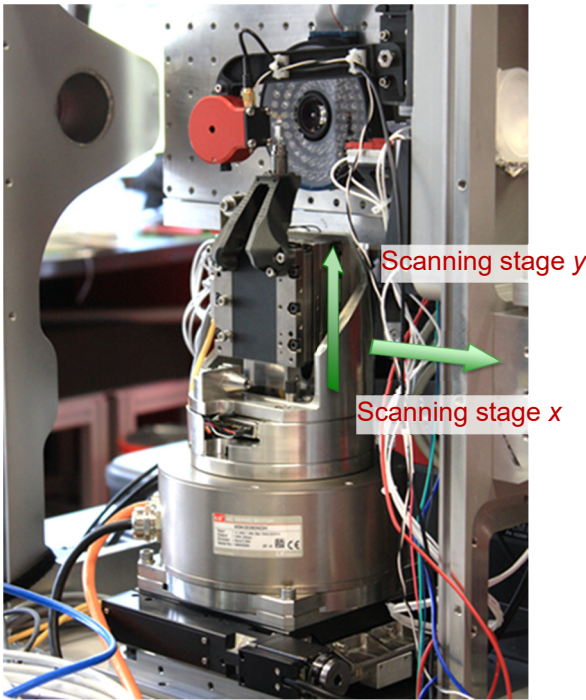

Figure 1: Sample diffractometer with sample holder and sample chip.

DESIGN OF THE SAMPLE HOLDER

To realize the sample holder, we considered both possibilities of aluminum material, i.e. by traditional CNC manufacturing, and by 3D printing with carbon fiber reinforced polyamide. In the Continuous Filament Fabrication (CFF) printing process, endless carbon fibers are printed layer by layer in predefined orientations and embedded in melted polyamide matrix material ([3]) to achieve high stiffness and low weight. The lack of material data for general 3D printing application limits the numerical predictions of the dynamical properties. In Table 1, material properties are given for uni-directional (UD) fibre orientation and for matrix material. UD composite shows the highest

---

† xinyu.wang@psi.ch

Core technology developments

New Technologies

MECHANICAL DESIGN OF A NEW PRECISION ALIGNMENT APPARATUS FOR COMPACT X-RAY COMPOUND REFRACTIVE LENS MANIPULATOR*

D. Shu[†], Z. Islam, J. Anton[1], S. Kearney, X. Shi, W. Grizolli, P. Kenesei, S. Shastri, L. Assoufid
Advanced Photon Source, Argonne National Laboratory, Argonne, IL, USA
[1]University of Illinois at Chicago, Chicago, IL, USA

Abstract

A prototype of compact x-ray compound refractive lens (CRL) manipulator system has been developed at the Argonne National Laboratory for dark-field imaging of multiscale structures. This novel full-field imaging modality uses Bragg peaks to reconstruct 3D distribution of mesoscopic and microscopic structures that govern the behavior of functional materials, in particular, thermodynamic phase transitions in magnetic systems. At the heart of this microscopy technique is a CRL-based x-ray objective lens with an easily adjustable focal length to isolate any region of interest, typically in the energy range of 5-100 keV or higher, with high precision positional and angular reproducibility. Since the x-ray CRL manipulator system for this technique will be implemented on a high-resolution diffractometer detector arm that rotates during diffraction studies, compactness and system stability, along with the ability to change focal length ("zooming"), became key design requirements for this new CRL manipulator system. The mechanical designs of the compact x-ray CRL manipulator system, as well as finite element analysis for its precision alignment apparatus are described in this paper.

INTRODUCTION

The macroscopic properties of functional materials (including most technologically relevant properties) are controlled by microscopic and nano-scale features and processes. It is important to deepen our understanding of couplings between such multi-scale structural features (e.g. as twin boundaries, grain orientations, lattice distortions, or magneto-striction) and average materials properties (thermodynamic, magneto-caloric, pinning, transport, critical current, etc.) as well as order parameters. Furthermore, the nature of hysteretic magnetic and/or structural transitions and related phenomena (e.g. memory effects, domain network, fluctuations, and relaxation) tuned in by magnetic fields at cryogenic temperature is of great interest. So, there is a growing need, especially in the wake of near diffraction-limited sources being on the horizon, to develop imaging techniques ideally suited for problems alluded to above and to complement well-known resonant and non-resonant diffraction methods.

While there is a plethora of x-ray microscopy techniques that are poised to provide high-resolution real-space images of inhomogeneous materials at multiple length scales and their evolution through phase transi-tions, dark-field x-ray microscopy (DFXM) stands out as a fast imaging method [1-6]. This full-field imaging modality uses Bragg peaks to reconstruct 3D distribution of mesoscopic and microscopic structures in materials. A Bragg peak is excited and its intensity distribution is recorded using an area detector. However, the diffracted beam is passed through an x-ray objective lens to magnify and project onto a scintillator before detection with a high-resolution CCD camera. The key is to collect diffraction data of a particular Bragg peak as the sample is rotated around the momentum transfer, with a high precision, over a range of full 360º.

A CRL-based x-ray objective lens [7-9] with an easily adjustable focal length to isolate any region of interest is a central piece of this microscopy technique. For such application CRL-based x-ray objective lens operating over a wide energy range (e.g. 5-100 keV, or even higher), with high precision positional and angular reproducibility, need to be implemented on a high-resolution diffractometer detector arm that rotates during diffraction studies. As such, compactness and system stability, along with the ability to change focal length, became key design re-quirements for this new CRL manipulator system.

In this paper, we present a proof-of-principle prototype design for the compact x-ray CRL manipulator along with its preliminary x-ray test results first, followed by the designs of the manipulators for 16-mm- and 32-mm-long CRL stacks, and conclude with the design options of the CRL manipulators integration.

PROOF-OF-PRINCIPLE PROTOTYPE

The novelty of the new mechanical design is the compactness and positioning stability as well as repeatability of its unique flexural lens holder alignment structure. It is using commercial high precision V-rail for linear roller bearing [10] as a reference base.

Figure 1 shows a 3D-model of the prototype for demonstrating proof-of-principle of operation. As shown in Fig. 1, the prototype CRL manipulator includes a base subassembly with stage support and a base V-rail, a lens holder V-rail with lens holder frame subassembly, a commercial miniature piezo-driven linear stage (SmarActTM 1720s) [11], and a multi-dimensional flexural link subassembly. As shown in Fig. 2, a group of eight CRL is confined by a thin metal lens confiner, which is mounted on the bottom of the lens holder frame. A short linear bearing V-rail is

APPLICATION OF INDUSTRY RECOGNISED DEVELOPMENT TOOLS AND METHODOLOGIES, SUCH AS SIX SIGMA TO FACILITATE THE EFFICIENT DELIVERY OF INNOVATIVE AND ROBUST ENGINEERING SOLUTIONS AT SYNCHROTRON FACILITIES

S.A.Macdonell[†], Diamond Light Source, OX11 0DE Didcot, UK

Abstract

Synchrotron facilities play a key part in the delivery of world leading science to facilitate research and development across multiple fields. The enabling technology designed by engineers at these facilities is crucial to their success.

The highly academic nature of Synchrotron facilities does not always lead to working in the same way as a commercial engineering company. However, are the engineering requirements at Synchrotrons different to commercial companies? Exploring the parallels between research and commercial companies, can we show that the tools and methodologies employed could benefit engineering development at Synchrotrons?

This paper provides a theoretical discussion on the commonality between engineering developments at Synchrotron facilities compared to commercial companies. How methodologies such as Design for Six Sigma and in particular tools such as stakeholder analysis, functional tree analysis, FMEA and DoE could be utilised in the design process at Synchrotrons. It also seeks to demonstrate how implementation could aid the development of innovative, robust and efficient design of engineering solutions to meet the ever-increasing demands of our facilities.

INTRODUCTION

Diamond Light Source [1], as other Synchrotron facilities around the globe, generates brilliant beams of light from infrared to X-rays, used for academic and industrial research. This research can be at the cutting edge of scientific discovery and therefore requires innovative enabling technology, engineered to meet unique requirements. Diamond Light Source like other facilities is a 'not for profit' organisation that is primarily government funded.

Commercial companies, on the other hand must develop innovative products that meet the needs of particular markets. Markets and the opportunity they present are constantly changing and companies must adapt and develop new innovative products and technology to meet these ever-changing needs. Commercial companies operate to make a profit that can fund business growth and the development of next generation products.

Synchrotron facilities and commercial companies oper-

ate and are funded differently, but at the heart of both of these organisations is a need to develop new and innovative solutions to meet unique engineering requirements. The ability to deliver to these unique engineering requirements determines the success of the organisation whether it be a Synchrotron facility or a commercial company.

Many commercial companies utilise Six Sigma approaches within their organisations. The many success stories of Six Sigma implementation include organisations such as [2] GE, Motorola, Honeywell, Bombardier, 3M Ford and Toshiba. Today, many large commercial organisations have implemented Six Sigma and are reporting large profits.

However, implementation of Six Sigma is not common at Synchrotron facilities. Given the funded research nature of these types of organisation, and headlines of profit associated with Six Sigma it is perhaps possible to understand why. Six Sigma also holds a statistical association that implies it is only useful for organisations creating products for mass production. This does not necessarily match with the single unique engineering developments carried out at Synchrotrons.

However, when we explore the Six Sigma methodology further and how and why it is used. We can see that the use of Six Sigma within an organisation can provide systematic approaches to process improvement, problem solving of existing designs and improve quality in new design

Since Synchrotron facilities utilise processes, can have a requirement to solve problems and do require high levels of quality in the design of their systems it is hard to believe that the Six Sigma approach or at least parts of it would not be beneficial. In fact, if we were to deploy some of the tools embedded in the Six Sigma approach at Synchrotrons could we save time in development, could we improve the performance and ultimately increase our ability to deliver world leading scientific research?

At Diamond Light Source Ltd, we have started to investigate the Six Sigma methodology and how we might apply this to the benefit of our organisation.

ENGINEERING DEVELOPMENTS AT SYNCHROTRON FACILITIES VERSUS COMMERCIAL COMPANIES

If we strip away the input and output factors of any engineering organisation, we see that there is a core process

---

† sarah.macdonell@diamond.ac.uk

A COMPACT AND CALIBRATABLE VON HAMOS X-RAY SPECTROMETER BASED ON TWO FULL-CYLINDER HAPG MOSAIC CRYSTALS FOR HIGH-RESOLUTION XES

I. Holfelder[†], R. Fliegauf, Y. Kayser, M. Müller, M. Wansleben, J. Weser, B. Beckhoff,
Physikalisch-Technische Bundesanstalt, 10587 Berlin, Germany

Abstract

In high-resolution X-ray emission spectroscopy (XES) crystal-based wavelength-dispersive spectrometers (WDS) are being applied for the characterization of the electronic structure of matter in various research fields like geosciences, chemistry or material sciences. Thereby, the von Hamos geometry provides high detection efficiency of spectrometers due to sagittal focusing using cylindrically bent crystals. To maximize the detection efficiency, a full-cylinder optic can be applied [1].

Based on this idea, a novel calibratable von Hamos X-ray spectrometer based on up to two full-cylinder optics was developed at the PTB. To realize the full-cylinder geometry, Highly Annealed Pyrolytic Graphite (HAPG) [2] was used. Besides its good bending properties, this mosaic crystal shows highly integrated reflectivity while offering low mosaicity, ensuring high resolving power [3]. The spectrometer enables chemical speciation of elements in an energy range from 2.4 keV up to 18 keV. The design and commissioning of the spectrometer will be presented. The spectrometer combines high efficiency with high spectral resolution (ten times better than in commercial WDS systems) in a compact arrangement also suitable for laboratory arrangements.

INTRODUCTION

Constant development of novel micro- and nano-materials in the industry is a huge challenge for metrology. As the research and development cycles are sometimes less than four months, reliable correlations of material functionalities and properties are called for while only few or no reference materials available. Therefore, reliable analytical methods for characterization of new material systems are needed that are not dependent on reference materials. An appropriate method is the reference-free X-ray spectrometry, which is based on the so-called fundamental parameter approach [4, 5, 6, 7, 8]. This method requires calculable synchrotron radiation and radiometrically calibratable instrumentation. In this work we present a novel compact wavelength-dispersive spectrometer that can be calibrated to ensure reference-free X-ray emission spectroscopy (XES). Due to its compactness and its high efficiency, it can be used in different experiments and at different beamlines. A laboratory X-ray source can be used as an excitation source as well.

† ina.holfelder@ptb.de

VON HAMOS SPECTROMETER

To ensure high efficiency, the von Hamos geometry was used. In the von Hamos geometry, the radiation source – which, in the case of the XES experiment, is the fluorescence radiation from the sample – and a CCD camera are placed along the cylinder axis of a sagittally bent crystal, see Figure 1. While the original design was based on a cylindrically bent crystal covering only a segment of a ring, the use of full-cylindrical optics allows maximizing the solid angle of detection [9, 10].
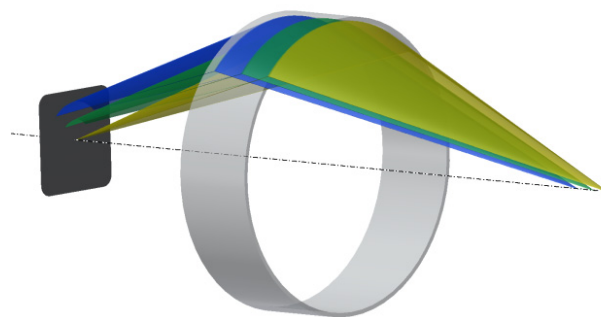

Figure 1: Von Hamos geometry.

To realize full-cylinder geometry, Highly Annealed Pyrolytic Graphite (HAPG) is especially suitable for this purpose, as it can be bent up to a 50 mm radius without any structural impact on the resolution. In the spectrometer presented here, 40 µm thick HAPG layers on cylindrical glass ceramic (Zerodur®) substrates were used. The HAPG is a mosaic crystal that consists of 50 µm to 80 µm mosaic blocks, which again consists of several approximately 1 µm sized crystallites that are tilted against each other [11]. Its mosaic structure leads to the highest integrated reflectivity of all known crystals, as all crystallites that are lying on the Rowland circle and fulfil the Bragg equation contribute to the crystal reflectivity. Simultaneously, HAPG has an especially small mosaic spread, the angle distribution function of the crystallites, and high resolving power.

For an additional increase of the resolving power, two HAPG optics are used in the beam path. An increase of the resolving power of around 40 % is expected [12]. This double reflection concept also increases the discrimination capability and improves the tailing of the spectral peaks.

DEVELOPMENT OF A NEW SUB-4K ARPES ENDSTATION AT PSI

D. Trutmann*, S. Maag, L. Nue, A. Pfister, A. Schwarb, K. Zehnder, S. Hasanaj, M. Shi, N. C. Plumb

Paul Scherrer Institut (PSI), 5232 Villigen PSI, Switzerland

Abstract

In spring 2016 a project was started to renew the high-resolution ARPES endstation of the Surface/Interface Spectroscopy (SIS) beamline at PSI. The focus lay on achieving sample temperatures below 4 K while maintaining 6 degrees of freedom.

This made it necessary to redesign all thermally active parts, such as the connection to the cryostat, the flexible braid that enables the tilt and azimuthal movement, the sample clamping as well as the thermal isolators that hold the clamping device in place. A newly introduced shield in the main analyser chamber, cooled by separate cryopumps, is used to remove nearly all radiation heat load.

A major milestone has recently been taken, by running cryogenic tests on a test stand. The simplified setup reached sample temperatures of 3.35 K. The temperature loss from the cryostat to the sample was as low as 0.6 K. Encouraged by these results, it is believed that the final endstation will be able to reach temperatures even below 3 K. With the new cryo concept, the thermal performance seems to be mainly limited by the radiative heat load emitted by the analyser lens.

The new endstation is planned to be in operation by spring 2019.

INTRODUCTION

Angle-resolved photoemission spectroscopy (ARPES) is a powerful technique to directly measure the electronic band structure and interactions in solids [1] that is widely employed at many synchrotrons. ARPES is primarily used to study materials at the cutting edge of condensed matter physics and solid state engineering. Practitioners in the field are generally interested in experimental systems that can reach ever-lower energy and temperature scales, as these provide access to many interesting, unstudied science cases and ideal conditions obtaining sharp spectra and discerning fine features.

Of course, the pursuit of lower temperature and better resolution always involves design tradeoffs. While the record lowest temperature for ARPES at a synchrotron currently is below 1 K using a He-3 cryostat [2], this level of performance is possible only by drastically reducing access to the sample in order to reduce the radiation load, which in turn introduces practical issues for sample handling, manipulation, alignment and data acquisition.

Considering the state-of-the-art in VUV beamlines – and, more importantly, the performance guarantees of commercially available ARPES analyzers – an optimistic estimate of the foreseeable best-case resolution at SIS beamline is

_____

* daniel.trutmann@psi.ch

about $\Delta E = 1$ meV. Equivalent thermal broadening occurs around $T \approx \Delta E/(4k_B) = 3$ K. Below roughly this point, we expect drastically diminishing scientific returns on any hard-fought improvements in the temperature. In light of the above, we have therefore conceived of the SIS upgrade as a new standard in high-throughput _workhorse_ systems for ARPES at synchrotrons, with the goal of sub-4 K temperature performance and an optimistic design target of 2 K to 3 K.

GENERAL OVERVIEW

The current endstation offers a six degrees of freedom (DOF) mechanical system, with no coupling between any DOF and only a negligible thermal drift along on the azimuthal axis and no drift along all other DOF. It further offers an open environment such that sample manipulation and alignment is easy. Overall, these features gives it a very competitive all-around performance among ARPES manipulators. Apart from maintaining the above features, the new endstation, figure 1 and 2, should improve or introduce new features, such as:
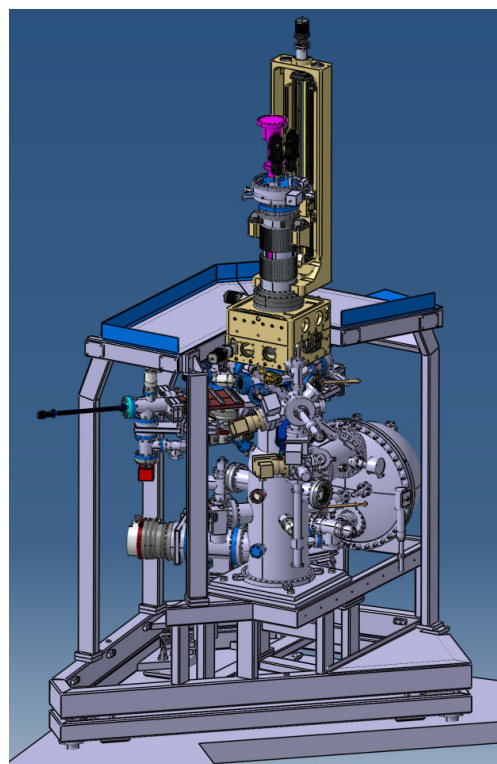

Figure 1: The current state of the new endstation.

- improved sample temperature from currently reachable 14 K (measured on the sample plate holder) to <4 K (measured on the sample plate itself)

EVALUATION OF ANISOTROPIC SIMULATIONS & REDESIGN OF THE BXDS HIGH ENERGY MONOCHROMATOR BENT LAUE DIFFRACTION CRYSTAL HOLDERS

M. J. P. Adam*, N. Appathurai†, Canadian Light Source Inc., S7N 2V3 Saskatoon, Canada

Abstract

The Brockhouse X-ray Diffraction and Scattering Sector (BXDS) High-Energy (HE) beamline includes a bent Laue diffraction monochromator. The BXDS HE monochromator achieves energy ranges of 35keV to 90 keV through the bent Laue diffraction of two silicon crystal wafers. Each wafer (460 μm & 1000 μm thick) is bent to achieve specific Sagittal Radius (R_s); subsequent anticlastic Meridional Radius (R_m) results from the anisotropic nature of silicon, creating the desired x-ray focusing parameters. During the initial conditioning of the BXDS HE monochromator spurious diffraction patterns were observed indicating that the crystal holder and crystal integrity failed. Alternative holder designs were evaluated using Finite Element Analysis (FEA; ANSYS) simulations to ensure that appropriate R_s and R_m values were achieved, verification of the crystal holder R_s was completed using contact 3D measurement (FaroArm/Leica T-Probe), and the crystal surface was assessed using 3D optical profiling (Zygo). A superior holder was chosen based on the results, and replaced. The performance of the BXDS HE monochromator has been characterized, indicating the new holder design has achieved x-ray focusing parameters.

INTRODUCTION

Each Si wafer is bent against a precisely machined cryogenically cooled block to achieve specific R_s; a subsequent anticlastic R_m results from the anisotropic nature of Si creating the desired X-ray focusing parameters [1–3]. The theoretical design values for the BXDS HE mono bending radius are found in Table 1), and describe values required for desired focus [1], Si (111) reflection for 35keV, Si (422) & Si (533) reflections for 60-90keV.

Table 1: Theoretical Radius of Curvature

Energy (Si thickness)	R_s [m]	R_m [m]
35keV (460μm)	0.37	-28.0
60-90keV (1000μm)	0.72	-37.0

BACKGROUND

The original BXDS HE crystal holder system was composed of two precisely machined blocks (specifically R_s, with dimensions from Table 1).

---

* madison.adam@lightsource.ca
† narayana.appathurai@lightsource.ca

During the initial conditioning of the BXDS HE mono spurious beam shapes were observed from both crystals. The patterns indicated that the crystal holder and crystal integrity had failed. The fluorescing patterns were observed during the initial low flux beam conditioning, suggesting that the crystal fracture resulted during cryogenic cool-down of the stage prior to x-ray attenuation.

The crystal assemblies were removed from the HE mono and inspected. Fractures for both wafers were observed (see Fig. 1), as well the crystal wafer had bonded to the indium foil, suggesting that the wafer was over constrained when assembled.
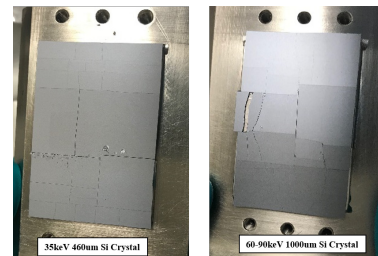

Figure 1: The fractured crystals after being removed. The silicon wafers fractured along the lattice planes (vertically & horizontally). The fractures per area were highest around the locations where the crystals were pressed against the indium foil and the cooling block.

The originally implemented design over-constrained the crystal, resulting in fractures and unusable beam (i.e. unfocused). Therefore, an evaluation of the crystal holders was required.

Objectives

1. Review the current holder design.
2. Confirm the radius induced when clamped against the cooling block & the effect of different clamps on the anticlastic radius.
3. Determine the expected performance (focusing, flux, etc.)

ANISOTROPIC SIMULATION

Initially a review of the original crystal holder was simulated using finite element methods (ANSYS 18.0) and evaluated to determine the resulting R_s & R_m. All simulations used anisotropic material properties for Si (111), and applied non-linear large deformation theory [4–7].

The original mask simulation results demonstrated an immediate issue; the R_m could not be achieved with the

THERMOMECHANICAL ANALYSIS OF SESAME HIGH-HEAT-LOAD FRONT ENDS COMPONENTS

M. AL-Najdawi[†], SESAME, 19252 Allan, Jordan

Abstract

New front-end beamline components at SESAME are designed to handle the high heat load produced by the insertion devices. A mini gap wiggler will be installed for the Material Science Beamline and the front end will receive 5.0 kW of total power and 7.79 kW/mrad^2 of peak power density. The power produced by the insertion device was simulated using SynRad+[1], a software using Monte Carlo simulation to simulate the synchrotron radiation from either an insertion device or any magnet source. The surface power density distribution generated by this software can be mapped directly to an FEA software to conduct a coupled thermo-mechanical analyses. The design, modelling, power source simulation and FEA analysis of the fixed mask, shutter and filter for the material science Beamline front end will be presented in this paper.

INTRODUCTION

SESAME is a third generation light source located in Allan Jordan operating with a 2.5 GeV electron beam and a design current of 400 mA. A mini gap wiggler as a source for the material science beamline will be installed and can deliver a power of over 5.0 kW with a peak power density of 7.79 kW/mrad^2 at 12 mm magnetic gap. The design of the fixed mask, shutter and filter had been done to handle the high heat load generated from the wiggler source, the upstream and downstream dipole magnets, to protect the first optical components in the beamline.

POWER CALCULATION

Mini-Gap Wiggler Parameters

The mini-gap wiggler will be installed in one of the storage ring long straight sections and the gap will be adjusted to 12 mm, the wiggler parameters shown in table 1 and power distribution in Figure 1.

Table 1: Mini-gap Wiggler Parameters

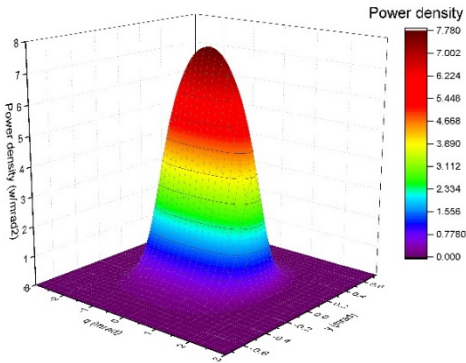|	
Overall length	2 m
Minimum magnetic gap	8 mm
Period length	60.5 mm
Number of poles (Np)	63
Maximum field (B_{max})	1.84 T
Effective field (B_{eff})	1.63 T
Deviation parameter (K)	8.6
Critical energy (E_c)	7.0 keV

---

† mohammad.najdawi@sesame.org.jo

Figure 1: Power distribution of the mini gap wiggler at 12 mm gap.

Power Calculation

The power calculations had been done using SynRad+, a software using Monte Carlo simulation to simulate the synchrotron radiation from either an insertion device or any magnet source. The surface power density distribution generated by this software can be mapped directly to an FEA software to conduct a coupled thermo-mechanical analyses. The benefit from using this type of simulation is to take the whole length of the insertion device as a distribution of source points, which give us more accurate results than the traditional way of assuming one source point. Also, in this type of simulations, we can introduce the effect of the heat load produced by the upstream and downstream dipole magnets as shown Figure 2.
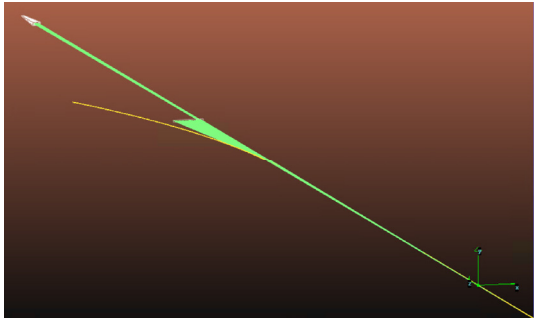

Figure 2: SynRad simulation for the wiggler source with upstream and downstream dipole magnets.

In order to have more accurate results, the tapered shape of the fixed mask had been introduced in the simulation and the power distribution has been calculated at each taper face. An example of the SynRad output is given in Figure 3 which shows the power distribution at the fixed mask from the wiggler and dipole magnet source.

DESIGN OF NEW BEAM INSTRUMENTATION FOR THE ISOLDE ISOTOPE SEPARATOR AT CERN

W. Andreazza, M. Duraffourg, G. J. Focker, A. Miarnau Marin, D. Smakulska, J. Tassan-Viol,
R. Veness, CERN, Geneva, Switzerland

Abstract

The ISOLDE radioactive ion beam separator facility at CERN produces beams of short-lived isotopes for experiments in physics, material and medical science. New requirements for more precise measurement of profile, position and intensity has pushed the CERN beam instrumentation group to start the study of a new generation of ISOLDE beam instrumentation dedicated to the specific needs of this facility.

This paper will describe the design and the development of a number of new ISOLDE instruments with the aim of achieving better performance, increased reliability and to facilitate maintenance in a radioactive environment.

It will explain how modern technologies such as magnetically coupled linear actuators and 3D additive machining have been used to make a modern, precise and reliable beam instrumentation design.

INTRODUCTION

The on-line isotope mass separator ISOLDE [1] is a facility dedicated to the production of a large variety of radioactive ion beams for a wide range of experiments in the fields of nuclear and atomic physics, solid-state physics, materials science and life sciences. The facility takes beam from the Proton-Synchrotron Booster (PSB) at CERN, the European Organization for Nuclear Research.

At ISOLDE, radioactive beams are produced in two fixed target areas, known as front-ends, and subsequently delivered to their respective isotope separators: the General Purpose Separator (GPS) and the High Resolution Separator (HRS). The GPS line has one mass separator magnet and the HRS line has two magnets. The extracted mass-separated beams are then delivered to different experimental lines.

BEAM DIAGNOSTIC REQUIREMENTS

Beam diagnostics in ISOLDE is comprised of wire Secondary Emission Monitor (SEM) grids, wire or needle scanners and Faraday cups in order to measure the properties of the beam during set-up and operation of the front-end and separators.

The SEM grids and scanners can be used to take beam profile measurements by moving them into the beam path. The charge depletion measured in the wires is proportional to the local beam density and thus allows for the reconstruction of the beam profile as a function of wire position. Faraday cups are used to take measurements of the beam intensity, however, in this paper the focus will be placed on SEM grids and needle scanners.

EXISTING SITUATION AND REASONS FOR CHANGE

The existing beam instrumentation was designed and built in the early 90's. The success of the ISOLDE facility, including a recent upgrade has meant that these instruments are operating far past their initial expected lifetime. Despite a surprising longevity, they are now showing their limits in terms of performance and reliability. New requirements for more precise measurement, more stringent vacuum acceptance constraints and a CERN-wide policy to reduce maintenance requirements in radioactive environments according to modern "As Low As Reasonably Achievable" (ALARA) guidelines has led to a project for the design, development and construction of a new generation of ISOLDE instrumentation.

USE OF NOVEL TECHNOLOGIES

The mechanisms that move a grid, wire or Faraday cup into the beam path do so using pneumatic actuators, lead-screws or pulleys. The current scanners use a system of in-vacuum motors and pulleys, which in turn rely on in-vacuum electronics and numerous small parts. These require frequent and costly maintenance in a hazardous area where there is a risk of radioactive contamination. Similarly, the combined scanner and Faraday cup instruments, which were recently redesigned, used pneumatic actuators coupled with edge welded bellows. Edge welded bellows allow a long movement for their nominal length, but are limited in fatigue life to some 10,000 cycles, are difficult to clean for ultra-high vacuum environments and are fragile, with the associated risk of leaks.

Magnetically coupled push-pull linear actuators (MPPL) were identified as a solution as they avoid these limitations. The MPPL is driven by a stepper motor and ball screw with a rated linear speed of 100 mm/s and a nominal linear resolution of 25 µm per half step of the stepper motor. The ball screw is connected to a thimble containing $SmCo_5$ magnets and running over a tube that creates the vacuum-air interface. The thimble is magnetically coupled to an in-vacuum shaft supported on a nose bearing. The MPPL is installed onto the instrument using a ConFlat® flange.

Existing MPPLs did not fully complying with CERN's requirements. A development was therefore made with a supplier to introduce some key modifications. Opto-couplers, which may fail under stray magnetic fields and radiation, have been replaced by micromechanical switches, and an over-travel hard stop has been incorporated to avoid damaging the push-pull. Finally, due to the rapid degradation of PTFE in a radioactive environment, the PTFE and

FINITE ELEMENT ANALYSIS OF A COMBINED WHITE BEAM FILTER AND VISUAL SCREEN USING CVD DIAMOND FOR THE BXDS BEAMLINE

D. M. Smith[*], M. J. P. Adam[†], A. Janis, G. Barkway
Canadian Light Source Inc., Saskatoon, Canada

Abstract

A white beam filter and visual screen are required for the undulator beamline at the Brockhouse X-Ray Diffraction and Scattering Sector (BXDS). Reusing a water-cooled copper paddle with a 0.1 mm thick chemical vapor deposition (CVD) diamond foil, a combined filter and screen design is presented. The Canadian Light Source (CLS) previously experienced failure of CVD diamond filters when exposed to high flux density white beam. Finite element analysis (FEA) was performed to determine if the CVD diamond would fracture under the BXDS undulator heat load. Conservative failure criteria are selected for CVD diamond based on available literature for the following failure mechanisms: high temperature, thermal fatigue, and temperature induced stress. Four designs are analyzed using FEA models simulating effects of clamping pressure and heat load on the CVD diamond. The simulations are verified by optimizing the model mesh, comparing results against hand calculations, and comparing theoretical absorbed heat load to simulated values. Details of the simulation method are reviewed and results for the different designs evaluated. Suggestions for future testing of CVD diamond in a synchrotron setting will be discussed.

INTRODUCTION

The BXDS undulator beamline at the CLS requires a white beam photon filter to reduce the heat load on downstream monochromators, and a visual screen for commissioning of the beamline. Originally planned as separate components, it was decided that a combined white beam photon filter and visual screen (PFIL/VSC) using a 0.1 mm thick CVD diamond filter could fulfill the functionality of both. A new FEA was initiated to accurately simulate the reaction of CVD diamond to a heat load and clamping forces. The purpose of this work was to apply an analysis based design process enabling good conceptualization of the design parameters for the PFIL/VSC.

FEA Objectives

1. Determine the Steady-State Thermal condition for the BXDS PFIL/VSC subjected to worst case heat loads,
2. Determine the Static Structural condition for the BXDS PFIL/VSC subjected to worst case heat loads, and
3. Determine a suitable design for BXDS PFIL/VSC.

---

* david.smith@lightsource.ca
† madison.adam@lightsource.ca

BACKGROUND

The primary purpose of the FEA was to determine if the PFIL/VSC could function under the undulator heat load using a recycled, water-cooled base, or whether a more robust cooling system would be required. The beam size 37.2 m from the center of the BXDS straight (the location of PFIL/VSC) is 13.0 mm (H) by 4.58 mm (V). The maximum power load and power density on the filter are 368.9 W and 6.42 W/mm^2 respectively when the storage ring current is 500 mA and the undulator gap is set to its minimum at 5.2 mm as shown in Fig. 1. The CLS typically operates at 220 mA, but designs require consideration for 500 and 250 mA too. For 250 and 220 mA, the absorbed power load will be 184.6 W and 163.8 W respectively.
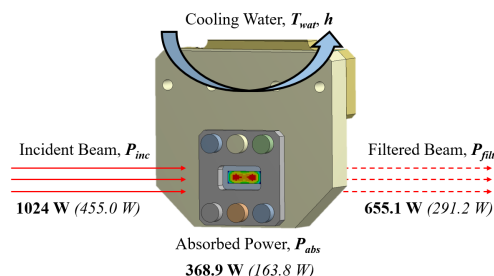

Figure 1: The undulator beam if filtered by the CVD diamond. The absorbed heat is removed while the filtered power continues downstream. Values in bold are for 500 mA and italicized values are for 220 mA.

Failure Criteria & Safety Factors

Conservative safety factors (SF) were favored from literature review when there was little experimental data available. Three failure methods are considered: high temperature, thermal fatigue, and stress.

Failure Due to High Temperature CVD diamond undergoes graphitization at high temperatures and optical degradation occurs at temperatures of 1300 °C in vacuum [1]. A SF of 1.5 allows for a maximum temperature of 866 °C on the CVD diamond foil.

Fracture Due to Thermal Cycling (Fatigue) of CVD Diamond Researchers have found that slow crack propagation, the main failure method in thermal fatigue, is not a concern with CVD diamond [2]. Therefore, fatigue effects will be considered negligible.

Simulation

FEA Methods

UPGRADE OF MAGNETIC MEASUREMENTS LABORATORY AT ALBA SYNCHROTRON

J. Campmany†, J. Marcos, V. Massana, L. Ribó, F. Becheri, R.A. Petrocelli
ALBA-CELLS, 08290 Barcelona, Catalonia, Spain.

Abstract

Along 2017 and 2018, a complete upgrade of hardware and software at ALBA magnetic measurements lab has been done. Regarding hardware, a relevant innovation has been the replacement of DC motors by step motors in new Hall probe, flipping and rotating coil benches. Up to now, these kind of continuous measurements usually were done with DC motors because steppers were considered unable to fulfil the required movement smoothness. However, recent innovations in drives made feasible its use. In our case, we tested the performance of upgraded benches and they reach the same accuracy than the former DC versions. In all upgraded systems, we used the ALBA standard IcePAP motor driver [1], taking advantage of firmware upgrades, including the possibility of triggering data acquisition by signals generated from different axes selectable via software. Regarding software, control systems have been unified to Tango package.

HALL PROBE BENCH

The Hall probe bench at ALBA, used to map the magnetic field over 3D regions, was originally built on 1997 by Ramem Company as shown in Fig. 1. It was fully characterized when it was initially commissioned [2], and over the years the system had undergone several hardware and software upgrades in order to improve its performance. In particular, in 2005-2006 the control system was completely revised in order to migrate it from EPICS to TANGO and to implement the on-the-fly measurement mode, which allows acquiring data while the system is moving [3].

However, one of the critical hardware components, the motion driving system, a Delta Tau VME PMAC, had never been replaced and by the end of 2016 it has become obsolete. Therefore it was decided to replace it by a state-of-the-art motion controller providing equivalent or even better capabilities. The selected system was a Delta Tau Power Brick AC unit, which integrates a Power PMAC controller. In parallel, it was also decided to develop a new version of the control system, having it up-to-date with ALBA standards, in order to take profit of the tools that have been developed last years. The objective has been to control ID laboratory benches with the same architecture and code versions used in the controls of both Beamlines and Accelerator at ALBA.

The hardware replacement took place in Oct-Dec of 2016. Afterwards, between Dec 2016 and Feb 2017 the

---

† campmany@cells.es

hardware was tuned and adjusted. Finally, in the period Feb-Apr 2017 the new control system was successfully commissioned and debugged. Its performance is the same as the old one.

Figure 1: Old Hall probe bench based in DC motors upgraded in 2016.

In parallel, we have built a new Hall probe bench entirely based on step motors and with a control system similar to the upgraded old bench. The new bench, presented and characterized as published elsewhere [4] can be seen in Fig. 2. Software and hardware improvements are sketched in Fig. 3.

Figure 2: New Hall probe bench based in step motors.

Hardware	Old system	Upgraded system	New system
Motion controller	VME PMAC	Power PMAC	ICEPAP
Motor	DC motors	DC motors	Step motors
Hall probe current source	Agilent E3631A	Lake Shore 121	Agilent E3631A
Software			
OS	Suse9	Debian8	Debian8
Control System	Tango5	Tango8	Tango8
Hardware controllers	Tango-ds compiled in C++	New Tango-ds, mostly in Python	New Tango-ds, mostly in Python
Experiment control		Sardana SEP6	Sardana SEP6
GUI	Java with Jdraw synoptics	Taurus 3.7.0 based on QT	Taurus 3.7.0 based on QT

Figure 3: Hardware and Software upgrades of the Hall probe benches at ALBA.

PHOTON BEAM APPLIED AS HEAT FLUX ON IRREGULAR SURFACES IN FEA*

D. Capatina†, Advanced Photon Source, Argonne National Laboratory, Lemont, USA

Abstract

The light source front ends and beamlines contain several devices designed to limit the size of, or completely stop, the photon beam. Most of these devices are meant to protect personnel and/or equipment, thus their failure would have serious implications for the facility operation. The photon beam carries extremely high energy, thus the system will experience very large thermal loads. Accurate temperature and stress distribution of these components, based on well-reasoned assumptions, is needed to accurately review the performance of these devices during the design process. Applying non-uniform heat flux as a thermal load in simulation presents a challenge. This work describes the steps of the thermomechanical numerical simulation for a typical component at the Advanced Photon Source (APS), subject to photon beam interception. The numerical algorithm used to apply the non-uniform heat flux distribution on an irregular type of surface is presented in detail. The algorithm was developed using the commercial Finite Element Analysis (FEA) software ANSYS Workbench of ANSYS, Inc.

PROBLEM FORMULATION

A photon mask (here after mask) is a front end or beamline component meant to limit the size of the photon beam presented to the downstream components. During normal operation the photon beam passes through the mask aperture. By several reasons the beam could be missteered from its normal trajectory, causing the beam to partially or fully strike the mask [1]. Accurate thermal simulation of this mask is needed to review the performance of this device under the worst case load and beam missteering scenarios.
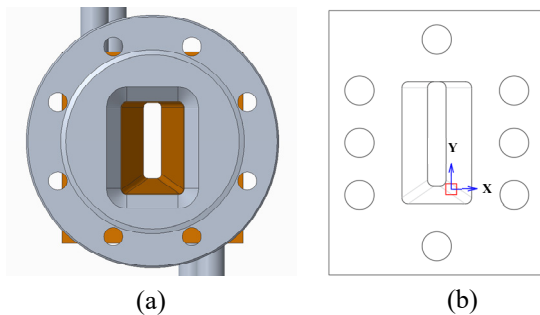

Figure 1: (a) CAD model of the mask assembly, front view; (b) CAD drawing of the mask model used in the analysis, front view, showing the beam footprint.

A typical mask design is the boxed-cone and the aperture of such component is shown in Fig. 1a. One of the most critical scenarios is when the beam strikes the corner of the taper. The beam footprint for this case is shown in Fig. 1b.

The power density distribution corresponding to the normal beam incidence assuming a 4th order Gaussian equation was calculated using SRUFF [2]. Equation (1), generated for a particular loading scenario for demonstration purposes, was used in ANSYS to apply the heat flux thermal load:

$$q = \exp(a + bx^2 + cy^2 + dx^4 + fy^4 + gx^2y^2) \qquad (1)$$

where   a=4.3828,   b=-0.037375,   c=-0.20196, d=-0.0023109, f=0.0045228 and g=-0.020031.

Equation (1) represents the coordinate-dependent power density, q, along the beam axis, z. The power absorbed by the mask surface and thus to be applied in ANSYS is the component of the q vector perpendicular to the surface, q_n. The heat flux vector decomposition is illustrated in Fig. 2.
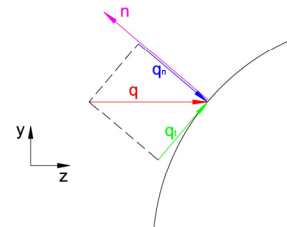

Figure 2: Heat flux vector decomposition.

Unlike the sides of the mask taper, which have a constant normal vector, on the corner surface the normal vector varies at each point of the surface. ANSYS does not have a build-in command to apply a coordinate dependent heat flux vector. The solution of this challenge is developing a code to provide the surface heat flux at each node of the element where the heat load is applied.

NORMAL VECTORS COMPUTATION

After meshing, ANSYS Workbench allows the user to obtain information about the mesh such as: element number and its nodes numbers, and coordinates with respect to the specified coordinate system [3]. In this case the coordinate system is user defined and its origin is situated in the middle of the beam footprint with respect to the x and y coordinates. Knowing the coordinates of two points one can compute a vector connecting the two points. In the same way, having the coordinates of three nodes of a surface element, one can compute two vectors which have a common point, each vector having the tail at the common

APPLICATION OF REMOTE INSTALLATION AND MEASUREMENT SMART VEHICLE IN ACCELERATOR*

J. X. Chen†[1], L. Kang[1], G. Y. Wang[1], J. S. Zhang[1], J. B. Yu[1], X. J. Nie[1], H. Y. He[1]
A. X. Wang[1], C. J.Ning[1], Y. J. Yu[1], L. Liu[1], D. H. Zhu[1]
Institute of High Energy Physics, Chinese Academy of Sciences, 100049 Beijing, China
[1] also at Dongguan Neutron Science Center, 523808 Dongguan,China

Abstract

The installation, alignment measurement and vibration monitoring of the accelerator equipment are cumbersome. In order to reduce the work intensity and exposure time of personnel, this paper has developed a smart vehicle that can automatically walk and automatically adjust the horizontal in the accelerator or beam line area. The smart vehicle can move forwards, sideways, oblique lines, rotations and combinations, and can automatically adjust the level according to different terrains. The auto-levelling accuracy is better than 0.001 degrees. By installing vibration measuring equipment or collimating equipment on the vehicle platform, vibration testing and collimation measurement of the equipment in the accelerator or beamline device can be performed.

INTRODUCTION

The remote measurement smart vehicle (Figure 1) is mainly composed of a body, McNamee wheels movement module, a lifting module, a parallel six-degree-of-freedom platform [1, 2], an electrical module and a control panel. The main body of the vehicle is constructed of high-strength hard aluminium alloy and aluminium profiles. The car is equipped with four sets of McNamee wheels motion platform, which can realize forward, horizontal, oblique, and rotation and combination sports. Lifting module maximum load is greater than 2000N, can achieve 0-500mm range of lifting movement. The six-degree-of-freedom platform mainly realizes the self-levelling and angle adjustment functions required for the vibration measuring equipment and the alignment equipment. Two 24V power interfaces are reserved for the walking platform to provide power to other on-board devices.
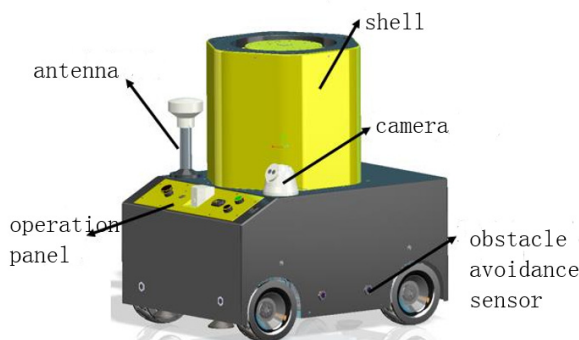

Figure 1: Structure of the smart vehicle.

SMART VEHICLE PERFORMANCE TEST

Smart vehicle walking tests mainly include automatic walking and manual walking. The vehicle and the upper computer control system communicate data through the wireless network. The automatic walking mainly realizes the straight running, left-turning, right-turning and stopping of the smart vehicle through the two-dimensional code identification and positioning technology. The vehicle walking movement information is recorded on each two-dimensional code. The smart vehicle scans the two-dimensional code to obtain the movement. The scanning range is φ200mm. Before detecting the action information of the next two-dimensional code, the smart vehicle will continue to maintain the previous command. Manual walking indicates the forward and backward rotation of the smart vehicle through the control button. The infrared obstacle avoidance sensor and image acquisition system are arranged around the whole vehicle, and the environment in front of the vehicle can be obtained in the upper computer. Figure 2 shows the smart vehicle measuring in a simulated accelerator tunnel. Figure 3 shows a two-dimensional code tracking test of the smart vehicle.
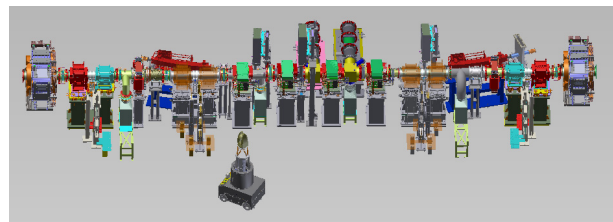

Figure 2: The smart vehicle measuring in a simulation accelerator tunnel.

SMART VEHICLE AUTO-LEVELLING TEST

When the vehicle is in place, in order to meet the level requirement of the alignment device, the level of the moving platform at the top of the smart vehicle needs to be adjusted [3]. According to the level requirement of the alignment measurement, the level of the platform needs to be better than 0.001°. After measurement, the three directions of the XYZ range of rotary angle travel are ±10° and the travel range is ±29mm. Figure 4 shows the position error curve of open-loop control of the horizontal adjustment mechanism of the smart vehicle. The open-loop position error is within 1mm. Figure 5 shows the attitude error curve of the open-loop control mechanism of the

VIBRATIONAL STABILITY OF A CRYOCOOLED DOUBLE CRYSTAL MONOCHROMATOR AT SSRF *

Y. Fan[†,1,2], F. Tao[1,2], Z. Li[1], H. Qin[1], W. Zhu[1]

[1]Shanghai Institute of Applied Physics, Shanghai 201800, P. R. China

[2] University of Chinese Academy of Sciences, Beijing 100049, P. R. China

Abstract

There is an increasingly critical demand on the angular stability of double crystal monochromator (DCM). This work focuses on a method to measure angular vibration directly at the DCM crystals using a dual-frequency interferometer. This method was applied to the off-line test of a newly developed cryocooled DCM at Shanghai Synchrotron Radiation Facility (SSRF), which can obtain a resolution of 8 nrad. The DCM was then tested on the X-ray Test Line. Both off-line and on-line results were referenced for DCM structure optimizations. In this paper, the DCM angular stability measuring method is presented, and detailed information of the results are shown.

INTRODUCTION

In the Phase-II beamline project of Shanghai Synchrotron Radiation Facility (SSRF), a fast x-ray imaging beamline will be constructed. To ensure the imaging quality, the beam stability is supposed to achieve 0.25μrad/10min, thus the influence on the spatial resolution can be controlled within 1μm. A cryocooled double crystal monochromator (DCM) has been designed and manufactured for this new beamline, which is under optimization at present. Main specifications of DCM stability are shown in Table 1 [1]. To achieve this target, a series of tests has been carried out on DCM stability, so as to provide references on the structure optimization.

Table 1: Angular Stability Specifications of DCM

Imaging Mode	Spatial Resolution (μm/pixel)	Angular Stability (μrad)
Monochromatic /White beam	1	≤0.25/10min
	2	≤0.5/10min
	5	≤1.5/10min

EXPERIMENTAL DESIGN

Principle and Instrument

To obtain the frequency information of DCM vibration, an Agilent®10719A differential interferometer was applied to angular measurement. As the interferometer is mounted with quarter-wave plates inside, direct measurement of a mirror or a polished crystal surface is available. Figure 1 shows the schematic of the interferometer [2,3].
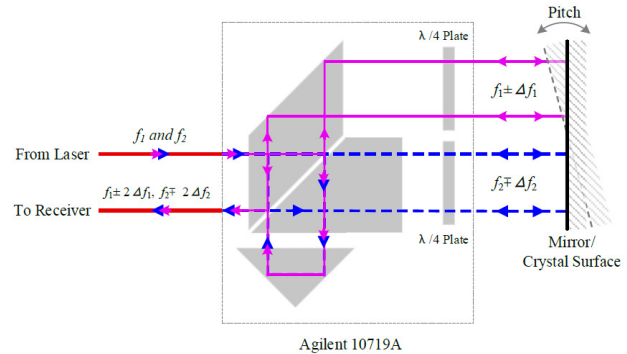

Figure 1: Schematic of 10719A.

According to Doppler effect, the angle can be worked out as:

$$\tan\theta = \frac{\lambda}{4D}\int_0^t \Delta f\, dt = \frac{N\lambda}{4D} \qquad (1)$$

With an upgrade of the monitor board from E1735A to N1230A, the resolution of this measuring system can be increased from 50nrad to 8nrad [3,4]. The upgrade is now in progress.

Methodology and Experimental Setup

With a mirror located by the outlet flange, angular vibration of double-crystal could be measured directly, as shown in Figure 2. This method can also be applied to the vacuum condition. All the off-line tests were carried out in Lab 1042 at SSRF, shown as Figure3, where the floor is only 0.12m thick with no pile underground [5]. The sampling rate was set to be 500 Hz to obtain the frequency information within 200Hz. As the experimental environment was not satisfactory, more attention was paid on the frequency information.
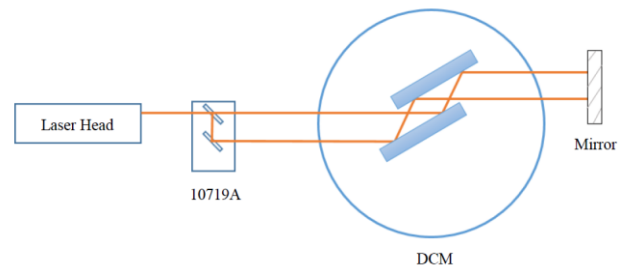

Figure 2: Direct measurement of double-crystal stability.

THERMO-MECHANICAL ASPECTS OF THE MOBIPIX, A COMPACT X-RAY IMAGING SYSTEM WITH EMBEDDED GPU*

A. Gilmour A Jr.[†], W.R. Araujo, J.M. Polli,
Brazilian Synchrotron Light Source (LNLS), Campinas, Brazil

Abstract

In the light of the high brilliance fourth generation synchrotron light sources, real-time imaging techniques became possible, boosting the demand for fast and reliable detectors. Mobipix project is a compact X-ray imaging camera designed for Sirius [1], based on Medipix3RX** [2,3]. The control and acquisition system uses System-On-a-Chip technology with embedded Graphics Processing Units (GPUs) where data processing algorithms will run in real time. The Mobipix X-ray detector is designed to perform as a video camera, enabling X-ray imaging experiments and beam diagnose, at thousands of frames per second (FPS), without external computers.

This paper presents the development of the Mobipix detector mechanics. The authors describe the path taken to design the structural aspects, ensuring robustness and versatility in the device installation to the beamlines, and the thermal aspects, regarding forced air cooling, high heat density, and small volume through which the flow will occur. The latter aspects were developed by exploiting Computational Fluid Dynamics (CFD) modelling.

The Mobipix has 28 x 28 mm² active area, composed by 260k pixels of 55 x 55 μm², and is planned to achieve continuous readout up to 2000 FPS.

INTRODUCTION

The Mobipix electronic design is composed of three boards, the upper board is the carrier board, responsible for housing a Nvidia Jetson TX-1 [4] and providing external connections. The lower board contains the analogical and digital electronics for Mobipix control and readout, being nominated Mobipix board. The board housing four Medipix3RX sensors is attached to the Mobipix board by a perpendicular connection, and is called the Medipix board. Figure 1, illustrates the three boards and their assembly disposition.
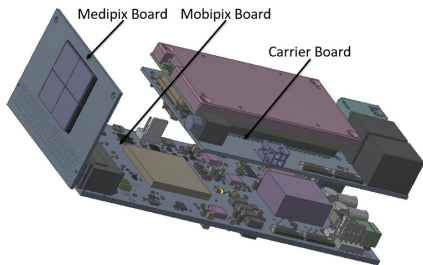

Figure 1: The three electronic boards that compose Mobipix, assembled.

Objectives

This work aimed at keeping the volume of the device as small as possible, while ensuring that the temperature of each component is kept within its given limits. There are two different kinds of semiconductor sensors intended to be coupled to Mobipix, one made of silicon (Si) and another made of cadmium telluride (CdTe). The thermal project must attend both possibilities.

Figure 2 and Figure 3 demonstrate the position of the main heat generating components, while Figure 4 lists their description and worst-case scenario heat dissipation, according to their datasheets [2-13].
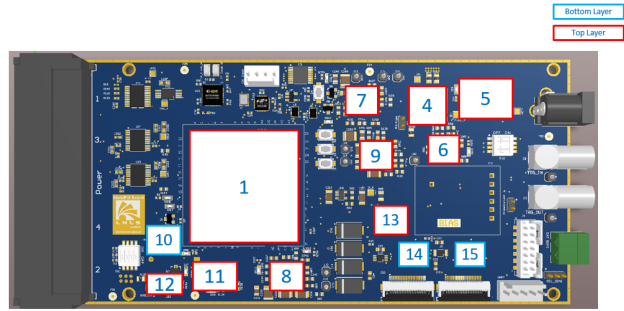

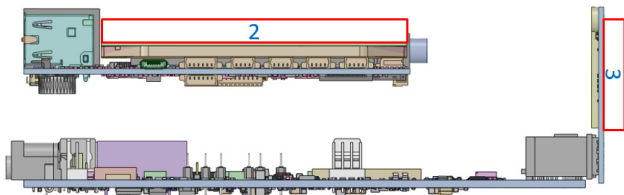Figure 2: Heat generating components in Mobipix board.

Figure 3: Heat generating components in the other two boards.

Component (ID no.)	Power [W]	P. Density [W/m³]	Allowed T [°C]
FPGA Kintek-7 Xilinx (1)	4	1.32E+06	80
Jetson TX-1 (2)	15	4.27E+05	80
Sensor Medipix-3RX (3)	6	6.56E+06	60
LTC4358 Protection Diode (4)	1	1.83E+07	80
BNX025H01B Source Filter (5)	1	2.65E+06	80
LTM4622 Tension Adjuster (6)	1.8	1.90E+07	120
LTM4622 Tension Adjuster (7)	0.9	9.52E+06	120
LTM4622 Tension Adjuster (8)	1.2	1.27E+07	120
LTM4622 Tension Adjuster (9)	1.5	1.59E+07	120
ADP1740ACPZ-1.5 Tension Adjuster (10)	0.2	1.48E+07	80
LT3071 Tension Adjuster (11)	0.82	5.69E+07	80
ADP1740ACPZ-2.5 Tension Adjuster (12)	0.16	1.19E+07	80
LT3080 Tension Adjuster (13)	1.1	1.43E+08	125
MC20902 MIPI Protocol Driver (14)	0.5	1.36E+07	80
MC20902 MIPI Protocol Driver (15)	0.5	1.36E+07	80

Figure 4: Heat Generation, Heat Density and Maximum Allowed Temperature for Each Component.

VIBRATION MONITORING AT TPS STORAGE RING*

K. -H. Hsu [†], H.-S. Wang, W. -Y. Lai, C.-K.Kuan, National Synchrotron Radiation Research Center, Hsinchu 30076, Taiwan

Abstract

In order to locate irregular vibrations caused by the installation of new equipment or malfunctioning of the machine, a vibration monitoring system was developed for the storage ring. Totally, 72 accelerometers and 10 velocity sensors were used to detect girder and ground vibrations, respectively. Continuous long-time observation results will be presented.

INTRODUCTION

For the low-emittance, high-brightness and high-stability Taiwan Photon Source (TPS), vibration issues have been studied. Before the TPS was constructed, D.J. Wang had recorded ground vibrations in 2006 at different locations across the NSRRC [1]. These measurements show that transverse vibrations were sometimes large than vertical vibrations for displacements at frequencies above 1.12 Hz but were almost the same above 3.5 Hz. However, we assume, that after more than ten years the situation is different now with significantly different environment. In recent years, the addition of vibration sources like the utility system, may have changed the vibration characteristic for the TPS. Since the utility equipment such as pumps, cooling water systems and air handling units (AHU) need to operate continuously over years, higher vibrations may get introduced when one component fails. In order to locate irregular additional vibrations caused by the installation of new equipment or the malfunction of the machine at the earliest time, we developed a vibration monitoring system to monitor the vibration status comprehensively and continuously.

Long-term girder and ground vibrations of the TPS storage ring were performed with the vibration monitoring system and we present in this paper observations of the vibration levels at various locations and variation of those vibrations with respect to day and night, work day and holiday.

EQUIPMENT AND METHODOLOGY

The TPS storage ring has a circumference of 518.4m composed of 24 Double-Bend Achromat lattice cells. Each TPS SR cell is composed of three magnet girders and the layout of 24 cells (R01~R24) of the TPS SR is shown in Fig.1. Accelerometers (PCB 393B31) were mounted on the first girder (G1) of each cell sensitive in three directions X, Y and Z, where X, Y and Z are the horizontal, vertical and longitudinal coordinates as shown in Fig.2. Tri-axial velocity sensors (Walesch MST-1031) were installed on the ground between G1 and G2 of each cell. However, there are only 10 velocity sensors installed

in R01, R03, R05, R07, R09, R11, R13, R15, R17, and R21 due to the limited availability of equipment. Totally, 72 accelerometers and 10 velocity sensors were used to measure the vibration of girders and ground of the TPS storage ring, respectively. The sensors installed evenly in 24 cells of the TPS storage ring are connected to the corresponding DAQ devices (NI PXI-4496) which are installed in a PXI chassis in 24 control and instrument areas (CIA) on the second floor.
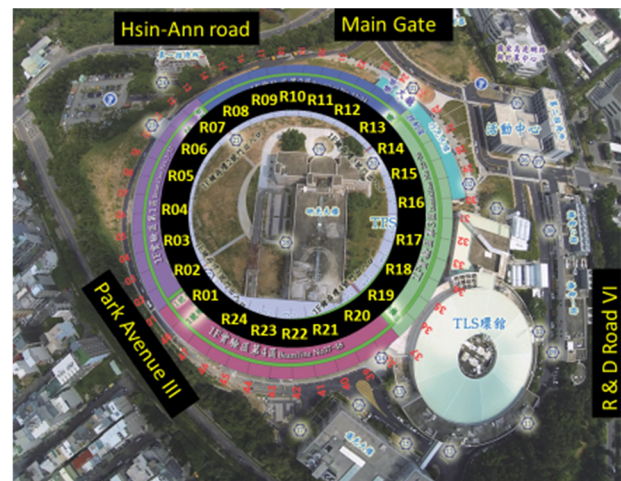
Figure 1: Layout of the 24 cells TPS storage ring on the NSRRC campus.
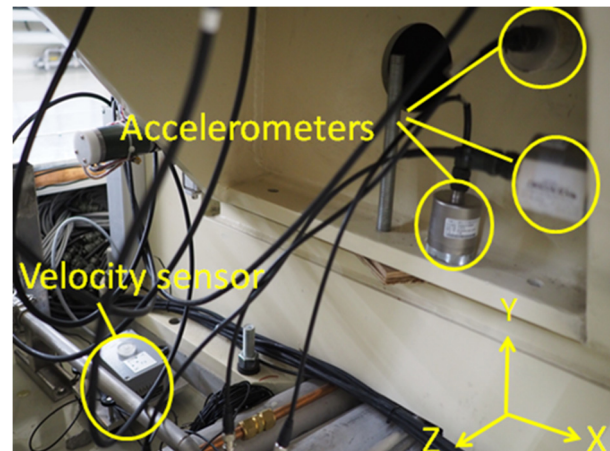
Figure 2: Vibration sensors are installed on the ground and girder of each TPS SR cell.

The Vibration signals were recorded, processed and analysed by a LabVIEW program with a sampling rate of 256Hz. We took 2048 data points for an FFT analysis to get the power spectrum density (PSD) [2]. The acceleration PSD and velocity PSD measured by accelerometers and velocity sensors are converted into displacement PSD by integration [3].

OPTOMECHANICAL OPTIMIZATION FOR A SAGITALLY BENT DOUBLE CRYSTAL MONOCHROMATOR, USING FINITE ELEMENTS AND RAY TRACING

N. Jobert[†], T. Moreno, M. Ribbens, E. Fonda, Synchrotron SOLEIL, Gif Sur Yvette, FRANCE

Abstract

Designing a second crystal for a sagitally bent Double Crystal Monochromator (DCM) requires dealing with a number of conflicting requirements. Especially when working with high-energy photons, the angular aperture (Darwin width) becomes very narrow (below 10 µrad for Si) while simultaneously the bending radius is decreasing (down to 1.2 m for typical beamline dimensions at 40 keV). In this situation, the cross-talk between tangential and sagittal curvature becomes a key parameter, and two strategies are generally used to overcome the issue: either using a flat crystal with a specific length/width ratio, or usage of a rib-stiffened crystal. In the frame of the upgrade of the SAMBA beamline DCM, both solutions have been explored, using a suite of scripts connecting a general purpose FEM code (ANSYS) and a ray-tracing code (SpotX). This has allowed a systematic evaluation of a wide number of configurations, giving insight in the interaction between geometric parameters, and ultimately resulting in a significant increase in the photon throughput at 30 keV without comprising neither spectral resolution nor spot size at sample location.

INTRODUCTION

During the upgrade of the SAMBA (Spectroscopy Applied to Material Based Absorption) beamline DCM, the second crystal needed to be replaced, along with its bending mechanics. Two improvements were requested by the beamline scientist. Firstly, it was desired to extend the 2nd crystal usable length so that the corresponding (longitudinal) translation stage could be removed, thus improving mechanical stability. Secondly, the photon throughput at high energies had to be as high as possible (preferably no less than 50% at 30 keV).

OBJECTIVES

The beamline layout is provided in Fig. 1. Combining the Bragg law for first order diffraction (eq. 1) and the equation for sagittal focusing (eq.2), the linear relationship between sagittal curvature and energy is derived (eq. 3).

$$2\,d\sin\left(\theta_{Bragg}\right) = \lambda \qquad (\text{eq. 1})$$

$$\frac{1}{p} + \frac{1}{q} = \frac{2\sin(\theta)}{\rho} \qquad (\text{eq.2})$$

$$\rho\,E = cte = \left(\frac{hc}{d}\,\frac{pq}{p+q}\right) \qquad (\text{eq.3})$$

Where, d is the spacing between crystal planes, λ is the wavelength, h is Planck constant, c is the light celerity, p and q are the object and image distances, ρ is the sagittal bending radius, E is the photons working energy.

A Si(220) monocrystal is used, so that the Bragg Angle and the curvature in the 5-40 keV energy range are as follows (Fig. 2):
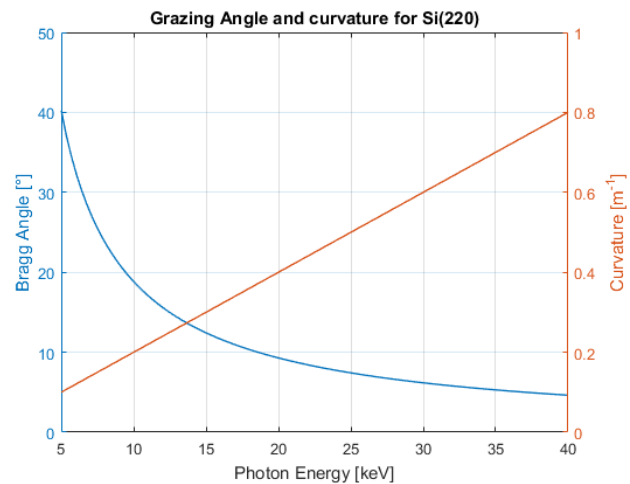
Figure 2: Bragg Angle and curvature.

In order to lose a minimal amount of photons, the parallelism between the first and the second crystals must remain well below the Darwin with of the crystal, which becomes increasingly small at high energies :

- @20keV: 9.3 µrad
- @30keV: 6.2 µrad
- @40keV: 4.6 µrad

Since the footprint has a length of about 10 to 20 mm, meeting the slope error criterion makes it necessary to have longitudinal bending radius larger than 1000 m. Compared to the sagittal curvature (slightly above 1 m), this in turn requires achieving a decoupling ratio of 1000 and above. The anticlastic effect must therefore be drastically minimized.

[†]nicolas.jobert@synchrotron-soleil.fr

EXPERIMENTAL MODAL ANALYSIS VIBRATION MEASUREMENT TO INFORM ENGINEERING DESIGN

J. H. Kelly, The Diamond Light Source Ltd, Harwell, UK

Abstract

Experimental Modal Analysis was performed on an existing 5 degree of freedom mirror system on beamline I08 at the Diamond Light Source, by impacting the structure and measuring the response at locations of interest. Commercial software was used to generate the frequency response functions and mode shape animations. This experimental information was used to inform and optimise a design iteration for a new mirror system. The new mechanism was designed, installed and tested on the J08 branch line at The Diamond Light Source to validate the expected improvements in stability, stiffness and resonant frequency. The mirror system fundamental resonant frequency was significantly increased from 20 Hz to 49 Hz.

INTRODUCTION

Experimental Modal Analysis is a technique which allows a mechanical system's vibration mode shapes to be identified, quantified and visualised. This information can then be used to inform future design & operation. It is commonly used for everything from aircraft to tennis rackets. Modal Analysis was used at the Advanced Photon Source during the development of new magnet support structures for example [1]. There are numerous commercial systems based upon different data capture methods from large scanning laser Doppler vibrometry systems [2] to single accelerometer techniques [3].

5 Degree of Freedom Mirror System

The I08 X-ray Microscopy beamline at the Diamond Light Source uses 3 mirror systems with identical supports. The new J08 branchline project required a new mirror system. Rather than order an identical copy of an existing mirror system, the opportunity for a design iteration was taken. The original systems which were procured from Instrument Design Technology Ltd.™ (IDT), have been in service since 2013. They have operated without fault and exhibit excellent thermal stability. The design uses an orthogonal system of slides, rails and vertical jacks to provide the 5 degrees of freedom (DOF). The mirror system moving platform is mounted without over constraint. A spherical bearing forms the "cone", a single free rail & spherical bearing forms the "vee" and 2 crossed free rails & a spherical bearing forms the "flat". A horizontally deflecting mechanical mirror bender is mounted within the vessel with a fine pitch piezo mechanism incorporated into the support. The vessel is pumped by a relatively small 200 l/s ion pump, mounted in top of the system, as there was no space underneath.

An image of the system under test is given in Figure 1. Up-stream of the mirror is a diagnostic vessel and down-stream is the radiation shutter.
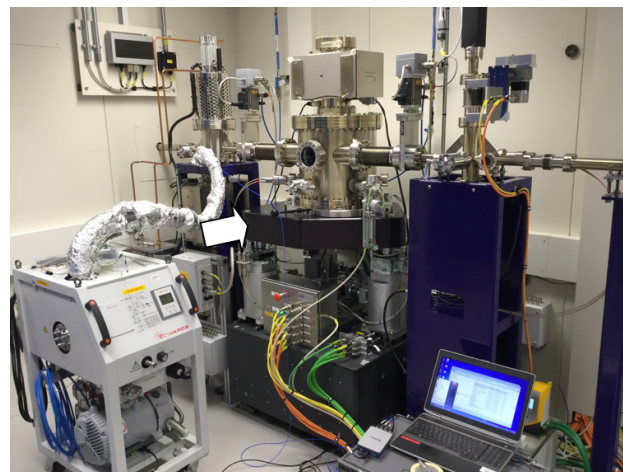

Figure 1: Mirror System I08-M4 at the Diamond Light Source. Impact location indicated by arrow.

Data Capture & Processing

The data presented within this paper was taken using a single triaxial accelerometer (PCB™ LW214478), an impact hammer (Bruel & Kjaer™ 8206), a 4 channel signal amplifier (National Instruments Ltd.™ cDAQ-9171) and software from M+P International Ltd.™ (Analyzer 5.1.0 software [3]).

The method chosen for this study was to manually impact the system at the same point and move the triaxial accelerometer around. The impact location was chosen to drive the resonant mode shapes most likely to cause X-ray beam motion. The direction and location are indicated in the image above (Figure 1). This force vector drives both horizontal and rotation modes of the horizontally deflecting optic. A course 3D model of the mirror system was created with node locations either corresponding to physical data capture locations or simply following data capture locations. For example, the granite block was modelled with 4 data points on the top surface close to the corners with an extra 4 virtual slave points to form the bottom surface. A total of 26 data points (5 impact average per point) were measured to give a clear picture of how the mirror system base, jacks, moving platform, vacuum vessel ports, ion pump and neighbouring vessel ports move. The software processes the accelerometer data using the time, amplitude and phase information from the calibrated impact hammer to create frequency response functions (FRF) & mode shapes. The modal analysis 3D model is shown below (Figure 2). Multiple data points were taken on the

THERMAL ANALYSIS OF HIGH HEAT LOAD MIRRORS FOR THE IN-SITU NANOPROBE BEAMLINE OF THE APS UPGRADE*

J. Knopp†, X. Shi, Argonne National Laboratory, 60439 Lemont, IL United States
J. Maser, R. Reininger, M. V. Fisher, Argonne National Laboratory, 60439 Lemont, IL United States

Abstract

The Advanced Photon Source (APS) is currently in the process of upgrading to a multi-bend achromat (MBA) storage ring, which will increase brightness and coherent flux by several orders of magnitude. The planned In-Situ Nanoprobe (ISN) beamline, one of the feature beamlines of the APS Upgrade (APS-U) project, is a 220 m long beamline that aims to focus the x-ray beam to a spot size of 20 nm or below by focusing with a KB pair. A double-mirror system, consisting of a high heat load mirror and a pink beam mirror, is designed to provide high harmonic rejection, reduce the power transmitted to the monochromator, and focus the beam along the vertical direction to a beam-defining aperture (BDA). One of the key issues is to manage the high power and power density absorbed by these mirrors. To attain the best focus at the BDA, the pink beam mirror needs to be mechanically bent to correct for thermal deformations on both mirrors. In this paper we report on the thermal responses of the mirror system to different undulator tunings and cooling schemes as calculated with Finite Element Analysis (FEA) and optical ray tracing.

INTRODUCTION

The ISN beamline will allow high-resolution imaging, spectroscopy, and tomography of energy materials and energy devices, as well as of other complex, hierarchical systems under in-situ and operando conditions. A flat high heat load mirror, M1, is located at 28 m from the source. A bendable pink beam mirror, M2, located 29 m from the source is used to focus the x-rays in the vertical direction from the source to the BDA, which is located at 26 m downstream of M2 (see Fig. 1). Both mirrors deflect the beam by 5 mrad (2.5 mrad grazing angle) in the vertical direction. Ray tracings show a focus at the position of the BDA without visible coma as expected from the near 1:1 focusing.
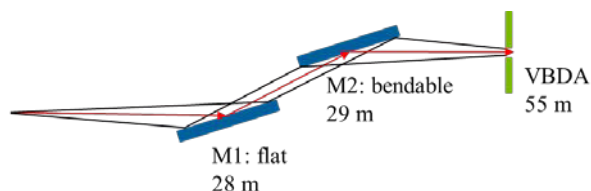

Figure 1: Schematic of the M1 and M2 mirrors of the ISN beamline focusing to the BDA.

M1, which is a flat mirror and deflects the white undulator beam is placed as close to the source as possible, to allow a secondary focus as far upstream as feasible, without reducing the size of the secondary source below the original source size.

To determine the effect of the heat load induced deformations on the spot size at the BDA location, the absorbed power by the mirrors was calculated using SRCalc [1] followed by several FEA calculations. The deformed output of the FEA was subsequently used in the ray tracings with and without the bending required to correct for the thermal deformation of the system.

THERMAL ANALYSIS

The insertion device designed for the ISN beamline has a 25 mm period and is 4.6 m long. Calculations were performed when the insertion device was tuned to emit photon energies between 5 keV to 12 keV at 1000 eV increments. The power absorbed by each of the mirrors was calculated assuming 200 mA stored in the 6 GeV storage ring. The power densities were imported into ANSYS and applied as a heat flux on the surface of the mirrors. The absorbed power density on the M1 mirror when the undulator is tuned to emit 5 keV is shown in Fig. 2. As seen in the figure, the absorbed power density does not vary significantly in the illuminated area. This is also the case for all energies investigated.

ANSYS Workbench version 18.2 was used in the steady state thermal analysis of the M1 and M2 mirrors. Both M1 and M2 mirrors are 400 mm long, 50 mm wide, and 50 mm thick.
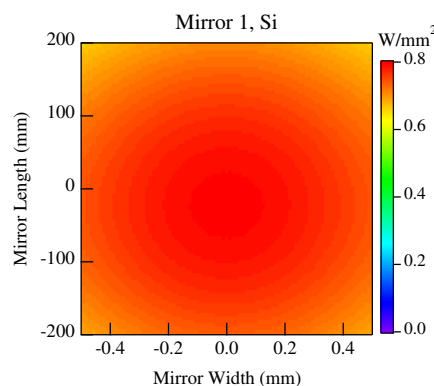
Simple Side Cooling

Figure 2: Absorbed power profile on M1 at 5 keV.

ADJUSTING MECHANISM OF INTER-UNDULATOR SECTION FOR PAL-XFEL

H.G. Lee, B.G. Oh, S.B. Lee, Y.G. Jung, H.S. Suh, S.H Jeong, D.E. Kim, K.H. Park, J.H. Han, H.S. Kang, H.S. Lee, Pohang Accelerator Laboratory, Pohang, Korea

Abstract

Pohang Accelerator Laboratory (PAL) has developed a SASE X-ray Free Electron Laser based on 10 GeV linear accelerator. The inter-Undulator (IU) support section was developed to be used in the intersections of the Undulator Systems. The IU supports consist of phase shifter, quadrupole magnet with mover, beam loss monitor, cavity BPM with mover, two corrector magnets and vacuum components. The adjusting mechanism of IU Support has manual alignment system to be easily adjusting the component. The mover of quadruple magnet and cavity BPM with submicron repeatability has auto-adjusting systems with stepping motor. The mover main specifications include compact dimensions and a ±1.5 mm stroke in the vertical and horizontal direction. Linear motion guide based on 5-phase stepping motors have been chosen. This paper describes the design of the stages used for precise movement and results of mechanical measurements including reproducibility will be reported.

INTRODUCTION

PAL-XFEL has been providing X-rays in ranges of 0.1 to 0.6 nm for hard X-ray line and 3.0 nm to 1.0 nm for soft X-ray line by using the self-amplified spontaneous emission (SASE) Schematic [1]. For undulator system, there are 20 undulators for hard X-ray line and 7 planar undulators with additional two EPUs (Elliptically Polarized Undulator) are expected for soft X-ray line. To generate X-ray FEL radiation, the PAL-XFEL undulator section requires high resolution beam position monitoring systems with <1 μm resolution for single bunch. It will be used in the intersections of the Undulator Systems to achieve high resolution requirement.

The inter-undulator sections, shown in Figure 1, consist of phase shifter, quadrupole magnet with mover, beam loss monitor, two corrector magnets, cavity BPM with mover and vacuum components. The quadrupole mover developed based on the EU-XFEL concept with some modifications [2]. It includes submicron repeatability for quadrupole magnet and a ±1.5 mm stroke in the vertical and horizontal direction. Compact linear actuators based on 5-phase stepping motors have been chosen. Vertical actuator works in a wedge configuration to take mechanical advantage. A closed-loop control system has been developed to achieve this repeatability. For the feedback, one LVDT sensor for each axis was used.

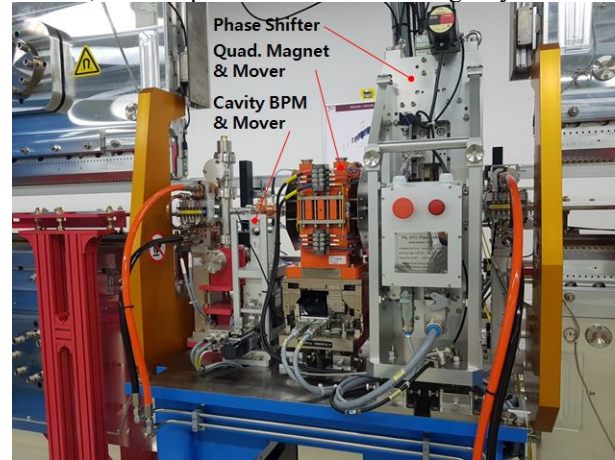Mechanical switches are used to limit movement. In addition, hard-stops are included for emergency.

Figure 1: Lay-out of inter-undulator section.

OVERVIEW OF CAVITY BPM MOVER

The cavity BPM(C-BPM) system has installed in between each undulator with other diagnostics tools. The cavity BPM Mover had been fabricated, tested and installed for the PAL XFEL [3]. The main specifications include submicron repeatability for a 10 kg cavity BPM with support within compact dimensions and a ±1.5 mm stroke in the vertical and horizontal direction. Linear motion guide based on 5-phase stepping motors have been chosen. For the measurement of the position, one digital probe sensor for each axis was used. Mechanical switches are used to limit movement. In addition, hard-stoppers are included for emergency.

Table 1: Main Specification for C-BPM Movers

	Value	Details
Dimensions	332x140x255.5 mm³	Long, wide, high
Axes	2(H & V)	±1.5 mm stroke
Load	10 kg	
Repeatability	< 3 μm	
Control Device	Digital probe closed-loop	EPICS
Ranges	±1.5 mm Limit Switch	±1.6 Hard Stopper
Driving System	5 Phase Stepping Motor	With brakes
Measure System	Digital Probe (DP/5/S)	< 0.15 μm
Limit Sensor	D4E-1C20N	

The main specifications for these movers are included in Table 1. The movers are composed of each stepping motor for horizontal and vertical, digital probe, limit switch and harder stopper. Figure 2 shows the 3D view of cavity BPM system. A robust and compact mover is required according to specifications therefore concept

OPERATION STATUS OF HLS SYSTEM INSTALLED TO MEASURE GROUND CHANGE OF LARGE SCIENTIFIC EQUIPMENT IN REAL TIME*

Hyojin Choi[†], Seung Nam Kim, Seung Hwan Kim, Sangbong Lee, Hong-Gi Lee, Jang Hui Han and Heung-Sik Kang,
Department of Accelerator, PAL-XFEL, Pohang, Korea

Abstract

Several parts that comprise the large scientific equipment should be installed and operated at precise three-dimensional location coordinates X, Y, and Z through survey and alignment to ensure their optimal performance. As time goes by, however, the ground goes through uplift and subsidence, which consequently changes the coordinates of installed components and leads to alignment errors ΔX, ΔY, and ΔZ. As a result, the system parameters change, and the performance of the large scientific equipment deteriorates accordingly. Measuring the change in locations of systems comprising the large scientific equipment in real-time would make it possible to predict alignment errors, locate any region with greater changes, realign components in the region fast, and shorten the time of survey and realignment. For this purpose, a WPS's (wire position sensor) are installed in undulator section and a HLS's (hydrostatic leveling sensor) are installed in PAL-XFEL building. This paper is designed to introduce performance enhancements to reduce observed phenomena and measurement errors in the HLS system operation process.

INTRODUCTION

All components of PAL-XFEL were completely installed in December 2015, and Hard X-ray 0.1nm lasing achieved through its beam commissioning test and machine study on March 16, 2017. The beam line users are use the hard X-ray since March 22, 2017 [1, 2].

The HLS and WPS system has been installed since September 2016 to measure and record changes of the building floor and devices in real-time [3, 4].

HISTORY OF HLS USED ON THE ACCELERATOR

HLS was developed by the Alignment and Geodesy group at the European Synchrotron Radiation Facility (ESRF) for long term monitoring and control of rapid realignment of the storage ring machine at 1990. The concept of the non-contact capacitive sensor developed at the ESRF has been considerably improved upon by the company FOGALE-Nanotech. Various types of HLS Sensors, including Capacitive and Ultrasonic, are developed and used in recent. European Council for Nuclear Research (CERN) announced the results of the comprehensive testing of HLS and WPS in many forms [5].

SELF-CALIBRATION FUNCTION

Deutsches Elektronen Synchrotron (DESY) conducted In-situ experiments to develop the Ultrasound sensor for HLS in 2001 and the basic design concept of Ultrasound sensor for HLS was built based on the result of the experiments [6]. The structure of Ultrasonic pulse hydrostatic level sensor developed by Budker Institute of Nuclear Physics (BINP) in Russia is described in Fig. 1. The sound reflector made of invar metal that has a low thermal deformation acts as an absolute ruler at an interval of 7.5mm and self-calibrates the differences of water density due to the changes in temperature (sound speed) and electrical properties of the transducer. The composition and operating principle of ULS Electronics developed by BINP and its results of field tests are described in more detail in related papers [7, 8].
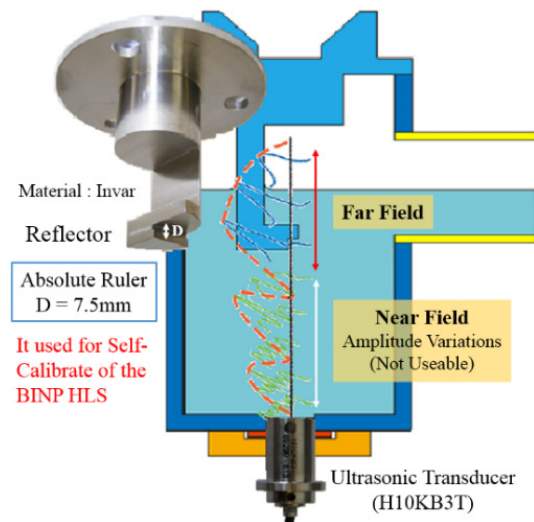
Figure 1: The HLS measurement concept using an Ultrasonic transducer and self-calibration.

INSTALLATION OF HLS AND WATERPIPE

Although it is best to survey the changing progress conditions of the building floor with a view to installing the HLS system, it is desirable to install it low and in close contact to the floor. However, since the concrete anchor, height controlling equipment, etc. is reflected in the support design, the HLS support of the Undulator section was designed to be 15cm in height and the waterpipe support to be 25cm in height. In order for the waterpipe to pass

A FAMILY OF REDUNDANT POSITIONING DEVICES FOR SYNCHROTRON APPLICATIONS

G. Olea[†], N. Huber, HUBER Diffraction GmbH & Co.KG, Rimsting, Germany

Abstract

A new family of reconfigurable devices able to work in synchrotron applications, especially in diffractometer's environments has been developed. It can provide six (6) or less than six (<6) degrees of freedom (dof) motion capabilities (F≤6) being able to pose a heavy load sample (instruments) with high precision towards an X-ray incoming beam. Based on the Parallel Kinematics (PK) Quatropod concept with redundant actuation (Rd=2), it was built around the fully (F=6dof) basic topology 6-4($2$13) where 2- actuated and 1, 3- passive joints, respectively. By altering the passive joints dof, structures with less than six dof (F<6) can be obtained, e.g. 5-4($2$13$_2$)/F=5, 4-4($2$13$_1$)/F=4, 3-4($2$13$_0$)/F=3 (3$_2$ and 3$_1$ and 3$_0$ stand for 3dof joint with constrained/less dof – f=2, 1 or 0/blocked). For a perfect symmetric arrangement and using only P, and S (P-prismatic, S-spherical) joints several useful positioning mechanisms are presented. And, in the design phase, 2dof linear actuators (2P), e.g. XY stages have been proved to be a successful choice, too.

INTRODUCTION

Today, the synchrotron light has been proved to be one of the most active tools to investigate the internal structure of materials. By using the actual and/or further advanced facilities and techniques, the mysteries of our ancient and future world are waiting to be deciphered.

The X-ray Diffraction (Df) is a well-established research technique for material characterisation. In its basic and/or modern forms [1] it is actually the largest investigative technique. Previously applied exclusively for crystalline materials, nowadays it extended to virtually any materials scattering X-rays. An appreciable number of research results have been obtained in the recent years.

The "workhorses" here have been the Diffractometers (Dm) machines. Built in standard or customized types for various specific applications they are manufactured by several companies (HUBER, NEWPORT, KOHZU, etc). Very often, the requirements are coming to use them for samples working in special environmental conditions (vacuum, cryo, magnetic) fields. These instruments could be sophisticated, large in size and heavy. In addition, they must be manipulated (together with the sample) with high precision, e.g. [2]. However, the existent working space inside of the Dm machines is relative small (constrains are coming from the beam line available room space / hutches, also). In order to comply with this restricted space (especially, height), the sample positioning systems designers must accommodate. Till now, in their concepts, they adopted a serial/stacked solution. (X, Y and/or Z motion xes have been materialized through single axis translation

and/or rotational positioning units called the stages). Subsequently, a sample (and, instrument) is posed in space in the desired position, but with relative low precision (accumulation of errors). The stages are commercially available in a large variety of standard typo-dimensions and can move a heavy load in all (6) or less than six (<6) degrees of freedom (dof). However, in the case of more than 3 dof, the available Dm working space in height sometimes is not enough for stacking all the axes, especially, when rotations around the Centre of Rotation (CoR) point are required. The CoR distance is predetermined (fixed).

Precision Hexapods based on Parallel Kinematic Mechanisms (PKM [3]) are gradually replacing them. They are precise and versatile, able to perform six (6) dof by freely choosing the CoR (variable distances), e.g. PI/Micos, SYMETRIE, NEWPORT, AEROTECH. However, they came with limitations regarding the available portfolio (standard typo-dimensions). The manipulated load & overall size (especially, the height) cannot fulfil always the specific requirements; they are too week or too big. They are not perfectly adapted to Dm environment [4]. Moreover, when less than 6 (dof<6) are necessary, another solutions must be considered.

In order to fulfil all these inconvenient, a new family of positioning devices is proposed. Based on the redundant and reconfigurable principles, at least one of the members could fulfil the above expectations. The main topological, kinematical and conceptual design features for the whole family and in particular for the members will be presented below.

RD-PPTD

HUBER Diffraction & Positioning company has been for a long time a promoter of synchrotron instrumentation pushing the limit of X-ray investigations [5].

A research project (2011) aiming to develop new positioning devices for synchrotron applications based on PKM has finally resulted into the development of a new family of Parallel Positioning Devices (P-PD) based on QUADROPOD (QP) [6]'species'.

By using only fundamental joints (f=1,2,3, f-joint dof), and in the same configuration on each level from the total of three (j=I,II,III) – costs saving and by choosing 2 dof actuation–compact joints, the findings resulted in three (sub) families of topological options. Each actuated level has eight dof capabilities (F$_j$)a=8, j=I,…,III where Fj – level dof (a-actuated) being from kinematics pov redundant one. One from the above QP6_2A (2A–2 dof actuation) (sub) families exhibits useful characteristics for positioning. The 2dof actuation subfamily having all the actuators on the base(Ia) has the advantages of low dynamical effects of motion comparing with another ones - (IIa) and (IIIa), respectively. The 6-4(2)13 (6-dof, 4-chains) representative

LE GUIDE FOR SUPPORT:
A COOKBOOK FOR MODELING OF ACCELERATOR STRUCTURES*

Curt Preissner†, Jeremy Nudell, Zunping Liu, Scott Izzo,
Advanced Photon Source, Argonne National Laboratory, Argonne, Il, 60439, USA

Abstract

The Advanced Photon Source-Upgrade (APS-U) project has stringent specifications and a 12 month installation schedule. Some form of these constraints appear to be common at all multi-bend achromat upgrade projects. At the APS-U, no full tests will be made of the final accelerator support design. The evaluation of the final design against the specifications will be based primarily on computer simulations using virtual inputs.

Ensuring that the final designs meet specifications solely based on simulations is much like cooking a complex, multicourse meal without a trial run. Producing a successful meal on the first try requires a prior understanding of the ingredients, techniques, and interactions between the constituents. A good cookbook can be essential in providing this understanding. Likewise, producing an accelerator support final design that meets the requirements requires a prior understanding of the materials, components, techniques, and interactions between them. This poster describes a cookbook-style approach that any design team can use to confidently predict important characteristics such as natural frequency and ambient vibration response with an error of around 10%.

MOTIVATION

Many third-generation synchrotrons are on a path to a high-brightness, multi-bend achromat (MBA) upgrade [1-3]. In addition to the orders-of-magnitude increase in brightness, these MBA upgrades are unusual in that they involve shutting down very productive machines for a period, removing and replacing the storage ring components, commissioning, and making them again available to the users in the shortest time possible. There is precedent for this in the United States with the SPEAR 3 upgrade project [4]. However, the aggressive project schedules of these MBA upgrades impose additional engineering constraints on the magnet support systems, beyond those driven by physics requirements or those found in greenfield synchrotron projects.

From the beginning of the design process the APS-U supports team assumed there would be a large reliance on computer simulation of magnet support mechanical behavior. Table 1 shows the stringent APS-U mechanical motion tolerances. In addition to these mechanical tolerances, there are space constraints dictated by installation, utilities, and front requirements. The short installation time requires magnets be grouped into larger structures and installed fully aligned and assembled, reducing in-tunnel assembly

time. These constraints all have to be met within the project schedule.

Table 1: APS-U Vibration Tolerances

Specified over 1-100 Hz	X (rms)	Y (rms)
Girder Vibration	20 nm	20 nm
Quadrupole Vibration	10 nm	10 nm

The APS-U magnet support design has evolved in parallel with the magnet, vacuum system, and revised physics requirements, moving beyond that described previously [5, 6]. The only full-scale magnet support prototype has a structure quite different that the final design.

Evaluating the final APS-U magnet support design against Table 1, from ref. [1], using only a numerical model, is challenging. Finite element (FE) model and vibration modelling is convenient due to the ease of incorporating CAD data. However, it is common for synchrotron engineers to expect FE results to be unrealistic [7], to tune a FE model *a posteriori* [8], or to use the FE model to confirm the behaviour of one particular design [9]. The APS-U supports team wanted a model and a process by which the final design could be checked against requirements, the effect of design trade-offs could be evaluated, and that could be used to accurately predict beam motions [10].

RECIPE

Ingredients

The APS-U magnet support systems consist of the following components, listed in order from the floor to the magnets: 1) a thin epoxy grout line, 2) a steel-reinforced concrete 'plinth', 3) a set of support and alignment mechanisms, 4) a cast iron 'girder', and 5) individual magnets. Measurements of the APS have shown the floor can be considered to be rigid. The most basic ingredients in any mechanical dynamic model are geometry, mass, stiffness, and damping. To obtain the final result, one more ingredient is necessary, the facility vibration. In this section we explain how these ingredients can be mixed to capture the behaviour of accelerator magnet support systems, using the APS-U magnet support system as an example.

The appropriate mixing of the ingredients for each component is key to producing an accurate FE model. For the epoxy grout, plinth, and girder, CAD geometry, combined with the material property data are sufficient to accurately capture the component behaviour. The epoxy manufacturer supplies modulus data. For the steel and concrete plinth, the steel reinforcing geometry is captured in the CAD model and can be used with common steel material properties, while the concrete vendor supplied modulus data on the proprietary concrete mix. Likewise for the girder, the

FEA SIMULATIONS OF THE ALUMINIUM VACUUM CHAMBER FOR LOREA INSERTION DEVICE AT ALBA SYNCHROTRON LIGHT SOURCE

M. Quispe[†], A. Gevorgyan, ALBA – CELLS Synchrotron, 08290 Cerdanyola del Vallès, Spain

Abstract

For LOREA, the new beamline at ALBA, the Insertion Device Apple-II helical out-vacuum undulator requires the installation of a suitable narrow – gap aluminium chamber.

The chamber design is based on the standard ALBA aluminium chamber which has an internal elliptical cross section, where NEG coating is deposited and bending magnet (BM) radiation from the upstream dipole is dissipated on the chamber walls. For the standard chamber the upstream distributed absorber cannot protect the entire chamber from direct BM radiation because there is a limitation for its design: the beam impedance of the machine.

Based on new studies of collective effects it has been concluded that it's possible to implement modifications on the upstream distributed absorber and protect the chamber from lateral collision of BM radiation keeping the beam impedance of the machine inside of a safe range. In spite of that still there is a contribution of the tails of BM radiation.

In this paper we describe the behavior of the new aluminium vacuum chamber for different thermal load conditions using water and air for refrigeration. Also we present the design of the modified OFHC upstream distributed absorber.

BACKGROUND

The Insertion Device (ID) for LOREA, the new beam line at ALBA for Low-Energy Ultra-High-Resolution Angular Photoemission for Complex Materials, will operate with a suitable chamber, a narrow-gap, NEG-coated, extruded-aluminium vacuum chamber.
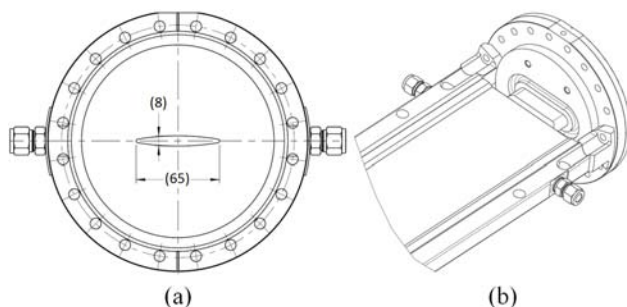

Figure 1: The ALBA narrow-gap, NEG-coated, extruded-aluminium vacuum chamber. (a) Internal elliptical cross section of 65 mm by 8 mm. (b) Detail of the end chamber joined to the flange.

The design model of this chamber is based on the standard aluminium vacuum chambers installed at ALBA. It has an internal elliptical cross section of 65 mm by 8 mm, where NEG coating is deposited (See Fig. 1).

Synchrotron radiation from the upstream dipole is dissipated on the chamber, thus two water cooling channels with 7 mm diameter each is used for cooling. The material used for the manufacturing is aluminium 6061 T6. At each end of the chamber, the aluminium extrusion is welded to an explosion-bonded bimetallic (stainless-steel/aluminium) flange to enable to make a joint to the flange (Spigot flange). The inlet and outlet flanges are bimetal made of AISI 316LN and aluminium 6061 T6. Flanges are CF type, fixed with a DN160 size.

In order to integrate the chamber into the straight section two vacuum components must be implemented: the OFHC upstream distributed absorber and the downstream tapered chamber connected to the current bellows (See Fig. 2).
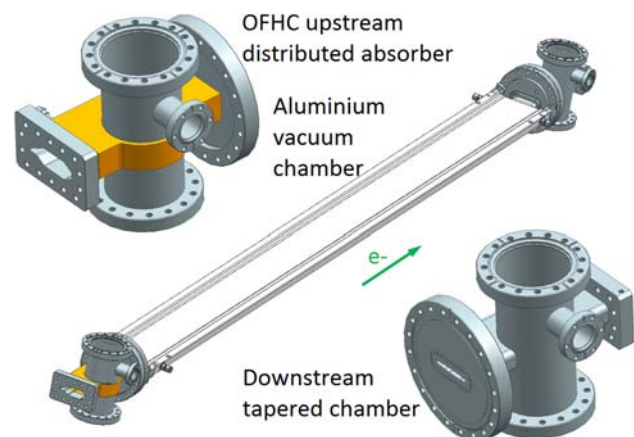
Figure 2: ALBA 3D model of the aluminium vacuum chamber, the OFHC upstream distributed absorber and the downstream tapered chamber.

For the current aluminium vacuum chambers at ALBA the BM radiation hits the wall laterally because the chamber is only partially protected by the upstream distributed absorber. This unwanted configuration is due to a geometrical restriction imposed for the design of the absorber: in order to keep the beam impedance of the machine inside of a safe range a minimum distance between the sharp end of the absorber and the electron beam trajectory must be fixed to 28.5 mm.

For LOREA, new studies of collective effect confirm the possibility to reduce the minimum distance from the sharp end of the absorber to the electron beam trajectory. Then it will be possible to avoid a lateral collision of BM radiation.

---

† mquispe@cells.es

Simulation

FEA Methods

DESIGN OF AN INTEGRATED CROTCH ABSORBER FOR ALBA SYNCHROTRON LIGHT SOURCE

M. Quispe[†], J. Campmany, A. Gevorgyan, J. Marcos
ALBA – CELLS Synchrotron, 08920 Cerdanyola del Vallès, Spain

Abstract

This paper presents the design of an Integrated Crotch Absorber for the new beamline LOREA (Low-Energy Ultra-High-Resolution Angular Photoemission for Complex Materials at ALBA). The LOREA Insertion Device (ID) consists of an Apple II undulator with a period of 125 mm.

For the current ALBA dipole chamber the ID vertical polarized light hits the upper and lower walls because of the very narrow vertical aperture between the cooling channels. To solve this problem some modifications must be implemented both in the dipole chamber and in the crotch absorber located inside of the dipole.

The new crotch absorber, named Integrated Crotch Absorber, must absorb a significant part of the ID vertical polarized light in order to avoid radiation impinging at the post dipole chamber.

The geometry of the Integrated Crotch Absorber is a combination of the conventional crotch and the distributed absorber done at PSI for ANKA. The design has been optimized taking into account the standard thermo-mechanical design criteria as well as the reflective effects of the ID radiation from the opening towards the walls of the dipole chamber.

INTRODUCTION

The ALBA synchrotron light source is currently installing the new beamline LOREA, for Low-Energy Ultra-High-Resolution Angular Photoemission for Complex Materials. It will operate in the range of 10 – 1500 eV and will use polarized light. To produce the light an Insertion Device Apple II undulator with a period of 125 mm has been chosen. The device can operate as an undulator at low energies and as a wiggler at high energies, reaching a wide energy range.

For the vertical polarization mode, the photon beam emitted by the ID at low photon energies has a large aperture angle of ±2.2 mrad, which is the worst case. Because of the very narrow vertical aperture between the cooling channels of the conventional ALBA dipole chamber, the ID vertical polarized light hits the chamber. To solve this problem two main modifications have to be introduced:

- Modification of the dipole chamber. The longitudinal cooling channels have to be removed to increase the vertical aperture.
- Modification of the Glidcop Crotch Absorber. Part of the ID radiation must be absorbed by the opening of the new crotch absorber in order to protect the post dipole chamber from any collision.

---

† mquispe@cells.es

This paper is dedicated to the design of a new Glidcop Crotch Absorber. For ALBA this new absorber is non-conventional because the device must face the Bending Magnet (BM) and ID radiation at the same time. We name this new absorber as Integrated Crotch Absorber because its geometry is a combination of the conventional crotch absorber and the distributed absorber made at PSI for ANKA [1].

Design aspects of the geometry, the effects of the ID beam reflection from the absorber to the walls of the vacuum chamber and FEA simulations of the Integrated Crotch Absorber are included in this paper.
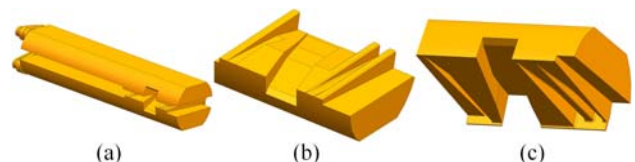
BASIC DESIGN

Figure 1: (a) Assembly of the Integrated Crotch Absorber, (b) The lower jaw and (c) The upper jaw.
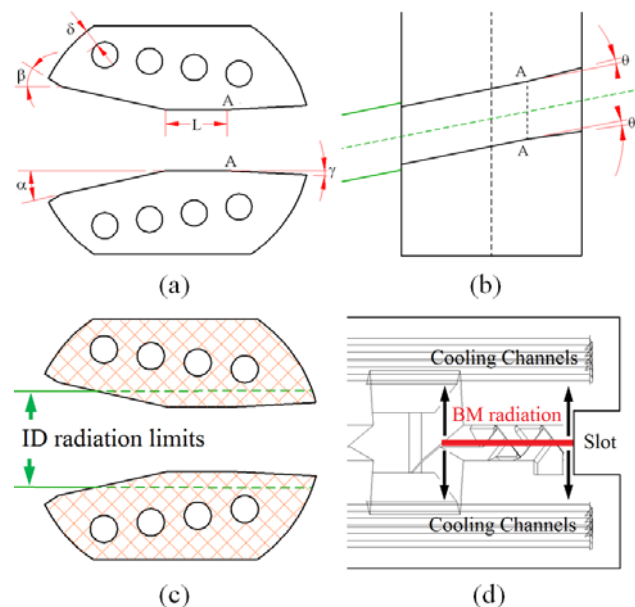

Figure 2: (a) Cross section view in the middle of the opening, (b) Details of the opening from the top view, (c) Details of the beam limits with respect to the cooling channels and (d) Position of the cooling channels with respect to the BM radiation on the teeth.

.

HIGH RIGIDITY GIRDER SYSTEM FOR THE SIRIUS MACHINE

M. C. Rocha[†], A. L. Mesa, A. R. D. Rodrigues, F. Rodrigues, P. P. S. Freitas, R. T. Neuenschwander,
R. J. Leão, T. Jasso, Brazilian Synchrotron Light Laboratory, Campinas, Brazil

Abstract

Sirius is a 4th generation synchrotron light source under construction in Brazil, with a bare emittance of 250 picometer rad, scheduled to have the first beam late this year. One of the most important aspects for this ultra-low emittance machine is the stability of the components, especially the magnets. This paper describes the main characteristics of the girder system, including the concrete pedestal, the levelling units, the girder itself, the clamping mechanism for the magnets and the measurements procedures. Each detail was considered in the design phase and the result is a high rigidity setup with a first horizontal mode close to 170 Hz.

INTRODUCTION

The Brazilian Synchrotron Light Laboratory – LNLS is currently installing the components of the new Brazilian light source (Sirius). This new machine will be a state-of-the-art synchrotron light source [1-2] with low emittance and capacity for 39 beamlines. First users are expected to 2019. For its proper operation, there are high demands in terms of stability of the storage ring components, especially the magnets. Their maximum vibration should not exceed 6 nm according to the specifications [3]. This tolerance implies that the whole building structure and the supports for the magnets should be designed accordingly.

When it comes to the decision as to where to install the storage ring magnets, the choice is usually to fix them on the slab, using intermediate support components such as bases, pedestals and girders. In most particle accelerators the solution is to fix concrete bases or metallic pedestals on the floor, followed by metallic girders that hold assemblies of magnets. Few studies propose girder-free magnet supports, notably [4].

To align the position of the components, levelling and positioning devices are used in-between pedestals and girders and in-between girders and magnets. For the Sirius supports, the concept of using metallic girders and concrete pedestals fixed to the slab is maintained. The main efforts were put into the design and manufacturing of the girders, although many innovations were applied to the concrete pedestals, the design of the levelling units and the fixation of the magnets on the girders. For the girder design, we built up on several girder designs, such as the Petra III [5], and optimized it in terms of rigidity.

One of the key issues for the Sirius building is its vibration characteristics, especially the special slab of the accelerators. Although this design and the civil construction details are of fundamental importance, a discussion about this is not within the scope of this paper. The intent of this work is to describe the main innovations and results related to the high rigidity girder system for Sirius, including design, manufacturing and tests.

SYSTEM DESIGN, MANUFACTURING AND TESTS

To maintain the displacement of the magnets within 6 nm, the vibrations coming from the ground must be attenuated. To achieve this, the vibration spectrum from the environment should not match the natural frequencies of the supporting structure. The goal is, therefore, design the supporting structure to maximize the natural frequency of its first modes of vibration. Also, the structure should provide a significative damping for the environmental vibrations. In terms of geometry of the girders, we performed a Topology Optimization starting from preliminary boundary conditions based mainly on dimensional constraints. Figure 1 shows the result of this study and the resulting geometry based on the study.
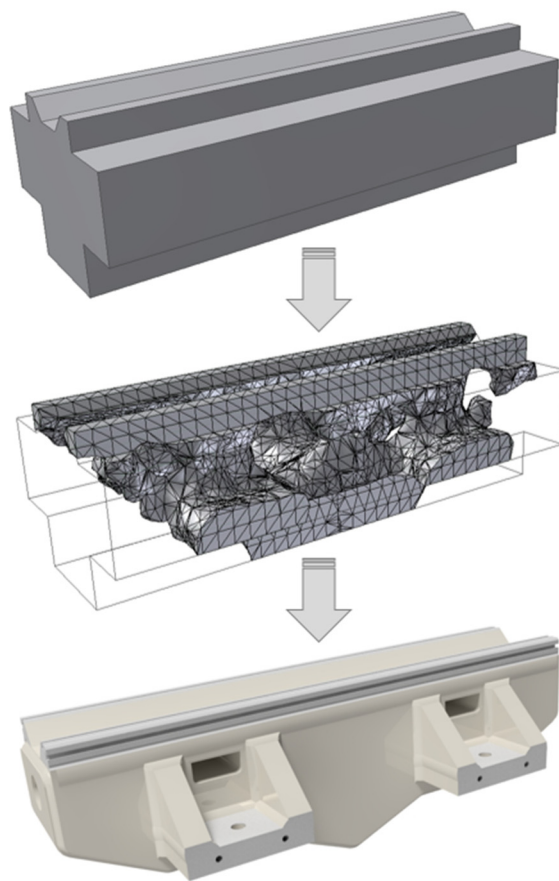

Figure 1: From the Topology Optimization to the final CAD model.

Finite Element Analyses – FEA shows that this "dolphin-shaped" design is indeed optimized in terms of vibration

---

† milton.rocha@lnls.br

A NOTE OF THERMAL ANALYSIS IN SYNCHROTRON RADIATION ACCELERATOR ENGINEERING

I. C. Sheng[†], National Synchrotron Radiation Research Center (NSRRC),
3007 Hsinchu, Taiwan, R.O. C.

Abstract

Thermal and thermomechanical analysis is one of the key process while designing accelerator components that may subject to synchrotron radiation heating. Even some closed-form solutions are available, and yet as to complex geometry numerical analysis such as finite element method (FEM) is commonly used to obtain the result. However due to its complexity of density distribution of the heat load, implementing such boundary conditions in the finite element method (FEM) model is relatively tedious.

In this report we provide a simplified, practical and more conservative method to apply heat load both for bending magnet and insertion device. In addition, a general purpose synchrotron radiation heating numerical modelling is also introduced, and a simple FEM model with EPU power heat load is also compared

INTRODUCTIONS

As to synchrotron accelerator radiation heat load issue, typically when it comes to analysing the designs of crotch absorber, fixed masks, photon stoppers…, etc., one finds that bending magnet (BM) and insertion device (ID) are two major heat sources. The synchrotron radiation (SR) is primary in Gaussian distribution in 1D or 2D. Unless one can compile embedded programming in the FEM tool (such as ANSYS), manually applying such non-constant power density on the nodes in the FEM model is a tedious work. On the other hand, the total heat flux input may be underestimated due to human error.

Due to high speed computer capability nowadays, we find that FEM modelling for this type of analysis, during material assignment element meshing as well as solving process are fairly straightforward. Instead, applying synchrotron radiation heat load distribution is the most time-consuming task among the entire modelling process. To speed up this process, we introduce two methodologies, a simplified and a realistic model for the analysis.

SYNCHROTRN RADIATION DISTRIBUTINOS

Bending Magnet

The power distribution function for the bending magnet can be found in [1]:

$$q\left[\frac{Kw}{mrad^2}\right] = 5.425E[GeV]B[T]I[mA]f(\gamma\varphi) = q_o f(\gamma\varphi)$$

$$(1)$$

_____
† email address shengic@nsrrc.org.tw

Where

$$f(\gamma\varphi) = \frac{1}{\left(1+\gamma^2\varphi^2\right)^{5/2}}\left(1+\frac{5}{7}\frac{\gamma^2\varphi^2}{\left(1+\gamma^2\varphi^2\right)}\right)$$

$$(2)$$

is the shape function of bending magnet, $\gamma = 1957E$ is relativistic energy and φ is the vertical opening angle. Kim [2] suggested that the shape function in equation (2) can be approximated as Gaussian distribution as follows:

$$f(\gamma\varphi) = \exp\left(-\frac{\varphi^2}{2(\sigma_o/\gamma)^2}\right)$$

$$(3)$$

Where σ_o is the standard deviation and is found to be

$$\sigma_0 = \frac{32}{21\sqrt{2\pi}} \approx 0.608$$

$$(4)$$

To simplify the FEM modelling, we can approximate the above shape function to be a Heaviside step function

$$q(\varphi) = q_o(H(\varphi - \frac{\sigma_c}{\gamma}) - H(\varphi + \frac{\sigma_c}{\gamma}))$$

.

As suggested in [3], the equilibrium beam half beam size σ_c is given as

$$\sigma_c = 0.608\sqrt{\frac{\pi}{2}} \approx 0.762$$

$$(5)$$

This assumption is valid because in general, the bending magnet beam size along vertical direction (Gaussian profile) is much smaller than that of the designed body itself. The benefit of utilizing this simplified power distribution are the following:

- Step function distribution gives more concentrated power distribution, which leads to more conservative thermal result.
- Easy to apply power to the FEM model. Only few nodes have to be meshed on the heating surface. This dramatically reduce the modelling time.

Insertion Device

As was given by [4] , power density of elliptical polarized undulator is

$$q[w/mrad^2] = 0.0844E^4[GeV]I[A]\frac{L[m]}{\lambda_o^2[m]} \times$$

$$f(k_x, k_y, \theta_x, \theta_y)$$

$$(6)$$

Where $f(k_x, k_y, \theta_x, \theta_y)$ is the shape function defined as

NSLS-II SITE VIBRATION STUDIES TO CHARACTERIZE BEAMLINE STABILITY

C. Spataro, F. Lincoln, S. Sharma, Brookhaven National Laboratory, Upton, NY, USA

Abstract

High performance goals of NSLS-II require stringent mechanical stability of its instruments such as BPMs, slits, mirrors, monochromators, and detectors. Mechanical stability of these components can be compromised by site-wide as well as local vibration sources (pumps, compressors, etc.). Several vibration studies have been performed at NSLS-II at the request of beamline users. This paper presents the results of these studies highlighting sources of vibration and mitigation strategies.

INTRODUCTION

Modern light sources, such as the NSLS-II at Brookhaven National Laboratory are designed to generate an electron beam with very low emittance and small beam size which requires a high degree of mechanical stability of the girder assembly and a low ground vibration level. The ground motion below 4 Hz is assumed to be correlated over the length of the storage ring cell (25m), and motion above 50 Hz is expected to be negligible.

MOTIVATION FOR MEASUREMENTS

Be it long (DC) or short term (AC), stability directly affects the operation and performance of NSLS-II. The beamlines also require precision mechanical and optical stability in order to meet their specifications and performance goals. At the request of the beamline users, a number of vibration studies were carried out to determine the sources of vibration instabilities that were affecting their operations.

SOURCES OF INSTABILITIES

Vibration sources can be broken down into four categories: natural, cultural, electrical and mechanical. Examples of natural sources are lunar tides, solar tides, earthquakes, wind, barometric pressure, and seasonal changes.

Heavy truck and traffic on the local expressway contribute greatly to the cultural instabilities. Mechanical vibration sources include AC handlers, water flow, liquid helium induced vibrations, and vacuum pumps. Electrical sources include power supply ripple as well as 60 Hz noise from power supplies, etc.

FLOOR MOTION OVER TIME

In October of 2012 vibration data was taken on the NSLS-II floor 2-ID SIX beamline every thirty minutes over a number of days. Measurements of the ground motion in the NSLS-II ring were made on a grouted floor plate as well as on a girder flange in cell 7 inside the tunnel. The results of the integrated displacement vs time from 2-100 Hz can be seen in Figure 1 below.
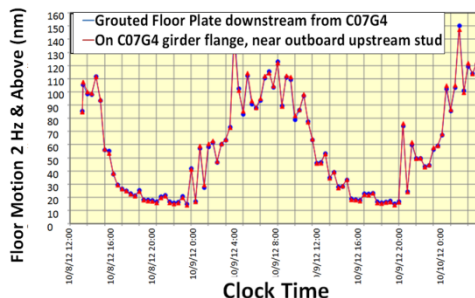

Figure 1: Vertical RMS Displacement vs Time.

The integrated displacement is periodic over a twenty-four hour period. The maximum day-time amplitude was about five times that of the night time amplitude. This was quite a surprise. The day time vertical RMS displacement from 2-100 Hz were upwards of 120 nm at mid-day while the night amplitudes dropped to 15-20 nm. Vibration measurements were taken over the next few months and were found to be very repeatable, though the weekend displacements measurements were slightly lower than the weekday and were also repeatable. The periodic nature of the vibration levels suggested the nearby Long Island Expressway which was later confirmed with measurements as the source of the vibrations.

11-BM VIBRATION MEASUREMENTS

Vibration studies have been performed over the last several years at bequest of the beamline users. The 11-BM (Bending Magnet beamline) was seeing a 200 μm fluctuation in beam position at a rate of 1 Hz during opera-tions. Below is Figure 2 that shows the layout of the beamline consisting of a number of optical benches, a sample chamber, two crys-tals and a single monochromator.

Figure 2: 11-BM layout

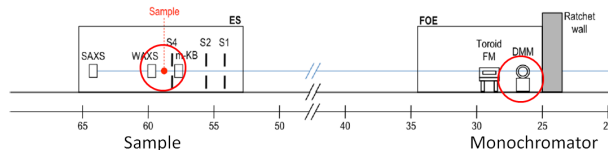Vibration measurements on the floor as well as along the entire beamline on the granite tables at beam height did not find the source of the 1 Hz signal. After a thorough inspection of the beamline, it was found that the spring-loaded screws for the kinematic mount for the 1st crystal were loose. [1] Tightening of these screws resulted in the dampening of the vertical motion as shown in Figure 3.

ENERGY EFFICIENT AIR-CONDITIONING SYSTEM DESIGN

Z. D. Tsai[†], W. S. Chan, C. S. Chen, C. Y. Liu, Y. C. Chung and Y. Y. Cheng, National Synchrotron Radiation Research Center, 30076 Hsinchu, Taiwan

Abstract

At the Taiwan Light Source (TLS) and Taiwan Photon Source (TPS), several studies related to energy savings in air-conditioning systems are underway, where heat recovery has been considered for laboratory applications. The performance of a run-around coil has demonstrated that heat recovery plays an important role in energy conservation. Based on this design of an air handling unit (AHU), we enhance this model by combining it with enthalpy control for seasonal changes. Here, we construct a new AHU to verify the practical impact of energy usage. The improvements show that both mechanisms can be achieved simultaneously.

INTRODUCTION

In general, thermal waste can be treated by circulating deionized water (DIW) and by air conditioning (AC). The main cooling water system at the TPS includes the cooling tower, chilled water, hot water, de-ionized water and heating, ventilation and air-conditioning (HVAC) systems. The air-handling units (AHU) located at the inner and outer rings provide very stable cooling air for the storage-ring tunnel, CIA, experimental hall and Linac area. The amount of HVAC systems must be well optimized so that the accelerator would be the least subject to thermal waste [1]. Besides the requirement to be stable, the utility system is designed carefully with a good satisfactory energy-efficiency ratio (EER) and coefficient of performance (COP). In general, a HVAC system always consumes energy for processes like dehumidification and reheating to maintain a constant temperature and humidity.

Since the utility system is essentially an energy wasting system, a preliminary study for energy efficiency in the HVAC system with heat moving and moisture recovery systems has been started by reviewing the designs in more detail [2]. Here, we address mainly specific designs with three flow piping schemes to verify energy efficiency. In addition, the HVAC system also should be equipped with enthalpy controls to deal with the return and fresh air damper. The control philosophy should have the goal to decrease usage of chilled water in the cooling coils.

ENERGY EFFICIENT AIR-CONDITIONING SYSTEM STRUCTURE

The main components of an AHU include dampers, supply fans, filters, humidifiers, dehumidifiers, heating and cooling coils, ducts and various sensors. We add a pre-cooling coil before the cooling coil, pre-heating coil before the heating coil and the corresponding flow piping.

---

† zdtsai@nsrrc.org.tw

The proposed AHU with extra two coils integrate into three modes, including a traditional mode, a cascade mode and a run-around mode to determine the performance among different flow methods.

The traditional mode as illustrated in Fig. 1a includes only cooling and heating coils, which serve as the basis of power usage. To maintain a suitable room humidity, the supply air temperature is controlled in a cooling coil to 12 °C, which is the dew-point temperature. To reach a final precise temperature control, the air temperature supplied by a heating coil must be maintained to a constant value of 22±0.05 °C.

Based on the traditional mode, pre-cooling and pre-heating coils are inserted and the water piping of the first three coils is also re-arranged to form a cascade mode as shown in Fig. 1b. The cascade mode has four coils including pre-cooling, cooling, pre-heating and heating coils. In principle, the larger the amount of heat transferred from the pre-cooling to the pre-heating coils by the circulating water, the greater is the required surface area of the coils and the larger is the required circulating water volume.

The run-around mode uses the same coils as the cascade mode with a circulating pump added as shown in Fig. 1c. The heat withdrawn from the warm air along the way to the pre-cooling coils is transferred by the circulating water to the pre-heating coils. The pre-heating coils then return the sensible heat to the cold air leaving the cooling coils and any heat added to the flowing air by the pre-heating coils is then exactly equal to the heat removed by the pre-cooling coils. The required refrigerating capacity thus decreases in the run-around cycle to reheat the cold air supply. In this arrangement, the required heating capacity is reduced as well.
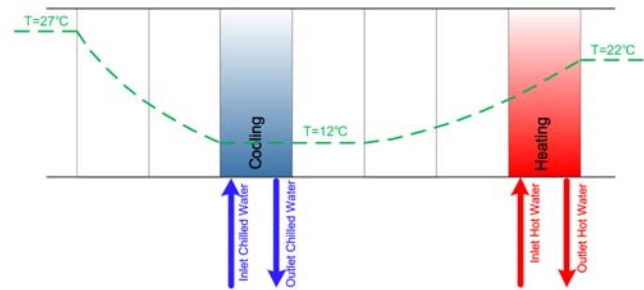

Figure 1a: Scheme of an AHU system operated in the traditional mode.

OPTIMIZATION METHOD USING THERMAL AND MECHANICAL SIMULATIONS FOR SIRIUS HIGH-STABILITY MIRRORS*

L. M. Volpe[†], G. V. Claudiano, R. R. Geraldes, S. A. L. Luiz, A. C. Pinto,
Brazilian Synchrotron Light Laboratory (LNLS), Brazilian Center for Research in Energy and
Materials (CNPEM), 13083-970, Campinas, Sao Paulo, Brazil

Abstract

The mirrors for Sirius, the new 4th-generation synchrotron at the Brazilian Synchrotron Light Laboratory (LNLS), have strict requirements regarding thermo-mechanical stability and deformations, with figure height and slope errors limited to a few nanometers and tens of nanoradians, respectively. Therefore, fixed-shape mirrors have been defined with horizontally-reflecting orientation (except for vertically-reflecting mirrors of KB systems), whereas their cooling schemes (namely, air, water or liquid nitrogen cooling) depend on the particular power load. A thermal and mechanical optimization method was developed to guide the design of mirrors through the evaluation of deformations caused by power load, cooling, gravity, tightening of the fastening screws, manufacturing errors and modal analyses. Up to now, this method was already used to define the mirrors of Sirius' beamlines, which include plane, cylindrical, elliptical and ellipsoidal mirrors, as well as KB systems for microprobe and nanoprobe stations. Two examples are presented to illustrate the method.

INTRODUCTION

Mirrors are critical components to ensure a good beam quality on beamlines. With the emergence of 4th-generation synchrotron accelerators, in which it is desired to have the photon beam size near the diffraction limit and a higher coherence, the deformation and stability specifications for the mirror's design have become extremely tight.

To reach these specifications, a new fixation system was developed based on deterministic models. Thermal and mechanical simulations using finite element analysis (FEA) were done to determine the shape of the mirror, minimizing the expected deformation in its operating condition. The simulations were performed using Ansys Workbench [1].

Firstly, the works related to the design of mirrors and deterministic models are presented. In the following sections are shown the optimization methodology used to define the mirror shape, the results obtained and the conclusions.

RELATED WORKS

During the last decades several solutions of water cooling of mirrors were presented and optimized, and with the requirements increasingly tight, these solutions became more complex, requiring methods of correction of the mirror shape, for example using heaters or actuators [2-3].

Cryogenic cooling solutions can also be applied to mirrors, but are often avoided due to cost, even if better results can be obtained than water cooling. This type of cooling is widely used in monochromator crystals due to the good thermal properties of the silicon at temperatures close to 125 K, such as a coefficient of thermal expansion close to zero and high thermal conductivity [4-8].

In order to achieve movement accuracy and stiffness never seen before in double-crystal monochromators (DCM), the Sirius High Dynamic DCM utilized deterministic concepts in its design [9]. A deterministic design is made in order to obtain a system that is highly repetitive, where cause and effect relationships are well known and controlled and random behaviors are negligible [10]. Only using such techniques it is possible to achieve the necessary requirements without divergences between the design and the final product, as it was done in the present study.

CONCEPTUAL DESIGN

Since Sirius' mirrors absorb powers of at most 50W, a simple cryogenic cooling solution using cryostats and copper braids can be used, benefiting from the good properties of silicon in relation to deformation and decoupling the vibrations from the cryostat to the mirror. Thus, a new fixture concept was developed for Sirius' mirrors based on the deterministic concepts used in HD-DCM: the optical element is fixed in an exactly-constrained flexure-based support with threaded rods that passes through holes in the substrate, which achieves high stability (eigenfrequencies above 150 Hz) and still accommodates thermal deformations resultant from system cooling. More details of the conceptual design of the Sirius mirrors mechanics can be seen in [11].

MIRROR DESIGN METHOD

In order to define the shape of the mirror, a method was developed to evaluate and optimize the deformation caused by several different effects, so that each effect can be evaluated individually and the mirror design can be optimized iteratively considering each effect at a time in a way that when all effects are added, the specifications are met. The main specifications required for the development of the project are: optical area size, mirror orientation, absorbed power and maximum permissible deformation for thermal and mechanical deformations. To illustrate the method two examples of Sirius' mirrors are presented, CAT-1-HFM from the Cateretê beamline and CAR-5-KB-VFM from the Carnaúba beamline. The specifications for these mirrors are shown in Table 1.

DESIGN OF A LAYERED HIGH PRECISION MAGNET GIRDER

Wang Guang Yuan，Zhang Junsong，Kang Ling，Yu Jiebin，Chen Jiaxin
Dongguan Branch of the Institute of High Energy Physics, Chinese Academy of Science (CAS),
523803 Dongguan, China

Abstract

In order to adjust the collimation of the light source magnet, a layered magnet girder is developed, which can adjust the six degrees of freedom accurately and reduce the mutual influence of the adjustment process between the various layers of the girder. The precision of the collimation is up to 5 microns.

INTRODUCTION

The HEPS is a high energy synchrotron source with the electronic energy of 5GeV and the emittance of 0.5nmrad in 13th Five-Year Plan. The synchrotron radiation source consists of two types of accelerators, the intensifier and the storage ring [1]. The synchrotron radiation source consists of two types of accelerators, the booster and the storage ring. The main equipment of the accelerator is all kinds of magnets (including: dipole magnet, quadrupole magnet, sextupole magnet, correction magnet).The magnet girder is a device used to support, adjust and locate the magnet. Its adjusting precision directly affects the collimating accuracy of the magnet [2]. This electric magnet girder is applied to support and position precision adjustment of the dipole magnet in the booster.

THE STRUCTURE OF GIRDER

In order to save the manpower and adjusting time of the magnet collimation adjustment, the girder adopts all electric control, which can realize three directions movement of X, Y, Z direction and Rotational motion around the axis of X, Y and Z. The girder realizes the precise collimation of magnets in a small area, and the adjustment range of the horizontal X, Y and Z directions is + 15mm. The structure of the electric adjusting girder is shown in Figure 1 below.
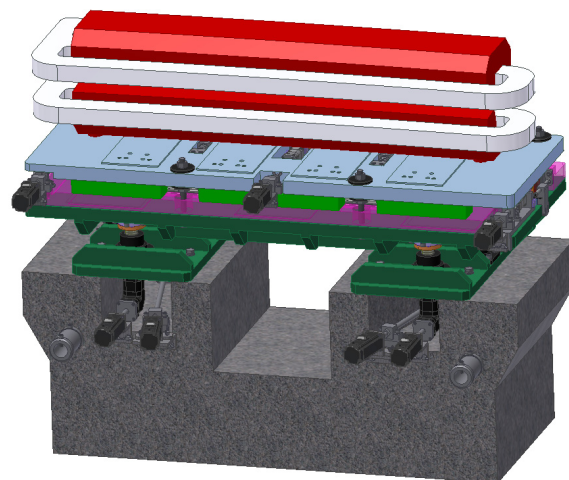

Figure 1: The structure of magnet girder.

The structure of the magnet girder is divided into two parts, namely the horizontal adjustment mechanism (shown in Figure 2) and the height adjustment mechanism (as shown in Figure 3). The horizontal adjustment assembly adopts a layering adjustment mode, and each layer realizes one direction adjustment independently. Height adjustment assembly realizes elevation adjustment by 4 adjusting mechanisms.

After the magnet collimating adjustment is completed, the girder is fixed by the height locking mechanism and the horizontal locking mechanism. The base of the magnet girder is made of marble, providing high stability support. The hoisting rod is used for lifting the whole magnet girder.
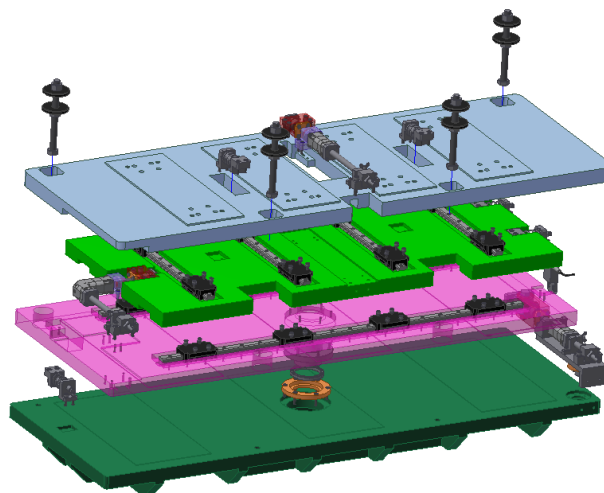

Figure 2: The horizontal adjusting mechanism.

RESEARCH ON ACTIVE VIBRATION ISOLATION SYSTEM*

J. B. Yu[1][†], L. Kang[1], G. Y. Wang[1], J. X. Chen[1], J. S. Zhang[1], A. X. Wang[1],
X. J. Nie[1], H. Y. He[1], D. H. Zhu[1], C. J. Ning[1], Y. J. Yu[1], L. Liu[1]
Institute of High Energy Physics, Chinese Academy of Sciences, Beijing, China
[1]also at Dongguan Neutron Science Center, Dongguan, China

Abstract

Based on the increase of accuracy requirements coming from increasing instrument precision, advanced isolation components are required, and active vibration control method is proposed. This paper mainly shows the experimental system, and some work has been done at present. Now that we are still at the beginning research of active vibration isolation, we hope it will be steadily used in the support systems of some precision equipment and instruments.

INTRODUCTION

Micro-vibration study is one of the important research project in synchrotron light sources, the girder system with passive vibration isolation and damping technology which are effective for beam stability has been widely researched in different institutes, active vibration isolation system, for some uncontrollable factors exist in the control system and actors, its application in synchrotron light source has been constrained. While for the increase of accuracy requirements coming from increasing instrument precision, alone use of passive vibration can't satisfy the requirements, active vibration will play an important role in high precision instruments [1]. This paper firstly shows active vibration isolation research in accelerator, and then the experimental system and some work we have been done at present will be introduced.

The active vibration isolation system in accelerator is mainly used in the future compact linear collider (CLIC) [2], two nanometre size particle beams are accelerated and steered into collision to create high energy collisions between electrons and positrons, to achieve the expected performance, the beams need to be vertically stabilized at the nanometre scale, many institutes have done much preliminary development, early in 1996, Christoph had researched the active stabilization of mechanical quadrupole vibrations with one piezo actuator used in one support system [3]. J. Frisch et al had constructed a prototype system by using of active vibration damping to control magnet motion [4]. C. Collette et al researched on the nano-motion control system for heavy quadrupoles by using two actuators in one support [5, 6]. R. Le Breton et al. had researched on the nanometre scale active ground motion isolator with four actuators in one support [1]. All these research experiments show that active vibration isolation can play a positive role on nanometre scle. Now that we are still at the beginning research of active vibration isolation, we hope it will be

steadily used in the support system of some precision equipment and instruments.

ACTIVE VIBRATION ISOLATION SYSTEM

A two stage support system which include passive stage and active stage is shown in Figure 1, the passive stage is composed of springs and damping, while the active stage is made up of springs and actuators. High stiffness springs, which result in high normal mode frequencies, provide relatively low amplitude motion and good stability in the absence of feedback, while low stiffness springs allow large amplitude low frequency motions, but attenuate high frequencies. This paper mainly research on the active stage.
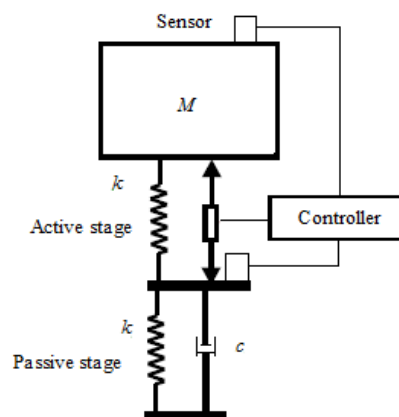
Figure 1: Single d.o.f support system.

To reduce expenditure, the active stage with three springs and one actuator is designed as shown in Figure 2. Different actuator technologies can be used for active isolation system, base on the advantages of high resolutions, wide bandwidths and strong forces, piezoelectric actuator is chosen in this stage. The load on the stage is about 100kg, and it's expected to be effective with the frequencies in the range 1-20 Hz.

FROM PLATE SCREENING TO ARTIFICIAL INTELLIGENCE: INNOVATIVE DEVELOPMENTS ON PROXIMA 2A AT SYNCHROTRON SOLEIL

Damien Jeangerard[1], Martin Savko[1], Lidia Ciccone[1], Kewin Desjardins[1],
Antoine Le Jollec[1], Ahmed Haouz[2], William Shepard[1†]

[1] Synchrotron SOLEIL, L'Orme des Merisiers, Saint Aubin BP 48, 91192 Gif-surYvette, France
[2] Pasteur Institute, 209-211 rue de Vaugirard, 75015 Paris, France

Abstract

PROXIMA 2A is a high performance 3rd generation synchrotron beamline dedicated to X-ray micro-crystallography on biological macromolecules. Since opening in March 2013, the experimental station has hosted a large number of users who have collected vast amounts of X-ray diffraction images from thousands of crystals. In order to streamline the throughput, enhance performance and add functionality, a number of developments have been launched on PROXIMA 2A. These cover all aspects of the beamline, from the practical to the visionary: such as the design, fabrication and implementation of a dedicated high-precision motorized stage to screen crystallization plates for *in situ* X-ray data collections, and the employment of artificial intelligence and computer vision technologies for the detection of samples under liquid nitrogen. Other notable beamline projects include the addition of a vertical translation table for the EIGER X 9M detector to permit the acquisition of ultra-high (0.6 Å) resolution X-ray data, the incorporation of a miniaturized Yttrium Aluminium Garnet (YAG) coupled photodiode within a beamstop and the determination of the sphere of confusion (SOC) of a recently added kappa arm to the goniometer.

INTRODUCTION

Modern macromolecular crystallography (MX) beamlines at synchrotron radiation centres have become highly automated systems that permit the high-throughput screening and X-ray data collection of a large number of protein crystals from academic and industrial users. However, as MX experiments have become increasingly sophisticated, there is a desire and need to record more information during the experiment (e.g. variations of the incident flux, sample shape, positions collected, X-ray dose, etc.). One of the direct consequences of maintaining higher throughput is that more complex situations need to be handled automatically without any human intervention. Given that every piece of instrumentation has its own technical limitations, there is a ceiling to the throughput efficiency obtainable. Similarly, every automated procedure is designed for a specific set of tasks, which tends to constrict the overall functionality of the experimental station. As such the automation of experiments sets its own boundaries in quality assurance, efficiency and functionality, and the mission of assuring reliability and broadening the frontiers is a continual process. Here we present some of the on-going projects on the PROXIMA 2A beamline at Synchrotron SOLEIL that improve upon the current automation available, extend the capabilities of the beamline, and add new functionalities for the user community.

RESULTS

In Situ Crystallisation Plate Screener

Crystals of biological macromolecules (proteins, DNA, RNA, and their complexes) are typically grown in 96-well SBS format crystallisation plates via sitting-drop vapour diffusion experiments. When crystals appear in a drop (few 100 nL), they are physically very fragile, sensitive to changes in humidity and temperature, and consequently difficult to harvest. Furthermore, as such crystals contain 30-80% water, flash freezing them in liquid nitrogen can destroy their crystal quality. Although collecting X-ray diffraction data from crystals in crystallisation plates has been reported previously from other beamlines [1–4], the micro-focussed X-rays on PROXIMA 2A with a beam cross-section of 5 μm full width half maximum (FWHM) necessitates a high mechanical resolution over the entire dimensions of a crystallisation plate (128 mm × 86 mm). Unfortunately, such a resolution can not be delivered by the robotic arm of the sample changer system (SOC ≈50 μm), and the travel range of our version of the Micro-diffractometer (MD2, Arinax, France) is too small to cover an entire crystallisation plate. Thus, we have launched a project to custom design and build a crystallisation plate screener that is suitable for a micro-focussed X-ray beam and tailored to the environment of PROXIMA 2A.

The crystallisation plate screener (Figure 1) is composed of five motorised translation tables: Three heavy duty, long range, high-resolution (100 nm) stages (Axmo Precision, France) to move the plate horizontally (Tx), vertically (Tz) and along the X-ray beam path (Ts), which also brings the drop into the focal plane of the coaxial microscope of the MD2. Two other stages (SmarAct, Germany) will align the crystallisation drop to the centre of the air-bearing ω rotation axis, which will ensure a limited movement in angular range (±45º). The supporting frame can hold SBS format crystallisation plates. A graphical user interface, written in Python Qt4, permits the user to move to any given crystallisation well and control the various data collection parameters (zone to

_____
† email address: william.shepard@synchrotron-soleil.fr

MECHANICAL DESIGN AND CONSTRUCTION OF THE COHERENT X-RAY SCATTERING BEAMLINE AT TAIWAN PHOTON SOURCE

H. Y. Yan[†], C. H. Chang, C. C. Chiu, C. Y. Chang, L. Lee, L. J. Huang, C. Y. Chen, J. M. Lin,
D. G. Liu, S. H. Chang, and Y. S. Huang,
National Synchrotron Radiation Research Center, 30076 Hsinchu, Taiwan

Abstract

The Coherent X-ray Scattering (CXS) beamline at Taiwan Photon Source has been completely constructed in the end of 2015 and opened for users in the next half year of 2016 successfully. Two In-vacuum Undulators (IU22) with lengths of 3 m and 2 m were used as the Insertion Device (ID) to provide intense synchrotron radiation for the CXS beamline. To achieve the coherent performance, the components setup in the beamline needs to be considered and designed carefully. As no white-beam diamond window was installed in the upstream beamline for the maintenance of coherent beam, a differential pumping mechanism was evaluated to prevent the worse vacuum condition influencing the front end and the storage ring. A single-crystal diamond filter was also adopted to maintain the coherence of x-ray. The protection of bremsstrahlung radiation for this beamline was designed specifically based on the optical layout. This paper will introduce the detailed mechanical design and current status for the CXS beamline.

INTRODUCTION

The Coherent X-ray Scattering (CXS) beamline, which is mainly dedicated to the experimental techniques of the Small-angle X-ray Scattering (SAXS), X-ray Photon Correlation Spectroscopy (XPCS), Coherent Diffraction Imaging (CDI), and so on with its highly coherent beam, is one of the phase-I beamlines at Taiwan Photon Source (TPS). The CXS beamline has been completely constructed and opened for users in 2016. The focused size of 10 x 10 μm^2

at sample with operating energy ranging from 5.6 to 20 keV was also accomplished. The preliminary mechanical design of the CXS beam was reported in [1]. Based on the following suggestion for optimization, the detailed design of the beamline was upgraded. This paper introduces the updated and optimized parts in the following sections, such as the radiation shields, optics, vacuum condition, and thermal analysis. The current status of the CXS endstation is also briefly described.

COMPONENTS SETUP

The latest layout of the CXS beamline and endstation is shown in Figure 1. The components setup in the beamline is mainly divided into several functional parts: The optics, radiation shields, vacuum condition, definition of beam size, monitor of beam position and size, and filter. The similar components for definition of beam size and monitor of beam position and size were introduced in [1-3]. In this section, we focus on the description for optics, radiation shields, and vacuum condition.

Optics

A liquid nitrogen-cooled Double Crystal Monochromator (DCM) manufactured by Kohzu Precision with two sets of crystals, which are Si (111) and Ge (111), was adopted for its mature technique in any sort of hard x-ray beamlines and located at 30.5 m. The crystals can be switched with a wide lateral translation. After reflected by the first and second crystals, the beam path offsets upward by 25 mm.
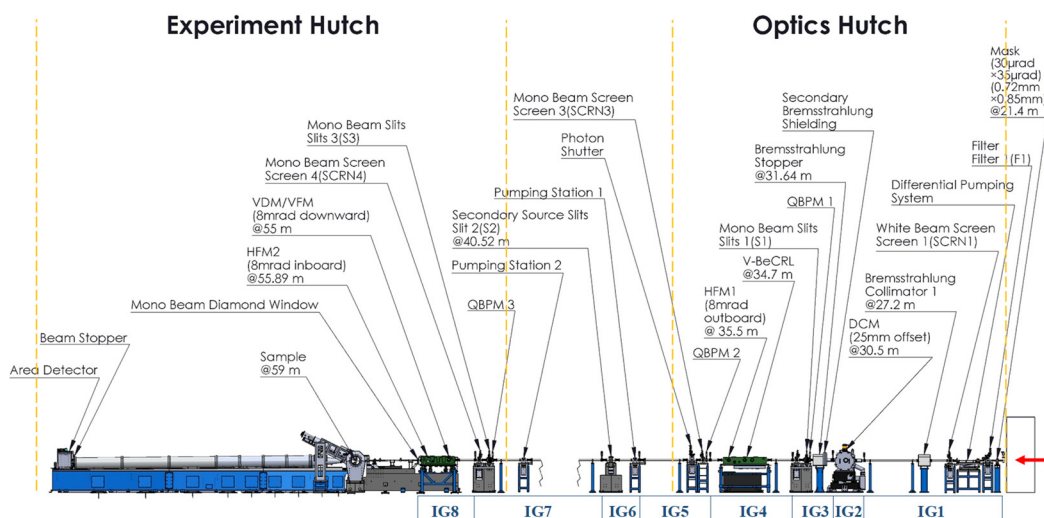

Figure 1: The layout of the CXS beamline and endstation.

---

† yan.hy@nsrrc.org.tw

VALIDATION RESULTS FOR SIRIUS APU19 FRONT END PROTOTYPE *

H. G. P. de Oliveira†, L .C. Arruda, C. S. N. C. Bueno, H. F. Canova, P. T. Fonseca, G. Rodrigues,
L. Sanfelici, L. M. Volpe, LNLS, Campinas, Brazil

Abstract

A Front End (FE) prototype for a 19-mm period length Adjustable Phase Undulator (APU19) beamline of the new Brazilian 4th-generation synchrotron, Sirius, was assembled in the LNLS metrology building in January 2017 to validate main design concepts. Regarding stability, flow-induced vibration (FIV) investigations were carried out on the water-cooled components, and modal analyses were made on the X-Ray Beam Position Monitor (XBPM) support. As for the vacuum system, final pressure levels were investigated and a vacuum breach was intentionally provoked to verify the performance of the equipment protection system (EPS). In addition, cycling tests of the Photon and Gamma shutters were conducted to verify the FE reliability. Moreover, the three-layer protection system, developed to limit the maximum aperture for the high-power slits, was functionally evaluated. Finally, the results were used to improve the FE to its final design. This paper describes the tests setups and results obtained during the validations.

INTRODUCTION

The Front-End comprehends the group of components connecting the storage ring (SR) to the beamline. They are responsible for defining the final aperture, absorbing exceeding beam power and providing radiation protection, storage ring vacuum protection and photon-beam diagnostics [1]. Figure 1 shows an overview of the FE design, highlighting its main components position. An APU19 front-end was first prototyped to validate its mechanical design concepts.

RESULTS AND DISCUSSIONS

Flow-Induced Vibrations

The FE components must handle a high-power load from the APU19 white beam, therefore they must be water-cooled. The total error budget allowed for each component is 1% of the beam size (which is ~30 mm for the APU19

FE). This analysis aimed to quantify the vibration contribution of the cooling system.

A 3D accelerometer from Kistler (8726A) was used to measure the vibration level in each component with and without a water flow of 3 m/s. With the data, it was possible to investigate the RMS displacement on the beam transversal plane. The results for each component are compiled in Table 1.

Table 1: RMS Displacement of the Front-End Components

Component	Flow on [nm]		Flow off [nm]		Variation (%)	
	X	Y	X	Y	X	Y
Mask	22	48	20	40	10	20
Photon	607	44	80	23	658	91
Slit 1	203	28	53	19	283	47
Slit 2	173	31	54	23	220	35
XBPM	15	52	15	36	0	30

The large influence of the cooling system on the Photon Shutter can be justified by the fact that its driving mechanism doesn't have a high stiffness in the X direction. As the water inlet is in the same direction, the disturbances are intensified. Even so, all the contributions are below 1% of the beam size.

XBPM Support Modal Analysis

The XBPM is the most sensitive component in the FE, demanding very strict stability requirements for it to be reliable [2]. It is mounted on the top of a granite block, which is designed for higher stiffness, aiming at the first eigenfrequency value above 100 Hz when tightened to the ground. A modal analysis of the XBPM support was conducted to verify its performance and compare the results with the Finite Element Analysis (FEA) simulation previously carried out using Ansys Workbench [3]. Simulations were firstly done considering the support as a free-body and then as rigidly attached to the ground (grouted).
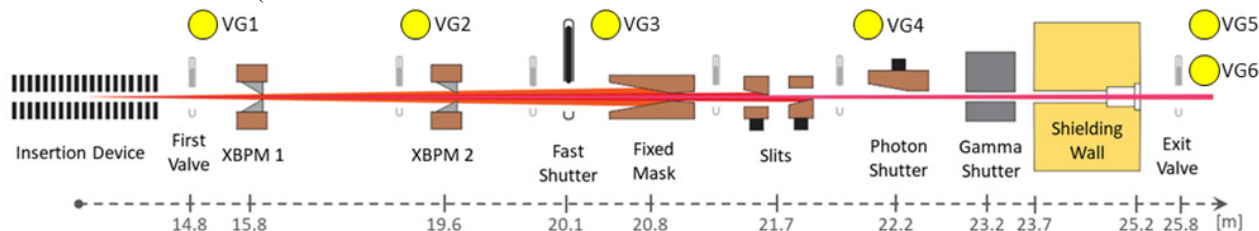

Figure 1: APU19 Front End general layout with each component's distance from the undulator. The vacuum gauges (VG) used to monitor the pressure level along the FE are represented by yellow circles. VG5 and VG6 are used in redundancy for the Fast Shutter (FS) actuation in case of an air inrush at the beamline.

THE DETECTOR ADJUSTMENT SYSTEM OF TAIWAN PHOTON SOURCE 24A

B. Y. Chen[†], G. C. Yin, M. Y. Hsu, X. Y. Li, D. J. Wang, L. J. Lai
National Synchrotron Radiation Research Center, 300 Hsinchu, Taiwan

Abstract

The soft X-ray tomography endstation of TPS has the ability to provide 3D biological cell images by fluorescence structured-illumination microscopy (SIM) and soft x-ray tomography (SXT). The electron energy is design to be in the range of 200 eV to 3 keV. The detector system equipped with an Andor® iKon-L Series imaging CCD, X-Z-roll-pitch adjustment stage, and long stroke bellows system. The detector system can adjust the CCD about 10 mm in both X and Z direction, and +-5 degree of roll. Moreover, the long stroke bellows system gives the CCD an extra degree of freedom in the Y direction and its range is up to 2500 mm. That can locate the CCD close to the sample to get a larger field of view, and far from the sample to get higher image resolution. In this study, the design and commission status of the detector system is studied and the mechanical structures are also presented.

INTRODUCTIONS

The soft X-ray tomography endstation (TPS 24A) is one of the phase II beamlines of Taiwan Photon Source. The main function of this endstation is aimed for the transmission full-field imaging of biological samples, such as thick cells or tissues. Most of the bio-cell or tissues are composed of carbon, oxygen, and nitrogen, etc. That gives a good chance to adopt the water window, which is between the K edge of carbon (284 eV) and oxygen (543 eV), to get the high contrast between biological sample and water. Moreover, the image contrast can be further improved when the x-ray energy decrease to the range of $2000 \sim 3000$ eV for phase contrast soft X-ray tomography [1-3].

BEAMLINE LAYOUT

The beamline layout of TPS 24A is shown in Fig. 1. The X-ray comes out from bending source and focused by the horizontal focused mirror (HFM) and vertical focused mirror (VFM). The x-ray is further pass through the plane grating mirror (PGM) and vertical refocusing mirror (VRFM). Finally, the x-ray is focused by the capillary condenser (CC) and shine on the biological sample. The fluorescence structured-illumination microscopy (SIM) is used to get the 3D biological cell images. Besides, the image can be projected by zone plate (ZP) and collected by the detector system, which is performed by Andor® iKon-L Series imaging CCD. The distance between detector system and the sample can be changed in a large range of 1390 mm to 3910 mm.
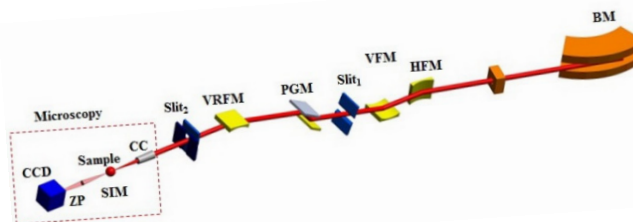
† chen.by@nsrrc.org.tw

Figure 1: Beamline layout of TPS 24A.

DETECTOR SYSTEM

The image of soft X-ray beamline is collected by the detector system, which is at the very end of this endstation. The detector system has three major parts, which includes (1) foundation, (2) long linear guide way, and (3) adjustment part. The detail design concept and components are described in this section.

Design Target

The phase contrast or absorption contrast signal comes from the sample, which is shining by the soft X-ray, will be collected by structured-illumination microscopy and Andor® iKon-L Series imaging CCD. The design target of the detector system is shown in the following: (1) system stability: The pixel size of Andor iKon-L series imaging CCD is 13.5 μ m x 13.5 μ m, thus, the vibration of the detector system shall be less than 2.7 μ m (20% of pixel size). (2) the position of detector: According to the optical design, the distance between detector and sample for different X-ray energy and magnification are in the range of 1390 mm to 3910 mm. (3) adjustment part: The resolution and travel range of the adjustment system is 1 μ m and 10 mm, respectively. This alignment part is necessary for adjusting the position of the detector with x-ray.

Foundation of Detector System

The allowable peak to peak vibration level is 2.7 μ m, this value is quite larger than the ground vibration, which is around 130 nm. But the foundation of the detector system still needs to design carefully, because the system has many degree of freedoms for adjustment. Therefore, stable and strong base is required.

Consider of the structure and thermal stability, the granite bases were adopted to form the reliable foundation of whole system. Each granite was placed on a 20 mm thick stainless steel, which is well aligned by laser tracker. The accuracy of vertical and horizontal position of both the stainless steel plate and granite is about several micro-meters. The foundation of detector system is shown in Fig. 2.

OPTIMIZING THE PETRA IV GIRDER BY USING BIO-INSPIRED STRUCTURES

S. Andresen[1], Alfred-Wegener-Institut Helmholtz-Zentrum für Polar- und Meeresforschung, Bremerhaven, Germany

[1]also at Deutsches Elektronen Synchrotron, Hamburg, Germany

Abstract

The PETRA IV project at DESY (Deutsches Elektronen Synchrotron) aims at building a unique synchrotron light source to provide beams of hard X-rays with unprecedented coherence properties that can be focused to dimensions in the nanometer-regime.

An optimization of the girder structure is necessary to reduce the impact of ambient vibrations on the particle beam. For this purpose, several numerical approaches have been made to simultaneously reach natural frequencies above 50 Hz, a high stiffness and a low mass.

In order to define an optimal girder support, a parametric study was conducted varying both the number and location of support points. Based on the resulting arrangement of support points, topology optimizations were performed to achieve a high stiffness and a high first natural frequency. The following transformation of the results into parametric constructions allowed further parametric studies to find optimal geometry parameters leading to the aimed girder properties. In addition to that, bio-inspired structures based on marine organisms were applied to the girder which likewise resulted in improved girder properties.

INTRODUCTION

DESY (**D**eutsches **E**lektronen **S**ynchrotron) plans to convert the PETRA III (**P**ositron-**E**lektron-**T**andem-**R**ing-**A**nlage) storage ring into an ultralow emittance synchrotron radiation source, able to provide beams of hard X-rays with very high coherence properties that can be focused to dimensions in the nanometer-regime and allows the analysis of physical, chemical and biological interactions which occur inside materials between atoms.

In order to receive such highly energetic and low emittance synchrotron radiation, it is fundamental to minimize the impact of ambient vibration on the girders which carry the magnets guiding the particles. An optimization of the girder design is therefore crucial to avoid resonance and minimize vibration amplitudes.

To achieve the best results, several approaches were followed in a systematic development of new girder designs.

As the definition of boundary conditions has a strong impact on the vibration characteristics and the stiffness, a support study was conducted which varied both the number and location of support points in order to find the optimal support point number and locations. Based on the resulting arrangement of support points, topology optimizations were performed to achieve a high stiffness in combination with a high first natural frequency. The goal of a topology optimization is to find the optimal design of a structure within a specified design space [1]. The applied loads and support conditions, the volume of the structure to be designed and potentially additional design restrictions are known, whereas the size, shape and connectivity of the structure are unknown. The subsequent transformation of the topology optimization result in parametric constructions allowed further parametric studies to determine optimal geometry parameters leading to the aimed girder properties. Furthermore, structures inspired by marine organisms were applied to the girder which also resulted into improved girder properties.

The objective of the conducted studies was to develop girder designs with natural frequencies higher than 52 Hz, a maximal deflection lower than 0.5 mm and a girder mass of maximal 2500 kg.

SUPPORT STUDY

Methods

An actual PETRA III girder assembly provided the basis for the study and led to the model layout shown in Fig. 1. The girder was abstracted as a hollow cuboid and meshed with shell elements with an averaged edge size of 0.08 m. The material was characterized by a Young's modulus of $2.1e11$ N m^{-2}, a density of 7830 kg m^{-3} and a Poisson's ratio of 0.3. The defined shell thickness of
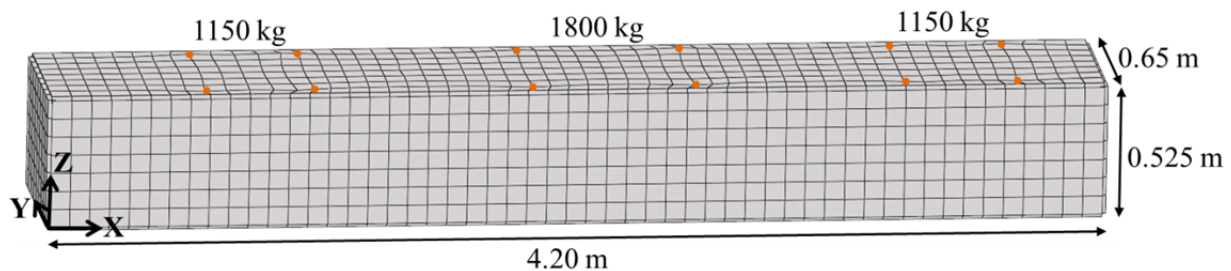

Figure 1: Model assembly considered for the support study. The orange dots show the defined point masses representing the three heavy magnets. The shell thickness of the elements is displayed.

MECHANICAL ENGINEERING DESIGN AND SIMULATION FOR SPIRAL2 ACCELERATOR @GANIL

C. Barthe-Dejean, F. Lutton, M. Michel, P. Gangnant, C.Michel, P. Lecomte, F. Daudin, C. Stodel,
R. Revenko, JL. Vignet, M. Di Giacomo, JF. Leyge, E. Petit, SPIRAL2-GANIL, Caen, France
M.Walter , CC-IN2P3, Lyon, France.

Abstract

The SPIRAL2 project at GANIL is based on a superconducting ion Continuous Wave LINAC with two associated experimental areas named S3 (Super Separator Spectrometer) and NFS (Neutron For Science). This paper reports the main contributions of Mechanical Design Group at GANIL to the project. Mechanical engineers have been highly involved since 2005 from the pre-design of the accelerator and its development until present to finalize the installation. During the development phase, design and numerical simulation were used throughout the complete process: from the ion sources, to the LINAC accelerator, then through beam transport lines to experimental halls equipped with detectors. The entire installation (process, buildings and systems) is integrated in 3D CAD models. The paper focuses on three equipments designed in collaboration with electronics engineers and physicists: the Rebuncher in the Mean Energy Beam Transport line (MEBT); the Instrumentation of Secondary Emission Monitors (SEM profilers), and the Target Stationin S3. SPIRAL2 also has to meet safety requirements, such as seismic hazard, therefore the dynamic simulations performed to demonstrate the mechanical strength in case of earthquake will also be detailed.

INTRODUCTION

The SPIRAL2 radioactive ion beam facility was launched in July 2005, with the participation of French laboratories (CEA, CNRS) and international partners. SPIRAL2 complex is built in two phases: a first one including the accelerator, the Neutron-based research area (NFS) and the Super Separator Spectrometer (S3); and a second one including the low energy RIB experimental hall called DESIR. The SPIRAL2 LINAC takes into account a wide variety of beams detailed in Table 1 to fulfill the physics requests.

Table 1: Beam Specifications [1]

Particles	H+	D+	ions	option
Q/A	1	1/2	1/3	1/6
Max I (mA)	5	5	1	1
Max energy (MeV/A)	33	20	15	8.5
Max beam power (kW)	165	200	45	51

The SPIRAL2 first phase facility is now built; the accelerator installation and connecting tasks are achieved, and the beam commissioning has started with encouraging and promising results. The goal is now to send the first beam for physical experiment in NFS in 2019.

MECHANICAL CAD INTEGRATION

One of the main task of the Mechanical Design Group was to integrate the CAD Models (CATIAv5 files) from the different laboratories participating to the project (Fig.1 and Fig.2). It was decided to use a common PLM (Product Life cycle Management) software: SMARTEAM. This PLM solution allows complex collaborative design development at large scale (Fig.3) . The software license, the installation and the training for all the users in different laboratories were organized jointly by GANIL Mechanical Design Group and IN2P3-CNRS Data Center.
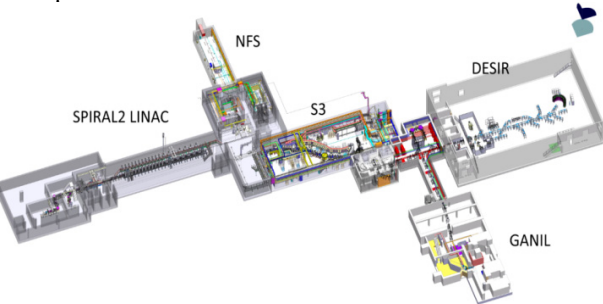

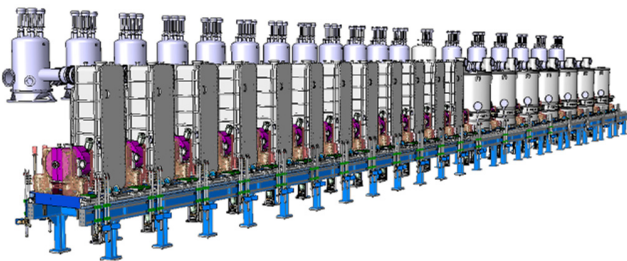Figure 1: SPIRAL2 CAD complete assembly model.

Figure 2: LINAC with its Cryomodules type A and B.

The complete SPIRAL2 CATIA v5 CAD file is 11 Giga-octets. It was assembled by GANIL designers, and is the most important CAD assembly of IN2P3 database. The CAD model of S3 experimental hall itself contains 2700 different sub-models.
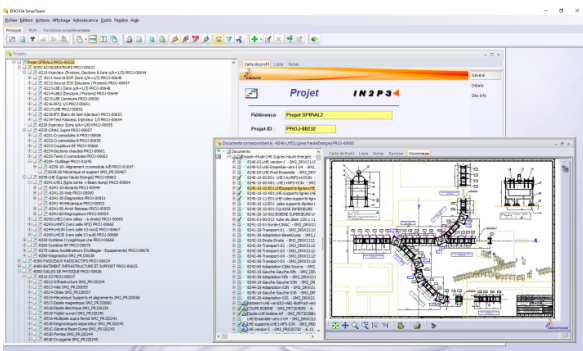

Figure 3: SPIRAL2 Project in Smarteam Data Base.

DESIGN AND FEA OF AN INNOVATIVE ROTATING SIC FILTER FOR HIGH-ENERGY X-RAY BEAM

W. Tizzano*, T. Connolley, S. Davies, M. Drakopoulos, G. E. Howell
Diamond Light Source, OX11 0DE Didcot, United Kingdom

Abstract

I12 Joint Engineering, Environmental, and Processing (JEEP) is a high-energy imaging, diffraction and scattering beamline at Diamond. Its source is a superconducting wiggler with a power of approximately 9 kW at 500 mA after the fixed front-end aperture; two permanent filters aim at reducing the power in photons below the operating range of the beamline of 50-150 keV, which accounts for about two-thirds of the total [1]. This paper focuses on the design and simulation process of the secondary permanent filter, a 4 mm thick SiC disk. The first version of the filter was vulnerable to cracking due to thermally induced stress, so a new filter based on an innovative concept was proposed: a water-cooled shaft rotates, via a ceramic interface, the SiC disk; the disk operates up to 900 °C, and a copper absorber surrounding the filter dissipates the heat through radiation. We utilised analysis data following failure of an initial prototype to successfully model the heat flow using FEA. This model informed different iterations of the re-design of the assembly, addressing the issues identified. The operational temperature of the final product matches within a few degrees Celsius the one predicted by the simulation.

INTRODUCTION

I12 is a high-energy imaging, diffraction and scattering beamline located on a straight section of Diamond storage ring. Its source is a 4.2 T superconducting wiggler, and the beamline operates at 50–150 keV, providing a hard X-ray beam capable of penetrating large dense samples, for

example engineering parts and assemblies (e.g., superalloy turbine blades [2], or steel and Al alloy internal combustion engines [3]). Table 1 summarizes the key parameters of the beamline and Fig. 1 shows its layout.

Table 1: I12 Key Parameters [4]

Source	Super-conducting wiggler, 4.2 T, 48 mm periodicity, 22 full field periods
Beam acceptance	1 mrad×0.3 mrad
Beam modes	White beam or monochromatic beam
Monochromator	Si (111) cryo-cooled double crystal bent Laue
Energy range	50–150 keV

The techniques available to I12 users include, among the others: static and time-resolved radiography and tomography, energy-dispersive diffraction, monochromatic and white-beam two-dimensional diffraction/scattering, and high energy Small-Angle X-ray Scattering (SAXS) [1].

The beamline has two in-line experimental hutches (EH), one inside Diamond Experimental Hall 51.7 m from the source (EH1), and the other in an external building 94.5 m from the source (EH2). EH1 allows experiments involving small and medium-sized samples and sample environments, whereas EH2 offers space for large or complex experiments [5].
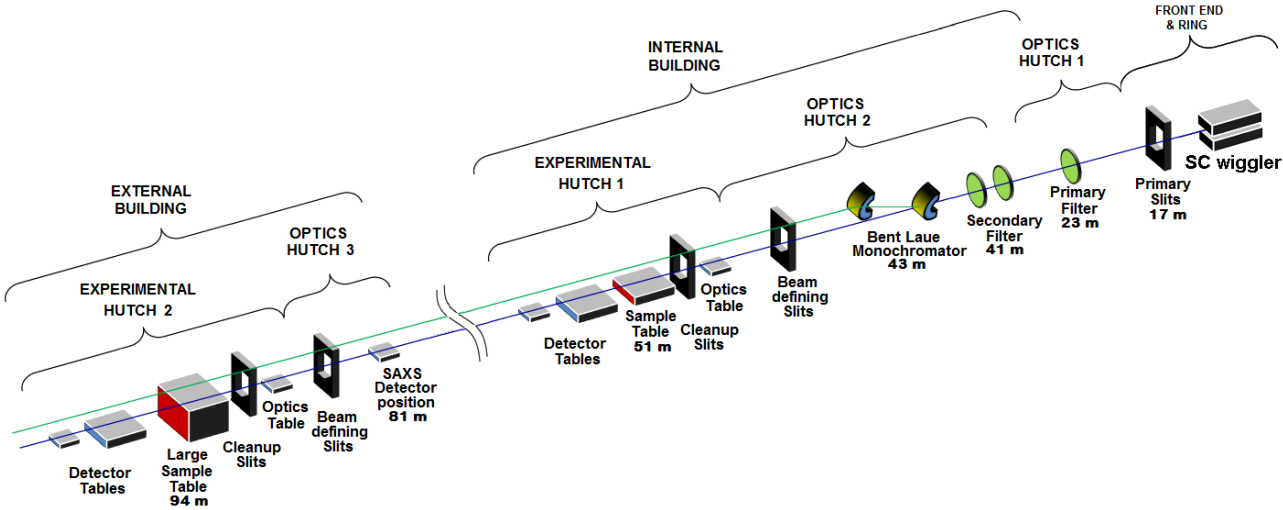
---

* walter.tizzano@diamond.ac.uk

Figure 1: Schematic optical and functional layout of the I12 JEEP beamline [4].

3D NUMERICAL RAY TRACING FOR THE APS-UPGRADE STORAGE RING VACUUM SYSTEM DESIGN

J. Carter, Argonne National Laboratory, Lemont, IL, USA

Abstract

The APS-Upgrade project will build a diffraction limited storage ring requiring a vacuum system design with small aperture vacuum chambers passing through narrow magnet poles. The small apertures dictate that the walls of the vacuum chambers act as distributed photon absorbers. The vacuum chambers must be designed robustly so a thorough understanding of the synchrotron ray tracing with beam missteering is required.

A MatLab program has been developed to investigate 3D ray tracing with beam missteering. The program discretizes local phase spaces of deviation possibilities along the beam path in both the horizontal and vertical planes of motion and then projects rays within a 3D model of the vacuum system. The 3D model contains elements in sequence along the beam path which represent both chamber segments and photon absorbers. Ray strikes are evaluated for multiple worst-case criteria such as local power intensity or strike offset from cooling channels. The worst case results are plotted and used as boundary conditions for vacuum chamber thermal/structural analyses. The results have also helped inform decisions about practical beam position limits.

RAY TRACING FOR THE APS-U STORAGE RING VACUUM SYSTEM

The APS-Upgrade will retrofit the existing 40 sectors, 1.1 km circumference APS storage ring with a new 6 GeV, 200 mA storage ring optimized for brightness above 4 keV. The new storage ring vacuum system will feature 22 mm inner diameter vacuum chambers to fit between narrow magnet apertures, see Figure 1. Each sector will have 5x copper photon absorbers to both funnel extracted photons towards the front ends and to shadow downstream components. Each sector will also have 14x independently mounted beam position monitor (BPM) assemblies. The BPMs are not water cooled and have sensitive features including RF liners and BPM buttons and each will need shadowing by compact inline absorbers built into the immediate upstream chambers.
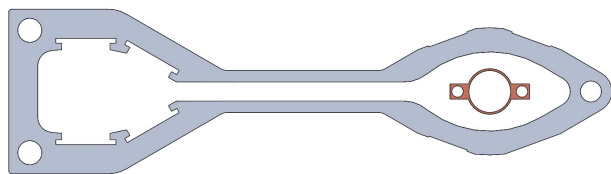

Figure 1: Cross section comparison of current APS-style vacuum chamber to new APS-U-style chamber.

In total the vacuum system will have 20x water-cooled vacuum components which will intercept synchrotron radiation either by design with a photon absorbing edge or along the chamber length as consequence of the small apertures. Figure 2 shows a cross section of three APS-U vacuum components in sequence. Here a slight taper on a vacuum chamber shadows a downstream flange joint of a compact copper inline absorber. The absorber then shadows the length of a BPM assembly past its downstream flange joint. The current APS has 6x total photon absorbing components compared to APS-U's 20x and this fits into a trend among diffraction limited light source vacuum systems with increasingly more compact vacuum chamber requirements. This increase in complexity leads to a need for more careful ray tracing constructions and calculations and considerations beyond the limits of conventional top view 2D ray traces.

A new MatLab program has been developed to investigate 3D ray tracing possibilities with missteering. Beam missteering possibilities and limits vary along the length of the lattice function and the ray tracing consequences differs from component to component in a complex system. Numerical methods are a more efficient approach to exploring missteering rather than individual CAD constructions. The new MatLab program calculates the local extents of missteering by discretizing local phase space ellipses and then projects the large quantity of rays downstream towards a model of vacuum elements. The quantity of ray strikes can be summarized to ensure the protection of sensitive components and to analyze worst case ray tracing outcomes unique to each vacuum component.
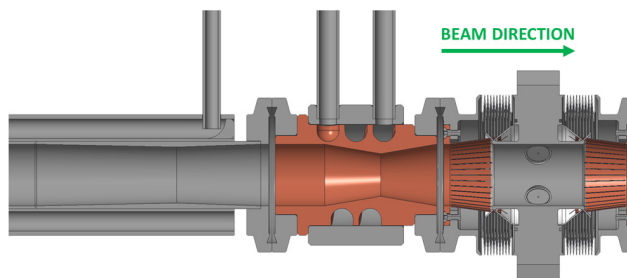
Figure 2: Top view cross section comparison of current APS-style vacuum chamber to new APS-U-style chamber.

SUMMARY OF APS-U'S 2D RAY TRACE

Building and analysing a conventional 2D ray trace remains critical as it sets the baseline for heat load distributions and shadowing of critical components. APS-U's storage ring ray trace is summarized in the table in Figure 3. APS-U's magnet lattice generates 14.3 kW per sector at 200 mA beam current. This excludes narrowly funnelled

A NEW X-RAY BEAM FOR THE ESRF BEAMLINES, OPTO-MECHANICAL GLOBAL SURVEY

Y. Dabin, R. Barrett, S. Jarjayes, M. Sanchez del Rio,
European Synchrotron Radiation Facility, 38043 Grenoble Cedex 9, France

Abstract

With the new Extremely Brilliant Source (EBS), ESRF beamlines (BL) will have to adapt their optical configurations to use the new beams optimally. Preparing the photon beam for an experiment by a BL implies successive interactions between the different components that produce, transport and manipulate this beam. A cascade of topics and cross-linked processes optimize the photon beam parameters. The scientific application defines the baseline parameters such photon energy, beam sizes and flux. These will in turn define the most appropriate source characteristics, for which an optical scheme must be developed and implemented to tailor the X-ray beam properties to the experimental requirements. In this phase simulation software tools such as OASYS, are employed for optics and source calculations and ANSYS and COMSOL for FEA thermoselastic analyses. Finally, the implementation phase interconnects the string of technical components, involving the whole spectrum of engineering issues. This paper deals with this cascade of tasks and describes the sequence of parameters and calculations flow required to exploit an X-ray light source.

INTRODUCTION

The EBS (Extremely Brilliant Source) [1] project is based upon a reduction of the horizontal emittance of the ESRF electron storage ring. Table 1 gives details on changes in major parameters.

The new EBS straight sections are reduced in length, leading to a need to adapt the existing collection of undulator carriages. Beamlines using canted undulators reset their source point and their location.

Table 1: Emittance and Straight Section Main Parameters for the Current ESRF and New EBS Storage Rings

Configuration	Current SR	EBS
Hor_Emittance (pm)	4000	147
Ver_Emittance (pm)	4	4
Straight section (m)	6 and 7	5.5
Bending magnet source	Dipole from DBA lattice	Small Insertion device

At the same time, new undulators require specific strategies for their gaps and periods. Recent cryogenic, in-vacuum undulators with 22, 18 and now 14mm periods, 6mm (and 5mm) gap increase peak flux and energy tunability. The recent topping-up hybrid mode (7/8+1) produces a reduced vertical size of the X-ray beam as seen at some BL, modifying as a consequence the optics illumination. Thus,

monitoring on-live the X-ray beam characteristics is a "daily issue" and an important topic. Scientists at the BL must react to any changes, in collaboration with the other engineering specialists like storage-ring, optics, mech. Eng. FEA. Since recent years, optics simulation tools are implemented in user-friendly software environment to make the chain of design and optimizing beamlines faster and easier. An example of such effort is OASYS suite [2].

FROM THE PRESENT STORAGE RING TO THE NEW EBS SOURCE

The photon beam is produced by an electron beam stored in a magnetic lattice. The fundamental properties of this X-ray beam are first determined by the electron ring. The ESRF electron storage ring, implemented in 1990, is based on a double-bend-achromat (DBA) lattice. It consists of al-ternating low- and high-beta straight sections for installing insertion devices, offering respectively an electron source of small size and large divergence, or large size and small divergence, in the horizontal plane Fig. 1 shows schemati-cally the horizontal emittance characteristics of this alter-nating
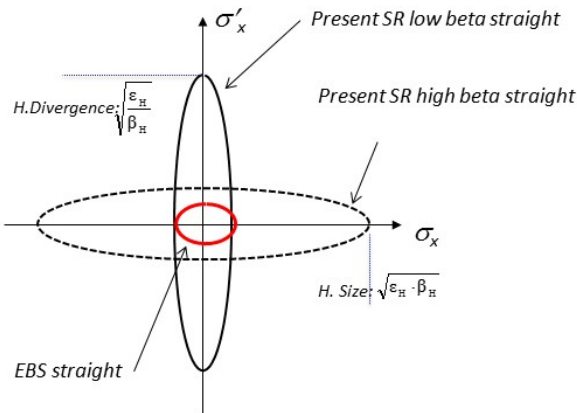
Figure 1: Schematic representation of the electron phase space in the horizontal plane comparing the case of present storage ring and the new EBS lattice. Originally the low beta was aimed at hosting wigglers, while the high beta hosted undulators. The emittance reduction factor of EBS is 1/30 as compared to the older facility.

The choice of a lattice configuration with high and low beta sections was driven at the time by the difficulties in building high performance undulators, as compared to less demanding wiggler technologies giving a broad energy spectrum without the need to tune the magnetic gap. With time and experience, undulator performance has improved

PIEZO TECHNOLOGY IN SYNCHROTRON

Boris Laluc, Aurélien Riquer, Thomas Maillard
CEDRAT TECHNOLOGIES, 38 000 Grenoble, France

Abstract

Synchrotrons need robust products. That's why the association of piezo actuator technology and CEDRAT TECHNOLOGIES (CTEC) know-how has been successful for synchrotron mechanisms projects. The technological brick is the "Amplified Piezo Actuator" (APA®) tested and widely used in space applications, it is often implemented in CTEC piezo mechanisms and provides a high level of robustness. Modifying the layout and the number of APA® allows several needs to be addressed within beamlines. Three applications developed in collaboration with the EMBL, PAL and SOLEIL will be presented in this paper. The first application consists of cutting a beam with a piezo shutter. The maximum beam diameter is 3 mm. The second mechanism allows the energy of a beam to be modified by using a series of piezo actuated filters. And the last mechanism aims at modifying the beam section shape with an active piezo micro-slits mechanism.

PIEZO TECHNOLOGY AND SYNCHROTRONS

Synchrotrons need reliable products because most of the time the actuators are working in vacuum environments and it is very time consuming and expensive to break the vacuum for a maintenance operation. That's why the association of the piezo technology and the CEDRAT TECHNOLOGIES (CTEC) know-how has been successful for synchrotron mechanisms projects around the world for over 15 years.

LINEAR ACTUATOR APA

The Amplified Piezo Actuator APA® [1] was developed, tested and approved for space applications and then industrialised to be used in other markets, for example instrumentation. Thus, the APA® can withstand more than 10^{10} cycles. The actuator is composed of a piezo ceramic which generates a translation motion. The piezo ceramic has only a 0.1 % active deformation: to get a 0.5 mm displacement motion the piezo ceramic size should be 0.5 m. That's why the APA uses a shell around the piezo-ceramic to amplify the movement and increase this deformation. As an example the APA600M with 0.55 mm stroke is only 15 mm-height. The active deformation ratio is then 3.7%. The full stroke of the APA® is achieved with a 170 V range (-20 to +150 V).
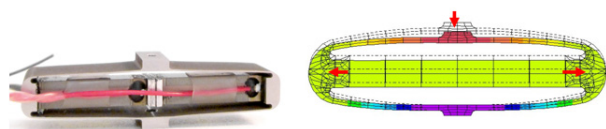

Figure 1: APA600M Actuator & Shell displacement.

In Figure 1 the dotted lines represent the actuator at rest thus not powered. When a positive voltage is applied the ceramic expands outwards and the shell moves downwards.

The robustness of the APA® is present in all CTEC mechatronics products and especially for synchrotron beamlines: the fast shutter, the fast beam attenuation actuator and the active micro-slits products.

FAST PIEZO SHUTTER (FPS)

For this mechanism 2 APA® face each other on a rigid frame, see Fig. 2. At rest the optical head cuts the beam and when a voltage is applied, the two APA200M retract and the shutter opens. The opening between the 2 APA is around 0.4 mm, giving a security factor, this shutter is designed for a beam diameter up to 0.3 mm.
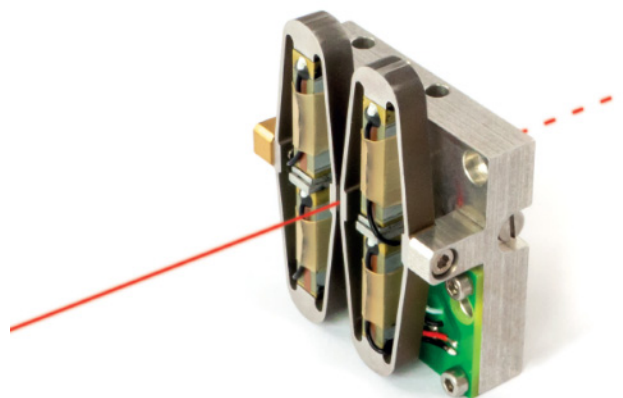
Figure 2: FPS200M.

These shutters are used to expose the sample behind it during a defined and controllable time. Aperture or closure time is directly linked to the resonance frequency of the actuator and so its stiffness. The APA200M has a mechanical resonance frequency of 900 Hz in blocked-free mode that is to say a period of 1.1 ms. The driver is optimised with a pre-shaped signal to minimise the excitation at this frequency. The mechanical ringing of the slits is reduced, even with a fast aperture and closing time of 2 ms. The APA200M actuator used in the FPS200M is a good compromise between stiffness required for fast response time, and aperture size. Other shutters FPS400M and FPS900M allow respectively a beam diameter of 0.7 and 1.1 mm with the same mechanical design but with larger strokes actuators.

If more stroke is needed, the FAPS400M (Fig. 3) developed for PAL uses a lever arm to amplify the APA movement. In this case the beam diameter could be up to 3 mm with a translation of each APA400M of 410 μm.

Beamlines

End Stations

BEAMLINE ENGINEERING OVERVIEW FOR THE APS UPGRADE*

O. Schmidt, E. Benda, D. Capatina, T. Clute, J. Collins, M. Erdmann, T. Graber, D. Haeffner,
Y. Jaski, J. Knopp, G. Navrotski, R. Winarski, Argonne National Laboratory, 60439 Lemont, IL,
USA

Abstract

The Advanced Photon Source (APS) is currently in the process of upgrading to a 4th generation high-energy light source. A new multi-bend achromat storage ring will provide increased brightness and an orders-of-magnitude improvement in coherent flux over the current facility. To take advantage of these new capabilities, we will be building nine new feature beamlines and implementing numerous additional beamline enhancements, all while ensuring the compatibility of existing programs. Clear challenges exist in advancing state-of-the-art optics and developing nano-resolution instrumentation. We also need to recognize and address project scheduling, labor resources, existing infrastructure, bending magnet parameters, and possible modifications to radiation shielding in order to achieve project success.

APS-U Overview

The APS-Upgrade (APS-U) will transform the APS into a next-generation synchrotron light source, exceeding the performance of today's storage ring by up to three orders of magnitude in brightness and coherent flux.[1]
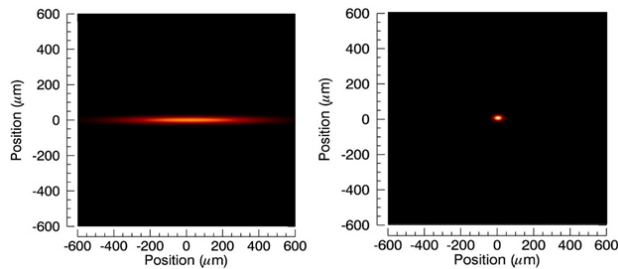

Figure 1: APS electron beam before and after upgrade.

The new storage ring will also produce a much smaller, more coherent beam (Fig 1). Currently we are in the planning and design phase of the project with the main installation planned for 2023 with one year of scheduled dark time.

Feature Beamlines

To take full advantage of the higher brightness and higher energy of the new storage ring, nine "feature" beamlines have been chosen to showcase these capabilities and provide world class scientific programs. Preliminary designs for each beamline have been completed along with detailed cost estimates and project schedules. Table 1 shows the list of feature beamlines that will be either brand new or greatly modified.

Table 1: Summary of APS-U Feature Beamlines

Sector	Name	Title
4-ID	POLAR	Polarization modulation spectroscopy
8-ID	XPCS	X-ray Photon Correlation Spectroscopy Beamline
9-ID	CSSI	Coherent Surface Scattering Imaging
19-ID	ISN	In Situ Nanoprobe
20-ID	HEXM	High-Energy X-ray Microscope
25-ID	ASL	Advanced Spectroscopy & LERIX
28-ID	CHEX	Coherent High-Energy X-ray Sector for In Situ Science
33-ID	Ptycho	Ptychography/ Spectromicroscopy
34-ID	3DMN/ ATOMIC	3D Micro & Nano Diffraction/ High-Resolution Atomic Imaging

Beamline Enhancements

In addition to the nine feature beamlines, another seventeen beamlines will see major enhancements to their optics and end station instrumentation to greatly enrich the capabilities of their current programs. Proposals for beamline enhancements were submitted in February of 2017. Beamlines were chosen based on scientific impact, degree of benefit to the general user program, and alignment with upgraded APS capabilities and APS strategic plans (high energy, coherence, etc.) Enhancements include new and upgraded mirrors, monochromators, and refractive lenses, along with station modifications and end station instrumentation and detectors. These smaller beamline enhancements essentially provide value and many can be completed before the main shutdown to free up resources during the main installation period.

Long Beamlines

In order to achieve extremely small focal sizes and make the best use of the improved beam coherence, two "long" beamlines will be developed which will extend beyond the current APS building footprint. The In Situ Nanoprobe (ISN), and High Energy X-ray Microscope (HEXM) beam-

A NEW PROCUREMENT STRATEGY TO CHALLENGE THE SUPPLIER CONSTRAINTS CREATED WHEN USING A FULLY DEVELOPED REFERENCE DESIGN

George Howell[†], Nick Baker[ζ] Steve Davies[η], Andrew Walters[β], Mirian Garcia-Fernandez[γ],
Houcheng Huang[δ], Stewart Scott[ε], Kejin Zhou[α1],
Diamond Light Source Ltd, OX11 0DE Oxford, United Kingdom

Abstract

A common procurement strategy is to produce a fully optimised reference design that makes assumptions about the manufacturing process and supplier capability. This approach can restrict the opportunities for some companies to include their own specialist manufacturing capability to provide a more effective and cost efficient solution. A new approach is suggested following the recent experience at Diamond Light Source. The manufacture of high stiffness welded fabrications up to 13 m in length for the I21 RIXS[2] [1] Spectrometer is used as an example. The I21 RIXS Spectrometer design was optimised for stiffness and control of vibration. The use of Finite Element Analysis[3] enabled different design options and compromises to be explored utilising the supplier's capabilities. The final design was tested during manufacture to verify the FEA model. With the I21 RIXS Spectrometer commissioned the data collected shows the final stability performance of the system including detector stability over full experiment durations has met the scientific goals of the design.

REFERENCE DESIGN DEVELOPMENT

The RIXS Beamline at Diamond followed the normal development process with Concept and Technical Design Review phases of Science Case and Technical Feasibility sign off. The beamline optical layout is typical for a soft X-ray beamline having a PGM[4] and Exit Slits with focusing optics either side. However to achieve the necessary photon throughput, energy resolution and stability enhancements have been necessary.

Construction of I21 RIXS Beamline at Diamond was a complex programme of Beamline, Spectrometer, External Building and Sample Vessel projects. The Spectrometer is a 16 m long assembly that supports a detector and optics. The complete assembly is able to rotate on a vertical axis

---

150 degrees around the sample vessel with the sample at the centre. The optics are a series of cylindrical gratings to focus scattered X-rays from the sample on the detector with energy distributed vertically. The gratings have 4 motions and in addition the whole assembly can travel 1.5 m in beam direction. The detector is able to rotate to align with the focus of the vertical energy distribution of the X-rays by moving radially and vertically.

Project Phases

The Spectrometer project had several stages starting with a concept stage that concluded with a review by the Technical Working Group, Science Director and Head of Engineering. The first phase of work on the Spectrometer involved developing concepts for the key aspects of the design. During this phase visits were carried out to the Address Beamline at the Swiss Light Source [2] and ID32 at the ESRF [3] to discuss the approach used for similar beamlines.

At this stage, the design intention followed recognised best practice to minimise risk through the utilisation of standard parts, using developed technology and where possible solutions previously used at Diamond. With this low risk strategy in place the design of individual assemblies could then be developed including the Spectrometer Frame.
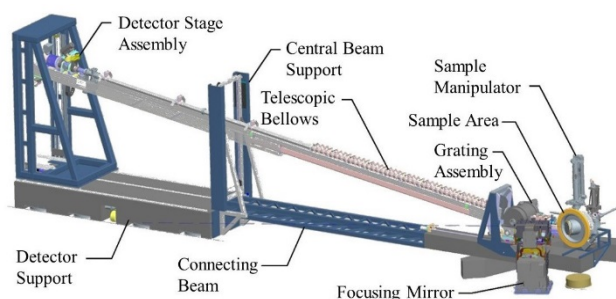
Figure 1: Concept Report Design January 2014.

In the design shown in Fig. 1 the Vertical Frame Assembly supporting the Detector Stage Assembly is able to move in the radial direction to control sample to detector distance. The range of this motion was extended in the final design to move detector from 10.3 m to 15.5 m. The completed Vertical Frame Assembly is able to move the detector 1.4 m vertically with a minimum height of 900 mm above the sample. At the concept stage it was expected the detector would need to be the same height as the sample for alignment. This requirement was later

---

† george.howell@diamond.ac.uk
α kejin.zhou@diamond.ac.uk
β andrew.walters@diamond.ac.uk
γ mirian.garcia-fernandez@diamond.ac.uk
δ houcheng.huang@diamond.ac.uk
ε stewart.scott@diamond.ac.uk
ζ nick.baker@diamond.ac.uk
1 Principle Beamline Scientist for I21
2 Resonant Inelastic X-Ray Scattering
3 Finite Element Analysis (FEA) or Finite Element Method
4 Plane Grating Monochromator

DEVELOPMENT OF LOW VIBRATION COOLING SYSTEMS FOR BEAM-LINE OPTICS USING HEAT PIPE TECHNOLOGY

J.R. Nasiatka*, S.S. Soezeri, O. Omolayo, H. A. Padmore, Advanced Light Source, Lawrence Berkeley National Lab, 94720 Berkeley, CA, USA

Abstract

Cooling of in-vacuum beamline components has always been problematic. Water cooling lines can transfer vibrations to critical components, and often require complex air guarding systems to ensure that the vacuum envelope is not breached in the event of a leak. These constraints increase design complexity, limit options, and provide challenges for assembly and maintenance.

Commercial heat pipes are inexpensive and readily available. Custom assemblies can be fabricated into vacuum flanges and may use non-water-based cooling mediums if required. A mockup of an optical assembly has been used to explore vibration reduction and cooling capacity. Other example beamline components such as a heat generating electromagnetic shutter, demonstrate the cooling capability of these heat pipes.

INTRODUCTION

A heat pipe [1] [2]is a device with a very high thermal conductivity that can transport large thermal loads. It is a passive, 2-phase device that comprises a sealed tube at sub-atmospheric pressure that contains a wicking medium and a working fluid. (Figure 1) At the hot end the working fluid absorbs energy and evaporates. It then migrates to the cold end where the thermal energy is released and the fluid condenses. The wicking material draws the condensed liquid back to the hot end. With proper design, the device can generally operate in any orientation, but if vertical with the hot end elevated, then gravity will help with the wicking.
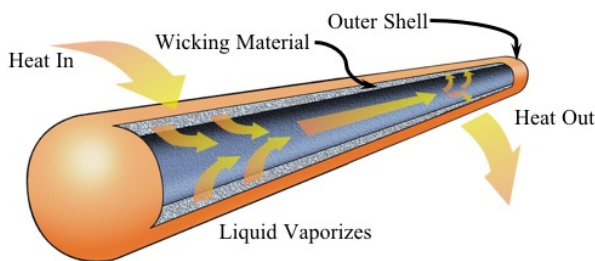

Figure 1: Heat Pipe Operation.

Table 1 lists thermal conductivities of various metals used in vacuum systems and the conductivity of a typical heat pipe. Heat pipes have an extremely high effective thermal conductivity compared to a solid metal conductor of the same size/shape ~x10-100. Internal design, orientation and working temperatures as well as heat loads need

to be considered for proper selection. [3] [4] Operation ranges can be anywhere from cryogenic to over 1500º C, and determine both the working fluid and outer shell. For 0-100º C operations water with a Copper shell is the most common and was used for these tests. Ethanol, methanol, and acetone can also be used. For use in UHV environments, sealing methods and materials are a factor. [5] This paper examines the suitability of heat pipes for cooling in-vacuum components on beamlines and endstations.

Table 1: Thermal Conductivities of Materials

Material	Conductivity (W/m•K)
Heat Pipe	10,000 +
OFHC Copper	390
6061 Aluminum	167
304 Stainless Steel	16.2

VACUUM COMPATABILITY

Standard Commercial Off The Shelf (COTS) heat pipes are typically fused and sealed by friction welding at the filled end. This end seal is the main potential point of failure that could result in leaking the working fluid into the vacuum. To determine vacuum suitability, two commercial heat pipes were ultra-high vacuum (UHV) cleaned and placed in a testing chamber that was then baked at 180º C for 2 days. Before and after bake residual gas analysis (RGA) scans were performed and after removal they were tested by placing them in a cup of hot water where they performed as expected.

Another heat pipe was cut in two and brazed onto a standard 2.75" Conflat flange so that the sealed ends of the pipe would be exposed to vacuum. (Figure 2) This was then UHV cleaned and mounted in a testing chamber equipped with an RGA. The assembly was exposed to repeated 180º C bake cycles of 24 hours with RGA scans performed after each cycle.

---

* JRNasiatka@lbl.gov

LCLS PULSE SELECTOR, A MULTIFUNCTION SHUTTER FOR THE LCLS-I 120 Hz FEL

R. R. Armenta[†], E. Paiser

Linac Coherent Light Source, SLAC National Accelerator Laboratory, Menlo Park, USA

Abstract

The Linac Coherent Light Source (LCLS) Pulse Selector was designed to pick specific pulses and reduce the repetition rate of the 120Hz LCLS pulse train in support of widely diverse, user defined experiments. It utilizes two rotating parallel plates to alternately transmit and block pulses in a single sweeping motion. A conventional stepper motor connected to the plates provides the rotation. The key to the system is its sophisticated timing scheme. Each sweep of the shutter is synchronized (with a precise delay) with the event codes normally generated with each pulse for data acquisition use. This shutter system has the capability of reducing the repetition rate of the LCLS x-ray to any frequency less than or equal to 60Hz in order to select a single pulse of LCLS x-ray beam at 120Hz. Since its installation, the pulse selector has been used in numerous experiments with great success providing independent pulse selection to individual beamlines at the same time.

INTRODUCTION

The Pulse Selector was commissioned to provide the hard x-ray beamlines (XPP, XCS, CXI, MEC, and later, MFX) with the ability to control pulse delivery without having to change accelerator machine modes/parameters. The key requirements were that (in addition to being able to fully attenuate the beam) the selector had to provide three main functions:

1. Provide single pulse selection (Mode 1)
2. Allow for multiple (n) sequential pulse selection (Mode 2)
3. Reduce the repetition rate of the 120Hz LCLS beam to up to 30Hz (Mode 3)

Initially the concept was to create a device similar in design to chopper/picker systems integrated at other synchrotron and FEL facilities e.g. the systems described by Kudo et al. [1] and Cammarata et al. [2]. These systems typically have a rotating disk or other shape with multiple apertures.

Material Considerations*

The pulse selector is required to block a certain number of x-ray pulses, i.e. attenuate the beam by more than about 20 orders of magnitude in the LCLS hard x-ray energy range (4-25 keV). While the required attenuation can be easily reached with small material thicknesses of high Z

_____
† Contact: rebeccaa@slac.stanford.edu
* Material investigations performed by Henrik Lemke, LCLS staff scientist (2012)

element containing materials, the short attenuation length in this material leads to the absorption of energy in a very small volume. Depending on the dose (energy per atom) the absorbed energy can be sufficient to melt and thereby damage the material. Melting doses for different elements are listed in the following Table.

Table 1: Melting Doses for Individual Elements

Element	Melting Dose / (eV / atom)
Al	0.186
W	1.2376
Si3N4	0.187
Co	0.554

The maximum FEL pulse energy to reach the damage dose depends on the beam size. From all hard x-ray hutches the beam size is smallest at XPP (500 um) and therefore the fluence is highest there.

The maximum pulse energy to reach the melting dose for W and Co, the main components in the stopper material selected for this application (WC/Co), is shown in Fig. 1 for the full energy range.
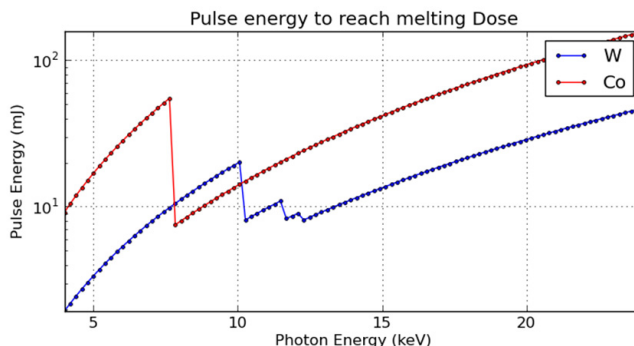
Figure 1: Pulse Energy to Reach Melting Dose.

Within the energy range of the first LCLS harmonic (4-10keV) damage might be reached. To prevent this, it was determined that coating with a lower Z material (Aluminum) would help for the following reasons reasons: The x-ray pulse energy is reduced by attenuation in the coating material, and the material prevents melted material from leaving the x-ray exposed region. Coating of the stopper material with a metal would have been most preferable as it is mechanically very stable. However, when evaluating

THE XBPM PROJECT AT MAX IV FRONTENDS, OVERVIEW AND FIRST RESULTS

A. Bartalesi[†], MAX IV Laboratory, Lund, Sweden

Abstract

All the frontends installed on the 3GeV storage ring at MAX IV are equipped with two X-Ray Beam Position Monitors. Having recently finished the installation of the acquisition system, it was possible to record and analyse data. This presentation describes the setup and shows the first results.

INTRODUCTION

Since the writing of the technical specifications for the MAX IV frontends [1], it was foreseen to include X-ray Beam Position Monitors in the design. Being the first real diagnostic tool for the photon beam, and being upstream of all the beamline optics, these devices are capable to decouple beam instabilities and fluctuations originated in the storage ring from the ones originated the beamlines. This makes them an important device when trying to pinpoint the source of a specific disturb. Additionally, they can be used to cross check the readouts of the ring BPMs, and possibly be included in closed loop orbit correction as feedback. Finally, being sensitive to energy and flux, and being the closest diagnostic tool to the synchrotron sources, they are interesting as a verification of the insertion device output.

WORKING PRINCIPLE

The XBPM working principle is based on the photoelectric effect: the emission of electrons from a material when light shine on it. Each XBPM is equipped with 4 tungsten blade that are placed in the outer region of the white beam, usually spaced in a way to have symmetries along X and Y in the beam cross section, as shown in Figure 1.
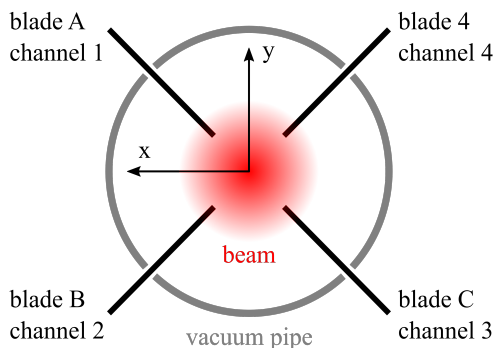

Figure 1: XBPM schematics.

These blades are then electrically connected to an elec-

_____
† antonio.bartalesi@maxiv.lu.se

trometer, so that when photons hit the blades and electrons are emitted, the electric current flowing out of the blades can be precisely measured. Knowing the photon cross-section of interaction of Tungsten, the energy and flux of the white beam and all the involved geometries, it is possible to calculate the theoretical current flowing out of each blade. But most importantly, if the symmetry is not broken anywhere else, imbalances between different blade currents are a direct sign of a difference between positions of white beam center and XBPM center.

This particular characteristic of being sensitive to *relative* signal differences makes these devices quite robust again other sources of error or uncertainties. For this reason, the XBPM are mounted on top of movable stages, and can be moved until the imbalances between different blade signals are zeroed. This placement is then fixed and maintained for long periods, so that short and long term beam movements can be both quantified.

Finally, there is one important complication: since the blades are usually close to each other, the electrons emittted from one blade can end up in another blade, and therefore alter the measurement. This is usually referred to as cross talk, but this issue can be avoided completely by applying a negative bias voltage to the blade themselves. The resulting electric field will then prevent emitted electrons from ending up in neighbouring blades, and each blade will show a reading that is closed to the theoretical one. Some XBPM designs take one step further in this direction and include an additional positive electrode in proximity of the blades, that distorts the electric field even more favourably.

Electric Measurement

The addition of a negative high voltage bias makes electric measurements slightly more complicated. Considering that we are interested in having really high accuracy, since we are interested in a differential measurement between similar blades, and also considering the small absolute value of the currents involved, it is important that all the current produced at a blade is transported to a high accuracy electrometer. The presence of the high voltage bias, however, can lead to very small, but problematic current leakages through the cable insulation. To avoid this problem, triaxial cables are adopted: they consist in a core at the bias voltage carrying the current from blade to electrometer, a first coaxial "shielding" named guard, that carries no signal but is elevated to bias voltage, and a third, proper shielding connected to ground. In this way, having the voltage difference between signal and guard equal to zero, we can guarantee no current leakages through the cable insulation. There will be leakages from guard to shield, but that has no effect on the measurement.

FAST X-RAY BEAM INTENSITY STABILIZATION FOR ABSORPTION SPECTROSCOPY AND SPECTROMICROSCOPIC IMAGING

M. Birri[†], V. A. Samson, D. F. Sanchez, B. Meyer, D. Grolimund[‡]
Paul Scherrer Institut, 5232 Villigen PSI, Switzerland
M. Willimann, DECTRIS Ltd, Baden, Switzerland

Abstract

We have designed and implemented a hardware component called "Wedges" with a closed-loop feedback system to achieve a constant incident X-ray flux I_0 at the sample during spectroscopic measurement at the microXAS undulator beamline at the Swiss Light Source. Compared to existing approaches, the new system has several advantages, in particular when used in combination with mini-gap, in-vacuum insertion devices or microfocusing optics. The attenuation strength required to maintain constant I0 flux can be adjusted in a fast, steady manner by simple linear translations of two wedge-shaped attenuators.

INTRODUCTION

The characteristics of synchrotron sources and beamline optics commonly result in systematic and random variations of the delivered photon flux. In X-ray absorption based measurements, for example, monochromator glitches [1] or the energy dependent gap size of small gap in-vacuum undulators [2] are intrinsic sources for changes in the I_0 flux. The measured signal intensity, I, has to be normalized by taking the ratio with I_0 to compensate for such variations in I_0. However, especially in the case of non-linear responses between the I_0 and I detectors, such normalization can introduce artifacts or signal distortions. Many types of x-ray experiments would benefit from a constant I_0 flux over the entire experimental parameter space.

Monochromator Stabilization (MOSTAB) is the current solution for most synchrotron beamlines with double crystal monochromators (DCM) to have a constant I0 from the monochromator output [3, 4]. The MOSTAB approach is acting on the relative alignment of the two monochromator crystals ('dynamic detuning') in order to stabilize beam intensity (or to maintain beam position). Obviously, any change in angular alignment of the monochromator crystals will not only result changes in the transmitted photon flux, but also induce deviations in the beam trajectory and photon energy distribution.

BEAMLINE LAYOUT

The beamline layout and relevant components are shown in Figure 1. A minigap in-vacuum undulator (U19) serves as radiation source providing high brightness X-rays in the energy range from 4 to 23 keV. The photon flux delivered at 12 keV is > 1012 photons/sec, while the optical scheme employed used ensure an energy resolution of ΔE/E <10-4. The optical layout of the beamline is composed of several pairs of slits, a bendable toroidal, horizontally deflecting mirror and a DC monochromator (Figure 1). The toroidal mirror unit serves three main purposes: (i) to collimate the beam in the vertical dimension, (ii) to allow for dynamic demagnification in horizontal dimension, and to act as a low-pass filter with an energy cut-off of ~23 keV given by the Rh coating. The horizontal focusing corresponds to the first part of a two-step focusing strategy that offers two main advantages: a secondary source with flexible size adjustment by precision slits (the capability of dynamical focusing and the possibility of optimizing the overall acceptance of the subsequent microfocusing optical system. The fixed–exit double-crystal monochromator is equipped with three different pairs of crystals: Si(111), Si(311) for higher energy resolution and Ge(111) for higher flux throughput. The first crystal is for energy selection while the fixed-exit is controlled by a piezo device acting the second crystal.

In the experimental hutch, the micro-probe set-up is installed on a stable optical table. Achromatic focusing in the entire energy range of 4-23 keV is done with an elliptical shape mirror pair in the Kirkpatrick-Baez (KB) geometry (or KB mirrors) producing a beam of about 1.0
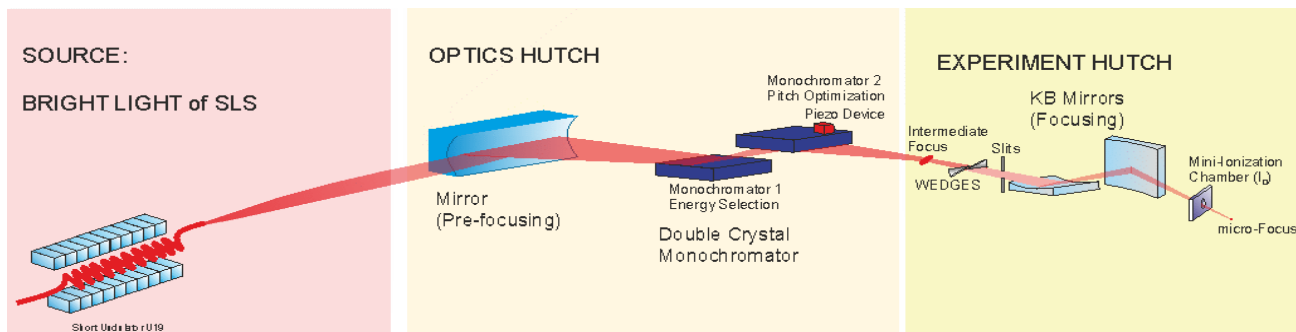

Figure 1: MicroXAS Beamline Layout.

---

† mario.birri@psi.ch
‡ daniel.grolimund@psi.ch

AN IMPROVED POLARISATION ANALYSER FOR THE I16 BEAMLINE AT DIAMOND

M. Burt, S. P. Collins, S. Green, I. Horswell, J. Li, G. Nisbet, R. Pocock, J. Spiers, K. Wilkinson
Diamond Light Source Ltd., Harwell Science and Innovation Campus, OX11 0DE, UK

Abstract

The project to upgrade the I16 polarisation analyser was necessary to increase its functionality and to introduce a more robust and reliable construction. The requirement that the device was to be mounted on the arm of a diffractometer meant the construction needed to be as lightweight and as compact as possible. This provided opportunities to explore new collaborative ways of working with both in-house and external suppliers.

The paper describes the approach taken to develop lightweight aluminium vacuum chambers using a company specialising in additive layer manufacturing techniques. In addition, the design of lightweight and compact slit assemblies are detailed; these were developed in collaboration with a supplier of driven linear stages.

The paper also describes the process of using additive layer manufacturing to model prototypes to optimise the design of cable management systems where previously basing the design on 3d CAD models had proved unsatisfactory.

Another novel requirement for this device is having an x-ray detector mounted on a rotation axis in vacuum. The results of working with the in-house detector group to develop a design to allow this to be realised with all the necessary thermal and electrical connections, are outlined.

POLARIZATION ANALYSER

Overview

The I16 beamline at Diamond is dedicated to the study of advanced materials using X-ray diffraction; part of this process is to use a device that can analyse magnetic scattering from samples. Magnetic scattering is different to, and weaker than, normal scattering and analysis of the polarisation of this scattering can be used to gain insights into the magnetic properties of materials. This information allows details of the three-dimensional magnetic structure of the sample material to be determined.

The device in question, known as a polarisation analyser (PA), allows a crystal/detector assembly to be rotated about the axis of the x-ray beam direction in a similar way to a polaroid polarizer being rotated in visible light. In addition, utilizing a high quality crystal with the analyser can give higher resolution diffraction that allows structures to be studied on length scales that range from the atomic to 10^{-3}m.

The design of the PA essentially comprises an assembly of vacuum chambers, sets of slits to remove unwanted scattering, and various detectors which are arranged to rotate about different axes. Data collected from the detectors as they are moved and rotated allow information on the polarisation of the scattering to be built up.

The project to upgrade the design of the existing polarisation analyser was an opportunity to increase its functionality and to introduce a more robust construction.

The analyser itself is mounted on the arm of a diffractometer so it was important that the construction was made to be lightweight (see Fig. 1). A lightweight construction would avoid the need for additional counterweights on the diffractometer which would reduce its performance.
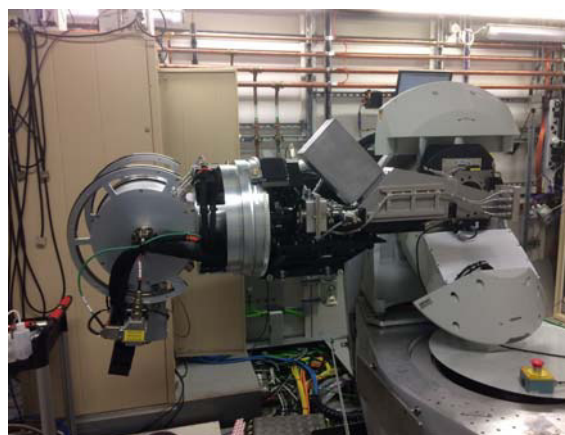

Figure 1: View of polarisation analyser mounted on diffractometer arm.

Lightweight Vacuum Vessels

A significant proportion of the structure of the PA comprises vacuum chambers. Conventionally these vessels had been constructed as two separate parts, a vessel body with a lid. In order to make an effective seal both parts have to be thick enough to accommodate an O-ring seal and also to be stiff enough to compress the seal. In addition, to compress the seal a large number of nuts and bolts are required, all of which add weight.

It was decided that by using additive layer manufacturing these vessels could be made as one piece. This would remove the need for flanges and the nuts and bolts; also the wall thickness of the vessels could be reduced to the minimum required to provide an air-tight and rigid shell.

Working in collaboration with a specialist additive layer manufacturing company: 3d-Alchemy [1], who advised on materials and minimum thicknesses to prevent porosity, the chambers were manufactured and the relevant sealing surfaces were machined to complete the finished chambers (see Fig. 2).

TMO - A NEW SOFT X-RAY BEAMLINE AT LCLS II*

J.C. Castagna[†], M. Holmes, J. James, P. Walter, T. Osipov, L Amores

LCLS, SLAC National Accelerator Laboratory, Menlo Park, CA, United States

Abstract

LCLS is building 4 new soft X-ray beamlines with the LCLS-II upgrade. The TMO (Time resolved Molecular Optical science) beamline aka NEH 1.1 will support many experimental techniques not currently available at LCLS. The beamline hinges around 2 main end stations, LAMP a multi configurable end station and DREAM, dedicated to COLTRIM type of experimentation. Both the existing LAMP as well as the newly built DREAM end-station will be configured to take full advantage of both the high per pulse energy from the copper accelerator (120 Hz) as well as high average intensity and high repetition rate (up to 100 kHz) from the superconducting accelerator. Each end station will have its own focusing optic systems (KB Mirrors) which can focus the beam down to 300 nm, and have laser pump probe experiments capability. Very demanding requirements for IR and X-ray overlap as well as beam stability, make the TMO beamline a major engineering challenge. The main components of the beamline (KB optics, DREAM end stations and diagnostics components) are built on granite stands. The building structure is being reviewed for thermal stability. First light on TMO is expected in February 2020.

SCIENCE DRIVERS

TMO stands for Time resolved Molecular Optical science instrument

LCLS-II will be a transformative tool for energy science, qualitatively changing the way that X-ray imaging, scattering and spectroscopy can be used to study how natural and artificial systems function. It will enable new ways to capture rare chemical events, characterize fluctuating heterogeneous complexes, and reveal quantum phenomena in matter, using nonlinear, multidimensional and coherent X-ray techniques that are possible only with X-ray lasers. This facility will operate in a soft X-ray range (250 eV to 1.5 keV), and will use seeding technologies to provide fully coherent X-rays in a uniformly spaced series of pulses with programmable repetition rate and rapidly tuneable photon energies.

NEH beamline 1.1 aka TMO will support many experimental techniques not currently available at LCLS. High operational efficiency will be achieved through utilization of 2 fixed endstations. Stable beam trajectories will be provided through streamlined X-ray alignment to the fixed interaction points. Delivering the beam to only a few fixed locations will optimize optical laser experiments and set-ups.

END STATIONS

The beamline hinges around 2 main end stations; LAMP a multi configurable end station and DREAM, dedicated to COLTRIM type experimentation.

Both the existing LAMP as well as the newly built DREAM end-station will be configured to take full advantage of both the high per pulse energy from the copper accelerator (120 Hz) as well as high average intensity and high repetition rate (up to 100 kHz) from the superconducting accelerator.

The new DREAM endstation will house a well-defined geometry and COLTRIMS type spectrometer as a standard configuration to accommodate extreme vacuum, sub-micron focus spot size, and target purity requirements dictated by the pump-probe class of coincidence experiments, while ac-cumulating data on the event-by-event basis at the rep rates in excess of 100 kHz fully utilizing the LCLS-II capabilities. Photon fluency in DREAM will reach over 1021 photons/cm2 with superconducting Linac X-rays, while with copper accelerator it will be over 1022 photons/cm2 at 120 Hz.

The LAMP endstation will be part of the Next generation Atomic, Molecular, and Accelerator Science and Technology Experiments (NAMASTE) and it will be optimized for performing high energy, high resolution, time, but also angular-resolved photoelectron spectroscopic measurements. NAMASTE will accept highly standardized modular endstations.

Pump-probe timing resolution of X-ray with optical laser pulses goal is sub 10 fs for both end-stations. Optical laser peak field power density will be over 1015 W/cm2 (of 800 nm) on target.

FOCUSING OPTICS

Each endstation will have its own focusing optic systems (KB Mirrors). The focus size in LAMP will be around 5μ and down to 300 nm in the DREAM end station. Both end station will have laser pump probe experiments capability. The KB mirrors will be used in "series". The focal point of the first set of mirrors for the LAMP end station being used as the source point for the second set of KB mirrors for the DREAM endstation. Only the first set of KB mirrors will be bendable to adjust focus in either endstation.

NANOSURVEYOR 2: A COMPACT INSTRUMENT FOR NANO-PTYCHOGRAPHY AT THE ADVANCED LIGHT SOURCE

R.S. Celestre, K.Nowrouzi [1], H.A. Padmore, D.A. Shapiro, Advanced Light Source, Lawrence Berkeley National Laboratory, 94720, Berkeley, CA, USA

[1]also at University of California, 94720,Berkeley, CA, USA

Abstract

The Advanced Light Source has developed a compact tomographic microscope based on soft x-ray ptychography for the study of meso and nanoscale materials [1,2]. The microscope utilizes the sample manipulator mechanism from a commercial TEM coupled with laser interferometric feedback for zone plate positioning and a fast frame rate charge-coupled device detector for soft x-ray diffraction measurements. The microscope has achieved scan rates of greater than 50 Hz, including motor move, data readout and x-ray exposure, with a positioning accuracy of better than 2 nm RMS and has achieved spatial resolution of better than 5 nm. The instrument enables the use of commercially available sample holders compatible with FEI transmission electron microscopes. This allows in-situ measurement of samples using both soft x-rays and electrons.

This instrument is a refinement of a currently commissioned instrument called The Nanosurveyor, which has demonstrated resolution of better than 20nm in both two and three dimensions using 750 eV x-rays. [3] The instrument has been installed on the new Coherent Scattering and Microscopy beamline at the Advanced Light Source and is in the final stages of commissioning. It will enable spectromicroscopy and tomography of materials with wavelength limited spatial resolution.

INTRODUCTION

X-ray ptychography holds the promise of overcoming the resolution, depth of field and efficiency limitations of imaging with conventional x-ray optics [1,2]. It instead relies upon phase retrieval from coherent diffraction data which can be measured to very high numerical aperture with high efficiency. The use of soft x-rays for microscopy, though limiting sample thickness to a few microns, provides very high contrast and exquisite sensitivity to electronic and magnetic states of matter. This, coupled with the high coherent flux available in the soft x-ray range at modern synchrotron sources allows for high spatial resolution with very short exposure times. The ability to image materials with near wavelength limited spatial resolution and functional systems with high time and chemical resolution has previously been demonstrated [2,3]. As x-ray source brightness increases, there is an ever increasing demand for high performance imaging systems. We present the operational instrument of an ultra-stable, high speed scanning x-ray microscope which is fully compatible with many electron microscopy sample holders. The microscope, called Nanosurveyor 2 (Fig. 1), enables wavelength limited x-ray microscopy and facilitate correlative imaging using x-rays and electrons.

MECHANICAL AND OPTICAL DESIGN

The nanosurveyor 2 instrument is derived from the sample area hardware of an FEI CM200 series TEM. We have modified the octagon sample area hardware to create a larger vacuum chamber incorporating both upstream and downstream sections in order to house the required beam conditioning hardware and the LBNL designed fast CCD [4]. This approach was taken in order to leverage the existing design of the TEM for high stability, which also utilizes air-side motor hardware for thermal stability, and to provide for ease of measurement of samples going between EM and XRM instruments. The sample is held and positioned by a standard FEI Compustage sample manipulator that has been upgraded to higher resolution optical encoders. Most functionality present in a standard TEM installation remains in our implementation of the system. This allows users to mount samples in commercially available sample holders designed for tomography, cryo-tomography and those holders specially designed for *in-situ* experiments.

The basic configuration of the system is similar to other scanning zone plate systems in use at the ALS in that the focusing optic is mounted into a high stiffness scanning piezo flexure stage with X and Y axes (orthogonal to the x-ray beam direction) [5]. The interferometer's fiber-optics heads are mounted to the fixed assembly which supports the sample goniometer such that mechanical path lengths to the sample are minimized. These interferometer beams are returned by a polished and gold coated surface on the zone plate mounting assembly in order to track position of the zone plate in XY while scanning. A compact, three axis order sorting aperture assembly is mounted within the frame of the piezo scanner in order to facilitate tracking of the focused x-ray beam with the order sorting aperture (OSA). The OSA assembly scans with the focusing optic. This enables us to utilize the entire 100 μm range of our XY scanning system rather than being limited to a fraction of the OSA diameter (typically 50 μm).

DESIGN OF INDIRECT X-RAY DETECTORS FOR TOMOGRAPHY ON THE ANATOMIX BEAMLINE

K. Desjardins[†], M. Scheel, J.-L. Giorgetta, T. Weitkamp, C. Menneglier and A. Carcy,
Synchrotron SOLEIL, L'Orme des Merisiers, 91192 Gif-sur-Yvette, France

Abstract

ANATOMIX is a new beamline for full-field tomography techniques at the French synchrotron SOLEIL. It will operate at photon energies from 5 to 30 keV and feature several operation modes via versatile optics configurations, including direct propagation of the polychromatic ("white") undulator beam to the experiment position. Two different experimental methods will be used: parallel-beam X-ray shadowgraphy, for spatial resolution down to the sub-micron range, and full-field transmission X-ray microscopy down to a spatial resolution of less than 100 nm. To cover the large panel of experimental possibilities, four dedicated indirect X-ray detectors have been designed. For pixels in the sub-micron size range, a micro-tomography revolver camera for versatility, a high-efficiency camera for flux-limited experiments, and a high-resolution camera for the largest optical magnifications will be available. For experiments with a large X-ray beam and pixel sizes from several microns upward, a "large-field" camera completes the set.

INTRODUCTION

Indirect X-ray image detection is the standard concept used today for full-field tomography techniques on hard X-ray synchrotron beamlines. Detectors based on this principle have been commonly used for 20 years [1,2]; they can be in-house developments [3-4] or commercially supplied (for example from Optique Perter, Lentilly, France or Hamamatsu Photonics, Hamamatsu, Japan). They convert the X-ray image to visible light with a scintillator screen and project the visible-light image on the sensor of a digital camera using visible-light lenses.

To match the large variety of needs of the new tomography beamline ANATOMIX [5] at the French synchrotron SOLEIL, the Detector Group, the Mechanical Engineering Group and beamline team have designed four models of indirect detectors. The "Revolver X-Ray Camera", a versatile assembly composed of a revolving cylinder with four microscope objectives, the "High-Resolution X-ray Camera" equipped with a very high resolution microscope objective, the "High-Efficiency X-ray Camera" for applications limited by X-ray flux and the "Large-Field X-Ray Camera" for fields of view of several centimeters width. Each of these models accepts different digital cameras and, with the exception of the "high-resolution" model, all are compatible with the intense white X-ray beam. In this article, we report on the different designs with the detailed components and expected performance of each solution.

---

† kewin.desjar@synchrotron-soleil.fr

INDIRECT X-RAY CAMERAS

Common Specifications

All X-ray detectors have been made to be easily customizable. The camera, objective, scintillator or mirror can be simply disassembled and changed.

The four X-ray detectors can accept different models of commercially-available digital cameras which can be plugged through a standard support (Fig. 1). Three different camera models are currently used at the beamline to cover the range of parameter space required by the user community.
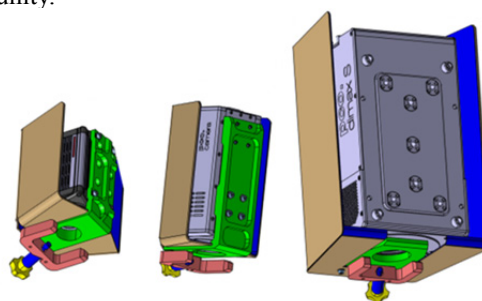

Figure 1: Standard camera support for ANATOMIX X-ray detectors. Left to the right: ORCA Flash4, PCO4000 and DIMAX HS4.

Firstly, the ORCA Flash 4 (Hamamatsu Photonics, Hamamatsu, Japan), with a scientific CMOS sensor array of 2048×2048 pixels of relatively small size of (6.5 µm) is a polyvalent camera with low readout noise (1 e⁻ rms) and high frame rate of 100 Hz. Secondly, the DIMAX HS4 (PCO AG, Kelheim, Germany), a high-speed CMOS camera with 2 kHz frame rate, 2048×2048 pixels (11 µm pixel size), especially used with the high X-ray beam flux to preform very quick tomography. Finally, the PCO 4000 based on a large CCD sensor (4008×2672 pixels of 9 µm size, sensor area 36×24 mm²) with a low dark noise < 0.05 e⁻/s. The camera bracket support is installed on a motorized rotation stage to align the pixel matrix with the tomography rotation axis (Fig. 2b).

The detectors (excepting the "high-resolution" model) have been also made to accept a polychromatic X-ray beam, so as to prevent radiation damage in lenses or electronics; all models have an L-shaped optical path, with the camera placed vertically, away from the X-ray beam path. A mirror between the scintillator screen and the objective redirects the visible light path toward the sensor (example in Fig. 2d for the revolver camera). The objectives are protected by millimeter-thick lead-glass windows which absorb the X-ray scattering from the air and mirror while remaining totally transparent to the visible.

LCLS-II FEL PHOTON COLLIMATORS DESIGN*

S. Forcat Oller[†], H. Wang, E. Ortiz, Y. Feng, J. Krzywiński, M.Rowen
SLAC National Accelerator Laboratory, Menlo Park, CA 94025, USA

Abstract

The unique capabilities of LCLS, the world's first hard X-ray FEL, have had significant impact on advancing our understanding across a broad range of science. LCLS-II, a major upgrade of LCLS, is being developed as a high-repetition rate X-ray laser with two simultaneously operating FELs. It features a 4 GeV continuous wave superconducting Linac capable of producing ultrafast X-ray laser pulses at a repetition rate up to 1 MHz and energy range from 0.25 to 5 keV. The LCLS-II upgrade is an enormous engineering challenge not only on the accelerator side but also for safety, machine protection devices and diagnostic units. A major part of the beam containment is covered by the FEL beam collimators. The current photon collimator design is no longer suitable for the high power densities of the upcoming LCLS-II beam. A complete new design has been conceived to satisfy this new constrains. Moreover, a special FEL miss-steering detection system based on a photo diodes array has been designed as an integral part of the photon collimator as additional safety feature. This paper describes the new LCLS-II FEL Collimators, their mechanical design and encountered challenges.

INTRODUCTION

Due to the possibility of having a X-ray FEL beam stray from its nominal path and strike surfaces of beamline components no able to handle the FEL power, the installation of collimators along the Front End layout is required to stop this mis-steered photon beam and also to only let pass the beam size defined by their aperture to the downstream components. The collimators are equipped with a fault detection mechanism that consists of four photo diodes that shall detect the beam scattering from miss-steered beam and inform the Machine Protection System (MPS) which will take actions such as deviating or even tripping off the beam if required.

LCLS-II BEAM PARAMETERS

The LCLS-II SXR beamline will be driven by the new superconducting radio-frequency Linac (SCRF) while the HXR beamline can be driven either by the SCRF Linac or by the normal copper radio-frequency Linac (CuRF).

The much higher average power possible with the SCRF Linac compared with the current LCLS FEL beam presents new challenges to the thermal management of the beam optics, diagnostics, slits and absorbers (see Table 1 and table 2).

Table 1: LCLS-II Soft X-ray Beam Parameters at 0.1 MHz, 300 Pc

Energy [eV]	Beam divergence [μrad]	Max integrated power [W]	Max single pulse fluence [mJ]
250	11.8	880	8.8
750	4.6	570	5.7
1250	3.2	339	3.4

Table 2: LCLS-II Hard X-Ray Beam Parameters at 0.3 MHz, 100 Pc

Energy [eV]	Beam divergence [μrad]	Max integrated power [W]	Max single pulse fluence [mJ]
1500	2.8	519	1.73
3250	2.0	185	0.62
5000	3.3	1.8	0.06

MECHANICAL DESIGN

Collimators in the Layout

A total of ten collimators are considered in the baseline for LCLS-II, five will be installed on the SXR line and five on the HXR. The Table 3 and Table 4 show the different aperture sizes and location of each collimator along the x-ray transport system. Aperture size was determined by beam stay clear and ray trace.

Table 3: HXR Collimators Location and Apertures Sizes (1.5 keV for the SC Linac and 1.5 keV for Cu Linac)

Coll. ID	Location[#] [m]	Beam size Ø [mm] SC/Cu	Beam Stay Clear Ø [mm] SC/Cu	Coll. aperture Ø [mm]
PC1H	84.2	2.92/2.44	7.69/6.73	8
PC2H	93.2	3.09/2.59	8.12/7.12	2.5
PC3H	100.9	3.24/2.72	8.49/7.46	2.5
PC4H	104.6	3.31/2.79	8.67/7.62	2.5
PC5H	98.2	3.19/2.68	8.37/7.34	2.5

[#]Location from the end of the undulator.

GRANITE BENCHES FOR SIRIUS X-RAY OPTICAL SYSTEMS

R. R. Geraldes, A. Sikorski, C.S.N.C. Bueno, M. Saveri Silva, G.V. Claudiano, V.Z. Ferreira, M.S. Souza, Brazilian Synchrotron Light Laboratory (LNLS), Brazilian Center for Research in Energy and Materials (CNPEM), 13083-970, Campinas, São Paulo, Brazil

Abstract

The first set of Sirius beamlines is expected to start operating in early 2019 and over the last few years many optical systems for the X-ray beamlines have been developed in-house at the Brazilian Synchrotron Light Laboratory (LNLS). Starting with the High-Dynamic Double Crystal Monochromator (HD-DCM), passing by the Double Channel-Cut Monochromator (4CM) and continuing with new standard mirror systems, a series of granite benches, based on high-resolution levellers, and a combination of embedded and commercial air-bearings, has been designed for high mechanical and thermal stability. Specifications, designs, and partial results are presented, showing the progressive increase in complexity according to a deterministic design approach.

INTRODUCTION

Sirius, the new Brazilian synchrotron light source, is currently under construction. As a fourth-generation machine, the synchrotron beam will have extraordinary properties in terms of size, divergence and flux. Consequently, the beamline optical elements, such as monochromators and mirror systems, must have corresponding performances to allow for proper energy selection and control of position and size of the beam at the sample, which begins with robust and stable mechanical supports (see Fig. 1).

Figure 1: Optical systems mounted on granite benches: (a) mirror; (b) double channel-cut monochromator (4CM); and (c) High-Dynamic Double Crystal Monochromator (HD-DCM) (Beam direction: +z. Vertical up: +y).

Following several successful beamline instrumentation examples [1, 2], granite was chosen as the base material for the new generation of mechanical benches, due its good elastic modulus over density ratio associated to a very low coefficient of thermal expansion, since this combination results simultaneously in good thermal and mechanical performances. Moreover, to improve the stability and reduce the complexity of the assemblies of the optical elements, it was made the choice of allowing only the essential degrees of freedom (DoF) in vacuum, whereas all other DoF needed for positioning and alignment should be provided by the benches [3, 4]. In the following sections, the practical implementation of these guidelines and partial results of the benches of the High-Dynamic Double Crystal Monochromator (HD-DCM), Double Channel-Cut Monochromator (4CM) and mirror systems are presented.

CONCEPTUAL DESIGN

Since positioning the optical elements along the beam axis (z) does not usually have strict specifications, the granite benches have been designed to allow for positioning and alignment in the remaining 5 DoF, namely: translations, in the horizontal and vertical axes, Tx and Ty, respectively; and the associated rotations, Rx, Ry and Rz.

With some effort, all the most demanding specifications of different optical elements could be meet in a standard conceptual design. At the bottom level, wedge-levellers developed for Sirius girders [5] allow for Ty_1, Rx and Rz, for basic short-range height positioning and levelling. Next, functional air-bearing arrangements allow for the additional DoF by positioning different granite blocks with respect to each other. In the monochromators, Tx and Ry are implemented to overcome initial assembly and alignment limitations, and to allow for either the exchange between crystal sets (HD-DCM) or for pink beam operation (4CM). As for the mirrors, with side-bounce deflection, in addition to these two DoF, a large-range Ty_2 has been introduced to allow for the selection of stripes with different coating materials.

The choice of functional air-bearings was driven by the intention of maximizing the overall mechanical and thermal stability, and effectively optimizing the stiffness of the bench as a whole. Indeed, with this solution, it is even possible to combine different DoF over a single interface, which allows for designing the minimum number of granite parts and direct interfaces. As the air-bearings are used only during alignment, once the air is off the bench should behave nearly as an extension from the floor up to the optical elements. With conventional guiding elements, there would be more elements in the stiffness chain and particularly a significant number of interfaces, which are prone to performance limitations. Finally, combining embedded
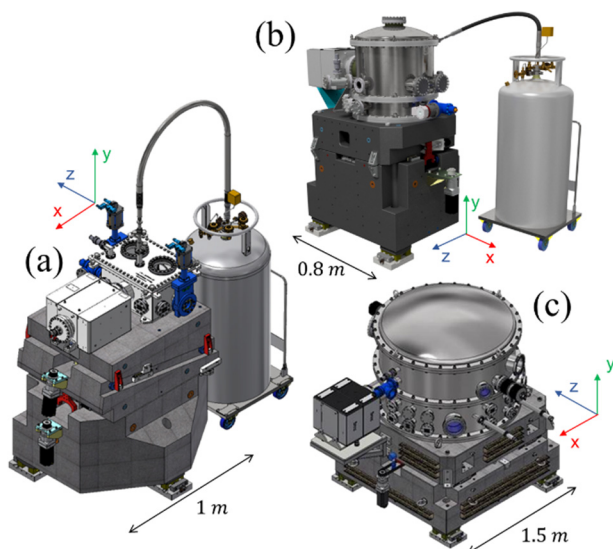
BEAM CONDITIONING OPTICS AT THE ALBA NCD-SWEET BEAMLINE

N. Gonzalez, J. B. González, C. Colldelram, M. Llonch, J. Ladrera, A. Fontserè, G. Jover-Manas,
J. C. Martínez, C. Kamma-Lorger, I. Sics, S. Ferrer and M. Malfois
ALBA Synchrotron Light Source, Cerdanyola del Valles, Spain

Abstract

The SAXS/WAXS Experimental End Station beamline (NCD-SWEET) at ALBA Synchrotron has undergone a major upgrade in the optics and the end station to perform state-of-the-art SAXS/WAXS experiments.

In order to reduce X-ray parasitic scattering with air and maximize the photon flux at the sample, an optimized beam conditioning optics has been designed and built in the end station, integrating previously used and new components in vacuum.

The beam conditioning optics includes a fast shutter, a set of commercial guard slits and a diagnostic unit comprising three filters and a four-quadrant transmissive photodiode. In addition, a set of refractive beryllium lenses allows micro focusing of the beam. The lens system can be removed from the beam path remotely. Finally, an on axis sample viewing system, with a novel design based on an in-vacuum camera mirror and a mica window minimizes the beam path in air up to the sample.

To facilitate the alignment of the elements with respect to the beam, all the subsystems are supported by a high-stability granite table with 4 degrees of freedom and submicron resolution.

INTRODUCTION

As part of the upgrade project of the the Non-Crystalline Diffraction beamline (NCD-SWEET) at ALBA, the end station has undergone a full re-design of the mechanical elements in addition to the installation of new equipment with the result of a new beamline configuration [1].

In order to improve the service to users and provide an improved basic configuration to perform transmission experiments, an enhanced beam conditioning optics system comprising new elements such as, a diagnostic unit and a set of micro focusing lenses, has been designed and built (Figure 1). Additionally, the vacuum section has been extended up to the sample and all the components have been located over an in-house developed 4-DOF granite table.
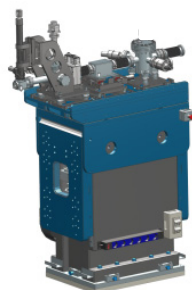

Figure 1: General overview of the Beam Conditioning Optics.

SYSTEM REQUIREMENTS

The main objective of the beam conditioning optics (BCO) upgrade was to maximize the beam transmissivity up to the sample, thus, all the elements, including the fast shutter and the on-axis sample viewing system (in air in the previous setup), were placed in vacuum. Besides, in order to have a diagnostic of the beam intensity just before the sample a new diagnostic unit compounded of a transmissive photodiode and 3 filters had to be installed. Additionally, a set of compound lenses were integrated. These lenses can be remotely inserted into the beam path in order to micro focus the beam.

So as to ease the alignment of the beam conditioning elements with respect to the beam for different optical configurations and energy ranges while ensuring the system stability, all the components had to be located over a high stability 4-DOF table.

The movement requirements of the support table are listed in Table 1.

Table 1: Motion Requirements of the BCO Support Table

	Range	Resolution
Vertical	15mm	2 µm
Transversal	± 5 mm	2 µm
Pitch	±0.5˚ (± 8.5 mrad)	±0.001˚ (17. 4 µrad)
Yaw	±0.5˚ (± 8.5 mrad)	±0.001˚ (17.4 µrad)

DESIGN DESCRIPTION

The beam conditioning optics system consists of a granite based table with 4 motorized degrees of freedom that allows the alignment of the elements with respect to the beam while ensuring the stability of the components. All the beam conditioning elements, namely, the fast shutter, the compound refractive lenses, the slits, the diagnostic unit and the sample viewing camera mirror are placed inside UHV vessels located over the table. The elements have external fiducial interfaces and individual alignment stages, with edge welded bellows in between, so that all the apertures could be pre aligned during the installation. Besides, the beryllium lenses system is located over two motorized stages that permit the in-out motion and the longitudinal positioning along the beam path for the focal position adjustment. This motion, together with the vertical movement of the on axis camera that permits the focusing adjustment, gives high versatility for using sample holders of distinct sizes.

Microfocusing Lenses

A set of 35 beryllium compound refractive lenses permit micro focusing the beam at 664mm from their centre. The lenses are positioned within a vacuum chamber lo-

A NEW HIGH PRECISION, FULLY MOTORIZED 6-DoF SAMPLE STAGE FOR THE ALBA PEEM ENDSTATION

N. González†, L. Aballe, A. Carballedo, C. Colldelram and M. Foerster
ALBA Synchrotron Light Source, Cerdanyola del Vallès, Spain

Abstract

A new 6-DoF sample manipulator has been designed for the ALBA Synchrotron PhotoEmission Electron Microscopy (PEEM) experimental station, based on a commercial Elmitec LEEM 3.

The new design includes full motorization of all 6 axes with position feedback, no backlash, and maximized stability, crucial to achieve the best spatial resolution of down to 8 nm (in so-called LEEM mode).

The in-plane longitudinal and transversal motions with sub-micron resolution are based on high precision linear guides, while the pitch and roll stages (sample tilt), guided by angular guides, are actuated by a double-flexure system, which enhances the overall rigidity of the system. The vertical stage is composed by a high rigidity recirculating roller screw and cross roller guides. Finally, 360° yaw rotation is supplied by a differentially pumped commercial rotary stage. On top of the stage, the sample support is mounted on a customized DN63CF flange.

This support keeps the original functionalities of the sample manipulator and holders, with 6 independent electrical contacts, and the possibility to heat the sample up to 2000 K and cool it to 100 K with an improved liquid nitrogen cooling system.

INTRODUCTION

The purpose of the project is to upgrade the PEEM endstation functionality by offering full automatization of the sample motions. In the present form, the vertical motion and the crucial sample tilt (which through non-geometrical effects is coupled with the measurement position (horizontal stage)) are still operated manually, preventing full remote control and programming of sequences.

Additionally the new design offers opportunities to improve repeatability of those motions already motorized, the easy integration into the control system through ICEpap motor controls and the improvement of the cooling stage efficiency which has deteriorated in the original design. Improvement of the sample stability, which is straight related with the microscope resolution, is also sought.

TECHNICAL SPECIFICATIONS

The main objective of the new design of the sample manipulator is to motorize the 6 degrees of freedom that allow the alignment of the sample with respect to the microscope (main) objective lens (field of view). The motions must guarantee the correct positioning of the sample and repeatability while most of all ensuring stability, which directly influences the microscope resolution. Besides, a longer vertical movement is required in order to move the sample holder to the transfer position.

In addition, the existing liquid nitrogen cooling system has to be improved in order to obtain 100K at the sample.

The stage must be placed over the analyser chamber at the PEEM experimental station (Figure 1) so the overall system must be as compact as possible to reduce the mass over the chamber, maximize stability and leave free space for the surrounding instrumentation.
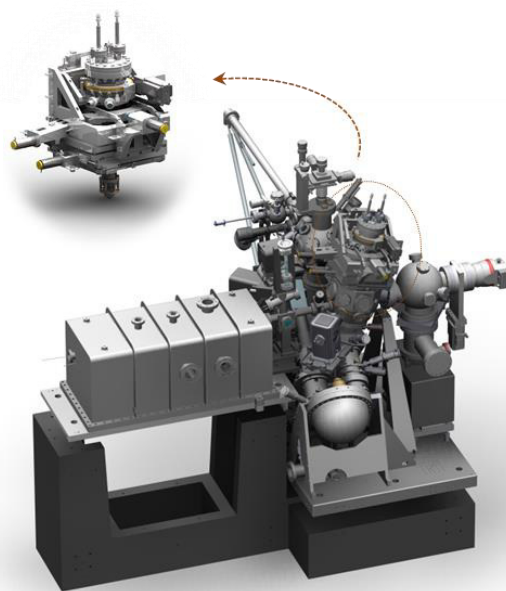

Figure 1: General view of the sample stage location at the PEEM End Station.

Moreover, the new sample stage must comply with the following specifications:
- To be UHV compatible and bakeable.
- To be compatible with the standard Elmitec sample holders.
- To keep 6 independent electrical contacts at High Voltage (20kV)
- Possibility to heat the sample up to 2000K.
- Possibility to cool the sample down to 100K.

---

† ngonzalez@cells.es

COMPACT MIRROR BENDER WITH SUB-NANOMETER ADAPTIVE CORRECTION CONTROL

N. González[†], J. González, C. Collderam, J. Juanhuix, C. Ruget and J. Nicolas

ALBA Synchrotron Light Source, 08290 Cerdanyola del Vallès, Barcelona, Catalonia, Spain

Abstract

We present a compact mirror bender with dynamic surface correction. The system is the evolution of an in-house development and will be the default focusing system for the new ALBA beamlines. The bender is now more compact and can introduce stronger curvatures, as required for microfocus applications. It allows for in-situ correction of the mirror surface, with resolution and stability below one nanometer. The bender can compensate parasitic deformations caused by thermal bumps, changes of focus, or stresses appeared during installation or bakeout.

INTRODUCTION

Surface quality of optical elements is essential to reach the performance of X-ray beamlines in 3rd and 4th generation synchrotron light sources and free electron lasers [1]. Mirror figure errors are usually the limit for the smallest achievable spot on sample and for the resolution of soft x-ray monochromators. In addition, they also limit the homogeneity of defocused beams [2,3]. In the last years, deterministic surface figuring techniques have been developed [4, 5], and sub-nanometer figure errors can be achieved by some mirror polishers [6]. On the other hand, beamline operation often requires certain adaptability: being able to change the focus position, tune the spot size, or compensate thermal bumps. This pushes for the development of active optics systems for x-ray mirrors, keeping the accuracy within the nanometer.

Existing active X-ray optical systems control the topography of the mirror surface by introducing deterministic deformation of its substrate. There are several systems that, to do this with sufficient resolution, use piezo-electric actuators [7-10]. Alternatively, the system we propose controls the deformation by applying point forces distributed along the substrate using spring-based mechanical correctors [11,12]. In order to achieve the required range, resolution, and stability of the applied force, we use a combination of springs and magnets as the elements generating the force.

Results obtained with a prototype demonstrate that the required mechanical performance is achieved, and is stable within several days.

SYSTEM DESCRIPTION

The mirror bender system we propose consists of three main parts: the frame that supports the bending actuators and the correctors, the bender actuators, that support and bend the mirror by applying forces at the ends of the mirror substrate, and the correctors, that apply smaller forces at

---

† ngonzalez@cells.es

discrete points along the mirror (see Fig. 1). The whole system is ultra-high-vacuum (UHV) compatible.

The main frame consists of two thick plates that offer a stiff reference for the supports and for the correctors. The plates have multiple slots to allow placing the correctors at any position along the mirror substrate. The two bending actuators are located at the ends of the frame. They support the mirror and provide the bending forces. These actuators are designed to be compact in the direction of the beam, so the complete system is just 20 mm longer than the mirror substrate, and most of the length of the substrate is also clear to install correctors, or cooling pads. The bending actuators include the supports of the mirror, as well as the contacts that apply the bending force on the mirror. All these elements have rolled articulations to minimize parasitic forces that could be applied to the mirror substrate. In particular, all contact points between the bender and the mirror are free to pitch and roll, except one of the supports of the mirror, which is fixed in roll. This fixes the orientation of the mirror but avoids introducing any parasitic twist. Also, all contact surfaces are cylindrical, in order to have a reproducible contact point on the mirror, with acceptable contact stress.
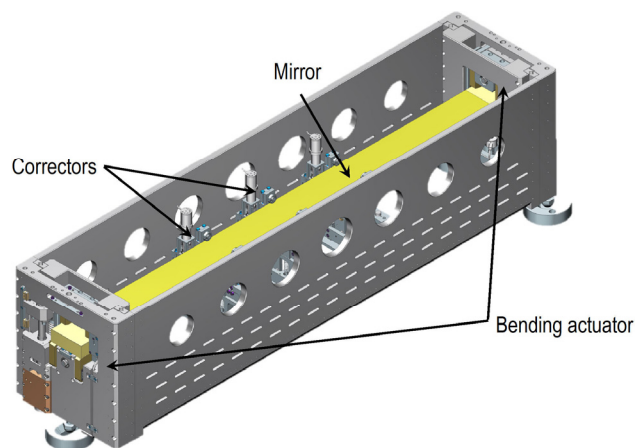

Figure 1. Illustration of the bender prototype, indicating the positions of the bending actuators and of the point correctors.

The bending force applied to each end of the mirror substrate is generated by compressing two helical springs which are connected on one end to a linear stage driven by a stepper motor, and to the mirror on the other end. In addition, the link between the spring and the mirror includes a load cell that provides feedback of the force applied to the mirror. The load cell is placed between braided cables, that compensate any misalignment that could introduce errors on the measurement of force. The load cell resolution is 0.01 N, which corresponds to a 0.5% error in a 100 km

NCD-SWEET BEAMLINE UPGRADE

J.B. González*, N. González, C. Colldelram, L. Ribó, A. Fontserè, G. Jover -Manas, J. Villanueva,
M. Llonch, G. Peña, A. Gevorgyan, Y. Nikitin, J.C. Martínez, C. Kamma-Lorger, E. Solano,
I. Sics, S. Ferrer, M. Malfois
ALBA Synchrotron Light Source, Cerdanyola del Valles, Spain

Abstract

The SAXS/WAXS Experimental End sTation (NCD-SWEET) at ALBA Synchrotron has undergone major improvements in three main areas, beam performance, SAXS detector data quality and beamline operability, in order to perform state-of-the-art SAXS/WAXS experiments. A new channel-cut monochromator system has improved the beam quality and stability, with current vibration amplitudes under 1% of the beam size. Two sets of refractive beryllium lenses have been installed for focussing the beam. One of the sets allows to microfocus the beam size. Besides this, the former SAXS CCD detector has been replaced by a single-photon counting pixel detector, a Piltatus3 S 1M. In the end station, a full redesign of the mechanical elements with sub-micron resolution movements together with the installation of new equipment has been completed, resulting in an improved beamline configuration, and a faster and safer rearrangement of the flight tube length. New upgraded configuration also allows for GISAXS experiments. Finally, other auxiliary improvements have been done in areas like radiation protection, air conditioning, health and safety, cable management, electronics and control.

INTRODUCTION

The NCD-SWEET beamline is dedicated to Small Angle X-ray Scattering (SAXS) and Wide Angle X-ray Scattering (WAXS) experiments at ALBA Synchrotron. SAXS experiments provide structural and dynamics information from coherently scattering entities within sample at a longer length-scale (up to several hundreds of nm). E.g. large molecular assemblies, fibres or higher order structures of proteins and polymers can be explored by this technique. WAXS technique explores structure at shorter length scales on the order of Angstroms. In addition, one of the objectives of the upgrade of beamline was to make it suitable for Grazing-Incidence Small-Angle Scattering (GISAXS) experiments which are being implemented at present.

The End Station of the beamline includes the last downstream section of beam conditioning optics, a sample environment, two detectors (SAXS and WAXS) and a flight tube on rails that permits changing the camera length and minimizing the air gap between the samples and the SAXS detector (Fig. 1).

Following some years of operations of NCD beamline, Scientific Advisory Committee suggested to perform an

upgrade of the beamline in order to improve its performance. After review process by a panel of experts as well as internal discussions, a major project was developed in order to achieve the state-of-the-art for SAXS/WAXS experiments at the beamline. Present paper discusses this multidisciplinary project including all of the changes made and features added to the beamline.

Figure 1: NCD-SWEET End Station.

BEAM PERFORMANCE

In the past, NCD beamline experienced poor beam stability due to undesired vibration in the double crystal monochromator system. In order to resolve this stability issue, the former double crystal monochromator (DCM) system has been replaced with a new channel-cut system while keeping the vacuum vessel, Bragg angle goniometer and other interfaces (Fig. 2). As a result, stability has improved substantially with current vibration amplitudes under 1% of the beam size instead of 39% before the change.
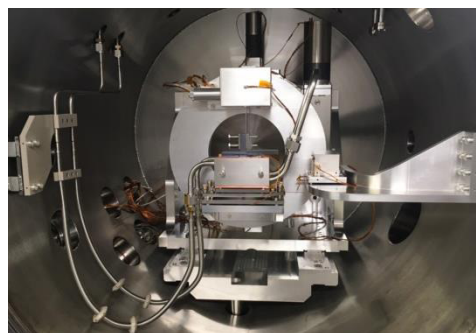

Figure 2: Channel-cut monochromator system.

In addition, two sets of refractive beryllium lenses have been installed for focussing the x-ray beam. One set is located in the Optics Hutch section of the layout while the second in the End Station of the beamline. The latter enables achieving microfocus beam size at the sample position (although with the associated loss in the flux). Addition of these beryllium lenses allows for switching between the existing toroidal-collimating mirror optics

A MULTI-SAMPLE HOLDER FOR THE MSPD BEAMLINE AT ALBA

J.B. González*, F. Farré, X. Serra, D. Roldán, P. Pedreira, F. Fauth,
ALBA Synchrotron Light Source, Cerdanyola del Valles, Spain

Abstract

At the high resolution powder diffraction end station of the Materials Science and Powder Diffraction (MSPD) beamline at ALBA Synchrotron, several samples are measured on a daily basis. Thus, an automatic sample exchanger is a great asset to the beamline, permitting a more efficient use of beam time. Even if a robot arm is the more suitable option for a sample exchanger device, in terms of cost, compactness and versatility MSPD needs another approach. ALBA engineering division has developed a multi-sample holder that allows the loading of up to eight samples and exchanging between them with a resolution of less than a micron. This new design consists of a customized and motorized linear stage that has been designed to fit into the present three-circles diffractometer, on top of the positioning stages, avoiding any possible collision with the Eulerian cradle. In addition, this new holder permits the use of different types of samples like capillaries in fast spinners, coin cell batteries and electrochemical cells. Finally, the system is compatible with the usual sample conditioning equipment on the end station such as the hot blower, cryostream, beamstop, chiller, etc.

DESIGN

The multi-sample holder consists of a customized and motorized linear stage (Fig. 1). The mechanism involves a ball screw and linear guides together actuated by a stepper motor. The ball screw presents low axial clearance (less than 5 µm) in order to assure good repeatability and the linear guides are slightly preloaded for stiffness purpose.

Due to space restriction on top of the positioning stages of the present three-circles diffractometer, the multi-sample holder has been designed to be as narrow as possible (up to 31.5 mm) in order to not shadow the Mythen and Multicrystal Analyser detectors (Fig. 2). Also the system has been designed to avoid any possible collision with the Eulerian cradle.
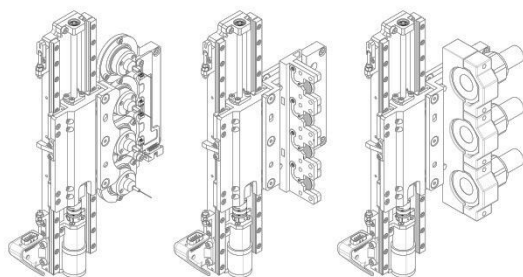

Figure 1: Multi sample holder in three configurations.

The multi sample holder permits the use of different types of samples like capillaries in fast spinners, coin cell

---
* jgonzalez@cells.es

batteries and electrochemical cells. For this purpose, a common interface is used for all sample holders, consisting of a plate with positioning pins and fixed by screws. This common interface will be compatible with all future sample developments in the beamline.

Finally, the complete system is suitable for sample conditioning equipment use on the end station such as the hot blower, cryostream, beamstop, chiller, etc. during normal operation.

TECHNICAL SPECIFICATIONS

The multi sample holder complies with the following specifications:

- Linear resolution of 0.3 µm.
- Repeatability of 0.75 µm.
- Range of 166mm (±83 mm).
- Compact and integrated in the Eulerian cradle.
- Compatible with sample conditioning equipment.
- It provides 4 positions for coin cell batteries.
- It provides 3 positions for electrochemical cells.
- It provides 4 positions for fast spinners in its current design or 8 in a new configuration in development.
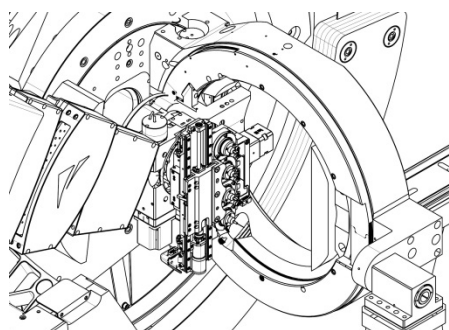

Figure 2: Multi sample holder on Eulerian cradle.

METROLOGY RESULTS

Metrology tests have been performed using a Renishaw ML10 Interferometer in order to evaluate the resolution, repeatability and other characteristics of the motion of the multi-sample holder in open loop.

Table 1: Metrology Results

Explored Range	0.156 m
Avg. resolution	0.1562 µm/hs
Backlash/Hysteresis	2.32 µm
Repeatability	0.75 µm
Linearity	4.39 µm
Sampling noise	18 nm

ENGINEERING DESIGN OF THE PDF & XPD BEAMLINE SAMPLE ENVIRONMENT FOR SAFE EXPERIMENTAL USE OF HAZARDOUS GASES

Edwin Haas, A. M. Milinda Abeykoon, PhD, Scott Buda, Eric Dooryhee, PhD, Sanjit Ghose, PhD, Christopher Stelmach, John Trunk, National Synchrotron Light Source II, Brookhaven National Laboratory, Upton, New York, 11973 U.S.A.

Abstract

The Pair Distribution Function (PDF) and X-ray Powder Diffraction (XPD) beamlines located at the 28-ID at Brookhaven National Laboratory's (BNL) National Synchrotron Light Source II (NSLS-II) require a means for safely supplying, containing, and exhausting hazardous gases to and from experimental samples. The PDF/XPD sample environment includes a sample holder, internal beam stop, sample chamber, and stages that provide eight degrees of freedom. A specially-designed window is also included for maximum X-ray transmission at minimum cost. Sensors, flow metering devices, and circuitry are included to provide proper purging, control hazardous and dilution gas flows, and integrate the safeguards needed for safe operation.

INTRODUCTION

The PDF and XPD beamlines collect X-ray pair distribution function and diffraction data from samples using high energy (i.e. > 25 keV) X-rays. A specially-designed Gas Handling System (GHS, see Acknowledgments) supplies a variety of hazardous and non-hazardous gases to an outlet port for in-situ and in-operando studies of chemical reactions. A specially-designed sample environment is needed to contain and supply gases to experimental samples, position samples quickly, accurately, and remotely, collect scattered X-rays over a wide-angle without distortion, dilute hazardous gases after flowing through the samples, and then safely exhaust the gas mixtures. Excluding inert and non-reactive gases, the GHS supplies hydrogen, methane, ethylene, oxygen, carbon monoxide, NO_x, SO_x, and CH_3S_x (e.g. methyl mercaptan and methional) gases and mixtures.

SAMPLE ENVIRONMENT DESIGN

The sample environment includes: a sample chamber, a sample holder and sample, an internal beam stop, and stages to remotely position the sample, sample chamber, and beam stop. The samples are contained in capillary tubes and retained by miniature collets in a holder designed to allow gases to pass through the samples. The sample chamber is vented externally and inert gas dilutes hazardous gases after flowing past each sample. Seals and materials are compatible with the gases used, and the sample chamber has windows to cost-effectively allow entrance of a .5 mm x .5 mm X-ray photon beam and undistorted exit of scattered X-rays over a wide (± 30°)

angle from the sample center. Lastly, the sample environment requires similar protections and safety provisions as the GHS. Two cameras, a goniometer, and X, Y, and Z stages are used to align the capillary tubes. Once aligned, electrical power is disconnected for safe operation when using flammable gases. The sample chamber is large enough to contain a goniometer and an internal beam stop (to prevent X-ray scatter from the downstream window) yet small enough for ± 30° unobscured collection of scattered X-rays. An image of the sample environment is shown in Figure 1.
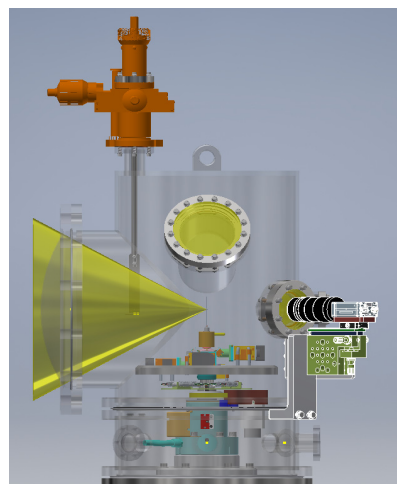

Figure 1: Sample environment with transparent sample chamber and ± 30° scattered X-ray exit cone.

The X-ray sample chamber is composed of two sections, the upper section has an upstream Be window for monochromatic photon beam input, a large port downstream to collect scattered X-ray data, an internal beam stop (with remote X and Y stages), two camera ports, and a view port. It connects to a lower spool section which contains the feedthroughs for gas inputs, exhaust, sensors, electrical power, and controls. The upper section can be removed quickly for non-hazardous gas experimental use.

To meet BNL safety requirements, the sample chamber materials must be compatible with all gases used and the chamber must withstand 1 atmosphere external pressure (and internal vacuum for leak-check verification) with a safety factor of 3.0 on yield stress. The chamber wall thicknesses were determined by iterative finite element analysis (FEA) modeling using standard material stock sizes. Since all gases used are compatible with stainless steel, 304/304L stainless steel

DREAM - A NEW SOFT X-RAY (DYNAMIC REACTION MICROSCOPY) COLTRIMS ENDSTATION AT LCLS-II*

M. Holmes[†], L. Amores, J. C. Castagna, J. James, T. Osipov, P. Walter
LCLS, SLAC National Accelerator Laboratory, Menlo Park, CA, United States

Abstract

SLAC National Accelerator Laboratory is building new soft X-ray beamlines to take advantage of the LCLS-II upgrade to 1 MHz. One of the new beamlines is called TMO (Time resolved Molecular Optical science) also known as NEH 1.1. It will be a soft X-ray beamline featuring a sub-micron X-ray focus at its second, most downstream interaction region where the DREAM (Dynamic REAction Microscopy) COLTRIMS (COLd Target Recoil Ion Momentum Spectroscopy) endstation will be situated.

DREAM will feature; large magnetic coils to provide a strong uniform magnetic field through the spectrometer, rigid in-vacuum laser in- & out-coupling optics decoupled from the chamber support stand for pump-probe experiments, a multi-stage differentially pumped gas jet with catcher, insertable diagnostics, a long-distance microscope, scatter slits, a steerable gas jet, jet slits, and an adjustable stand to bias the spectrometer off-center from the interaction region.

In order to achieve a spot overlap spec of 0.5 um; the KB mirrors, laser optics, & beam position diagnostics all sit on a common granite support structure to minimize mechanical vibrations and thermal drifts. An in-vacuum UHV hexapod will be utilized for fine positioning of the laser in-coupling optic.

BACKGROUND

For the new DREAM endstation at SLAC National Accelerator Laboratory, the required X-ray spot size is 0.3 um, and the required pump laser spot size is 5 um. They need to be overlapped with incredibly tight precision to achieve spatial overlap of the pump laser with respect to the X-ray laser with sub-micron repeatability. In addition to this challenging requirement the DREAM endstation needs to achieve an outstanding UHV (Ultra High Vacuum) base pressure of 3e-11 Torr. It also needs to have a multi-stage differentially pumped gas jet for delivering the sample and a Helmholtz coil pair for generating a magnetic field around its COLTRIMS spectrometer at the center of the chamber. Figure 1 shows the complete model of the DREAM endstation and labels its major components.
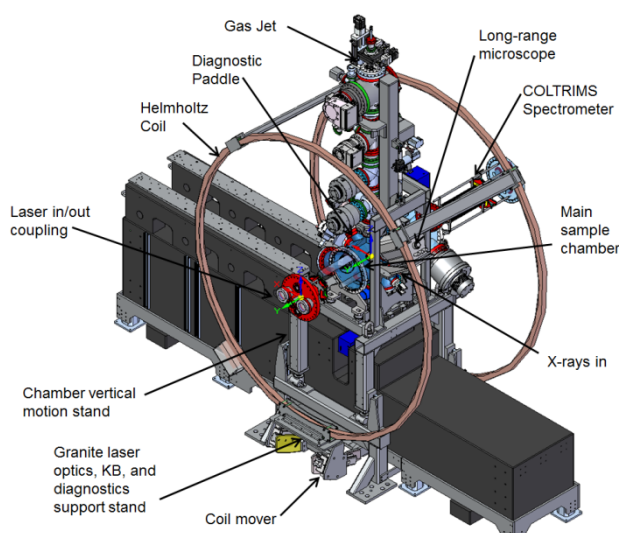

Figure 1: The DREAM endstation in its preliminary design phase. The major components of the endstation are listed.

HELMHOLTZ COILS

A pair of high-power Helmholtz coils is used for providing a linear magnetic field of up to 30 Gauss through the central ion/electron spectrometer. The coils will each be built by winding 16 turns of hollow rectangular copper tubing around a fixture, and curing a high-temperature fiberglass/epoxy mixture. At a diameter of approximately 2.2 meters, the total cross sectional amperage needed for each main coil ring is about 3800 amps; therefore each section of coil tubing will have 1/16th of the total; about 240 amps. The expected voltage required to drive both coils in series is 16 volts DC, resulting in a total power requirement of 3.7 kW. The Helmholtz coils will be water-cooled to keep them safe to touch while additionally not contributing unwanted thermal currents to the surrounding air near the endstation.

In order to correct the magnetic field vector of the earth, the coils have two motorized angular degrees of freedom to correct both roll and yaw of the coils. This will ensure the resultant magnetic field vector from the combination of earth's magnetic field and the coil's magnetic field is running axially horizontal along the center of the main chamber perpendicular to the two detectors in the spectrometer.

INTERLOCK SYSTEM FOR A MAGNETIC-BEARING PULSE SELECTOR

H. Ishii, J. Adachi, H. Tanaka, T. Kosuge,
High Energy Accelerator Research Organization, Tsukuba, Ibaraki, Japan

Abstract

A new pulse selector with a magnetic bearing has been developed for a hybrid operation mode which has been introduced in the Photon Factory (PF) 2.5 GeV ring of the High Energy Accelerator Research Organization. The pulse selector is used to permit only the passage of an X-ray pulse that comes from the single-bunch part of the hybrid filling pattern. It is mainly comprised of a slit dish-shaped disk fixed at a rotation axis and a motor system synchronized with the radio-frequency signal of the ring. We have adopted a commercially available motor system with a very low jitter of the rotation, which was developed not for a heavy load. The slit disk is so heavy that a rapid deceleration of the rotation can cause a large current to flow back to the motor driver. To avoid the current flow-back problem in the pulse selector system, we have implemented a software interlock and have developed a prototype of a programmable logic controller–based interlock system. The operation of the interlocks in five possible situations has been checked.

INTRODUCTION

A hybrid operation mode has been introduced in the Photon Factory (PF) 2.5 GeV ring of the High Energy Accelerator Research Organization (KEK) [1]. A pulse selector, a type of optical chopper, is used to permit only the passage of an X-ray pulse that comes from the single-bunch part of the hybrid filling pattern. We have developed a new pulse selector which comprises of a magnetic bearing, a dish-shaped and many-slit disk fixed at the rotation axis, a phase-locked-loop (PLL)-controlled motor system, and other parts. The speed and phase of the rotating disk are controlled by transistor-transistor logic (TTL) signals obtained by dividing the radio-frequency (RF) signal of the PF 2.5 GeV ring. A commercially available motor system has been adopted for a sufficiently low jitter of the rotation. The slit disk for the new pulse selector was so heavier than the previous disks in our previous pulse selectors with an air bearing that a rapid deceleration of the rotation can cause a large current to flow back to the motor driver, causing it to fail. An interlock to avoid the current flow-back problem in the pulse selector system is required. We have implemented a software interlock and have developed a prototype of a programmable logic controller (PLC)–based interlock system.

INTERLOCK SYSTEM FOR MAGNETIC-BEARING PULSE SELECTOR

The magnetic-bearing pulse selector system consists of an amplifier module, trigger and clock delay module, pulse-selector controller, magnetic-bearing controller, pulse-selector main body, and interlock system (Fig. 1).
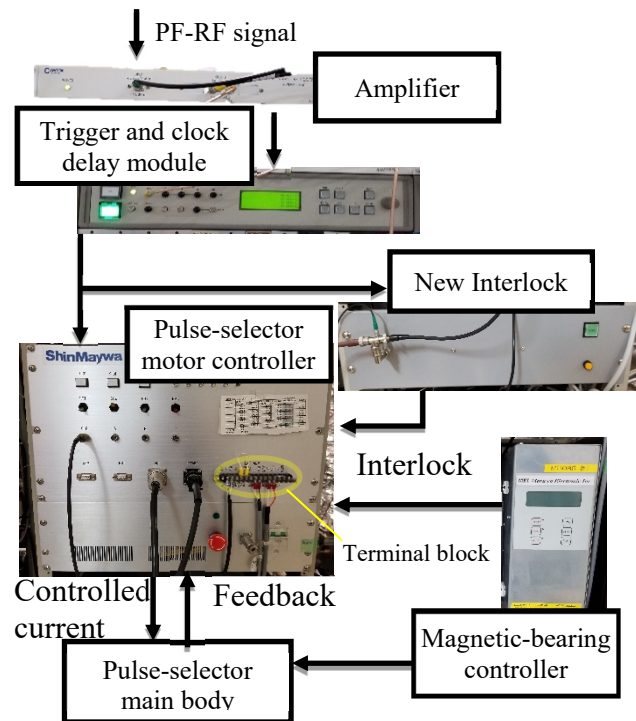

Figure 1: Pulse-selector control system.

The RF signal for the PF 2.5 GeV ring is amplified by the amplifier module and input into the counter circuit. The trigger and clock delay module divides the amplified RF signal into TTL-pulse sequences with a frequency-dividing rate. The TTL-pulse sequence is sent both to the new interlock system and to the pulse-selector motor controller. The pulse-selector motor controller drives the motor of the pulse selector with monitoring encoder. The new interlock system responds according to the TTL-signal frequency to protect the pulse-selector motor controller from the ill effects of the current flow-back.

The pulse-selector motor controller has an emergency button and a terminal block for the external input to protect the equipment. The terminal block is connected to the following three types of interlock.

- Power-off detection
- Detection of magnetic-bearing controller errors
- Newly developed PLC-based interlock system

The slit disk part of the pulse selector is floated by the magnetic bearing and the controller is connected to an uninterruptible power supply (UPS). If a power stoppage to the UPS input is detected, the drive signal of the pulse selector will be cut immediately. The magnetic-bearing controller is connected to the terminal block to signal an error to the motor controller.

FRONT END DESIGNS FOR THE ADVANCED PHOTON SOURCE MULTI-BEND ACHROMATS UPGRADE *

Y. Jaski[†], F. Westferro, S. Oprondek, S. Lee, B. Yang, M. Abliz, J. Downey, J. Mulvey
and M. Ramanathan, Argonne National Laboratory, Lemont, IL 60439, U.S.A

Abstract

The Advanced Photon Source (APS) upgrade from double-bend achromats (DBA) to multi-bend achromats (MBA) lattice is underway. This upgrade will change the storage ring energy from 7 GeV to 6 GeV and beam current from 100 mA to 200 mA. All front ends must be upgraded to fulfil the following requirements: 1) Include a clearing magnet in all front ends to deflect and dump any electrons in case the electrons escape from the storage ring during swap-out injection with the safety shutters open, 2) Incorporate the next generation x-ray beam position monitors (XBPMs) into the front ends to meet the new stringent beam stability requirements, 3) For insertion device (ID) front ends, handle the high heat load from two undulators in either inline or canted configuration. The upgraded APS ID front ends will only have two types: High Heat Load Front End (HHLFE) for single beam and Canted Undulator Front End (CUFE) for canted beams. This paper presents the final design of the HHLFE and preliminary design of the CUFE.

OVERVIEW OF APS FRONT ENDS

APS has a total of 35 sectors that can extract user beams. Currently there are 33 existing ID front ends (FE) and two vacant ID ports. The APS upgrade (APSU) will build out all 35 ID front ends with either a HHLFE for inline undulators or a CUFE for canted undulators. Out of the 33 existing ID front ends, 21 of them were built in the 1990s and are not capable of handling the heat load of the APSU ID sources and must be replaced with new FEs. The remaining 12 front ends that were built in the 2000s are capable to handle the heat load but must be retrofitted to have the next generation XBPMs and the clearing magnets. The APS existing ID front ends and their heat load limit is shown in Table 1.

Table 1: APS Existing ID Front Ends Heat Load Limit

Type of FEs	FEv1.2	FEv1.5	CUFE	HHLFE
P_{total} (watts)	6.9	8.9	10×2	21
P_{peak} (w/mrad^2)	198	245	281	590
Existing Qty.	17	4	7	5

HIGH HEAT LOAD FRONT END

The original HHLFE was designed in 2003 [1]. The original design was focused on the design of high heat load components. All photon masks and photon shutters were designed to handle the heat load limit of 21 kW total power and 590 kW/mrad^2 peak power density, equivalent of two inline 3.3-cm-period undulators at 10.5 mm gap at 180 mA. This heat load limit was sufficient for the APSU and was adopted as the design requirement for the APSU front ends. The first major redesign of the HHLFE was in 2012 to incorporate the next generation XBPMs into the front end [2]. Since then many improvements have been made to the front end. This paper presents the new HHLFE for APSU MBA to include a clearing magnet in the front end and refine the design of the XBPMs to reduce cost and ease alignment, and introduce a new design of exit mask and XBPM2 combined unit. The layout of the new HHLFE is shown in Fig. 1. The aperture of key components are shown in Table 2. The design will be initially installed in the vacant port of 28-ID for the current storage ring to test out the new designs of the XBPM system.

Table 2: HHLFE Aperture Table for APSU MBA

Components	Aperture H×V (mm)
Pre-Mask	36×26
FM1	38×26 (inlet)/ 20×16 (outlet)
FM2	24×20 (inlet)/ 9×12 (outlet)
Clearing Magnet	13×20 (optical minimum)
	18 (magnet gap)×65 (stay clear)
Lead Collimator	19.5×19.5 (optical)
	26×26 (shielding)
GRID-XBPM	15.3×50 (inlet)/ 1.6×50 (outlet)
FM3	16×47.8 (inlet)/ 3.6×6 (outlet)
Photon Shutter	10×47.8 (inlet)/ 5×47.8 (outlet)
Safety Shutter	72×20 (optical)
	72×20 (shielding)
Wall Collimator	27×17 (optical)
	37×26 (shielding)
Exit Mask	10×38 (inlet)/ 2×2 (outlet)
Exit Collimator	5×5 (optical)
	5×5 (shielding)

MECHANICAL CONVERSION OF A VERTICALLY REFLECTING ARTIFICIAL CHANNEL-CUT MONOCHROMATOR TO HORIZONTALLY REFLECTING*

S. P. Kearney[†], E. Dufresne, S. Narayanan, A. Sandy, D. Shu, Advanced Photon Source, Argonne National Laboratory, Argonne IL. 60439, U.S.A.

Abstract

The mechanical conversion of a high-resolution artificial channel-cut monochromator (ACCM) from a vertically reflecting orientation to a horizontally reflecting orientation is presented. The ACCM was originally commissioned for the 8-ID-I beamline at the Advanced Photon Source (APS), Argonne National Laboratory [1, 2]. The ACCM was intentionally designed at commission to have the potential to be reoriented to the horizontal direction. After nearly a decade of operation in the vertical orientation the ACCM was rotated to the horizontal orientation. The details of the design which allowed this conversion and the preparation steps needed to assure the continued performance of the ACCM will be discussed.

INTRODUCTION

An ultra-high-vacuum double crystal monochromator (DCM) was previously designed for the 8-ID-I beamline at the Advanced Photon Source [1]. The DCM was designed to meet the same stability performance as a single channel-cut crystal using an overconstrained weak-link mechanism for positioning alignment of the second crystal [3]. In addition, features were incorporated into the design for the potential conversion of the vertically reflecting geometry to horizontally reflecting. This paper will discuss the mechanical conversion of the DCM from vertical to horizontal reflecting geometry and the optical results.

MECHANICAL CONVERSION

The original vertical orientation can be seen in Fig. 1(a-b). For the conversion to work the entire vacuum tank was designed so that when rotated 90° about the x-ray beam path (Fig. 1(a)) the crystal assembly would be at the same height. The support frame was designed with this in mind, which can be seen in Fig. 1(b), and the table was also designed with a hole through the top plate for clearance of the main Bragg rotation stage flange. Rotation of the DCM was done in the end station with little modification and the final horizontal orientation can be seen in Fig. 1(c). Internal components were kept in place during the rotation and only the x-ray vacuum lines, cooling lines, and electrical components were detached. Modifications included new supports for the ion pumps shown in Fig. 1(c), and two internal support straps, Fig. 2, for the water cooling lines. The straps were installed to reduce the strain on the connection points due to gravity. All crystal mounts, stages, and supports needed no modification for the new orientation.
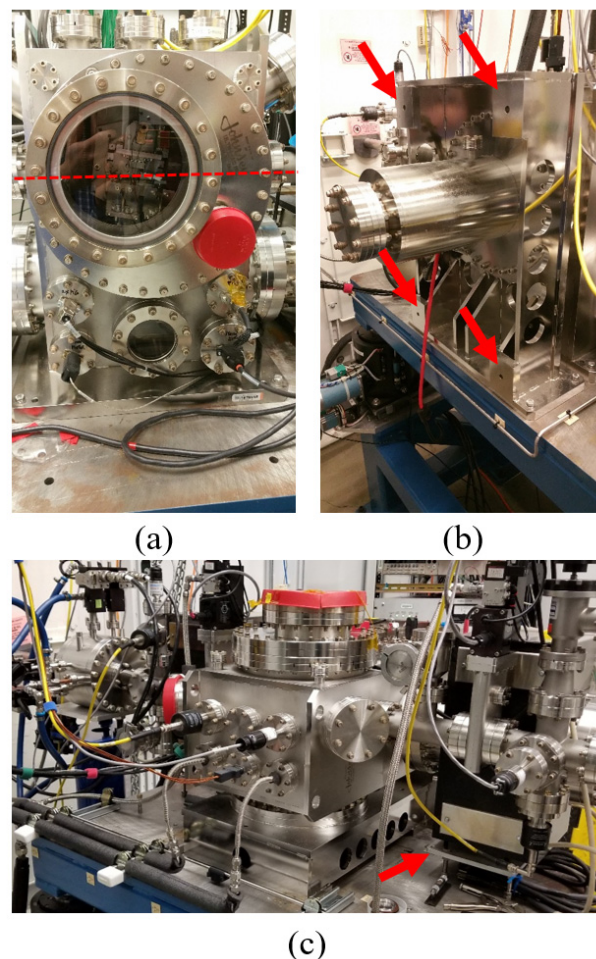

Figure 1: (a) Front view of DCM in vertical orientation with a dashed line representing x-ray path. (b) Back view of DCM showing new mounting surfaces (red arrows) for horizontal orientation. (c) Isometric view of DCM in the new horizontal orientation with red arrows showing new ion pump supports.

MECHANICAL DESIGN OF A COMPACT NON-INVASIVE WAVEFRONT SENSOR FOR HARD X-RAYS

S. P. Kearney[†], L. Assoufid, W. Grizolli, T. Kolodziej, K. Lang, A. Macrander, Y. Shvyd'ko, X. Shi, D. Shu, and M. Wojcik,

Advanced Photon Source, Argonne National Laboratory, Argonne, IL 60439, U.S.A.

Abstract

This work describes mechanical design of a prototype compact wavefront sensor for in situ measurement and monitoring of beam wavefront of hard x-ray beamlines. The system is based on a single-shot grating interferometer [1, 2] and a thin diamond single-crystal beam splitter. The beam splitter is designed to be inserted in the incident beam and oriented to diffract a fraction of the incident beam bandwidth into the interferometer, for wavefront measurement and reconstruction. The concept is intended to study the feasibility of a non-invasive wavefront sensor for real time wavefront monitoring and diagnostics, with possible application in adaptive mirrors for wavefront preservation and control [1, 3]. The design focus was on compactness to enable easy portability and implementation in a beamline.

Z8-83 OVERALL DESIGN

The wavefront sensor, see Fig. 1 and 2, was designed for in situ measurement and monitoring of beam wavefront of hard x-ray beamlines. It works by placing a single-crystal beam splitter into the incident x-ray beam and then using the grating interferometer to measure the diffracted wavefront in a non-invasive manner. The design is based on the designs in [1, 2] with the focus being compactness so that it could be easily implemented in any beamline. The entire assembly is only 26 kg (Table 1), which can be easily lifted by two people without lifting equipment. A total of 9 controlled stages were used in its various sub-assemblies and the camera and grating assemblies were designed to be manually positioned along the rotation arm. The support structure is modular such that the legs can be removed completely or replaced with longer legs all while maintaining alignment of the crystal rotation axis and main diffraction axis.

Figure 1: Fully assembled wavefront sensor.
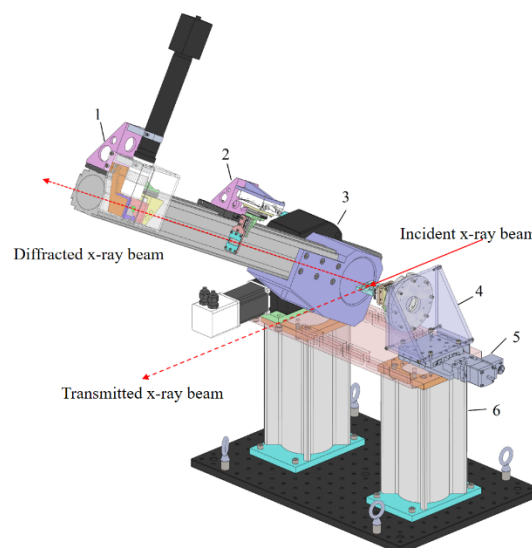
_____
[†]skearney@aps.anl.gov

Figure 2: Complete assembly of Z8-83 wavefront sensor: (1) camera assembly, (2) grating assembly, (3) rotation arm, (4) crystal assembly, (5) Kohzu Precision Co. linear stage, and (6) modular support table.

Z8-830200 Crystal Assembly

The crystal assembly holds the single-crystal beam splitter, see Fig 3. A SmarAct SR-7021 rotation stage is used to rotate the crystal to diffract a fraction of the incident beam, all other stages are used for fine positioning alignment of the crystal. The crystal holder is designed with a U-shaped cut-out to let the incident beam pass through non-invasively.
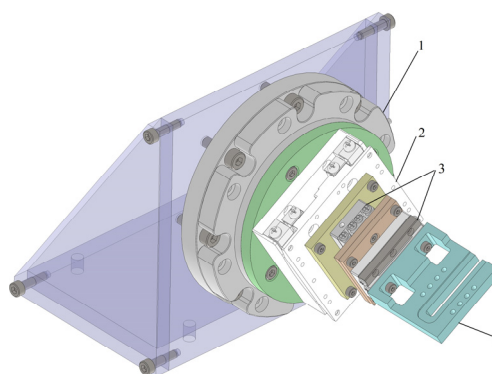

Figure 3: Z8-830200 crystal assembly: (1) SmarAct GmbH SR-7021 rotation stage, (2) SmarAct GmbH SGO-60.5 tilt stage, (3) SmarAct GmbH SLC-1730 linear stage, and (4) crystal holder.

THE DEVELOPMENT OF PAL-XFEL BEAMLINE

Seonghan Kim*, Seungnam Kim, Myeongjin Kim, Seonmin Hwang, Hyojung Hyun,
Intae Eom, Kisoo Park, Jaehyun Park, Jaeku Park, Kyungsook Kim, Sangsoo Kim,
Sunam Kim, Chaesun Lee, Seungyu Nah,
Pohang Accelerator Laboratory, POSTECH, Pohang, Gyeongbuk 37673, Republic of Korea

Abstract

Pohang Accelerator Laboratory X-ray Free Electron Laser (PAL-XFEL) is a research facility, which is designed to generate extremely intense (assuming 1×10^{12} photon/pulse at 12.4 keV) and ultra-short (10-200 femtosecond) pulsed X-rays. Now two beamlines were constructed, the one is hard X-ray and the other is soft X-ray. Each beamline is consisted of UH (Undulator hall), OH (Optical hall), and EH (Experimental hall). We have two hutches, XSS (X-ray Scattering Spectroscopy) and NCI (Nano-crystallography and Coherence Imaging) in hard X-ray beamline. They are connected each other, and sharing main optics (Mirrors and DCM, etc). PAL-XFEL is a very precise facility and has very large heat power, so mechanical analysis is required. Now vacuum components of beamline are installed and completed performance test. In here, beamlines of the PAL-XFEL is introduced in briefly, and two components, GMD (Gas Monitor Detector) and MICOSS (multifarious injection chamber for molecular structure study), are also reported.

INTRODUCTION

PAL-XFEL (Pohang Accelerator Laboratory X-ray Free Electron Laser) project, which provides 10 times the brightness of the beam than the third generation and a very short pulse of <100 fs, started construction in 2011. The installation of all machines and devices was completed at the end of 2015 and the commissioning was proceeded in 2016. The XFEL (X-ray Free Electron Laser) has been officially provided to users from 2017. Figure 1 shows the PAL-XFEL installed near the PLS-II (Pohang Light Source II).

Figure 1: Scene of PAL-XFEL and PLS-II.

The PAL-XFEL features as the world's most notable source of radiation in recent years are using higher electron energy and a longer undulator than PLS-II to produce much shorter and stronger light. The average brightness is about 100 times and the maximum brightness is more than 100 million times stronger, and the pulse length is shorter than 1/100, which makes it suitable for dynamic phenomenon research. PAL-XFEL beamline is divided into UH (Undulator hall), OH (Optical hall) and EH (Experimental hall). There are three experimental area at EH, which are XSS (X-ray Scattering Spectroscopy), NCI (Nano-crystallography and Coherence Imaging), and SSS (Soft X-ray Scattering and Spectroscopy).

Beamline [1,2]

Figure 2 shows the layouts of the hard X-ray and soft X-ray beamlines. The performance of various optical devices which are consisted of beamline were verified during the commissioning. In the PAL-XFEL beamline, the role of the diagnostic device is very important and needs to be developed separately. Therefore, various diagnostic devices were developed. GMD (Gas Monitor Detector) that one of the diagnostic device has been developed with a lot of verification test and modification and installed at the beamline. In experimental area, NCI beamline's SFX (Serial Femtosecond Crystallography) experiment uses micro focused X-ray pulse and needs to provide efficient operational performance. Thus, the MICOSS (the multifarious injection chamber for molecular structure study) is developed. By using this system, clear diffraction patterns can be obtained for lysozyme microcrystal experiment.
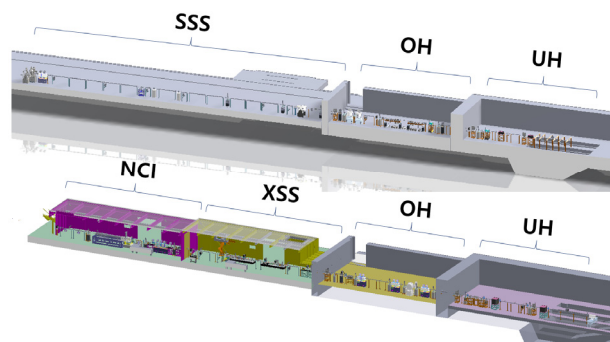

Figure 2: The layouts of hard x-ray beamline (bottom) and soft x-ray beamline (top).

*kimsh80@postech.ac.kr

DESIGN OF A FLEXIBLE RIXS SETUP

D. Meissner*, S. Adler, M. Beye, A. Bühner, H. Krüger,
R. Platzer, T. Reuss, M. Röhling, E.-O. Saemann, E. Saithong
Deutsches Elektronen-Synchrotron DESY, 22607 Hamburg, Germany

Abstract

We present a new mechanical design for a RIXS experiment setup consisting of a sample environment vacuum chamber and corresponding spectrometer. It allows variable beam incidence angles to the sample as well as observation angles of the spectrometer.

The dispersive element of the spectrometer can be aligned in five DOF by motors inside the UHV chamber. The alignment of the CCD detector can be adjusted independently in the lateral and longitudinal position as well as incidence angle. In combination with a tiltable detector chamber this design allows for multiple observation methods, not limited to variable energies but also for use of different optics or direct observations of the sample.

REQUIREMENTS AND EXPERIMENT SETUP

Requirements for the setup are according to Fig. 1, as well as Table 1. In Addition the entire spectrometer Setup must rotate around the Sample Chamber.

The setup need not support changing the entire scattering angle field without breaking vacuum. Rather a cost effective yet easy to use and quickly changeable support structure has to be chosen.

The design of the sample chamber is fixed from the beginning of the design phase which also restricts placement of mechanics and supporting infrastructure.

To observe RIXS photons at the energy spectrum from 50 eV to 650 eV the positions of grid and detector have to be changed. The optical parameters are optimized to space constraints (available area at end station as well as placement of objects and assembly space required) and imaging qualities on the detector.

In addition to the ranges of movement of grid and detector according to Fig. 1 and Table 1 the setup can move the detector to any position in the rectangle defined by the two extreme points. Also horizontal view from sample to detector is possible.

SAMPLE ENVIRONMENT AND SUPPORT STRUCTURE

Figure 2 shows an overview of the experiment. The sample is located in a vertical, cylindrical vacuum chamber and is inserted from the top. Figure 3 shows the sample holder mechanism. The top flange of the chamber is a rotating feedthrough which supports the sample holder and addi-

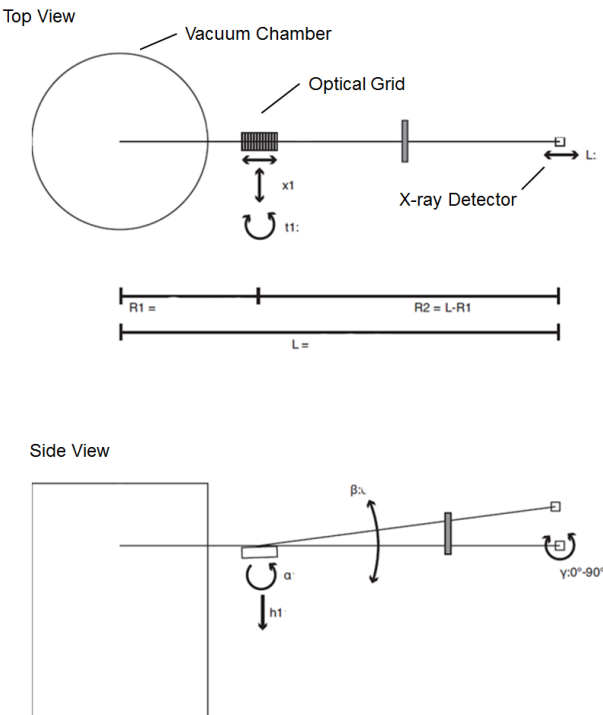---

* daniel.meissner@desy.de

Figure 1: Position and movement parameters for optical elements.

Table 1: Correlation of RIXS Photon Energy and Positions of Optical Elements (Refer to Figs. 2 and 5)

Energy eV	R_1 mm	L mm	α deg	β deg	γ deg
50	300	1347	87,9	75,8	53,5
200	364	1240	87,9	82,7	23,1
400	399	1183	87,9	84,6	17,4
650	422	1146	87,9	85,6	13,9

tional infrastructure. The sample can be cooled to 25K or heated to about 350K.

To vary the angles between beam incidence on the sample and observation angle of the spectrometer a cost-effective solution was chosen. The beamline is connected to the chamber by a motor driven bellow system (see Fig. 4) that can vary incidence angles of $\pm 15°$. For larger changes of incidence angle however the vacuum connection has to be broken and the bellow system has to be attached to another flange. By using all ports on the sample chamber any scattering angle can be reached.

The chamber is mounted on a support structure that can be adjusted to multiple beam heights above the floor and has

DUAL BEAM VISUALIZER - INTENSITY MONITOR
FOR LUCIA BEAMLINE AT SOLEIL SYNCHROTRON

C. Menneglier[†], V. Pinty, D. Vantelon, D. Roy and K. Desjardins,
Synchrotron SOLEIL, L'Orme des Merisiers, Saint-Aubin, 91190 Gif-sur-Yvette, France

Abstract

LUCIA is a micro-focused beamline dedicated to X-ray fluorescence and X-ray absorption spectroscopy at SOLEIL Synchrotron. With its recent optical upgrade and photons flux increase, the three pink-beam diagnostics of the beamline have been upgraded to sustain a beam flux reaching 10^{13} ph/s and a power deposition of 20 W/mm². This paper presents the thermomechanical study and the realization of new diagnostic detector adapted to the current constraints of use, making possible to both visualize the shape of the pink beam and to measure its intensity simultaneously in the same compact device. The X-ray beam is visualized by a piece of Al_2O_3 - Cr ceramic, soldered to a copper heat sink, whose fluorescence image detected in visible light with a suitable camera and optical system. The measurement of the photonic intensity is made by a polarized CVD diamond used as a photosensitive element, the current reading is made by a suitable low noise current to voltage amplifier. The design of this dual beam visualizer and intensity monitor, made by the SOLEIL Detector group with thermomechanical studies done by the Mechanical Design Office, will be presented in details in this paper. In-lab measurements will be also presented.

INTRODUCTION

The LUCIA beamline [1] is dedicated to micro-X-ray Absorption Spectroscopy (µXAS) and micro-X-ray Fluorescence (µXRF) experiments in "tender" X rays range of energy 0.6 - 8 keV. The range of energy offered by LUCIA allows µXAS experiments at the K-edge of the elements from sodium (Na) to iron (Fe) and L-edges of nickel (Ni) to gadolinium (Gd) and to the M-edges of rare earths and actinides. It makes it possible to apply these two non-destructive techniques to the measurement of heterogeneous samples, to make elementary maps at the photon spot scale (2 µm × 2 µm), and to describe the local environment around these elements. In order to adjust the beam on the focusing and low-pass mirror, and on the monochromator, the beamline has several imagers and intensity monitor in pink beam. The monochromatic beam is finally sent on a sample placed on an x-z translation stage. (Fig. 1).

Typical imagers consist of a YAG scintillator screen placed perpendicular to the beam and a visible light camera

oriented at 45 ° to the screen. The intensity monitors consist of AXUV100 diode in the direct beam. Both are motorized for insertion/extraction.
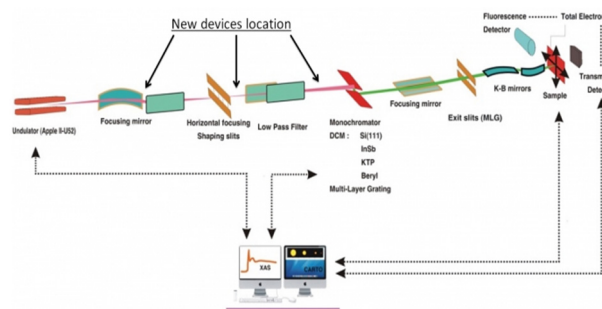

Figure 1: General layout of the Lucia Beamline.

TECHNICAL ISSUES

As a result of an upgrade of the first focusing mirror of the beamline, and a gradual increase in the intensity of the SOLEIL electron beam, the diagnostic elements of the line have undergone constraints exceeding their initial design limit. Degradations and alterations of their performance have appeared over time.

In addition, the orientation of the camera with respect to the scintillator screen requires closing the diaphragm of the camera to increase the depth of field. A long exposure time is necessary to compensate for the loss of light. This prevents detection of beam movement and creates latency during direct visualization of the beam for adjustment of optical alignments. This device had to overcome these limitations.

TECHNICAL SPECIFICATION

The new diagnostic devices must meet several functional needs:

- Image and monitor the X-ray beam;
- Totally extractable;
- Compatible with the pink beam properties;
- A incident power density of 20 W/mm²;
- A maximum beam size of 300 µm (H) × 1.2 mm (V).

The new diagnostics must also take into account technical constraints specific to the beamline:

- The imager and the intensity monitor must be designed on a single package (compact design), but will not be used simultaneously;
- They must be compatible with a level of 10^{-8} mbar vacuum;

---

† claude.menneglier@synchrotron-soleil.fr

DIRECT LN2 COOLED DOUBLE CRYSTAL MONOCHROMATOR

Tetsuro Mochizuki[†], Kazuteru Akiyama, Katsumi Endo, Hirotsugu Hara, Takumi Ohsawa,
Junki Sonoyama, Tetsuya Tachibana, Hisataka Takenaga, Koji Tsubota,
TOYAMA Co. Ltd., Kanazawa, Japan
Klaus Attenkofer, Eli Stavitski, BNL, Upton, Long Island, New York, USA

Abstract

A liquid-nitrogen-cooled (LN) X-ray double crystal monochromator has been designed and built for the high power load damping wiggler beamline of the NSLS2. It was designed as the direct LN first crystal to dissipate the max heat load of 2 kW and the second is in-direct-braid LN. It is designed to operate for beam energy 5 to 36 keV with fixed exit beam mode, and for QEXAFS compatible with channel cut mode. It is designed to rotate the Bragg axis with using AC servo motor and achieve up to 10 Hz scan.

INTRODUCTION

Directly fin-cooling cryogenic crystal is designed and built for the first crystal of NSLS-II ISS beam line monochromator. The ISS damping wiggler source incident power to the first crystal is total power of 2 kW and its power density of 7 W/mm^2.

Directly water cooled silicon crystal was designed and built for use in high power synchrotron radiation beamlines. The fin-cooling crystal used at KEK-PF BL16 multi pole wiggler source beamline showed its cooling effectiveness at the total incident power up to 1.6 kW and power density up to 0.7 W/mm^2 [1]. The total heat load is comparable to the incident power of ISS monochromator but the power density is one tenth.

Another crystal cooling method of direct LN2 cooling was designed and used for cooling the high heat load and high power density source at AR-NE3 in-vacuum undulator beamline [2, 3]. The maximum heat load is 800 W and the power density is 4.2 W/mm^2. The crystal is cooled by LN2 pool boiling. The power density is comparable to that of the ISS crystal but the total power is about half.

Cryogenic internal cooling and side cooling crystals were tested at NSLS on beam lines X25 and X17[4]. The tests are carried out for power density: 150 W/mm^2, total power: 75 W and power density: 0.5 W/mm^2, total power: 100 W. The power density is very high but the total power is small.

As cryogenic silicon crystal is adequate thermo-mechanical property for cooling the high power density radiation source and directly fin-cooling crystal can handle the high heat load, a new direct fin-cooling cryogenic silicon crystal was designed and fabricated for the ISS monochromator first crystal. The design of this crystal depends on critically on a number of mechanical dimensions. One is the Si thickness between the diffracting surface and the top of the LN2

channel. As this thickness is reduced, but the temperature and the heat flux on the LN2 channel are increased. If the temperature of the channel exceeds the starting point of nucleate boiling, LN2 boiling begins on the cooling channel surface. When the heat flux go through the critical heat flux, the heat transfer is suddenly decreased, and part of the channel surface is insulated with a vapour film and then cooling of the crystal fails.

The individual widths of the cooling channels and Si fins, and the geometry of the crescent inserts influence the effectiveness and uniformity of the cooling, and should be matched to the parameters of the cooling system.

The Si top thickness, the channel widths, the geometry of inserts, the over-all Si thickness and the coolant flow rate were optimized by the simulation with using FEA analysis.

DESIGN OF SI CRYSTAL

The Si (111) first crystal is a cylindrical shape and has a disc shape thick flange in the middle of it with which it is mounted to a manifold and seals the vacuum. The cooling semi-circular channels are cut into the backside through which LN2 is circulated. The size of the crystal is 62.5 mm in height, 77 mm in top surface diameter, 125 mm in flange diameter.
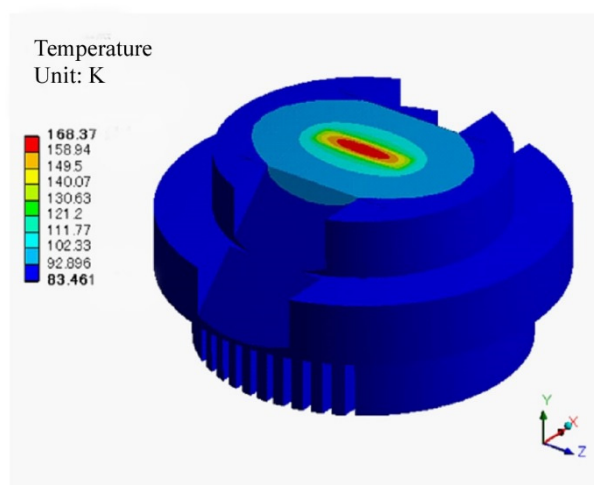

Figure 1: Temperature profile of the first crystal. Total heat load=2 kW; power density=7 W/mm^2; foot print=33.6 mm x8.51 mm (H x V); T-LN2=80 K; h=0.0103 W/mm^{2}K. This calculation model is for the thermal design phase.

_____

† mochizuki@toyama-jp.com

ENGINEERING CHALLENGES FOR THE NEH2.2 BEAMLINE AT LCLS-II*

F. O'Dowd[†], D. Cocco, J. Defever , S. Guillet, C. Hardin, D. Morton, M. Owens, T. Osier, D. Rich,
L. Zhang, G. Dakovski, SLAC National Laboratory, Menlo Park, USA

Abstract

SLAC National Accelerator Laboratory is developing LCLS-II, a superconducting linear accelerator based free electron laser capable of repetition rates up to 1MHz. The NEH2.2 Instrument at LCLS-II will use this combination of exceptionally high flux of monochromatic photons to achieve multidimensional and coherent X-ray experimental techniques that are possible only with X-ray lasers. The challenges, which emanate from delivering the beam from the sub-basement level to the basement of the Near Experimental Hall (NEH) along with the stringent requirements for providing a stable beam at the interaction points, necessitate unique engineering solutions.

With this paper we present the conceptual design for the NEH2.2 Instrument along with an overview of the R&D program required to validate design performance. Furthermore, it will show the design of the proposed Liquid Jet Endstation (LJE) and Resonant Inelastic X-Ray Scattering Endstation (RIXS) that will be installed on the beamline. After introducing the context and the layout of the beamline, this paper will focus on the main technical challenges and present the mechanical design solutions adopted for beam delivery and other strategic components.

INTRODUCTION

The LCLSII is a nextgeneration facility based on advanced superconducting accelerator technology (continouswave RF) and tunable magnetic undulators. The Xray FreeElectron Laser (FEL) is being designed to deliver photons between 200eV and 5keV with an unprecedented flux, approximately 10^{18}ph/s (0.1mJ/pulse = 10^{12}ph/pulse), at repetition rates as high as 1MHz using a superconducting RF linac (SCRF) while still providing pulses at short wavelengths and high Xray pulse energy over the photon range of 1 to 25keV using the existing copper RF (CuRF) LCLS linac at 120Hz.

The unique LCLS-II capability opens the possibility to follow chemical dynamics with time resolved x-ray absorption and emission spectroscopy as well as time resolved inelastic X-ray scattering. LCLS-II will enable the full implementation of time-resolved resonant X-ray Raman spectroscopy (resonant inelastic X-ray Raman scattering, RIXS). RIXS uniquely provides information on both occupied and unoccupied valence states probed from core levels to achieve chemical specificity.

NEH2.2 BEAMLINE

The NEH2.2 beamline fulfils the need for high throughput spectroscopic and resonant scattering applications with the high repetition rate LCLS-II beam (see key requirements in Table 1). It will take advantage of the unprecedentedly high flux of narrow-band, nearly transform-limited femtosecond soft X-ray pulses to open new scientific opportunities for spectroscopic studies of elementary excitations. The major components include a beamline monochromator, bendable re-focusing optics, pump laser integration and two endstations: Resonant Inelastic X-ray Scattering (RIXS) Endstation and Liquid Jet Endstation (LJE).

Table 1: Key Requirements

Parameter	Range	Comment
Photon Energy	250-1600eV	Reject 3rd harmonic at O
Beamline Transmission	20%	Zero Order
Bandwidth Control	>50,000; 5-10,000	High resolution RIXS
Spot Size	2-1,000μm	Adjustable

X-ray Optical Layout

The layout of the beamline stretches from the Front End Enclosure (FEE) into the Near Experimental Hall (NEH) and ultimately to the upper level, as shown in Figure 1. The beam will be deflected vertically by the soft X-ray monochromator (through a combination of mirrors and a grating) and will rise at an angle of ∼7º. A horizontally deflecting flat mirror directs the beam south by ∼3º towards NEH 2.2, while the straight-through beam continues to NEH 2.1. The beamline exits the FEE high on the east wall and enters Hutch 1 (AMO), where the exit slit is mounted. The beam continues in Hutch 1, penetrates the ceiling and continues to the basement level of the NEH. The beam is then deflected back down by a combination of a flat and vertically re-focusing mirror, so it is again horizontal, and enters the RIXS Sample Chamber, Figure 2.

The beamline monochromator is projected to house four gratings ruled at different groove densities. Three of them are used to provide very high spectral resolution. The fourth one has a low groove density (50l/mm) and will provide transform limited beam with resolution between 5 and 10,000. The footprint of the beam on the grating is controlled using the elliptical bendable mirror upstream of the monochromator. For the very high resolution option, approximately 10^{15}ph/s, in first diffraction order, at resolving power (RP) up to 50,000 will be made available at the sample location in high repetition rate mode.

___
*fodowd@slac.stanford.edu

MAGSTAT V3: AN IN-VACUUM VARIABLE-GAP QUADRUPOLE WITH ROTARY PERMANENT MAGNETS

V. Pinty, H. Popescu, N. Jaouen, F. Marteau, P. Prout

Synchrotron SOLEIL, L'Orme des Merisiers, Saint-Aubin, 91190 Gif-sur-Yvette, France

Abstract

MAGSTAT is a quadrupole designed to magnetize samples with a variable magnetic field in flow density and in directions. Four rotary permanent magnets allow the user to specify a direction for the field and changing in situ the gap between the poles drives the field intensity. The first prototype was realized in 2016 on the SEXTANTS beamline in the framework of SOLEIL-MAXIV collaboration; a second version has been manufactured for MAXIV SoftImax beamline. This third version shows a significant evolution of the mechanical design, guaranteeing a much better stiffness in high field configurations. Samples up to Ø74mm can be placed in this quadrupole, and the tiny ones which may fit in a Ø10mm circle or smaller, can be magnetized with a 1T local field. The angle of each magnet is driven by a dedicated stepper motors with a big reduction ratio. The total gap is ensured by a single motor, and its motion is symmetrically transferred to the magnets through an Archimedean spiral. The first prototype is installed permanently at COMET endstation dedicated to the coherent scattering of soft X-ray in transmission for imaging magnetic materials via the Fourier Transform Holography or ptychography techniques.

SPECIFICATIONS

The initial specifications were:
- The quadrupole should fit in CF100 DN flange so it can be transferred to or removed from the sample through the CF100 vacuum chamber fittings.
- The horizontal magnetic field should be driven by four motorized rotating magnets, with a variable motorized gap.
- The magnetic field should reach ~1T, at minimum gap on the center of the quadrupole.
- All motorized movements should be encoded.

FIRST AND SEDOND MAGSTAT PROTOTYPES

Mechanical Description

In order to drive magnets rotations, each magnet has a dedicated UHV stepper motor and is coaxially mounted on it. The maximum field of 1T is reached only when gap of the magnets is about 12mm, with Ø26mm permanent magnets made of NdFeB. The closest motor size is Ø22mm, with the highest reduction ratio, the output torque is 1.5N.m.

Each motorized magnet block is mounted on a linear translation oriented towards the centre of the poles. To drive the four linear translations, the motorized magnets

mounts are locked in a double Archimedean spiral (green part in Fig. 1) path which crosses the translation path [1].
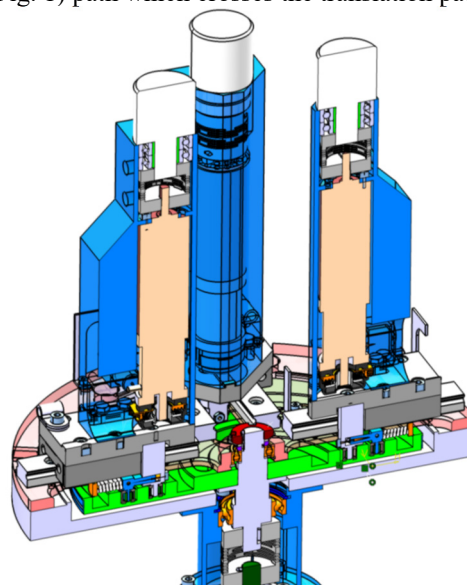

Figure 1: Section view of CAD V1 MAGSTAT prototype.

This solution ensures a great radial compactness since there is only one motor for the four symmetric linear displacements, and it is coaxially mounted with respect to the poles.

Performance

The first prototype (Fig. 2), realized in 2016 was able to achieve good performance in most field configurations and is being use on the SEXTANTS beamline.
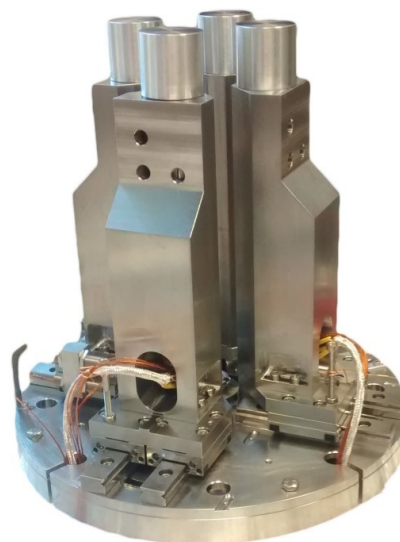

Figure 2: MAGSTAT V1 prototype main parts overview. Bottom disk diameter is less than Ø100mm.

DESIGN & DEVELOPMENT OF AN INNOVATIVE 6 AXIS SAMPLE MANIPULATOR

M Purling [†], Diamond Light Source Ltd., Oxfordshire, UK

Abstract

The accurate positioning & alignment of sample specimens within the experimental test chamber on a beam line is always a challenge. The ability to move in any direction and angle to very precise increments with repeatable positioning is crucial for being able to focus on the exact part of the sample required in the correct orientation. This is more complex when the sample is required to work within the Ultra High Vacuum environment and cooled to cryogenic temperatures of below 20k. Initially in conjunction with St Andrews University, Diamond Light Source Ltd. have developed their own manipulator for this purpose, it has six degrees of freedom for alignment of the sample and easy remote sample plate loading via a transfer arm system. (Fig.1 & Table 1)

This paper describes the developments made from initial design to working manipulators with increased functionality for bespoke requirements on four different beam lines within Diamond.
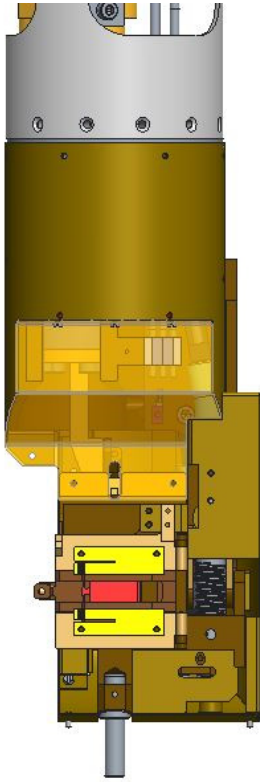

Figure 1: Manipulator Lower Half.

Table 1: Manipulator Motion Specification

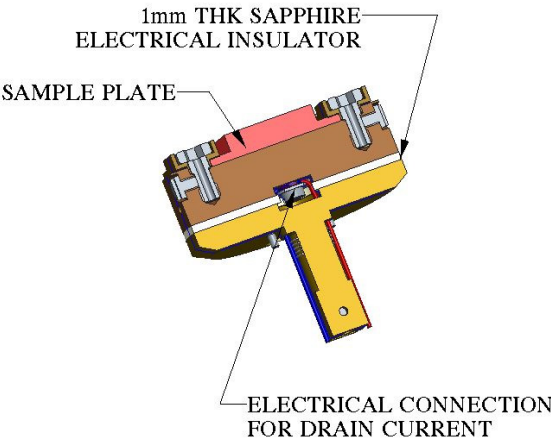| Axis	Range	Resolution	Repeatability
x	+/-12mm	0.5 micron [1]	1 micron [1]
y	+/- 12mm	0.5 micron [1]	1 micron [1]
z	100mm	1 micron [1]	1 micron [1]
Polar	360°	100 nrad [2]	10 µrad [2]
Azimuth	+/- 90°	0.01°	+/- 0.05°
Tilt	-10/+45°	0.1°	+/- 0.05°

DRAIN CURRENT MEASUREMENT

Figure 2: Section Showing Drain Current Connection.

Certain types of experiments, Photo Emission Spectroscopy and Absorption Spectroscopy use & measure the drain current flowing to the sample. It is important that the sample remains at a neutral potential but electrons are allowed to flow to the sample replacing ones emitted during the experiment. A new azimuth drive (Fig. 2) was designed to enable this to be done. A top and bottom made from copper, for good thermal conduction that are separated with a 1mm thick piece of sapphire which kept the top & the sample electrically isolated from earth. A wire is connected to the underside of the top and this is used for the drain current is measurement.

Sapphire was used as it has the properties of an excellent electrical insulator, 1×10^{14} Ωcm [3], with good thermal conductivity.

_____
† martin.purling@diamond.ac.uk

NOVEL COMPREHENSIVE UHV LENS CHANGER AT THE PETRA III BEAMLINES P22, P23 AND P24

J. Raabe[†], K. Ederer[†], C. Schlueter, R. Grifone, D. Novikov
Deutsches Elektronen-Synchrotron DESY, Notkestraße 85, 22607 Hamburg, Germany

Abstract

We present the design of a compact UHV-compatible X-ray transfocator for beryllium compound refractive lenses (CRL).

CRLs are nowadays commonly applied for beam focusing, collimation and aperture matching in a lot of experimental techniques based on synchrotron radiation. Aim of the current project was the development of a low-maintenance lens for the reliable use under ultrahigh vacuum conditions. We discuss two variants of the device, one designed for 2D lenses and the other one operating with 1D lenses. Precise and reproducible alignment is achieved by pneumatic actuators that press the lens stacks against a high precision prism. All actuators and position sensors are placed outside the UHV vessel. Alignment is facilitated by integrated beam monitors and alignment apertures. The transfocator construction allows an easy adaptation for any desired number of lens stacks. In the current version, the 2D lens changer adapts 12 stacks of up to 8 single lenses each, and the 1D variant – 8 single lenses or apertures.

INTRODUCTION

Refractive optics is of key importance for synchrotron beamlines aiming for micrometer and sub-micrometer beam sizes. Small dimensions of the lenses allow for very compact and cost effective solutions for beam focusing applications [1, 2]. Consequently, CRLs became widespread in the synchrotron community, particularly for hard X-ray beamlines.

Three new beamlines went into operation in the Ada Yonath hall at the high brilliance PETRA III storage ring at DESY (Hamburg, Germany) in 2017. At all beamlines compound refractive lenses are employed for in-vacuum X-ray beam focusing, collimation and conditioning [3].

In this project, great importance was attached to a robust and low maintenance design of the lens changing mechanics which was implemented with some minor variation at all three beamlines. Here we present a lens changer design, with particular emphasis on 2D focusing requirements at the In-situ and Nano Diffraction beamline P23 and at the Chemical Crystallography beamline P24.

LENS CHANGER DESIGN

The beamline optical configurations require the positioning of lenses in the optic hutches in an UHV environment, making a compact and scalable design, high reliability and low-maintenance operation as well as compliance with the stringent DESY vacuum guidelines key objectives of the design task.

Requirements

Basic specifications for the lens changer include :
- Main functionality: high precision for positioning of the lenses
  - with exact coaxial orientation of the lenses to the synchrotron radiation beam and to each other
  - high positional reproducibility
- UHV environment with extremely low residual hydrocarbon content
- Simplified adjustment mechanics with four motorized degrees of freedom for alignment with respect to the X-ray beam – y (horizontal, perpendicular to the beam), z (vertical), pitch and yaw
- all alignment mechanical parts should stay outside of vacuum for easy service and troubleshooting
- Integrated alignment screens
- CF-flange viewport(s) for inspection and alignment
- flexible remote control via a TCP/IP interface

Design of P23 Transfocator

The general design of the transfocator is comprised of a vacuum vessel with lens stacks, alignment prism, out of the vacuum support and positioning mechanics. Single lenses are stacked in groups depending on experimental requirements (i.e. energy, focusing conditions, photon flux optimization). To achieve optimal focussing at discrete energies one can select suitable combinations of lens stacks carrying different numbers of lenses [4].

The lens stacks are pressed with a spring sheet into a high precision prism. The prism is the core element of the design. It has very tight shape and position tolerances and serves as a reference plane for reproducible alignment and ensures exact positioning. The manufacturer we have chosen provides a permitted variance of the guide plane parallelism to the reference planes of 2μm over the whole length of a range [300…1000] mm.

The stacks are inserted into the beam path by a rotational lever mechanics pushed by pneumatic drives. The simple and robust layout inside the vessel allows for fast and reliable switching between different configurations.

For alignment and beam monitoring, pinholes and X-ray fluorescence screen are incorporated into the system.

The assembly is shown in Figure 1.

---

† jana.raabe@desy.de
† katrin.ederer@desy.de

TRAINING THE NEXT GENERATION OF ENGINEERS FOR PHOTON BASED LIGHT SOURCES

S.M.Scott, Diamond Light Source, OX11 0DE Didcot, UK

Abstract

The continued increase in the number of Light Sources, their beamlines and the need for upgrades of both machine and beamlines requires an increasing supply of suitably qualified and experienced engineers. If there is a world wide shortage of Engineers where will facilities find these engineers and how can they be trained to the required   level?
This paper discusses these issues by looking at the growth of demand for engineers within light sources, the evidence of shortages of engineers, the changes in attitudes to work by younger people, the skills necessary, training opportunities and the issues in attracting people into the light sources industry.

GROWTH OF LIGHT SOURCES

The first observation of radiation from accelerating electrons was in 1947. At first, synchrotron radiation was obtained from electron synchrotrons built for other purposes such as for high-energy physics. Dedicated machines started to appear in the 1970's and since then there has been a constant increase in the number of synchrotrons operating throughout the world. As well as an increasing number of facilities, the size and complexity of each synchrotron is increasing. The larger number of beamlines per facility, the demands for higher levels of stability, smaller beam sizes, higher power and faster throughput all require Engineers with a high level of expertise and experience.

IS THERE A WORLD SHORTAGE OF ENGINEERS ?

Some of the recent headlines would indicate a shortage of engineers in many parts of the world.

"By 2025, we might need 500,000 engineers, said Olof Persson, chief executive, of Volvo Group, the world's second-biggest truckmaker" [1].

"Peter Löscher, chief executive of Siemens, Europe's largest engineering group, said "the skills shortage, particularly in Germany, is a big issue" [1].

"Washington Post editorial published on August 4th 2011 warns of an approaching disaster in the shortage of professional engineers in the US."

As well as the media sound bites there are well researched reports.

"According to a recent Engineering labour market study by Engineers Canada, the country's rapid growth in the mining, energy, and transportation sectors, coupled by the anticipated retirement of approximately 95,000 Canadian engineers in the next 7 years, has resulted in a worrisome shortage of experienced engineering talent" [2].

The "skills panorama" are part of the European commission and monitor skills shortages. They report that across the EU, the top five skill shortage occupations include engineering professionals [3].

Within the UK, the Royal Academy of Engineering's report highlighted a shortage of Engineers within the UK across all sectors of the economy [4], the Institution of Engineering and Technology (IET) 2017 skills survey [5] concluded that engineering skills shortages and gaps continued to be a huge problem for employers.

In India, about 1.5 million engineers graduated from more than 3,500 engineering colleges across India in 2014. But at a recent meeting to discuss the Indian aerospace indus-try the conclusion was that only 4 to 7 per cent of engineers are actually fit for jobs in the core engineering sectors [6].

However one of the problems in developing a global view is the lack of reliable data. In a recent report by Emma Smith [7], she concludes that while the shortage debate has a long history, it is one that is characterized by poor quality data as well as methodological and conceptual challenges.

IS THERE A SHORTAGE OF ENGINEERS FOR LIGHT SOURCES?

If accessing a shortage of Engineers worldwide is difficult, can we say anything about the shortage within the light source community?

One way of examining the need would be to review the number of vacancies that exist. The vacancy pages of the web sites of each facility may give information as well as generic web sites such as www.lightsources.org. The problem with this approach is that the recruitment and supply of staff varies between facility and country. For example SOLEIL Light source have a limit in staff numbers as part of the legal structure and any shortfalls have to be met with contractors. In the USA, some beamlines are operated by university departments that are separate from

FRONTEND SLITS FOR CLOSELY-SPACED WIGGLER BEAMS

S. Sharma[†], C. Amundsen, F. DePaola, J. Tuozzolo, NSLS-II, BNL, 11973 Upton, NY, USA

Abstract

A high energy x-ray (HEX) beamline facility will be constructed at NSLS-II for R&D in energy storage technologies using different x-ray imaging techniques. A 4.3 Tesla superconducting wiggler will be used to produced x-rays of total power of approximately 56 kW in 8 keV – 200 keV range. The nominal horizontal fan of ~ 10 mrad will be split into three closely spaced beams of 0.2 mrad, 1.0 mrad and 0.2 mrad fans. Each beam is required to have a frontend slit with four distinct apertures. The conventional L-shape design of the slit is not feasible for these closely spaced beams because of constraints on side cooling and horizontal travel of the slits. In this paper we propose two solutions for these slits using a beam pass-through design, vertical-only travel and optimized cooling configurations.

INTRODUCTION

NSLS-II is presently designing a state-of-the-art HEX beamline facility for fundamental research in energy storage technology and associated materials [1]. The facility will support three beamlines integrating multiple high energy x-ray imaging techniques. The beamlines will enable in-situ experiments on real materials and systems under real operating conditions.

The x-ray source will be a 4.3 Tesla superconducting (SC) wiggler that will produce highly intense x-rays of total power of 56 kW in 8 keV – 200 keV range. As shown in Fig. 1(a) this source has a large horizontal fan of 9.87 mrad as compared to the narrow vertical fan of 0.88 mrad. The peak power density is 28.4 kW/mrad².
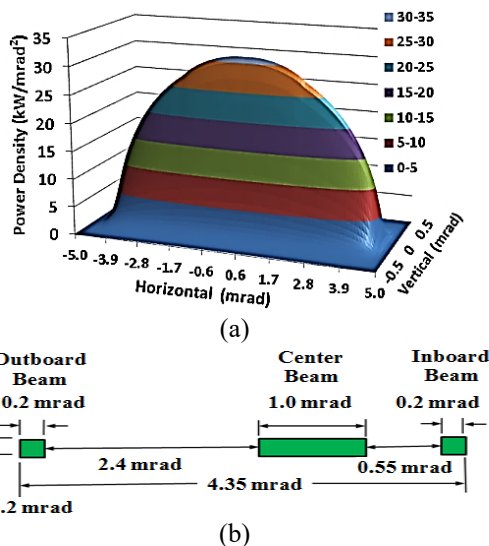

(a)

(b)

Figure 1: HEX wiggler x-ray source and beams, (a) power distribution of 4.3 Tesla SC wiggler, (b) 3 beams, fan sizes and spacings.

† sharma@bnl.gov

A fixed mask in the frontend, placed at 18 m from the source, divides the horizontal fan into three beams of 0.2 mrad (outboard), 1.0 mrad (center) and 0.2 mrad (inboard) as shown in Fig. 1(b). The separation between the outboard and center beams is 2.4 mrad, whereas it is only 0.55 mrad between the center and inboard beams.

Three slits are provided downstream of the fixed mask to reduce the beam size for each beamline independently (Fig. 2(a)). The conventional design of a pair of L-shaped slits is not possible for these closely spaced beams because there is no room for any significant horizontal travel. The HEX slits will, therefore, have four discreet apertures [2] ranging from a full beam size exiting the mask to a smallest size of (0.05 mrad H x0.05 mrad V). The apertures for the center-beam slit, separated vertically by ~ 10 mm, are shown in Fig. 2(b). Each slit will also act as a beam stop. Single axis high-precision linear stages will be used to provide vertical motion to the slits for remotely selecting one of the apertures.

(a)

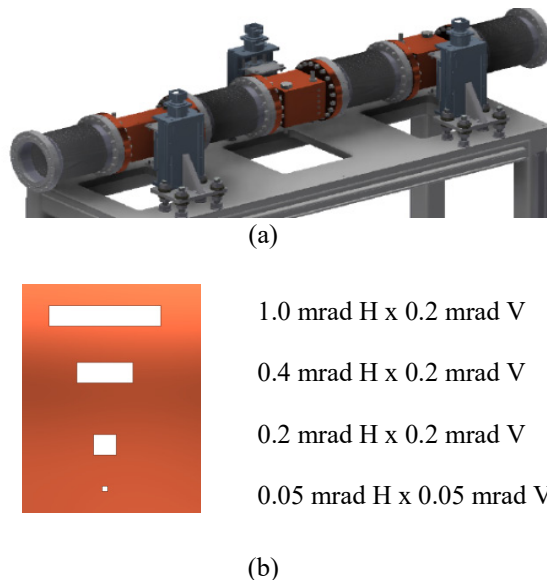| 1.0 mrad H x 0.2 mrad V |
| 0.4 mrad H x 0.2 mrad V |
| 0.2 mrad H x 0.2 mrad V |
| 0.05 mrad H x 0.05 mrad V |

(b)

Figure 2: Slits in the HEX frontend, (a) 3-slits assembly on a table, (b) 4 apertures of the center-beam slit with vertical separation of ~ 10 mm.

Two slit designs are described in this paper, one for the case when the narrow spacing between the beams is not sufficient to include cooling channels of reasonable size (> φ 6 mm). This design will be applicable to the center and inboard beams. The second design, applicable to outboard beam, is for the case where it is possible to include cooling channels between the beams, even if slightly smaller than φ 6 mm. For comparison both designs are discussed with respect to the center-beam slit.

NEW HOLDER FOR DUAL-AXIS CRYO SOFT X-RAY TOMOGRAPHY OF CELLS AT THE MISTRAL BEAMLINE

R. Valcárcel*, N. González, C. Colldelram, A. J. Pérez-Berná, A. Sorrentino, E. Pereiro,
ALBA Synchrotron Light Source, Cerdanyola del Valles, Spain

Abstract

A new dual-axis sample holder has been designed and built for the Transmission soft X-ray Microscope (TXM) at the MISTRAL beamline (ALBA Synchrotron) [1, 2] to perform cryo-soft X-ray tomography of cells with dual tilt configuration to reduce the missing wedge.

The design, with restricted dimensions Ø7x30mm, enables using commercial Auto-Grid support rings that give rigidity to the sample grid handling. It consists of a guided miniature handle with a spring system that allows sample rotation by 90º around the beam axis inside vacuum and in cryogenic conditions by using the TXM sample loading robot keeping a rotation of ±65˚ at the sample stage. Two magnets fix the positions at 0˚ and 90˚. The two tilt series can be collected consecutively and the use of Au fiducials permits combining both improving the final quality of the 3D reconstructions. In particular, cellular features hidden due to their orientation with respect to the axis of rotation become visible. The main frame is made in aluminium bronze to enhance the thermal conductivity and in addition, all the pieces have undergone an ion implantation treatment in order to reduce friction and improve the anti-seizure property of the parts.

INTRODUCTION

Structural Cell Biology demands detailed structural and functional descriptions of the different cellular components which must be correlated with a topological 3D map of these components at the whole cellular level. In this frame, an emerging technique such as cryo-SXT can provide structural information at the level of a whole cell without further sample preparation except for the cryo-fixation required to prevent radiation damage while collecting the data. The penetration power of soft X-rays in the so-called water window spectral range, between the inner-shell absorption edges of carbon and oxygen (from 284 eV to 543 eV), allows penetrating water layers of up to 10 µm thickness while carbon-rich structures are visualized with good absorption contrast. Thus, frozen-hydrated specimens can be imaged close to their native state providing significant complementary information to existing biological imaging techniques at a spatial resolution of 30 nm. Cryo-SXT generates, as in electron tomography, 3D absorption maps of the specimen from a series of 2D soft X-ray microscopy projections recorded with a CCD [3]. In the current TXM design at Mistral we use TEM grids as sample support on which the cells are grown. Due to the choice of the flat sample support and the reduced distance from the sample to the objective lens, the available tilt range is ± 70º. This angular restriction results in a region empty of information in the Fourier space, the so-called "missing wedge" (see Fig. 1), which in real space produces an elongation of every point of the reconstructed volume along the beam direction. In addition to this well-known effect, in the reconstructions some cellular features will not be visible due to their orientation with respect to the axis of rotation. A way to reduce the missing-wedge effect in the reconstructed volumes is therefore by doing dual-tilt tomography (see Fig. 1)
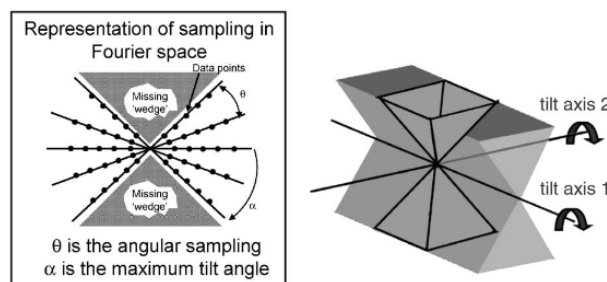

Figure 1: Representation of the sampling in Fourier space showing the limited tilt range (left) leading to a missing wedge 3D reconstruction in a single tilt tomography (right) and the sampling achieved by dual axis tomography which is reduced to a missing pyramid (right). [4]

TECHNICAL SPECIFICATIONS

The dual-axis holder must comply with the following specifications:

- Two orthogonal tilt axis.
- High vacuum compatible (10^{-7}mbar).
- Good thermal conductivity to get 100K at the sample.
- Motions inside TXM.
- Compatibility with AutoGrid sample support.
- Sample visibility in the range ± 65º degrees for the existing tilt.
- Second tilt with two fixed positions (0º- 90º).

DESIGN

The design consists of tiny mechanism of metal parts that have been treated with an ion implantation process to improve the anti-seizure property and reduce the friction in cryogenic temperatures. The holder body is produced in aluminium bronze to achieve a good thermal conductivity and it is manufactured with precision to fit perfectly in the motorized sample stage of the TXM. The

---

* rvalcarcel@cells.es

Beamlines

End Stations

A HIGH HEAT LOAD DOUBLE CRYSTAL MONOCHROMATOR AND ITS CRYO COOLING SYSTEM FOR HEPS

Hao Liang[†], Gang Cao[1], Lidan Gao, Yongcheng Jiang, Weifan Sheng[†, 1], Shanzhi Tang[1], Aiyu Zhou,
Institute of High Energy Physics, 100049 Beijing, P. R. China,

[1]also at University of Chinese Academy of Sciences, School of Physics, 100049 Beijing, China

Abstract

A high heat load double crystal monochromator and its cryo cooling system were designed and their prototypes were fabricated for the future HEPS. The mechanical and cooling structure of the DCM are introduced. The FEA results show the DCM is capable of cooling 870 watts of heat load. The cryo cooling system is also introduced. Test results show the pressure stability of the cryo cooling system is less than 2 mbar RMS. Offline heat load test of the DCM were carried out by a ceramic heater attached to the center of the incident surface of the first crystal, and 834 watts heat load were applied by the heater without boiling the liquid nitrogen. Offline absolute vibration measurement of the second crystal assembly was carried out by a laser interferometer under different cryo pump speed, pressure and heat load conditions, to find out the stability performance accordingly. An absolute vibration of 41 nrad RMS was measured, with the pump running at 45 Hz, which has a cooling capability of 400 watts.

INTRODUCTION

HEPS is a new generation light source which employs multi-bend achromat lattices and aims to reach emmitance as low as 60 pm•rad with a circumference of about 1296 m. [1] It will start construction at the end of this year in Beijing. With the new light source there will be very small beam size and high-power density for the monochromator, and cryo cooling of crystals is favourable under those conditions. In the first phase of HEPS there will be 14 beamlines, a batch of cryo cooled monochromators and cryo cooling systems will be needed. Monochromator relates directly with beam intensity and stability issues and affects the overall beamline performance. Beijing Synchrotron Radiation Facility of IHEP is a first-generation light source which contains no cryo cooled optics. It is necessary to develop prototypes of a DCM and a cryo cooling system in order to get a better understanding of the technical challenges during the process and meet the requirements of HEPS beamlines in the future.

The following sections will introduce the design of the DCM and the cryo cooling system, offline heat load test and vibration test, and online test results of the prototypes.

DESIGN OF THE DCM

During the designing phase only, the techniques that had past the proven of principle stage were adopted. By applying those techniques which has never been used in BSRF

---

† Email addresses: lianghao@ihep.ac.cn and shengwf@ihep.ac.cn.

before, successful running of both the prototypes was the major target.

Table 1 shows the general specifications of the DCM during design phase.

To have a good stability performance wasn't among the original design objectives of the DCM. Later on, after the prototype was built, with the growing concern on the stability performance, the target was set to 100 nrad.

Table 1: DCM Specifications

Parameter	Description
Energy range:	5-20 keV
Crystal type:	Si<111>
Bragg angle range:	-4°–40°
Angular resolution:	0.5 µrad
Fixed offset:	25 mm (upwards)
Absolute stability of exit beam:	100 nrad
Heat load to be handled:	800 Watts
Rocking-curve broadening:	<10%
1st crystal size:	30(W)×60(L)×40(T) mm^3
2nd crystal size:	30(W)×200(L)×30(T) mm^3
1st crystal adjustment:	fixed
2nd crystal adjustment:	Pitch, roll, gap
1st crystal cooling:	Indirect LN$_2$
2nd crystal cooling:	Indirect by copper foils
Vacuum:	10^{-5} Pa

Cooling of Crystals

To design a high heat load monochromator, a heat load of 870 watts with 2D Gaussian distributions were assumed to irradiate onto the first crystal. Assumed distribution of heat load absorbed on the surface of the first crystal is shown in Fig. 1 and Fig. 2.
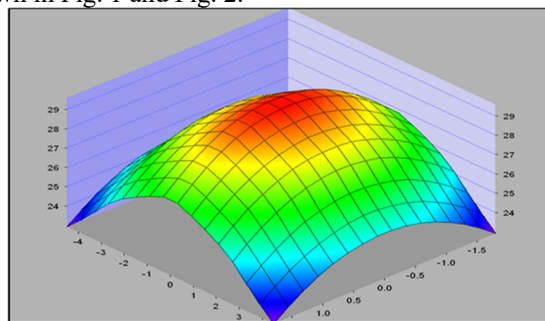

Figure 1: Heat load distribution, total power: 870 watts, power density: 29.6 W/mm^2, divergencies (RMS): 25(H)×10(V) mrad^2.

ENGINEERING DESIGN AND COMMISSIONING PERFORMANCE OF THE ESM AND SIX SOFT X-RAY BEAMLINES AT NSLS-II*

Y. Zhu, S. O'Hara, M. Idir, E. Vescovo, I. Jarrige, S. Hulbert[†], National Synchrotron Light Source II (NSLS-II), Brookhaven National Laboratory, Upton, New York 11973, USA

Abstract

Two of the five NSLS-II Experimental Tools (NEXT) project insertion-device beamlines developed for the NSLS-II facility at Brookhaven National Laboratory are state-of-the-art soft X-ray beamlines covering the 15 eV-2300 eV photon energy range. The engineering challenges of these two beamlines included: accurate and realistic optical simulations, nearly perfect optical figure and metrology, and advanced diagnostics systems developed in-house. The measured preliminary performance (flux, spot size, resolution) of these two beamlines closely matches the calculated values. Here, the engineering design and performance measurements of these two beamlines are presented.

INTRODUCTION

The Electron Spectro-Microscopy beamline (ESM) and Soft Inelastic X-ray Scattering beamline (SIX), as part of the NEXT project funded by the Department of Energy, have recently been commissioned at NSLS-II and are now in operation.
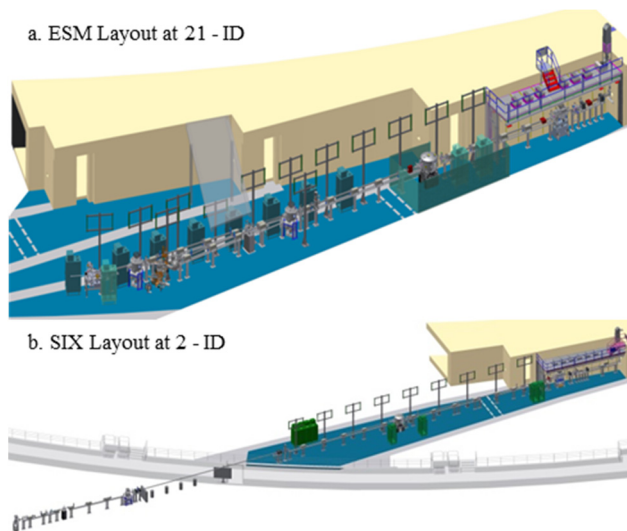

Figure 1: ESM and SIX on the NSLS-II Floor.

ESM is an insertion device beamline installed in sector 21-ID shown in Figure 1(a), a low-beta, non-extended floor space sector of the NSLS-II experimental floor. Two in-line, elliptically polarized undulators (EPU), a 2.8 m long

EPU105 and a 1.4 m long EPU57, serve as the beamline sources to cover a large photon energy range: 15 to 1500 eV. Downstream of a shared plane grating monochromator, the beam is deflected horizontally into one of two branches, the A-branch or P-branch (A for a high-resolution Angle-Resolved PhotoEmission Spectroscopy (μ-ARPES) and P for a full-field photoelectron microscopy (XPEEM)) by vertical selection of one of two identical elliptical cylinder mirrors (M3-A and M3-P).

The 105 m long SIX beamline is installed in sector 2-ID shown in Figure 1(b), a high-beta insertion device straight section feeding beam through an extended floor space sector to a satellite building. The SIX beamline covers the 180-2300 eV photon energy range by using a 3.5 m long EPU57 (upgradable to 7.0m) and is optimized to achieve a resolving power of 100,000 at 1,000 eV.

BEAMLINES OVERVIEW

ESM and SIX adopt the same type of optical scheme [1] (Figure 2; Table 1 lists beamline parameters). A horizontal internally water-cooled plane mirror (M1) serves to remove unwanted power and to separate the rest of the beamline from the Bremsstrahlung cone. The next component, a Variable Line Spacing (VLS) Plane Grating Monochromator (PGM), contains an internally water-cooled plane pre-mirror (M2) which illuminates one of four VLS gratings (300 l/mm, 600 l/mm, 800 l/mm and 1200 l/mm) for ESM and one of three VLS gratings (500 l/mm, 1200 l/mm, and 1800 l/mm) for SIX. The diffracted beam from the gratings is focused, vertically by the VLS grating and horizontally by an elliptical cylinder mirror (M3), at a plane occupied by high precision horizontal and vertical slits which define the energy resolution (vertical) and serve as a secondary source. A refocused image of the secondary source is produced at the sample position by either an ellipsoidal mirror (M4, at SIX and ESM B-branch) or by a KB mirror pair (ESM A).
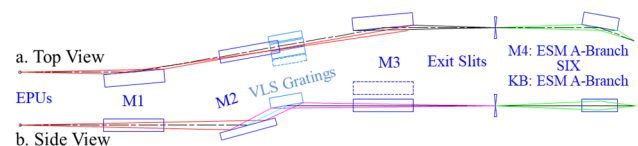

Figure 2: ESM and SIX optical schemes. The dashed rectangles represent the 4th ESM grating and the 2nd ESM M3 mirror.

ESRF DOUBLE CRYSTAL MONOCHROMATOR PROTOTYPE PROJECT

R. Baker, D. Baboulin, R. Barrett, P. Bernard, G. Berruyer, J. Bonnefoy, M. Brendike, P. Brumund,
Y. Dabin, L. Ducotté, H. Gonzalez, G. Malandrino, P. Marion, O. Mathon, T. Roth, R. Tucoulou,
European Synchrotron Radiation Facility, 38043 Grenoble, France

Abstract

Spectroscopy beamlines at the ESRF are equipped with a generic model of double crystal monochromator (DCM), originally acquired in the 1990's. After over 20 years of continuous service, their conception, although pioneering at that time, can no longer meet the challenge of present and future scientific goals in terms of position and angular stability, thermal stability, cooling system, vibration, control and feedback, particularly in view of the ESRF - EBS upgrade.

Considering the above issues, a feasibility phase was launched to develop a prototype DCM dedicated to future spectroscopy applications at the ESRF. Specifications - derived from expected performance of the EBS upgrade and scientific objectives - are extremely challenging, especially in terms of mechanical and thermal stability and impose the adoption of several innovative design strategies. The prototype is currently in the assembly phase and tests of the complete system are planned before the end of 2018.

This article gives an overview of the DCM prototype project including specifications, major design options implemented and various validated concepts. Current project status and first test results are also presented.

INTRODUCTION & SPECIFICATIONS

Beamlines applying experimental techniques such as X-ray Absorption Spectroscopy (XAS) in the tender to hard X-ray energy range (>2keV) are among the most demanding applications for monochromator systems. Typically such beamlines use fixed-exit double-crystal monochromators which permit scanning of the X-ray beam energy without realignment of the downstream optical components or sample. Achieving the required stability and repeatability of such devices both in terms of beam trajectory and selected photon energy is particularly challenging. This difficulty is accentuated by the progressive improvement of source and focusing optic quality as well as the challenges of management of the absorbed X-ray power which have meant that the monochromator can often be a key component limiting beamline performance.

Table 1 shows the critical target specifications for a new ESRF DCM. The values are derived from typical ESRF beamline geometries, the upgraded EBS source characteristics and the stability and precision of the energy selection. The overall specifications are particularly demanding and cannot be met by currently available devices. Consequently a new, vertically-deflecting DCM has been designed which is intended to replace ageing devices on several ESRF spectroscopy beamlines.

Table 1: Summary of Critical Specifications

Crystal parallelism	Units	Value
Pitch for Δ Bragg <1°	nrad fwhm	15
Pitch for Δ Bragg <5°	nrad fwhm	30
Pitch for Δ Bragg <20°	nrad fwhm	75

Bragg angle	Units	Value
Precision	μrad	2 - 5
Bidirectional repeatability	μrad fwhm	25
Unidirectional repeatability	μrad fwhm	0.2

Figure 1 indicates the 3 stage design philosophy behind the DCM concept: a strong user request is for the DCM to continue functioning, albeit in a "downgraded mode" in the case of failure of the correction and feedback loops. Every effort has therefore been made at the design stage to attain 0.1 - 0.3μrad/° crystal parallelism in this mode (A). Repeatable errors can be corrected after characterisation (B) and ultimate performance is achieved by using the real time control system (C).
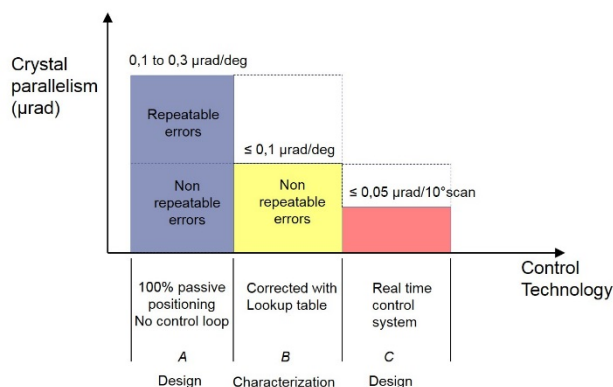

Figure 1: ESRF DCM design philosophy.

ARCHITECTURE

Several architecture options have been evaluated:
- Cantilever cage concept
- Cantilever or split bearing cages , all in vacuum
- Split bearing and drum cage concept

Advantages and drawbacks were established for each solution, but the cantilever design was favoured, firstly due to the numerous possible identified areas of improvement over the existing concept and secondly, because the six ESRF DCMs are due for replacement and